Genetic profiling of phaeochromocytoma and paraganglioma: towards precision medicine

Dr Amanda Seabrook

A thesis in the fulfilment of the requirements for the degree of

Doctor of Philosophy

Faculty of Medicine, The University of Sydney

Declaration

The work in this thesis was carried out by the candidate, except where specific acknowledgement has been made.

I declare that no part of this thesis has been previously submitted for the purpose of obtaining any other degree.

Amanda Seabrook

March 2024

Acknowledgements

The work presented in this thesis would not have been possible without the guidance and support of my supervisors and collaborators.

Firstly, to Professor Rory Clifton-Bligh for providing me with the opportunity to undertake a PhD within the Cancer Genetics laboratory. His guidance, encouragement and mentorship over my candidature has been invaluable. His passion for research to improve patient care is unwavering and inspiring. I would also like to thank Dr Trisha Dwight for her time and patience teaching a newcomer how to navigate the wet lab and perform the basics of genetic testing. The day I received my own set of pipettes (on loan) was very exciting for a clinician moonlighting as a scientist.

I am forever indebted to Dr Cathy Luxford, my 'lab mum', for her knowledge and guidance both within the laboratory and outside, who would always take time from her own busy work to nut out problems. And, of course, for editing large sections of my manuscript. I would also like to thank Dr Marty Bullock, always calm and collected, for helping with RNA extraction and analysis. I am grateful for the support of the other members of the Cancer Genetics laboratory, including Dr Dindy Benn, Ann Louise Richardson and Rozelle Harvey for their insights and support over the years. To my fellow PhD students, particularly Dahlia Davidoff who was forever positive and upbeat, and Marthe Chehade, Grace Lim, Ayanthi Wijewardene and Chris Muir.

I would like to thank Professor Anthony Gill and Loretta Sioson in the Department of Anatomical Pathology, Royal North Shore Hospital, for providing tumour samples and histopathology review at all times. I would also like to thank present and past members of the Kolling Institute Tumour Bank, including Ussha Pillai, Sam Yuen, and Katherine Markoulis for providing me with the samples vital for my studies.

I am fortunate to have had the opportunity to collaborate with experts outside of the Cancer Genetics laboratory, including Dr Ryan Davis, Neurogenetics Research Group, University of Sydney, for his insights into mitochondrial disease, and A/Professor Richard Tothill and Dr Aidan Flynn, University of Melbourne, for their guidance with mitochondrial sequencing and RNA sequencing analysis.

To the Cancer Geneticists and Genetic Counsellors, particularly A/Professor Kathy Tucker and the whole team at Prince of Wales Hospital and Royal Prince Alfred Hospital Hereditary Cancer Services, who have been exceptionally supportive and gracious during the final sprint for submission, allowing me to take time during my full time clinical work to complete this thesis.

Finally, I would like to thank my family for their love and support over the course of this candidature. To Christof, for his continual encouragement as our lives have become more and more chaotic with a growing family. To our little boys Alex and Henryk who are my world. To my mum, Julia, for her endless support throughout my life, and for our little family, constantly travelling from Perth when life becomes a challenge to help in any way possible.

Table of Contents

List of Tables

List of Figures

List of Appendices

Abbreviations

µg – Micrograms

µL – Microlitre

µM – Micrometers

4EBP1 - Eukaryotic translation initiation factor 4E binding protein

Ach - Acetylcholine

ACMG - American College of Medical Genetics

ACT - Australian Capital Territory

AGRF - Australian Genome Research Facility

ARS - Antihypertensive response score

ATP Adenosine triphosphate

BAM - Binary alignment map

DBH - Dopamine beta hydroxylase

cDNA - Complimentary DNA

CGDL - Cancer Genetics Diagnostic Laboratory

CHIP - Clonal haematopoiesis of indeterminate potential

COSMIC – Catalogue of Somatic Mutations in Cancer

CT - Computerised tomography

CVD - Cyclophosphamide, vincristine and dacarbazine

DCR - Disease control rate

DNA - Deoxyribonucleic acid

DOTATATE - 1,4,7,10-tetraazacyclododecane-1,4,7,10-tetraacetic acid

EBRT - External beam radiotherapy

ETC – Electron transport chain

FCS - Familial Cancer Service

FDR - False discovery rate

FFPE – Formalin fixed paraffin embedded

FH – Fumerate hydratase

Ga68 - Gallium 68

GIST – Gastrointestinal stromal tumour

HGVS - Human Genome Variation Society

HLRCC - Hereditary leiomyomatosis and renal cell carcinoma

HU - Hounsfield units

I-123 - Iodine-123

IHC – Immunohistochemisty

ICGC – International Cancer Genome Consortium

KITB - Kolling Institute Tumour Bank
L-AADC - L-aromatic acid decarboxylase
L-DOPA - L-3,4-dihydroxyphenylalanine
LC/MS - MS liquid chromatography/tandem mass
LOH - Loss of heterozygosity
MAX - MYC-associated factor X
MD – Mitochondrial disease
MDS - Multidimensional scaling
MEN - Multiple endocrine neoplasia
MIBG - Metaiodobenzylguanine
MLPA - Multiplex ligation probe amplification
mtDNA - Mitochondrial DNA
MPS -Massively parallel sequencing
MRI - Magnetic Resonance Imaging
mTOR - mMmmalian target of rapamycin
NET – Neuroendocrine tumour
NF1- Neurofibromatosis type 1
NGS - Next generation sequencing
NSW - New South Wales
ORR - Overall response rate
OXPHPOS – Oxidative phosphorylation
PC – Phaeochromocytoma
PDGFR - platelet derived growth factor
PGL – Paraganglioma
PI3K-AKT - phosphoinositide 3-kinase-Akt
PNMT - Phenylethanolamine
PRRT - Peptide receptor radionuclide rherapy
PV -Pathogenic variant
RCC - Renal cell carcinoma
RET- Rearranged during transfection
RNA - Ribonucleic acid
RNSH - Royal North Shore Hospital
SBP - Systolic blood pressure
SDHA - Succinate dehydrogenase subunit A
SDHAF2 - Succinate dehydrogenase complex assembly factor 2
SDHB - Succinate dehydrogenase subunit B
SDHC - Succinate dehydrogenase subunit C

SDHD - Succinate dehydrogenase subunit D

SDHx - Succinate dehydrogenase subunits A-D

SNV - single nucleotide variation

TCGA – the Cancer Genome Atlas

TERT – Telomere reverse transcriptase

TH - Tyrosine hydroxylase.

TKI - Tyrosine kinase inhibitors

TMEM127 - Transmembrane protein 127

TMM - Trimmed Mean of M-values

RNSH - Royal North Shore Hospital

S6K1 - Ribosomal S6 kinase

TCGA - The Cancer Genome Atlas

UMAP - Uniform Manifold Approximation and Projection

VAF - Variant allele frequency

VCF - Variant call format

VHL - Von Hippel Lindau

VUS - Variant of uncertain significance

WHO – World Health Organisation

Abstract

Phaeochromoctyoma and paraganglioma (PC/PGL) are rare neuroendocrine tumours of neural crest origin, arising within the adrenal medulla and sympathetic/parasympathetic chain. Morbidity and mortality arises from an excess of catecholamine secretion (adrenaline, noradrenaline and/or dopamine which causes hypertension, palpitations and headaches) or mass affect or tumour invasion. High heritability is a unique feature of PC/PGL with up to 30% of tumours developing in the context of an underling germline pathogenic variant (PV). More recently, sporadic causes have come to the forefront with somatic PVs being identified in up to 40% of patients with PC/PGL. Germline and somatic PVs occur broadly within two clusters: Cluster 1 involving pseudohypoxia and culminating in HIF stabilisation, and Cluster 2 which involves kinase signalling pathways. Genotype-phenotype correlations are well recognised for syndromes associated with Von Hippel Lindau disease (*VHL*), Multiple Endocrine Neoplasia Type 2 syndrome (*RET*) and Familial Paraganglioma Syndrome Types 1 and 4 (*SDHD* and *SDHB*, respectively). However, newly discovered genes implicated in PC/PGL development, with lower penetrance, present diagnostic and management challenges. Genetic testing to elucidate hereditary causes of PC/PGL has advanced from single gene testing to massively-parallel sequencing (also known a next generation sequencing) allowing a large number of genes to be investigated concurrently. Next Generation Sequencing creates large volumes of data which requires expert bioinformatic analysis and variant curation.

The initial work of this thesis comprised validating Next Generation Sequencing as a highly sensitive and timely genetic testing modality to diagnose hereditary causes of PC/PGL. This approach streamlined the time from resection of PC/PGL to a result from molecular analysis when compared to the current standard of care. Additionally, through paired blood-tumour sequencing we gained insights into the germline and somatic mechanisms driving PC/PGL development.

A frequent consequence of genetic testing is identifying variants of uncertain significance. These present a management conundrum as there is insufficient or conflicting evidence to allow definitive classification and ‘benign/likely benign’ or ‘pathogenic/likely pathogenic’, thus being uninformative for clinical decision making. The American College of Medical Genetics recognises *in vivo* or *in vitro* functional studies as ‘strong evidence’ for variant interpretation. Thus, RNA sequencing was explored as a diagnostic adjunct to assist with variant curation of a rare gene known to cause hereditary PC/PGL, *TMEM127*. Patients harbouring a *TMEM127* PV typically present with PC/PGL in midlife, often with multifocal/bilateral disease. RNA sequencing techniques included *TMEM127* expression levels, differential gene expression, and copy number analysis. This approach showed promise as a functional assay to assist with variant curation.

Emerging phenotypes in poorly described cohorts were explored; firstly, within rare, newly discovered genetic drivers of PC/PGL (*MAX* and *EPAS1*) and subsequently in paediatric and adolescent patients diagnosed with PC/PGL. Rare phenotypes pose a challenge to clinicians in terms of establishing tailored gene specific surveillance guidelines, which are drawn from evidence of age of development of PC/PGL, disease behaviour and penetrance. *MAX* PVs, implicated in ~2% of PC/PGL, were found to be associated with a high burden of endocrine and non-endocrine tumours, including multiple parathyroid adenomas and prolactin secreting pituitary adenoma. *EPAS1*, a somatic driver of PC/PGL, has been identified in 6-10% of cases. Post-zygotic mosaicism of *EPAS1* causes Pacak-Zhuang 'syndrome' characterised by the co-occurrence of PC/PGL, polycythemia from a young age and/or somatostatinoma. A literature review was performed to better define the phenotype of this syndrome which highlighted an early age at diagnosis of PC/PGL with multifocal disease being a frequent occurance. Further, although females are disproportionately affected, men were diagnosed at a significantly younger age. Somatic *EPAS1* was then identified in a cohort of 'apparently sporadic' cases through genetic testing of fresh frozen PC/PGL tissue. Although further investigation for Pacak-Zhuang syndrome in these individuals was not possible (due to pandemic restrictions), this finding still provided a molecular diagnosis for these patients. Finally, the exceptionally rare nature of paediatric and adolescent PC/PGL has made it challenging to establish genotype-phenotype correlations and disease frequency in young patients, however the prevalence of a germline PVs within this cohort approaches 80%. A high prevalence of germline PVs was detected, particularly in *VHL* and *SDHB*. Furthermore, these patients were found to have a high likelihood of developing aggressive features with clinical implications.

The electron transport chain is comprised of five complexes embedded in the inner-membrane of the mitochondria. Mitochondrial complex II, comprising SDH subunits A-D in which PVs are associated with PC/PGL, are nuclear encoded. The remaining complexes (mitochondrial complex I, III, IV and V) are encoded by the mitochondrial genome, a compact circular genome of which there are many copies within a single cell. A potential relationship between PC/PGL tumours containing bi-allelic *SDHB* PVs and somatic mitochondrial high and moderate impact PVs was found such that somatic mtDNA PVs occur more often in complex I and high/moderate impact variants were more frequent in recurrent/metastatic disease. This provides a potential insight into the relationship between somatic mitochondrial PVs and disease behaviour.

Inoperable and metastatic PC/PGL are incurable and pose a treatment challenge for clinicians. There are several therapies available, however the optimal choice remains unclear. Therefore, a retrospective audit of patients receiving radionuclide therapy was undertaken which found I-131 MIBG and Lu-177 DOTATATE both resulted in symptom control, a fall in systolic blood pressure and reduction in blood pressure medication requirements, and reduction in serum catecholamines levels. Tumour response,

using RECIST 1.1, was modest with an overall response rate of 8%, however a disease control rate of 100% with a significant proportion of patients demonstrating stable disease.

Overall, this thesis has described contemporary methods for investigating hereditary causes of PC/PGL and variant interrogation, emerging phenotypes of newly discovered genetic drivers of phaeochromocytoma and paraganglioma, uncovered somatic mitochondrial variants as influencing PC/PGL disease behaviour, and recent advances in therapeutic options for inoperable and metastatic disease.

Publications arising from this thesis

Seabrook A[+], Harris J[+], Velosa S, Kim E, McInerney-Leo A, Dwight T, Hockings J, Hockings N, Kirk J, Leo P, Love A, Luxford C, Marshall M, Mete O, Pennisi D, Brown M, Gill A, Hockings G*, Clifton-Bligh R*, Duncan E*. Multiple Endocrine Tumors Associated with Germline *MAX* Mutations: Multiple Endocrine Neoplasia Type 5?, *The Journal of Clinical Endocrinology & Metabolism*, Volume 106, Issue 4, April 2021, Pages e1163–e1182

[+] A Seabrook and J Harris contributed equally to the manuscript

*G Hockings, R Clifton-Bligh and E. Duncan contributed equally to the manuscript

Seabrook A, Vasudevan A, Neville K, Gerstl B, Benn D, Smith J, Kirk J, Gill A, Clifton-Bligh R, Tucker K. Genotype–phenotype correlations in paediatric and adolescent phaeochromocytoma and paraganglioma: a cross-sectional study. *Archives of Disease in Childhood* 2024;**109:**201-208.

Abstracts presented during candidature

Seabrook A, Hsiao E, Chan D, Robinson B, Bernard E, Clifton-Bligh R. Efficacy of Radionuclide Therapy (I-131 MIBG OR Lu-177-DOTATATE) in the Treatment of Inoperable or Metastatic Phaeochromocytoma and Paraganglioma. Oral Presentation (Abstract ID 168) , Endocrine Society of Australia Annual Scientific Meeting, Brisbane, Australia, November 2023

Other publications and abstracts arising during the candidature of this thesis

Seabrook A, Wijewardene A, De Sousa S, Wong T, Sheriff N, Gill A, Iyer R, Field M, Luxford C, Clifton-Bligh R, McCormack A, Tucker K. MEN4, the MEN1 Mimicker: A Case Series of three Phenotypically Heterogenous Patients With Unique *CDKN1B* Mutations, *The Journal of Clinical Endocrinology & Metabolism*, Volume 107, Issue 8, August 2022, Pages 2339–2349.

Authorship attribution statement: chapters published as papers

Chapter 5 of this thesis published as **Seabrook A**[+], Harris J[+], Velosa S, Kim E, McInerney-Leo A, Dwight T, Hockings J, Hockings N, Kirk J, Leo P, Love A, Luxford C, Marshall M, Mete O, Pennisi D, Brown M, Gill A, Hockings G*, Clifton-Bligh R*, Duncan E*. Multiple Endocrine Tumors Associated with Germline *MAX* Mutations: Multiple Endocrine Neoplasia Type 5?, *The Journal of Clinical Endocrinology & Metabolism*, Volume 106, Issue 4, April 2021, Pages e1163–e1182.

- I designed the study, analysed the data and wrote the draft manuscript with the co-first author Jessica Harris. Only work undertaken independently by myself has been included in this thesis. My supervisor, Professor Roderick Clifton-Bligh, is the corresponding author.

Chapter 7 of this thesis published as **Seabrook A**, Vasudevan A, Neville K, Gerstl B, Benn D, Smith J, Kirk J, Gill A, Clifton-Bligh R, Tucker K. Genotype–phenotype correlations in paediatric and adolescent phaeochromocytoma and paraganglioma: a cross-sectional study. *Archives of Disease in Childhood* 2024;**109:**201-208.

- I designed the study, extracted and analysed the data and wrote the draft manuscript. My supervisor, Professor Roderick Clifton-Bligh, is the corresponding author.

As supervisor of the candidature upon which this thesis is based, I can confirm that the authorship attribution statements are correct.

Professor Roderick Clifton-Bligh
09.04.2024

CHAPTER 1

Review of the literature

CHAPTER 1. Review of the Literature

This thesis will describe contemporary methods for investigation of hereditary causes of phaeochromocytoma and paraganglioma, emerging phenotypes of genetic drivers of phaeochromocytoma and paraganglioma, challenges in predicting disease behaviour, and discuss recent advances in therapeutic options for inoperable and metastatic disease. The detailed literature review below outlines the context in which this thesis arises, including embryological origins, clinical characteristics, diagnosis, and treatment of phaeochromocytoma and paraganglioma; genetic mechanisms underlying somatic and germline tumour development; and finally, introduces the landscape of molecular analyses for cancer susceptibility genes and their application to hereditary phaeochromocytoma/paraganglioma syndromes.

1.1 Introduction to phaeochromocytoma (PC) and paraganglioma (PGL)

1.1.1. Discovery of PC/PGL

The term 'chromaffin' originated from the brown discoloration occurring when tissues from the adrenal medulla were fixed in chromate salts in 1857 by Bertholdus Werner [1]. Discovery of similar groups of cells within the paraxial sympathetic nerves and carotid body was subsequently made by Alfred Kohn who proposed that these cell groupings arose from the same neural progenitors [2]. Consequently it was recognised this distinctive colour change arose from oxidation of catecholamines from the chromaffin reaction. Embryological studies using lineage tracing and functional markers have since conclusively established similarities (and differences) of 'paraganglia' at difference sites [2].

Neuroendocrine tumours have two distinct lineages; those arising from epithelia and those from paraneurons [2]. Paragangliomas are non-epithelial neuro-endocrine neoplasms and express the transcription factor GATA3, essential for differentiation of sympathoadrenal tissue [3]. Although this factor is not specific for paraganglioma (as GATA3 has also been shown to be expressed in thyroid and pituitary neuroendocrine cells), further biomarkers, transcription factors, hormones and enzymes have been utilised to aid in the differentiation of this tumour [2, 4]. Unique to PC/PGL are the catecholamine-synthesising enzymes tyrosine hydroxylase (TH), dopamine beta-hydroxylase (DBH), and phenylethanolamine N-methyltransferase (PNMT) [5, 6].

1.1.2. Epidemiology of PC/PGL

The annual incidence of PC/PGL is estimated to be 0.8 per 100 000 person-years [7]. This may be an underestimation based on series identifying up to 50% of PC/PGL being incidentally diagnosed on autopsy [7, 8]. PC/PGL most commonly develop between the fourth to sixth decade of life with equal gender distribution [9]. PC/PGL are estimated to occur in less than 0.2% of hypertensive patients [10].

There is an exceptionally high hereditary predisposition with 30-40% of PC/PGL occurring in patients with an underlying germline pathogenic variant [11].

1.1.3. Definition, embryological origins and anatomical location of PC/PGL

The 5th series of the World Health Organisation Classification of Endocrine and Neuroendocrine tumours published in 2022 has upgraded the nomenclature to classify all phaeochromocytoma and paraganglioma under the term 'paraganglioma' [2]. Sympathetic paraganglioma arise from chromaffin cells within the adrenal medulla (phaeochromocytoma, PC) or within the prevertebral and paravertebral sympathetic ganglia of the thorax, abdomen and pelvis (sympathetic paraganglioma, PGL). Approximately 80% of sympathetic paraganglioma develop within the adrenal gland and frequently produce an excess of catecholamines [12, 13]. Conversely parasympathetic PGL mostly occur in the neck and base of skull and are typically non-hormone secreting [14, 15].

Paraganglioma are of neural crest origin with the peripheral autonomic nervous system arising from the neuroectoderm. In the human embryo neural crest cells develop in a cranio-caudal sequence and migrate ventrolaterally through the sclerotome (blocks of mesodermal cells which differentiate into vertebral cartilage) to form the adrenal medulla, sympathetic trunk and pre-aortic nerve plexuses [16, 17]. The adrenal glands, located above the kidneys, are comprised of the outer cortex (important for the production of steroid hormones including glucocorticoids, mineralocorticoids and androgens) and the aforementioned inner medulla (important for the production of catecholamines)[16, 18]. The sympathetic or parasympathetic ganglia are a bilateral chain of ganglia and nerve fibres and are classified into four groups [19].

i. Branchiomeric group: In the region of the embryological branchiomeres (jugulo-tympanic ganglion, carotid body, laryngeal ganglion, subclavian ganglion, aorticopulmonary ganglion). There is a close relationship with blood vessels.
ii. Intravagal group: In the region of the parasympathetic nerves (jugular ganglion, nodose ganglion). They have their origin within the perineurium.
iii. Aorto-sympathetic group: In the region of the sympathetic nerves of the aorta.
iv. Visceral autonomic group: In the nervous system of the heart, digestive tract, liver hilus, and bladder.

Key locations of PC/PGL are summarised in Figure 1.1. Sympathetic PGL develop most frequently in the abdomen (75%), particularly at the aortic bifurcation (junction of the vena cava and renal veins) or at the organ of Zuckerkandl (the origin of the inferior mesenteric artery), followed by the thorax (10%) [20]. Sympathetic PGL have also been described in soft tissue organs particularly the prostate and bladder [21, 22]. Parasympathetic PGL (often referred to as head and neck PGL, HNPGL) develop

along the branches of the glossopharyngeal nerves arising most frequently from the carotid body, less frequently from the jugulo-tympanic and vagal paraganglia, and rarely from the laryngeal paraganglia[15].

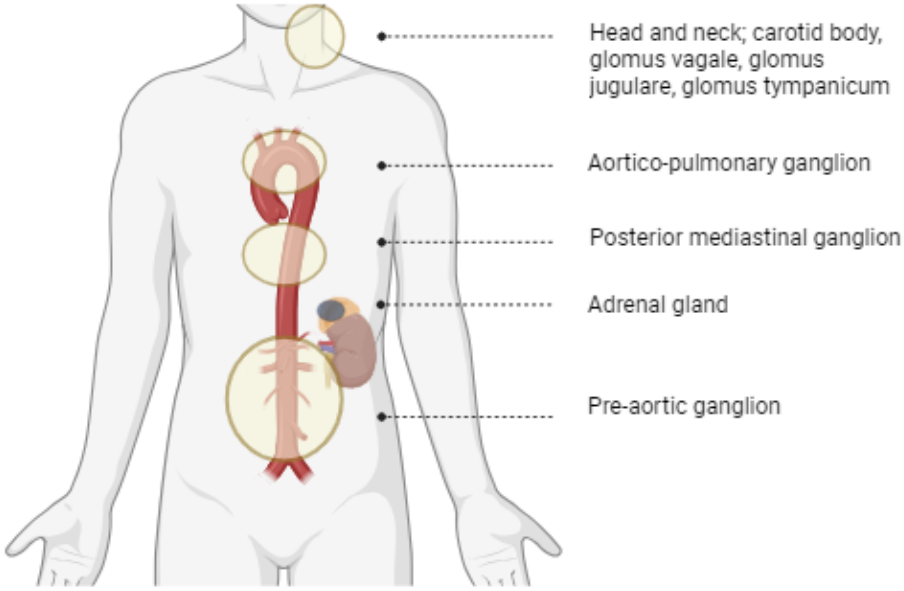

Figure 1.1 Anatomical locations of phaeochromocytoma and paraganglioma. Phaeochromocytoma arise within the adrenal gland (represented in blue) above the kidney and paraganglioma occur within sympathetic and parasympathetic ganglions (common sites shown in yellow). Image adapted from Crona *et. al.*[23]

Catecholamines, namely dopamine, noradrenaline, and adrenaline, form an essential component of the autonomic nervous system and function as both neurotransmitters and hormones [24, 25]. Their primary role is within the 'fight or flight' response. Following an external stimulus which triggers a stress response sympathetic splanchnic nerves release acetylcholine (Ach). Ach binds to nicotinic receptors on chromaffin cells causing exocytosis of catecholamine-filled vesicles into the bloodstream. Catecholamines bind to alpha- and beta-adrenergic receptors resulting in sympathetic nervous system stimulation which collectively increases blood pressure, enhances contractility of skeletal muscle, bronchodilation, and increase blood glucose [25, 26].

Catecholamine synthesis commences with conversion of tyrosine to 3,4-dihydroxyphenylalanine (L-DOPA) catalyzed by tyrosine hydroxylase, a rate limiting enzyme (Figure 1.2) [27, 28]. Aromatic-L-amino acid decarboxylase then converts L-DOPA to dopamine which in turn is converted to

noradrenaline by dopamine beta-hydroxylase within vesicular secretory granules. Noradrenaline is converted to adrenaline by phenylethanolalamine N-methyltransferase (PNMT) within the cytoplasm. Due to differences in enzyme location, biosynthesis requires production of dopamine into secretory granules followed by leakage of noradrenaline into the chromaffin cell cytoplasm where it is converted into adrenaline and then stored as epinephrine secretory granules[12, 25].

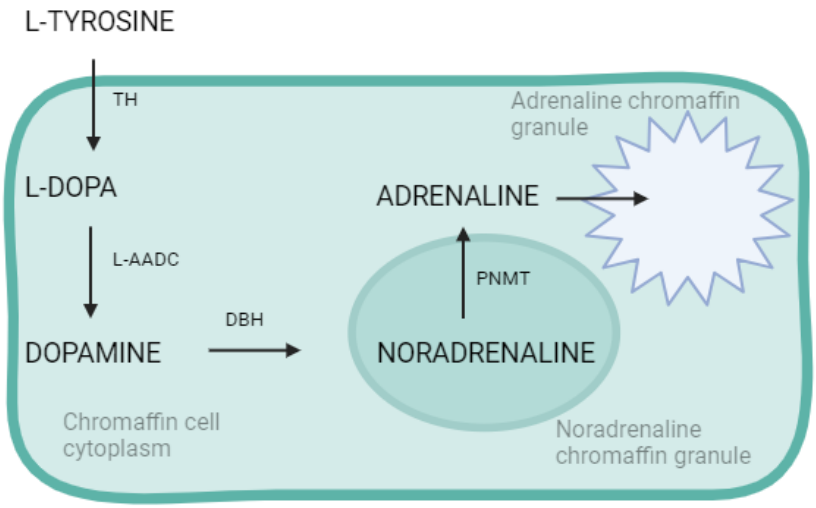

Figure 1.2. Catecholamine production and secretion

Schematic diagram showing the biosynthesis of catecholamines within the chromaffin cells of the adrenal medulla. Abbreviations: DBH, dopamine beta hydroxylase; L-AADC, L-aromatic acid decarboxylase; L-DOPA, L-3,4-dihydroxyphenylalanine; PNMT, phenylethanolamine-N-methyltransferase; TH, tyrosine hydroxylase. Image adapted from Eisenhofer *et. al.*[12]

All phaeochromocytoma and paraganglioma have malignant potential with the World Health Organisation (WHO) recently replacing the term 'malignant phaeochromocytoma or paraganglioma' with 'metastatic phaeochromocytoma or paraganglioma' [2]. The incidence of metastasis increases with tumours > 5cm, and are more likely from extra-adrenal PGL (20%) than from PC (10%); metastasis is uncommon from HNPGL [29, 30]. Familial syndromes are also associated with risk of metastatic disease, particularly in patients harbouring germline pathogenic variants in *succinate dehydrogenase subunit B* (*SDHB*) [29, 30]. Metastatic disease is strictly defined as the presence of chromaffin cells in embryologically-unrelated tissue (e.g. lymph nodes, lung, liver and bone) [2]. Histopathological features (Ki-67 index, pS100 staining, expression of heat-shock protein 90) and scoring systems (such as phaeochromocytoma of adrenal gland score) provide limited prognostic information to risk of recurrence or metastases [31, 32].

1.2 Clinical presentation, diagnosis, and management of PC/PGL

Diagnosis of PC/PGL should be suspected in the following scenarios; suggestive signs or symptoms, hypertension, an adrenal incidentaloma or on imaging as part of routine surveillance in those with a known hereditary PC/PGL syndrome.

1.2.1 Clinical features of PC/PGL

Symptoms are reported in approximately 50% of patients with phaeochromocytoma and may be due to hypersecretion of catecholamines or mass effects from the tumour [10]. The classic triad of symptoms of PC/PGL include episodic headache, sweating, and tachycardia. Hypertension is the most commonly seen clinical feature (either sustained or paroxysmal, 85-95%) [33, 34], followed by headache (in up to 90%)[33], or generalised sweating (60-70%) [35]. Other reported symptoms include palpitations, pallor, or anxiety. Attacks may occur frequently (daily, weekly), or more sporadically (once every few months), with most episodes lasting under an hour. Rarely seen features include hypotension, cardiomyopathy, acute hypertension in certain scenarios (surgery, stress, medications), and diabetes [36-38]. Interestingly, approximately 10% of PC/PGL are diagnosed following the discovery of an adrenal incidentaloma [39].

1.2.2 Diagnosis of PC/PGL

Biochemical investigation

Measurement in plasma or urine of catecholamine *O*-methylated metabolites (normetanephrine, metanephrine and 3-methoxytyramine) is superior for diagnosis of PC/PGL than measurement of adrenaline, noradrenaline or dopamine, due to sustained elevation of metabolites in between "spells" of elevated catecholamine release [12]. Measurement of free metabolites by liquid chromatography/tandem mass spectrometry (LC/MS-MS) provides advantages of fewer false-positive results compared with deconjugated metabolites. Recent studies confirm diagnostic accuracy is highest measuring free metanephrines in plasma rather than urine, providing the blood sample is collected fasting and after remaining supine for 30 mins; collecting blood from seated subjects can result in a 6-fold increase in false-positive results [27, 40]. Other pre-analytic steps to optimise diagnostic accuracy include withholding (if safe) interfering medications (such as tricyclic antidepressants, levodopa, amphetamines, prochlorperazine, and decongestants) for a minimum of two weeks prior to testing, and avoiding intense exercise, catecholamine-rich food (such as nuts, tomatoes, fruit) and caffeine immediately prior to blood or urine collection.

Biopsy of PC/PGL generally considered contra-indicated due to the risk of catecholamine-related complications including worsening of catecholamine-related symptoms, myocardial infarction, hypertensive crisis, and Takotsubo cardiomyopathy [41].

Radiological and nuclear medicine investigation

Computerised tomography (CT) or magnetic resonance imaging (MRI) can both be considered as frontline clinical assessment tools if a PC/PGL is suspected biochemically, as both methods are considered to be highly sensitive (98-100%) [42]. CT involves exposure of the patient to a low dose of radiation and iodine contrast, and may be contra-indicated in pregnancy or if there is a history of renal impairment. MRI may be more appropriate for patients with renal impairment, an allergy to CT contrast, or for patients in whom radiation exposure should be limited (pregnancy, lifelong surveillance, children) [43].

On CT, PC are typically present as heterogenous and occasionally display cystic areas, calcifications or haemorrhage [44]. Pre-contrast density of PCs is almost always > 10 Hounsfield Units (HU) and show delayed contrast washout of less than 50% at 10 minutes following administration. On T2 weighted MRI imaging , PC often demonstrate high signal intensity (a bright lesion compared to that of the physiologic levels observed in the liver) with increased tumour vascularity or cystic/haemorrhagic changes [45].

Functional imaging may be appropriate in selected cases, particularly if there is a high degree of suspicion for metastatic disease, such as a PC greater than 5cm or an underlying hereditary syndrome [46]. Historically, functional imaging was performed using Iodine-123 metaoidobenzylguanidine (I-123 MIBG), whereby MIBG mimics noradrenaline and is taken up by adrenergic tissue. Gallium 68 (Ga68) DOTA-0-Phe1-Tyr-3 octreotate positron emission tomography (Ga-68 DOTATATE PET) has more recently emerged as a sensitive imaging modality, whereby the chelated radio-analogues bind to somatostatin receptors present on PC/PGL cells [45].

Histology

Macroscopically PC/PGL have a fleshy red-brown to gray appearance with a thin capsule and consisting of epitheloid cells grouped in cell nests or trabecular arrangements [47, 48]. Spindle shaped sustentacular cells surround the chief cell nests. The nuclei of the chief cells are located centrally and comprise of finely clumped chromatin and a moderate amount of eosinophilic, granular cytoplasm. Chief cells contain dense core neurosecretory granules which store catecholamines. Histological features may show some similarity to other tumours (such as meningioma, rhabdomyoma, sarcoma and melanoma). Thus, immunohistochemical staining is important to confirm neuroendocrine origin of the

chief cells which demonstrate strong positivity for neuron-specific enolase, synaptophysin and chromogranin [47, 48].

1.2.3 Management of PC/PGL

Resection of PC/PGL is recommended for unifocal tumours, and best performed by surgeons and anaesthetists with surgical experience with a high volume of these patients, and with practical expertise in managing surgical risks associated with intra-operative haemodynamic instability.

Pre-operative preparation

Medical therapy with alpha-blockers is usually considered pre-operatively to prevent hypertensive crisis [42]. Phenoxybenzamine is a nonspecific and long-acting alpha-adrenergic blocker, usually commenced at 10 mg twice daily increasing up to 1 mg/kg in divided doses as required to control blood pressure and achieve a mild postural drop before surgery. Common side effects include nasal congestion, fatigue and orthostasis. The selective alpha-1-adrenergic blocker prazosin or calcium channel blockers are preferred by some centres. Beta-blockers are only required to control tachycardia and must be commenced after adequate alpha-blockade, as blockade of the vasodilatory peripheral beta-adrenergic receptors with unopposed alpha-adrenergic stimulation can lead to sudden and severe hypertension [49].

A high sodium diet is recommended following alpha-adrenergic blockade to counteract the effects arising from the catecholamine-induced volume contraction and orthostasis from alpha-adrenergic blockade. Medications to be avoided include the dopamine D2 receptor antagonist metoclopramide, peptide and corticosteroid hormones (including glucagon and glucocorticoids), which may precipitate a catecholamine crisis [20].

Primary unifocal PC/PGL

A minimally invasive approach with adrenalectomy for small, solitary intra-adrenal PC is the current procedure of choice. The retroperitoneal approach offers several advantages to anterior laparoscopic procedures [50]. Most abdominal PGLs can be approached laparoscopically [51]. Complications include intraoperative tumour capsule rupture into the retroperioneum.[52] PGL identified in less common areas, including the neck, chest and bladder, require specialised techniques; i.e. carotid sheath tumours require proximal and distal vascular management, and chest PGL usually require median sternotomy [53, 54].

Multifocal, metastatic, or inoperable PC/PGL

At present there are no curative treatments for metastatic PC/PGL. Some studies suggest survival is improved following resection of the primary tumour, even in the presence of metastatic disease, and may improve symptoms related to catecholamine excess or mass effect [55, 56]. Differing to unifocal localised disease, open procedures are often required for multifocal and metastatic lesions [57].

Traditionally PC/PGL were thought to be resistant to external beam radiotherapy (EBRT). It has since been shown that doses > 40Gy can be effective in control of tumour growth in 81%, and report symptomatic improvement in 94% of patients [58]. EBRT has been used to target numerous sites including base of skull and neck, thorax, and painful bony metastases. A key role of this therapy has been in the treatment of skull base and neck PGL which historically have proven to be anatomically difficult to operate on. 'Gamma knife' or 'cyber knife' may be used to provide precise targeting of high dose radiation for glomus jugulare tumours [59].

Systemic therapy can be divided into cytotoxic chemotherapies, molecular targeted therapies, and radionuclide therapies. Cytotoxic chemotherapy has predominantly been studied in the clinical scenario of rapidly progressive metastatic paraganglioma. Combinations of cyclophosphamide, vincristine and dacarbazine (CVD) has been most extensively investigated with objective response rate of 25-50% [30]. Temozolamide is a single agent that has also shown some efficacy in patients with *SDHB* pathogenic variants [60].

Tyrosine kinase inhibitors (TKIs) are pharmacological agents that block the signal transduction pathways of protein kinases (enzymes) involved in malignancy, including cell growth and angiogenesis. Sunitinib is a multi-kinase inhibitor which binds to multiple receptors including vascular endothelial growth factor (VEGF), platelet derived growth factor (PDGFR), and re-arranged during transfection (RET). Sunitinib was evaluated in a randomised, placebo controlled phase II trial in patients with metastatic PC/PGL (First International Randomised Study in Malignant Progressive Phaeochromocytoma and Paraganglioma: FIRST-MAPPP) and 12-month progression-free survival was 14 of 39 patients (36%) in the sunitinib group *vs*. 7 of 39 patients in the placebo group (19%) [61]. Other TKIs presently under investigation include cabozantinib (which targets VEGFR2 and cMET), pazopanib (which target VEGF), and lenvatinib.

Radionuclide therapy regimes currently consist of Iodine-131 (I-131) MIBG (radiolabelled iodine (I-131) attached to MIBG) and Peptide Receptor Radionuclide Therapy (PRRT); both deliver beta-emitting isotopes to PC/PGL. I-131 MIBG is structurally similar to noradrenaline with uptake into

chromaffin cells. Tumour regression or stabilisation, and improvement of symptoms has been demonstrated in multiple small series [62-65].

1.3 Genetics and molecular characterisation of PC/PGL

Oncogenesis is associated with DNA mutations in specific genes, occurring either somatically (in sporadic cancers), or in the germline (in hereditary cancer syndromes). Disease-associated variants, historically referred to as 'mutations', are now termed 'pathogenic' or 'likely pathogenic' by the American College of Medical Genetics [66]. Reference to 'pathogenic variants' (PV) in the remainder of this literature review includes both the pathogenic and likely pathogenic variants.

PVs implicated in the development of PC/PGL can be categorised as causing exclusively hereditary or sporadic disease, or be implicated in both. In 2017, utilising data from The Cancer Genome Atlas (TCGA), a comprehensive genomic characterisation was performed on 173 patients which provided estimates of the prevalence of PV in PC/PG (Figure 1.3) [67]. The highest rate of germline PVs was reported to occur within *SDHB*, *SDHD*, *VHL,* and *RET*, identified in 27% of cases; and the highest rate of somatic PV located within *NF1, HRAS, EPAS1,* and *RET*, identified in 39% of cases. These estimates are broadly comparable in other studies and are summarised in Table 1.1. There was a low somatic mutation rate (mean 0.67 mutations per megabase) compared to other cancer types [68]. Copy number alterations were seen in germline *SDHB* (chromosomal location 1p), *VHL* (3p), *SDHD* (11q), *TP53* (17p), and *NF1* (17q). A key finding was of mutual exclusivity of most PVs [67]. Further studies identified the presence of somatic driver PV in 32% and 37% of phaeochromocytoma and paraganglioma respectively, with *HRAS, NF1, RET,* and *VHL* being the most frequently affected genes.[69, 70] Of note, through these recent studies mosaic *SDHB* and *VHL* PV were also identified.[67, 70, 71]

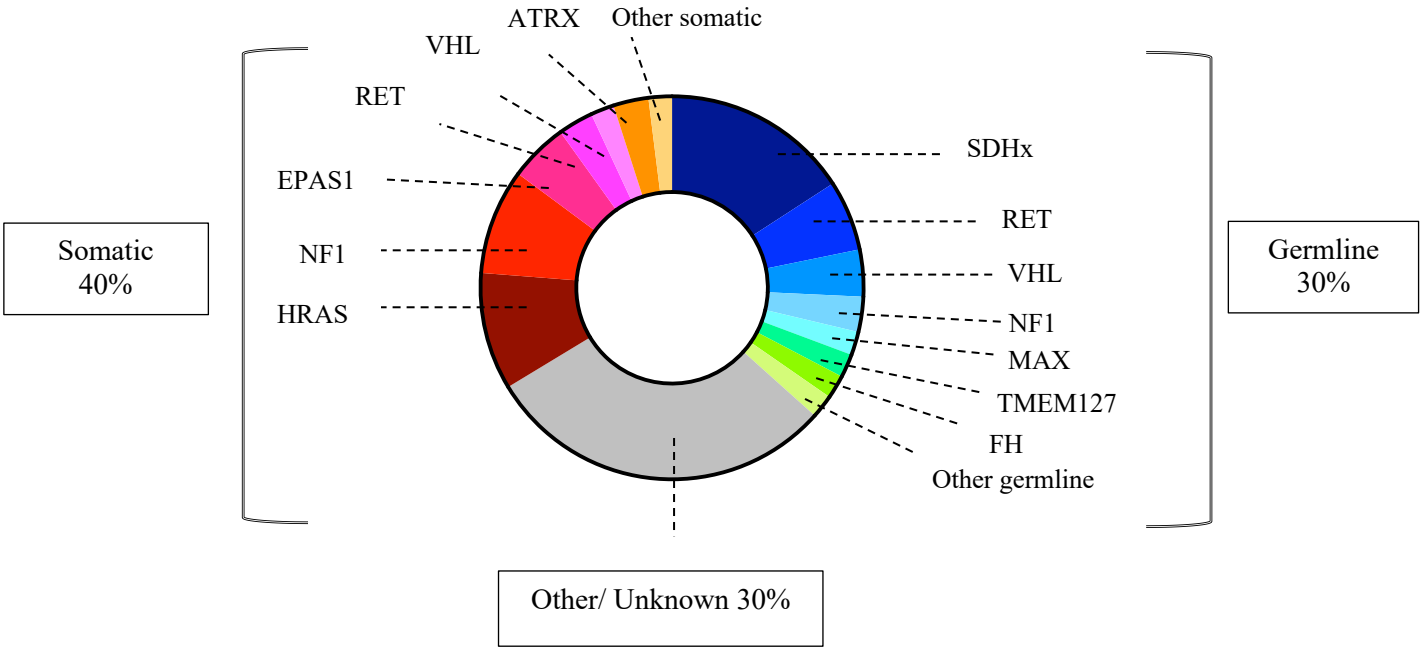

Figure 1.3 Estimation of germline and somatic pathogenic variants implicated in the development of PC/PGL. Pie-chart sections on the left depicts the proportion of PC/PGL harbouring somatic variants and sections on the right depicts the proportion of germline pathogenic variants. The underlying cause remains undefined in 30% of cases of PC/PGL. Image adapted from Fishbein *et al.[67]*

Table 1.1 Summary of most frequently occurring pathogenic variants implicated in the development of PC/PGL

Gene	Fishbein *et al.[67]*	Toledo *et. al[72].*
HRAS	10% S	5-7% S
SDHB	9 % G	8-10% G
ATRX	2% S	10% S
VHL	4 % G | 2 % S	7-10% G
RET	6 % G | 3% S	5-7% G|S
EPAS1	5% S	5% S (mosaic)
NF1	3 % | 9% S	3% G | 20-25% S
SDHD	2% G	5-7% G
MAX	1% G	1-2% G|S
TMEM127	0.6% G	1-2% G

Abbreviations: S, somatic; G, germline

A seminal paper published in 2005 by Dahia *et al*., followed by a further publication by the same author in 2014, identified clustering of genes involved in PC/PGL through differential gene expression [73, 74]. Unsupervised hierarchical cluster analyses showed two clusters – now referred to as Cluster 1 and Cluster 2 PC/PGLs. Cluster 1 is enriched for genes associated with hypoxia, and Cluster 2 includes genes which activate kinase signalling and protein translation. Subsequently in 2017 Fishbein *et al.,* identified a third cluster of PC/PGL including genes involved in the Wnt/beta-katenin pathway [67]. All genes identified from such analyses were tumour suppressor genes, with the exception of *EPAS1, HRAS, RET*, and *TMEM127*, which are categorised as oncogenes. Single nuclei sequencing has recently refined these clusters into seven distinct groups each associated with a specific genetic signature: C1A1 – *SDHx*, C1A2 – *SDHx*-HN, C1B1 – *VHL*, C1B2 – *EPAS1*, C2A – kinase, C2B1 – *MAX*, C2B2 – *MAML3*, and C2C – cortical admixture [75].

1.3.1 Cluster classification

Cluster 1: pseudohypoxia-driven PC/PGL

Cluster 1 PC/PGL (Cluster 1A and Cluster 1B) are characterised by activation of hypoxia-inducible factors (HIFs) [74]. In normal conditions this transcription factor is induced in response to low cellular oxygen levels. Pseudohypoxia is the phenomenon whereby the HIF pathway is constitutively activated despite normoxia with subsequent upregulation of HIF-target genes [23]. Cluster 1A PVs impair mitochondrial oxidative phosphorylation through severe disruption of the Krebs cycle leading to accumulation of oncometabolites including succinate and fumarate [76]. Most Cluster 1A PVs are germline, but 4-12% are also somatic [74]. Key Cluster 1A genes include those encoding components of the succinate dehydrogenase (SDH) complex (*SDHA, SDHB, SDHC, SDHD, SDHAF2*; collectively referred to as SDHx), *FH, MDH2, IDH, GOT2, SLC25A11,* and *DLST.* Downstream implications of aberrations within these genes which include promotion of DNA hypermethylation, inactivation of PHD1/2 and direct HIF-alpha stabilisation. Cluster 1B PVs are directly involved in hypoxia signalling and include *PHD1/2, VHL,* and *EPAS1*, of which the former play a role in hydroxylation of the HIF-alpha subunit for proteasomal degradation, and the latter is the oncogene that encodes HIF2-alpha. Notably, while *VHL* and *PHD1/2* PVs can be germline, *EPAS1* PVs are typically somatic or mosaic [77].

Cluster 2: kinase-signalling driven PC/PGL

Cluster 2 PC/PGLs are characterised by increased pro-growth signalling involving receptor tyrosine kinases and activation of RAS, PI3K-AKT and mTOR [74]. mTOR activation triggers cell growth and proliferation, gene transcription and tumour metabolism. Key Cluster 2 genes include the proto-oncogene *RET* and tumour suppressor genes *NF1, MAX,* and *TMEM127* [67, 74]. Elucidation of the roles of *BRAF, HRAS, FGFR1, MERTK, MET,* and *MYCN* is an emerging field of investigation [23].

Cluster 3: Wnt-signalling driven PC/PGL

Cluster 3 PC/PGL arising due to PV within the Wnt/beta-katenin pathway were first described by Fishbein *et al.*, in 2017 [67]. The Wnt pathway is important for the regulation of cell proliferation, adhesion, and motility. Somatic PVs include the cold shock domain-containing E1 (*CSDE1*) and mastermind-like transcriptional coactivator 3 (*MAML3*) fusion genes.

Disease modifiers: *ATRX, TERT, SETD2*

Studies show that aberrations in genes involved in telomere maintenance have an impact on disease behaviour. *ATRX* encodes the transcriptional regulator ATRX [78]. The role of this chromatic remodelling protein is in histone deposition in telomeres and chromosome segregation in the cell cycle. *ATRX* PV were first identified in *SDHB*-mutated PC/PGL, whereby alternative telomere lengthening was demonstrated by fluorescence *in situ* hybridisation (FISH), and to be associated with aggressive disease [79, 80]. *TERT* (also involved in telomere maintenance) and *SETD2* (involved in chromatin maintenance) also appear to modify disease behaviour [11, 81].

1.3.2 Germline genes implicated in hereditary PC/PGL

Germline PVs in *SDHx* are the most frequent genetic cause of PC/PGL occurring in approximately 25% of cases, followed by *VHL*, *RET,* and *NF1* [82]. Distinguishing clinical features of key hereditary PC/PGL syndromes are summarised in Table 1.2.

Table 1.2 Summary of well recognised hereditary PC/PGL syndromes

	Gene	Distinguishing Clinical Features					
		Most frequent tumor type	**Frequency multifocal disease**	**Biochemical phenotype**	**Metastatic risk**	**MOI**	**Penetrance ****
C1	*SDHA*	PGL, PC	Single	Mixed	Low	AD	10%
	SDHAF2	PGL (skull base & neck)	~90% multiple	Unclear	Low	Paternal	Unknown
	SDHB	PGL	~20% multiple	Noradrenaline, non-secreting	24-58%	AD	21.8-26.4%
	SDHC	PGL	~20% multiple	Noradrenaline	Low	AD	25%
	SDHD	PGL (skull base & neck most common)	~75% multiple	Noradrenaline, often non-secreting	<5%	Paternal	43.2%
C2	*MAX*	PC	~60% bilateral	Mixed	25%	Possibly paternal	Unknown
	TMEM127	PC, rarely PGL	~25% bilateral	Mixed	Low	AD	Unknown
	VHL	PC, occ PGL	~ 50%	Noradrenaline	Low	AD	30%

Abbreviations: C1, cluster 1; C2, cluster 2; PC, phaeochromocytoma, PGL, paraganglioma, MOI, mode of inheritance; * Multifocal defined as multiple or bilateral PC/PGL ; ** probands
Table adapted from GeneReviews[83]

1.3.3.1 Von Hippel-Lindau disease

The von Hippel-Lindau (*VHL)* gene (OMIM: 193300, cytogenic location 3p25) was mapped in 1993 [84]. VHL protein is an E3 ligase which ubiquinates HIF1-α, targeting this molecule for degradation by the proteosome. Defective VHL expression or function causes inappropriate accumulation of HIF1-α resulting in inappropriate activation of target genes involved in cell growth and metabolism [85].

Von Hippel-Lindau syndrome (VHL) includes risk of PC/PGLs, retinal angiomas, cerebellar and/or spinal haemangioblastomas, renal cell cancers, endolymphatic sac tumours, epididymal ligament cysts and pancreatic neuroendocrine tumours [86, 87]. VHL Type 1 disease is associated with a low risk of developing PC (type 1A) or PC and renal cell cancer (type 1B, results from deletions which includes *BRK1* gene) with a high risk of other syndromic neoplasms [88]. Patients with VHL Type 2 disease are at high risk of PC and are subdivided based on the low incidence of RCC (type 2A), high incidence of RCC (type 2B), or PC only (type 2C). VHL displays an autosomal dominant pattern of inheritance.

Compared with sporadic disease, PCs in VHL are more likely to be diagnosed at a younger age and to be bilateral or multifocal. Two large studies from the National Institute of Health and Mayo Clinic defined the phenotype of PC in VHL syndrome [89]: PCs develop in 18% of patients (PGLs less so) with VHL at a median age 30 y. Catecholamine production was almost exclusively noradrenergic [24].

1.3.3.2 Familial paraganglioma syndromes

SDHA, SDHB, SDHC, *SDHD* (collectively referred to as *SDHx*) encode the four sub-units of complex II of the mitochondrial respiratory chain [90-95]. Complex II plays an essential role in electron transfer and ATP generation through the process of oxidative phosphorylation. *SDHAF2* encodes a protein required for flavination of the SDHA subunit [96]. A PV within any of these genes increases the risk of PC/PGL and potentially other tumours.

Paraganglioma syndrome 1 (PGL1)

PGL1 arises due to a PV in the *SDHD* gene (OMIM: 602960, cytogenic location 11q23). *SDHD* is maternally imprinted meaning only offspring who paternally inherit the variant are at risk of developing disease. Head and neck PGL (HNPGL) are common in PGL1 and typically parasympathetic and multifocal, however metastatic disease is uncommon. In a cohort of 289 affected patients 93% had PGL and 24% PC. PGLs were typically parasympathetic (84%) and multifocal (56%) with metastasis rare (4%) [97, 98]. When paternally inherited the lifetime risk of PC/PGL is 64%, of which 7% occur in childhood, and 75% of carriers manifest disease by age 40 y [82, 99]. Renal cell carcinoma has been reported in 8% and pituitary adenoma in < 1% [82]. There is a founder pathogenic variant in patients with Dutch heritage, particularly in those presenting with HNPGL; 83% of patients with HNPGL carried a *SDHD* pathogenic variant, of which 72% were the single founder variant [100].

Paraganglioma syndrome 2 (PGL2)

PGL2 arises from a PV in the *SDHAF2* gene (OMIM: 613019, cytogenic location 11q12.2). This rare syndrome occurs in patients with HNPGL and to date has been described in only two European kindrids [96]. Within the affected patients PGL developed by age 45 y, were parasympathetic and multifocal in

87% of cases [97]. PGL only developed in patients with an affected father, suggestive of maternal imprinting [101]. Association with other syndromic features is currently unknown.

Paraganglioma syndrome 3 (PGL3)

PGL3 arising from an *SDHC* pathogenic variant (OMIM: 602413, cytogenic location 1q21) cause predominantly parasympathetic HNPGL [102]. In a cohort of 42 affected patients all PGL were benign, of which 93% were parasympathetic, 7% sympathetic, and 17% multifocal [97]. Other studies reported up to 10% of *SDHC*-related PGL occurred in the thoracic cavity [102, 103]. Malignancy appears rare with only a single reported case developing metastatic disease [104]. The lifetime risk of PC/PGL in PGL3 is estimated to be 18% by age 80 y [105].

Paraganglioma syndrome 4 (PGL4)

PGL4 arises from pathogenic variants in *SDHB* (OMIM: 185470, cytogenic location 1p36) and is the most common cause of hereditary PC/PGL. In a cohort of 378 affected patients with an *SDHB* PV, PGL occurred more frequently than PC at 78% *versus* 25% [97]. Key features included sympathetic catecholamine secreting PGL which develop in the abdomen, pelvis or thorax, with HNPGL occurring less frequently [106, 107]. PGL4 is associated with greater morbidity and mortality attributed to the younger age at diagnosis, hormone secretion, and higher malignancy rate [108]. The lifetime risk of PC/PGL is estimated to be 37% with malignant disease in 12% [13]. Renal cell cancer is reported in 14%, gastro-intestinal stromal tumour in 2%, and pituitary adenoma in < 2% [82].

Paraganglioma syndrome type 5 (PGL5)

PGL5 is associated with pathogenic variants in *SDHA*, a large gene comprising of 15 exons spanning 2390 base pairs (OMIM: 619259, cytogenic location 5p15). PGL is more common than PC in this syndrome [109, 110]. These tumours are almost always unifocal but may present with highly aggressive disease [111]. The lifetime risk of PPGL is less than 5% [112].

1.3.3.2 Fumarate hydratase

FH (OMIM: 136850, cytogenic location locus 1q43) is a tumour suppressor gene responsible for converting fumarate to malate [113]. Accumulation of the precursor metabolite fumarate, resulting from deficiency in FH, leads to inactivation of prolyl-hydroxylate (PHD) and stabilisation of HIF.

Pathogenic variants in *FH* have been implicated in the development of Hereditary Leiomyomatosis and Renal Cell Cancer (HLRCC). The resultant phenotype of cutaneous leiomyomata, uterine leiomyomata (fibroids), and/or renal tumours has been well described. PC/PGL have been reported in a small number

of kindreds and it is estimated that ~ 1% of patients with PC/PGL will harbour a germline *FH* pathogenic variant, and this often occurs in the absence of a personal or family history of syndromic tumours [114, 115]. To date, 18 cases of *FH* PV have been described in the literature, with an older age of onset (range 6- to 7-year) and with a high incidence of metastatic disease (25%) [115]. Emerging evidence supports genotype-phenotypes correlations whereby nonsense pathogenic variants predispose to HLRCC, whereas missense predominantly PC/PGL [115, 116].

1.3.3.3 Multiple Endocrine Neoplasia type 2 syndrome

The rearranged during transfection (*RET*) proto-oncogene is comprised of 21 exons and is located on chromosome 10 (10q11.2) [117]. *RET* encodes a transmembrane receptor tyrosine kinase comprised of three functional domains; extracellular ligand-binding, transmembrane, and cytoplasmic tyrosine kinase domains. RET appears to transduce growth and differentiation, particularly in tissue derived from the neural crest [118].

A heterozygous germline *RET* gain of function PV causes multiple endocrine neoplasia type 2 (MEN2) syndrome [117]. Currently, 95% of cases are subtyped as MEN2A (including familial medullary thyroid carcinoma [FMTC]), with the remaining 5% as type MEN2B. The majority of PV in MEN2A affect the cysteine-rich region of the extracellular domain (encoded in *RET* exons 10 and 11). Conversely germline PV in the intracellular tyrosine kinase domain (encoded by exons 13-15) are predominantly associated with FMTC, and account for only a small proportion of cases [119]. There is an autosomal dominant pattern of inheritance, with up to 30% of patients with MTC being reported as harbouring a germline *RET* PV. 6-7% of these patients will have no family history of MEN2A-associated endocrine disease, attributed to *de novo* disease [119].

MEN2 is associated with a high risk of medullary thyroid carcinoma (MTC) and PC, and MEN2A is also associated with primary hyperparathyroidism. MTC is usually the first manifestation and typically presents before the age of 30 y (penetrance 90%) [117]. Phaeochromocytoma (PC) develops in 4-25% of patients with MEN2. Primary hyperparathyroidism usually develops many years later (penetrance 2-12%)[119]. Multifocality is a feature of all MEN2A neoplasms. Genotype-specific risk management guidelines have been developed for MEN2A syndrome by the ATA Taskforce [117]. This reflects the near complete disease penetrance and aggressive nature of MTC thus usually recommending prophylactic thyroidectomy and biochemical surveillance for PC and primary hyperparathyroidism. A small number of families will develop pruritic cutaneous lichen amyloidosis, a lichenoid skin lesion over the back [120].

1.3.3.4 Multiple endocrine neoplasia type 5 syndrome

MAX is a tumour suppressor gene (OMIM: 154950, cytogenic location 14q23.3) encoding an essential component of the MYC-MAX-MXD1 'network' of transcription factors which regulate cell proliferation, differentiation and apoptosis [121]. There is evidence that disruption of this pathway plays a role in the development of neural crest tumours, including neuroblastoma [122]. *MAX* PVs have been identified throughout the gene however were particularly frequent in exons 3 and 4, which transcribe into important residues in the bHLH-Zip domain of MAX [123]. There appears to be a paternal mode of inheritance with a parent of origin effect [121].

The median age of diagnosis is 34 y (range 13-58 y) with a penetrance of 70% by age 40 y [124]. PC are most common with a high frequency of bilateral or multiple PC (21%), a 48 fold high rate ($p<0.001$) than *MAX*-negative cases.[123] PC/PGL were predominantly normetanephrine secreting and metastatic disease has been reported in 7-25% of cases [121, 123]. There was phenotypic heterogeneity with less than 35% of patients reporting a family history.

1.3.3.5 Transmembrane protein 127

TMEM127 (OMIM: 613403, cytogenic location 2q11) encodes a multi-spanner transmembrane protein. Whilst a biological role has not been clearly established, it has been suggested that TMEM127 is associated with nutrient sensing and handling of glucose [125, 126]. Evidence suggests TMEM127 signals through the mammalian target of rapamycin (mTOR) pathway, frequently disrupted in human cancer [127].

TMEM127 PVs are found throughout the coding region of the gene, with truncating variants (n=66) occurring more frequently than non-truncating (n=42) [127]. Genotype-phenotype correlations occurred with patients harbouring non-truncating PV being more likely to present with PGL or RCC (in the absence of PC.) Patients present at a similar age to sporadic PC with a mean age of diagnosis at 45 y. PC was most frequent (85.5%) compared with PGL (9%) and renal cell carcinoma (5.4%) [127]. Multifocal disease occurred in one-third of patients however metastatic disease was rare (2.8%). A family history was reported in 15.4% of patients carrying *TMEM127* PV.[127].

1.3.3.6 Neurofibromatosis 1

The Neurofibromatosis 1 (*NF1*) gene (OMIM: 162200, cytogenic location 17q11.2) encodes the protein neurofibromin produced by nerve cells, oligodendrocytes and Schwann cells [128]. Neurofibromin is a guanosine triphosphate hydrolase (GTPase)-activating protein that stimulates intrinsic GTPase activity in the RAS p21 family. Ras activates a number of signalling pathways including mammalian the target of rapamycin (mTOR) and mitogen-activated protein kinase (MAPK) pathways [128, 129].

Neurofibromatosis type 1 (NF1) occurring due to pathogenic variants with the *NF1* gene is a multisystem disorder characterised by café au lait macules, cutaneous neurofibromas, learning disability and plexiform neurofibromas[130]. The prevalence of PC/PGL in NF1 is currently estimated as 2.9% with a median age of diagnosis 41 y (range 14-67 y). Bilateral PC/PGL has been described in 17% of patients and metastatic disease in 7.3% [131].

1.3.3.7 Others

The rapidly evolving field of identification of the genetic drivers of PC/PGL disease has recently identified further rare germline genes, of which the frequency of PC/PGL is suspected to be < 5% and lifetime risk of PC/PGL is still being established include *EGLN1*, *FGFR1*, *H3F3A*, *MDH2*, *MERTK*, *GOT2*, *SLC25A11* and *DLST* [23, 67].

1.3.4 Somatic genes implicated in sporadic PC/PGL

There is overlap with germline and somatic PV, primarily *RET*, *VHL* and *NF1* [132, 133]. Somatic PVs in *SDHx* are rare [132].. There are several exclusively somatic genes worthy of note.

1.3.2.1 Harvey rat sarcoma viral oncogene homolog

The *H-RAS* gene (OMIM: 190020, cytogenic location 11p15), which belongs to the RAS oncogene family along with KRAS and NRAS, encodes G-proteins which reside on the inner surface of the cell membrane [134]. These proteins transmit signals arising from cell-membrane tyrosine kinases and G-protein coupled receptors along the MAPK, PI3K/AKT and other pathways [135]. mRNA expression profiling grouped *HRAS* with Cluster 2, with activating PVs in this gene being implicated in several solid cancers, including follicular thyroid cancer [67]. PV in exon 2 and 3 hotspots have been identified in 7% of PC (G13R, Q61R, Q61K) and 7.1% of PGL (Q61L) [134]. *HRAS* has been found in sporadic PC/PGL and did not co-occur with other PC/PGL susceptibility genes. All cases were benign [134] however the mean tumour size was larger when compared with *HRAS* wild-type PC/PGL (58 *versus* 45mm.). Overall mutation frequency is 5.2% and this increases to 8.8% among apparently sporadic cases [134, 136].

1.3.2.2 Endothelial PAS domain protein 1

EPAS1 (OMIM: 611783, cytogenic location 2p21) encodes the transcription factor HIF2-alpha, involved in the downstream regulation of genes regulated by oxygen [137]. Somatic gain-of-function mutations in the *EPAS 1* exon 9 and 12 hotspot region result in defects in the proline residues at the hydroxylation site of HIF-2 alpha impairing degradation and stabilisation of this transcription factor [138]. As described previously, stabilisation of HIF2-alpha results in cell proliferation and increased

vascularisation [139]. Somatic HIF-2 alpha PC/PGL has been shown to co-occur with somatostatinoma and polycythaemia (Pacak-Zhuang syndrome) arising due to post-zygotic mosaicism [77].

1.3.2.3 *Cold shock domain E1 (CSDE1) and mastermind like transcriptional coactivator 3 (MAML3)*

CSDE1 (OMIM: 191510, cytogenic location 1p13) and *MAML3* (OMIM: 608991, 4q.31) are two genes that have been identified as exclusively somatic PV which are thought to be implicated in 5-10% of sporadic PC/PGL [67]. Gain of function UBTF-MAML3 gene fusions lead to DNA methylation and activation of the Wnt signalling pathway [67, 140]. *CSDE1* encodes a tumour suppressor protein which controls cell apoptosis and differentiation, and mRNA stability [141]. An aggressive phenotype has been reported with recurrent and metastatic disease [67].

Further somatic variants including *IDH1*, *FGFR1* and *BRAF* have been reported in PC/PGL albeit they are rare occurrences [67, 70].

1.3.3 History and evolution genetic testing in hereditary cancer syndrome

It is a widely accepted statistic that 5-10% of all cancers are inherited, with most following an autosomal dominant pattern of inheritance with variable penetrance [142]. Hereditary retinoblastoma set the paradigm for the understanding of hereditary cancer syndromes. Alfred Knudson's two hit hypothesis was established from his study of this tumour type in 1971 [143]. This model defined heterozygous tumour suppressor genes in the germline with loss of heterozygosity (loss of both alleles or carrying the pathogenic variant) in the tumour. Since this time more than 200 hereditary cancer genes have been described [142]. Highly penetrant pathogenic variants, defined as a relative risk of > 5, are relatively rare [144]. Key syndromes seen in Familial Cancer Services include hereditary breast-ovarian cancer syndromes (*BRCA1, BRCA2*), Familial adenomatous polyposis (*APC*), Lynch syndrome (*MLH1, MSH2, MSH6, PMS2*) and Li Fraumeni Syndrome (*TP53*). Characteristic features of hereditary cancer syndromes include the following; early development of cancer than is typical; multiple primary cancers in an individual; multiple family members of the same lineage affected; or a specific grouping of cancers known to be associated with a syndrome [142].

A combination of benign and malignant tumours is common and when grouped together most syndromes approach complete penetrance by age 70 [142]. A further 15-20% of patients will show a familial clustering of cancer without a pathogenic variant being detected in a high-risk cancer susceptibility gene. An explanation for this may include multiple low-moderately penetrance alleles, that when combined, increase risk. This concept of polygenic disease (interactions between genes) and genes and environments is becoming a key focus of cancer risk [144].

1.3.4 Evolution of genetic testing techniques

Historically, single-gene analysis of a select group of high-risk cancer susceptibility genes based on the individual and family history of malignancy was performed. Sanger Sequencing, the method developed by Sanger, Maxam and Gilbert in 1977, is considered 'first' generation sequencing and involves analysing DNA fragments of approximately 500-900 base pairs (BP) [145]. This technique now comprises of denaturing template DNA which is mixed with short DNA primers, DNA polymerase and deoxynucleotide triphosphates and modified di-deoxynucleotide triphosphates (responsible for terminating DNA strand elongation), followed by amplification of fragments by polymerase chain reaction and finally dye-terminator sequencing to create an electropherogram [146].

Sanger sequencing has been superseded by Next Generation Sequencing (NGS) whereby many genes are sequenced simultaneously [147, 148]. This approach is time and cost efficient compared with the stepwise approach implemented in cascade testing via Sanger Sequencing [149]. DNA is fragmented and unique adaptors added to each of the fragments, allowing samples from many individuals to be pooled[150]. Fragments bind to a glass flow cell and bridge amplification occurs adding fluorescently tagged deoxynucleotide triphosphates. 'Sequencing by synthesis' occurs whereby the tagged nucleotides give off an emitted signal when added with each cycle and this number of cycles determines the read length.

NGS generates several million-billion short read sequences of DNA ranging from 75-300bp. Bioinformatic analyses include computational, mathematical and statistical tools to analyse the large volume of data generated from NGS.[151] A typical bioinformatics pipeline consists of generating FASTQ files which store short sequences as plain text. The raw short sequence reads are then aligned to the human reference genome in the format of a binary alignment map (BAM) file. BAM files are then used to generate a range of genetic information including single nucleotide variations (SNV), insertions and deletions and tumour mutational burden and copy number alteration.[151, 152] SNV and Indels are stored as variant call format (VCF) files which contain quantitative information including variant location, variant allele fraction, and depth of coverage. Standard analyses used to classify variant pathogenicity include assessing population allele frequency in large genomic databases (e.g. gnomAD), functional impact using *in silico* databases (MutationTaster, Provean, SIFT, REVEL or Bayes), and previous inclusion in databases of clinical significance (ClinVar [153], COSMIC[154]).

NGS has become essential as the discovery of genes implicated in hereditary cancer syndromes have expanded and where it is difficult to predict which gene may be implicated based on personal or family history alone [155]. For example, in familial breast cancer a panel of 11 genes are routinely tested in clinical care (*ATM, BARD1, BRIP1, CDH1, CHEK2, PALB2, PTEN, RAD51C, RAD51D, STK11* and *TP53*)[156].. Similarly in familial PC/PGL syndromes, over 20 germline cancer susceptibility genes have been identified to date, of which 15 have been extensively validated as being

associated with familial disease and includes the following genes: *EGLN1/PHD2, EPAS1, FH, KIF1B, MAX, MET, RET, SDHB, SDHD, SDHC, SDHA, SDHAF2, TMEM127, VHL* [72]. Clinical utility remains fundamental regarding inclusion of genes on a panel test; only test if identification of a pathogenic variant would change management for the patient and/or their family [149].

1.3.5 Variant curation and standardised reporting of variants

The American College of Medical Genetics and Genomics have published standards and guidelines for the interpretation of sequence variants using typical types of variant evidence (e.g., population data, computational data, functional data, segregation data) [66]. Variant nomenclature aligns with the Human Genome Variation Society (HGVS). Specific standard terminology to classify and report variants that cause Mendelian disorders as 'pathogenic', 'likely pathogenic', 'uncertain significance', 'likely benign', and 'benign'. Each pathogenic criterion is weighted as very strong (PVS1), strong (PS1–4); moderate (PM1–6) or supporting (PP1–5). These criteria are then combined according using a scoring system to classify variants in to the five categories.

1.3.6 Genetic counselling and consent

Exponential discovery of germline cancer predisposition syndromes and resultant implications to individuals and families resulted in considerable medical, psychological, and ethical considerations. Professional organisations (Human Genetics Society of Australasia) developed guidelines for the practice of genetic counselling[157]. Genetic counselling aims to provide both current information and support for patients with a potential hereditary cancer syndromes, and traditionally falls under the care of a genetic counsellor or clinician (cancer or clinical geneticist). Key elements of genetic counselling include advice regarding the appropriateness of genetic testing, explaining medical facts surrounding particular genetic conditions and explaining how hereditary conditions contribute to risk. In practice this includes pre-test counselling (where consent is obtained) and post-test counselling (when the result of genetic testing is discussed)[157].

1.4 Summary and aims

PC/PGL are distinct tumours with a diverse molecular biology. Genomic characterisation through massively parallel sequencing, including NGS, has helped define prevalence of historically well-established driver PVs and uncovered new genes involved in the development of these rare tumours. Challenges with variant curation and disease behaviour have come to the forefront with the discovery of infrequent genes implicated in PC/PGL, including *TMEM127 MAX*, and *EPAS1*. Similarly, the rare occurrence of paediatric PC/PGL has impeded genotype-phenotype correlations. As such, the establishment of surveillance recommendations for these groups of patients has been hindered.

PC/PGL behaviour is another ongoing challenge in the clinical care of these patients, absent histopathological features predicting metastatic disease. The lack of reliable markers of disease behaviour is particularly pertinent to patients harbouring a germline *SDHB* PV, which have the highest rate of metastases. Uncovering a potential disease modifier of *SDHB* PC/PGL disease behaviour would help guide clinicians who are involved in the ongoing surveillance of these patients. Further, once PC/PGL metastasise treatment options are limited with no curative therapies. Radionuclide therapy is one treatment option which has become more widely accessible and shows promise for disease control.

The overarching aim of this thesis was to explore the role of genetic profiling to establish personalised management pathways, known as precision medicine. Specifically, the aims were:

1. To assess sensitivity and timeliness of paired tumour-blood sequencing of PC/PGL using NGS as a streamlined pathway to diagnosis of hereditary PC/PGL
2. To examine the utility of RNA sequencing in variant curation of *TMEM127*
3. To expand the phenotypic characterization of rare genes implicated in development of PC/PGL, including *MAX* and *EPAS1*.
4. To establish genotype-phenotype correlations in paediatric and adolescent PC/PGL
5. To explore the impact of mitochondrial variants within *SDHB* mutated PC/PGL
6. To assess the efficacy of radionuclide therapy in patients with inoperable or metastatic PC/PGL

CHAPTER 2

Methodology and Materials

CHAPTER 2. Methodology and Materials

2.1 DNA protocols

2.1.1 DNA extraction from fresh frozen tissues

DNA was extracted from PC/PGL tissue using the DNeasy® Blood & Tissue Kit (Qiagen, Germany) according to the recommended manufacturer's protocol, briefly described below. All reagents were supplied within the commercial kit unless otherwise described, and all reagents supplied as concentrates were pre-prepared as directed in the DNeasy® Blood & Tissue Handbook.

To enable efficient lysis, fresh tissue samples (approximately 25mg) were macerated using sterile scalpels on clean, sterile petri dishes, and then transferred into 1.5ml microcentrifuge tubes. The tissues were resuspended by addition of 180µL Buffer ATL (tissue lysis buffer) containing 20µL Proteinase K (supplied as 600mAU/ml solution or 40mAU/mg protein). Samples were briefly vortexed and incubated at 56°C until samples were completely lysed (1-3 hr). Samples were vortexed for 15s, then treated by the addition of 200µL Buffer AL and 200µL absolute ethanol (≥ 99.9%, AnalaR grade), and samples mixed again by brief vortexing. Individual lysed tissue mixtures containing the crude DNA lysates were transferred into corresponding fresh, single-use DNEasy Mini spin columns held within 2ml collection tubes. The DNA contained within the lysates was bound to membranes within DNEasy mini spin columns during centrifugation at 6000 x *g* for 1 minute. The flow throughs were discarded. The DNEasy mini spin columns were placed into a new 2mL collection tube and the bound DNA was washed by addition of 500µL Buffer AW1 (pre-mixed with ethanol as per manufacturer's protocol), and centrifugation for 1 minute at 6000 x *g*. The flow throughs were again discarded. The DNEasy Mini spin columns with bound DNA were then transferred to new 2ml collection tubes, and bound DNA underwent a second wash by addition of 500µL Buffer AW2 (pre-mixed with ethanol as per manufacturer's protocol) to each column, and the samples were centrifuged for 3 minutes at 20 000 x *g* to remove residual ethanol from the column membranes. The DNEasy Mini spin columns containing the bound DNA were placed in clean 1.5ml tubes and elution of the purified DNA was performed by careful pipetting of 200µL Buffer AE directly onto the DNEasy membranes. The DNA samples within columns were incubated at room temperature for 1 minute and then centrifuged for 1 minute at 6000 x *g* to elute the purified DNA. DNA concentrations contained within the eluates were measured at A_{260} using NanoDrop ND-1000 and stored at 4ºC.

2.1.2 *EPAS1* DNA amplification by Polymerase Chain Reaction

2.1.2.3 Primer design

Primers were designed to encompass exon 12 of *EPAS1*. The DNA sequence was obtained from National Centre for Biotechnology Information Entrez Gen Refseq. Primers were designed using the 'UCSC In-silico PCR' program (https://genome.ucsc.edu/cgi-bin/hgPcr) with an expected PCR product of 641 base pairs (bp), the chromosomal region of amplification being chr246380136-46380776, with a forward primer melting temperature of 60.9°C and reverse primer melting temperature of 58°C. Primers were synthesised by Sigma Aldrich, Sydney Australia.

Table 2.1 *EPAS1* primers

	Forward primer (5'-3')	**Reverse primer (3'-5')**
***EPAS1* Exon 12**	agatgaatggctctgcagga	ttactagtgggtgcctctcg

2.1.2.4 Polymerase chain reaction

Polymerase chain reactions (PCR) were performed using *Amplitaq* 360™ DNA polymerase master mix (2x; Applied Biosystems) [containing *Amplitaq* 360™ DNA polymerase (5U/µL), *Amplitaq* 360™ PCR buffer, $MgCl_2$ (25mM), deoxynucleotide triphosphates (dNTP (2.5mM); adenine (dATP):cytosine (dCTP):guanine (dGTP):thymine (dTTP), 1:1:1:1)]. *Amplitaq* 360™ DNA polymerase master mix was added to nuclease-free water, forward and reverse primers (20µM each), and DNA at 4°C to a final volume of 10µL per reaction (Table 1).

Table 2.2. *EPAS1* exon 12 PCR reaction volumes

***Amplitaq* 360™ DNA polymerase master mix (2x)**	**5µL**
***EPAS1* exon 12 F primer**	0.5µL
***EPAS1* exon 12 R primer**	0.5µL
H_20, nuclease-free	3µL
DNA	1µL

Once the samples were prepared the template was amplified using the ProFlex PCR System Thermal Cycler (ThermoFisher Scientific, Australia) following the specified amplification settings (Table 2).

Table 2.3 *EPAS1* PCR amplification thermal cycler settings

Temperature (°C)	Time (min)	Cycles
95	10	1
95	0.5	30
66	0.5	30
72	0.5	30
72	7	1
11	Infinite hold	1

2.1.2.5 DNA electrophoresis

PCR products were checked for size and relative concentration on 4% (v/v) polyacrylamide gels (acrylamide/Bis-acrylamide [19:1]), containing ammonium persulfate (0.08% (w/v)), 23µL N,N,N',N'-Tetramethylethylenediamine (TEMED; 0.15% (v/v)) in 0.5 x Tris-Borate-EDTA (TBE) buffer. Samples of the PCR products (between 1.5-2µL) were electrophoresed on the 4% polyacrylamide gels at 120V (30min) to confirm the success of the PCR reaction. A pUC/*Hpa*ll marker (*Geneworks,* Cat no: DMN-P1) was used as a comparator for size estimations of PCR fragments. The DNA/PCR fragments gel were visualised using SYBR® Safe DNA Gel stain (ThermoFisher Scientific) and images obtained using the White/Blue light Transilluminator MUV21-254/312 (Major Science, Scientifix, Australia) and SmartView Pro 1100 Imager System (Major Science, Scientifix, Australia).

2.1.3 Massively parallel sequencing

Massively parallel sequencing (MPS) experiments were performed by Dr Catherine Luxford (Cancer Genetics Diagnostic Laboratory [CGDL], Kolling Institute). Testing of genes associated with phaeochromocytoma/paraganglioma (PPGL) using MPS was performed using a custom panel (Custom 46 gene Solution by SOPHIA GENETICS pre-validated capture kit, Switzerland) encompassing the protein-coding regions of genes associated with hereditary PC/PGL syndromes (Table 2.4) that were sequenced on an Illumina MiSeq platform. Sequencing data was then analysed using Illumina MiSeq Reporter (instrument specific software that assessed sequencing quality, aligned sequencing reads to the reference human genome [hg19] and identified variants). Variants were annotated (using ANNOVAR [158]to assist with interpretation of pathogenicity.

Table 2.4 Genes included in the PC/PGL NGS panel

GENE	Chr	RefSeq NM_	RefSeq NG_
SDHAF3 (ACN9)	7q21	NM_020186.2	?
ATRX	Xq21	NM_000489.5	NG_008838.3
DNMT3A	2p23	NM_022552.4	NG_029465.2
EGLN1	1q42	NM_022051.2	NG_015865.1
EGLN2	19q13	NM_080732.3	?
EGLN3	14q13	NM_022073.3	?
EPAS1	2p21	NM_001430.4	NG_016000.1
FH	1q43	NM_000143.3	NG_012338.1
H3F3A	1q42	NM_002107.4	?
GOT2	16q21	NM_002080.3	?
HIF1A	14q23	NM_001530.3	NG_029606.1
HIF3A	19q13	NM_152795.3	NG_029679.1
IDH1	2q34	NM_015040.3	NG_023319.2
IDH2	15q26	NM_002168.3	NG_023302.1
IDH3B	20p13	NM_006899.4	NG_012149.1
KIF1B	1p36	NM_015074.3	NG_008069.1
MAX	14q23	NM_002382.4	NG_029830.1
MDH1	2p15	NM_005917.3	NG_028144.2
MDH2	7q11	NM_005918.3	NG_052976.1
MERTK	2q13	NM_006343.2	NG_011607.1
MET	7q31	NM_000245.3	NG_008996.1
MYCT1	6q25	NM_025107.2	?
NF1	17q11	NM_000267.3	NG_009018.1
RET	10q11	NM_020975.4	NG_007489.1
SDHA	5p15	NM_004168.3	NG_012339.1
SDHB	1p36	NM_003000.2	NG_012340.1
SDHC	1q23	NM_003001.3	NG_012767.1
SDHD	11q23	NM_003002.3	NG_012337.3
SDHAF1	19q13	NM_001042631.2	NG_016869.1
SDHAF2	11q12	NM_017841.2	NG_023393.1
SLC25A11	17p13	NM_003562.4	?
TMEM127	2q11	NM_017849.3	NG_027695.1
VHL	3p25	NM_000551.3	NG_008212.3

TERT	5p15	NM_198253.2	NG_009265.1
TERT*	5p15	NM_198253.2:c.1-124C>T	?
TERT *	5p15	NM_198253.2:c.1-146C>T	?
MEN1	11q13	NM_000244.3	NG_008929.1
CDKN1B	12p13	NM_004064.4	NG_016341.1

* promotor hotspot

2.1.4 Sophia Genetics DNA Library Preparation Methodology

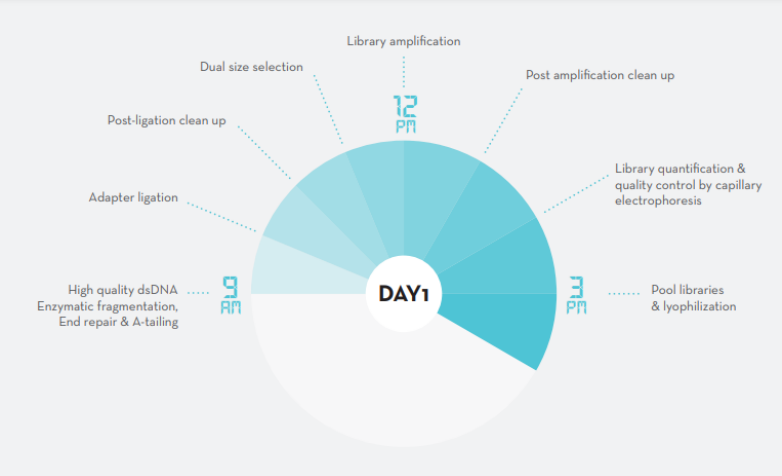

Figure 2.1 Day 1 NGS library preparation workflow summary. Image from Custom Bundle Solution by Sophia Genetics User's Guide.

2.1.4.1 Library preparation

Genomic DNA (gDNA) samples were diluted to produce 200ng gDNA in a final volume of 30µL using IDTE buffer (IDTE; low TE buffer supplied with the Sophia Genetics Custom Bundle Solution library preparation kit). All samples were mixed briefly by careful pipetting followed by a brief spin in a microcentrifuge to settle contents of the tubes. All pre-mixes volumes listed below were used in the preparation of 24 MPS sample reactions.

Pre-mixes and reagents preparation

The DNA Library Prep Kit by SOPHIA GENETICS was removed from -20°C storage and thawed on ice. Once thawed the reagents were mixed by inverting 5-10 times and briefly spun in a microcentrifuge to settle tube contents. AMPure XP beads were removed from 4°C storage and left to equilibrate at room temperature for at least 30 minutes, then mixed thoroughly. FX reaction pre-mixes (as stated above, for 24 sample reactions) were prepared by combining 150µL FX Buffer (10 x) and 300µL FX Enzyme Mix. Pre-mixes were mixed thoroughly as above, then kept on ice. The ligation

pre-mixes were prepared by combining 600µL DNA Ligation Buffer (5 x), 300µL DNA ligase, and 450µL nuclease free water. Pre-mixes were mixed thoroughly as above. The PCR pre-mixes were made by combining 690µL HiFi PCR Master Mix (2x), 41.4µL Primer Mix Illumina Library Amp and 96.6µL nuclease-free water. Pre-mixes were mixed thoroughly as above, then kept on ice.

Genomic DNA preparation for fragmentation

The diluted individual gDNA samples (200ng in 300µL) were transferred into individual tubes within a sterile 8-tube PCR strip. To each 30µL of gDNA sample, 5µL of the FX enhancer was added, followed by gentle mixing. All samples were kept on ice until enzymatic fragmentation reaction setup.

Enzymatic fragmentation, end repair and A-tailing

Samples were kept on ice before and after the incubations to block non-specific enzymatic reactions. The thermal cycler was programmed for FXFrag with the settings outlined in table 2.1. The FXFrag program was started and paused when the block reached Step 1 - 4°C. The reactions were assembled as follows: 15µL of FX reaction pre-mix was added to each of the 35µL of gDNA samples. The samples were mixed thoroughly and briefly spun in a microcentrifuge. The samples were placed in the thermal cycler and the FXFrag program was continued.

Table 2.5 FXFrag thermal cycler settings

	Temperature (°C)	Time (minutes)
Lid	70	
Step 1	4	1
Step 2	32	5
Step 3	65	30
Step 4	4	hold

Ligation

The thermal cycler was set at 20°C. Dual Index Adaptors plate was removed from -20°C storage and thawed on ice. After thawing the plate was briefly spun to settle well contents. Three new 8-tube strips with 5µL of different Dual Index Adaptors per tube were prepared, based on the indexing strategy for each run. The reaction was assembled as follows: 50µL of the FX fragmentation reaction products were added to the 8-tube strips containing 5µL of Dual Index Adaptors stock. The samples were mixed thoroughly and centrifuged briefly to settle tube contents, then 45µL of Ligation pre-mix was added to each of the Adapter/FX fragmentation reaction products. The samples (final volume 100

µL) were mixed thoroughly and centrifuged briefly to settle tube contents. Samples were incubated in the thermal cycler at 20°C for 15 minutes (with no heating to the lid).

Post-ligation clean-up

Immediately after the ligation incubation, 80µL of AMPure XP beads were added to each of the 100µL gDNA-ligation reaction products within the 8-tube strips. The samples were mixed thoroughly by pipetting, followed by incubation at room temperature for 5 minutes. The gDNA-ligation reaction products within the 8-tube strips were placed on a 96 well plate-format magnetic rack for 3 minutes, and then the supernatant was carefully discarded. Keeping the tubes containing the gDNA-ligation reaction products on the magnetic rack, each sample was washed with the careful addition of 200µL of freshly prepared 80% ethanol (v/v) directly onto the bead pellets. The samples were then incubated at room temperature whilst on the magnet for 1 minute, and then all ethanol was carefully discarded. This step was repeated. The gDNA bound-bead pellets were air dried for 5 minutes at room temperature. The tubes containing the gDNA bound-bead pellets were removed from the magnetic rack and 105µL of nuclease free water was added to each sample directly onto the beads and mixed thoroughly, and incubated at room temperature of 5 minutes. The 8-tube strips containing the gDNA bound-beads were then placed on a 96-well plate format magnetic rack for a further 3 minutes, then 100µL of each supernatant (containing ligated reaction products) was carefully transferred to new labelled 8-tube strips.

Dual Size Selection

To each 100µL ligated reaction product, 60µL of AMPure XP beads were added. The samples were mixed thoroughly by pipetting and then incubated at room temperature for 5 minutes. The 8-tube strips containing the ligated reaction product and beads were placed on a 96-well plate format magnetic rack for 3 minutes, then 140µl of each of the supernatants was transferred to new labeled 8-tube strips containing 20µl of AMPure XP beads. The sample and bead mixtures were mixed thoroughly by pipetting and then incubated at room temperature for 5 minutes. The samples were again placed on a 96-well plate format magnetic rack for 3 minutes, and then 150µl of the supernatant was carefully discarded. The beads bound with the gDNA samples were retained on the magnet.

With the tubes kept on the magnetic rack, 200µl of freshly prepared 80% ethanol (v/v) was added to each of the gDNA-bound bead samples which were then incubated at room temperature for 30 seconds. All ethanol was carefully discarded, and this wash step was then repeated. Residual ethanol was carefully removed, and the beads were left to air-dry at room temperature for 5 minutes. Tubes were removed from the magnetic rack and the bound gDNA dual size selected reaction products were resuspended by the addition of 20µl of IDTE. The samples were mixed thoroughly by gentle pipetting.

Library amplification (LibAmp)

The thermal cycler was programmed for LibAmp outlined in Table 2.2.

Table 2.6 LibAmp Thermal Cycler settings

	Temperature (°C)	Time (minutes)
Lid	99	
Initial step	98	120
1st step	98	20
2nd step	60	30
3rd step	72	30
Final step	72	60

* Hold reactions at 10°C at the end of the program

The PCR reaction was assembled as follows: 30µl of PCR pre-mix was added to the dual size selected ligation products and bead mixtures, the samples (final volume 50µl) were mixed thoroughly, and the tubes were placed in the thermal cycler and then amplified using the LibAmp program as described above.

Post-amplification clean-up

Post-amplification clean-up of the amplified PCR samples was performed by the addition of 50µL of AMPure XP beads to each of the 50µL PCR products, and samples were mixed thoroughly and incubated at room temperature for 5 minutes. The 8 tube strips containing the PCR products and bead mixtures were placed on a 96-well plate format magnetic rack for 3 minutes and then the supernatants were carefully discarded. The tubes were kept on the magnetic rack for the following washing steps: 200µL of freshly prepared 80% ethanol (v/v) was added to each of the bead pellets. The samples were left to stand for 30 seconds, then ethanol was carefully discarded. These steps were repeated, and any residual ethanol was then carefully removed, and the bead pellets were air dried at room temperature for 5 minutes.

With the tubes kept on the magnetic rack, 20µL of nuclease-free water was added to each of the bead pellets. The samples were mixed thoroughly and incubated at room temperature for 5 minutes. The 8-tube strips containing the samples were placed on a 96 well plate magnetic rack for 3 minutes, then 18µL of each supernatant was carefully transferred to a new correspondingly labelled library storage tube.

Individual Library Quantification and Quality Control

Briefly, 2µL of each sample was diluted 1:4 by addition of 6 µL nuclease-free water, then 2µL of each diluted sample was quantified with the fluorometric method Qubit dsDNA HS quantification. Quality of the libraries was assessed by analysing sample product profiles via capillary electrophoresis using the Agilent Bioanalyzer. Library fragments were deemed of high quality if a size distribution between 300bp and 700bp was observed on bioanalysis electropherograms.

2.1.4.2 Capture

After quantification of each individual library, 12 libraries were pooled by combining 150ng of each to yield a total of 1800ng per pooled library per capture in a DNA low-binding tube. To each of these pooled library mixtures, 2µl of Blocking oligos x Gen Universal Blockers – TS Mix and 5µL of Human Cot DNA was added. The pooled library samples were mixed thoroughly, then dried using a vacuum DNA concentrator until the mix was completely lyophilized.

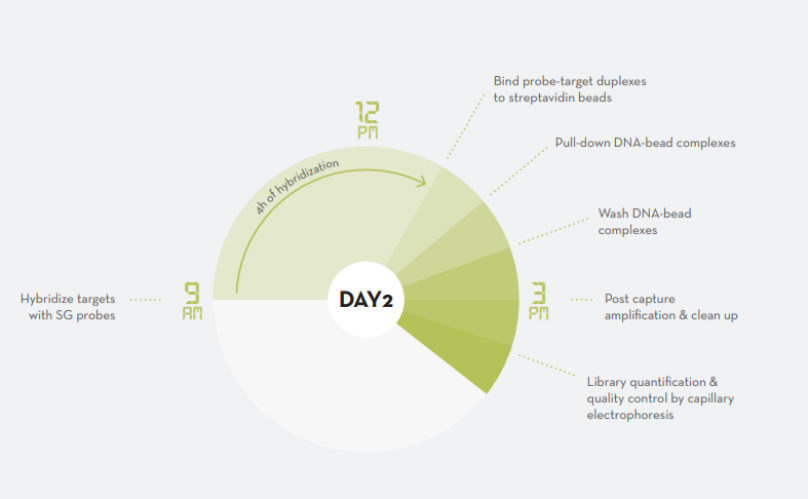

Figure 2.2 Day 2 NGS library preparation workflow summary. Image from Custom Bundle Solution by Sophia Genetics User's Guide.

Hybridisation

The thermal cycler was pre-warmed to 95°C (with the lid temperature set to 99°C). After the 10 minutes of denaturation the thermal cycler was switched directly to 65°C. The lyophilised pellets were resuspended in 13µL of the hybridisation mix (consisting of 8.5 µL of hybridisation buffer (2 x); 3.4µL of Hybridisation Buffer Enhancer; 1.1µL of nuclease free water per sample). Pre-mixes were prepared in advance according to the amount required for the capture reactions. Resuspended samples (13µL) were transferred to PCR tubes (one tube per capture reaction) and incubated in the thermal cycler at 95°C for 10 minutes. To each sample, 4 µL of probes was added and the samples mixed thoroughly, followed by incubation in the thermal cycler at 65°C for 4 hours. The wash buffers were

prepared in advance during the hybridisation reaction as per Table 2.3, and incubated to optimal temperature as described below.

Table 2.7 Wash Buffer preparation

	Stock Buffer (µL)	Water (µL)	Final volume 1 x (µL)
10 x Wash Buffer I	66	594	660
10 x Wash Buffer II	44	396	440
10 x Wash Buffer III	44	396	440
10 x Stringent Wash Buffer	88	792	880
2 x Bead Wash Buffer	550	550	1100

*1 x Stringent Buffer was pre-warmed and an aliquot of 220µl of 1 x Wash Buffer I was incubated at 65°C for at least 2 hours. The remaining Wash Buffer I was kept at room temperature.

Streptavidin Beads Preparation

The streptavidin beads were mixed by vigorous vortexing and then 100µL of the bead suspension was transferred per capture to a single 1.5ml tube. Each tube was placed on a magnetic rack, left to stand until the solution became clear, and then the supernatant was carefully discarded. Then 200µL of 1 x Bead Wash Buffer was added per capture and vortexed for 10 seconds. Tubes were placed on a magnetic rack and left to stand until the solutions became clear, then supernatant was carefully discarded. This step was repeated. Following these wash steps, 100µL of 1 x Bead Wash Buffer was added per sample tube and the tube was vortexed for 10 seconds, and 100µL of cleaned beads were transferred to a new 250µL PCR tube (one tube per capture). All tubes were placed on a 96-well plate format magnetic rack and left to stand until the solution became clear. The supernatants were then carefully discarded.

Binding of Hybridized Targets of the Beads

This step was performed quickly to ensure the temperature of the solutions remained close to 65°C to minimize off-target binding. The hybridisation reactions were removed from the thermal cycler and briefly spun down to settle tube contents. For each reaction 17µL of the hybridisation reaction solution was transferred to one PCR tube containing the cleaned beads. The beads were resuspended by pipetting up and down. The DNA was bound to the beads by placing the tubes into the thermal cycler set a 65°C (lid at 75°C) and incubating for 45 minutes. During the incubation the samples were gently pipetted up and down every 15 minutes to ensure the beads remained in suspension.

Streptavidin beads were washed to remove unbound DNA.
This step was performed quickly to ensure the temperature of the solutions remained close to 65°C. At this point, 100µL of 1 x Wash Buffer I (at 65°C) was added to each of the hybridised target/streptavidin beads tubes. The mixtures were transferred to new DNA low-binding 1.5ml tubes and the tubes were placed on a magnetic rack and left to stand until the solution became clear. The supernatant was carefully discarded, then 200µL of 1 x Stringent Wash Buffer (at 65°C) was added to each tube. The beads were gently resuspended by pipetting and each sample was then incubated at 65°C for 5 minutes. The tubes were places on a magnetic rack and let stand until the solution became clear and the supernatant carefully discarded. This step was repeated. Working at room temperature, 200µL of 1 x Wash Buffer II was added to each tube and the contents vortexed for 1 minute. The tubes were placed on a magnetic rack and allowed to stand until the solutions became clear, then supernatants were carefully removed and discarded, then 200µL of 1 x Wash Buffer III was added to each of the tubes, which were then vortexed for 30 seconds and spun briefly. Tubes were then placed on a magnetic rack and left to stand until the solution became clear and the supernatant was carefully discarded, then 200µL of 1 x IDTE was added to each tube and the beads were resuspended and the sample was spun briefly. The tubes were placed on a magnetic rack and left to stand until the solution became clear. The supernatant was carefully discarded. At this step, all remaining IDTE was completely removed. The beads were then resuspended gently by the addition of 20µL of nuclease-free water, and the samples then transferred to a new PCR tube.

Post Capture amplification (Post CapAmp)
The thermal cycler was programmed for Post CapAmp using the settings outlined in Table 2.4. The program was held at 10°C at the end of the program.

Table 2.8 PostCapAmp Thermal Cycler settings

	Temperature (degrees C)	**Time (minutes)**
Lid	99	
Initial step	98	45
1st step	98	15
2nd step	60	30
3rd step	72	30
Final step	72	60

A master PCR mix was prepared as follows for the number of reactions required. For example, per reaction, 25µL 2 x KAPA HiFi HotStart ReadyMix, 2.5µL 10 x Library Amplification Primer Mix, and 2.5µL Nuclease-free water. Then 30µL of the PCR pre-mix was added to each 20µL of DNA-bead suspension (final volume of 50µL) which was mixed thoroughly by pipetting, and all tubes were placed in the thermal cycler and the PostCapAmp program was run.

Post capture amplification clean-up

Each 50µL PCR reaction product was mixed thoroughly with 50µL of AMPure XP beads and all samples were then incubated at room temperature for 5 minutes. The tubes containing the samples were placed on a magnetic rack for 3 minutes, and the supernatant was carefully discarded. Sample tubes were kept on the magnetic rack during the following steps: the bead pellets were washed by the addition of 200µL of 80% ethanol (v/v) with incubation for 30 seconds. The ethanol was carefully discarded, and this wash step repeated. All residual ethanol was removed, and the bead pellets were air dried at room temperature for 5 minutes. The tubes containing the washed beads were removed from the magnetic rack and 20µL of IDTE was added directly onto the beads, which were then mixed thoroughly by pipetting. All samples were incubated at room temperature for 5 minutes. All tubes were placed on a magnetic rack for 3 minutes and then 18µL of the supernatant was transferred to a new labeled library storage tube.

Final Library Quantification and Quality Control

Each captured library pool was quantified with a fluorometric method (i.e. Qubit™ dsDNA HS Assay quantification using 2µL of the library). Quality control of the captured libraries was performed by analyses via capillary electrophoresis, with library DNA fragments being deemed to be of optimal quality having a size distribution between 300bp and 700bp.

2.1.4.3 Sequencing

The molarity of each pool, with average size of the library (peak size in base pairs) and concentration (ng/µL) was obtained. Each pool was diluted to 4nM and then each pool was combined in equal amounts. A x pM dilution of the denatured libraries was loaded. Library pools were prepared and sequenced on a MiSeq platform (Illumina) using the 2 x 150 bp paired-end cycle protocol. MiSeq Reporter software (v2.3, Illumina) was used to demultiplex indexed reads; generate FASTQ files (containing reads for each sample and their quality scores); perform alignment (of reads to the human genome [hg19] using a banded Smith-Waterman algorithm); and perform variant calling (using the Genome Analysis Toolkit [159]). Annotation of variant calls was performed using ANNOVAR [158] while visualization of data was performed with the Integrated Genomics Viewer (IGV, v2.3, www.broadinstitute.org).

2.7. MAX1 Immunohistochemistry

Immunohistochemistry assessing MAX expression was performed by A/Professor Anthony Gill (Anatomical Pathology Department, Royal North Shore Hospital, Sydney) on FFPE tissue sections from parathyroid adenoma and lung adenocarcinoma using a commercially available rabbit anti-MAX1 polyclonal antibody C-17 (cat no: sc-197, Santa Cruz Biotechnology) at a dilution of 1 in 1000 after heat induced epitope retrieval in alkaline solution for 30 minutes at 97° C

2.8. Statistical analysis and software

Mean, median and range were calculated for numerical values and groups compared using the Mann-Whitney *t*-test. Categorical variables were compared using Fisher's exact test. A p-value of < 0.05 was set for significance for all analyses. Statistical analyses were performed using GraphPad Prism 8 (version 8.4.3, June 2020).

2.9 Kits and reagents

Table 2.9 chemicals and reagents

Chemical kit	Supplier
Acrylamide/Bis-acrylamide (19:1 [40% (w/v)])	Astral Scientific, Australia
Ammonium persulfate	Merck, Germany
AmpliTaq Gold360™ DNA polymerase and Master Mix	ThermoFisher, USA
Boric acid	Merck, Germany
Bromophenol blue	International Biotechnologies, Australia
Buffer AL	Qiagen, Germany
Buffer ATL	Qiagen, Germany
Buffer AW1	Qiagen, Germany
Buffer AW2	Qiagen, Germany
DNA Library Prep Kit by SOPHiA GENETICS 48 reactions	SOPHiA GENETICS, Switzerland
Ethyl alcohol (ethanol, molecular grade)	Merck, Germany
Gentra ® Puregene ® Blood Core Kit B	Qiagen, Germany
KAPA ™ Library Amplification kit KK 2620 (Roche Cat. No 07958978001)	SOPHiA GENETICS, Switzerland
Microseal ® 96-well PCR plates	Bio-Rad, Australia
Microseal ® A PCR plate sealing film	Bio-Rad, Australia
MiSeq ® Reagent Kit	Illumina Australia Pty Ltd., Australia

N, N, N',N'-Tetramethyl ethylenediamine	Merck, Germany
pUC19 DNA/*Msp*I(*Hpa*II) Marker	ThermoFisher, USA
Proteinase K	Qiagen, Germany
Petri dish, Sterilin	ThermoFisher, USA
Qubit™ dsDNA HS Assay Kit	Molecular Probes, Life Technologies
Sodium hydroxylate pellets	Merck, Germany
Sucrose	Merck, Germany
SYBR Safe DNA Gel stain	ThermoFisher, USA
TBE Buffer	Merck, Germany
Tris (hydroxymethyl)aminomethane	Merck, Germany
Tris hydrochloride	Merck, Germany
TruSeq ® Custom Amplicon Index Kit	Illumina Australia Pty Ltd., Australia

Table 2.10 Equipment and software

Equipment	**Supplier**
Agencourt® AMPure® XP magnetic particles	Beckman Coulter, Australia
Biological Safety Cabinet Class II, Model 212524	Gelaire, Australia
Centrifuge, Beckman J2-21	Beckman Instruments Inc, USA
Chromas chromatogram viewer	https://technelysium.com.au/wp/chromas/
DNA low binding 1.5ml tubes	
ProFlex Thermocycler	ThermoFisher Scientific, Australia
Dry Block Heater	Thermoline, Australia
Electrophoresis Cell Apparatus, ready Gel	Bio-Rad Laboratories, USA
Eppendorf MixMate	ThermoFisher Scientific, Australia
FujiFilm Image Reader FLA-3000 Transilluminator	Fuji Photo Film Co., Ltd., Japan
GraphPad Prism version 8.4.3	GraphPad Software, USA
Incubator, CO_2 Quantum Scientific	Sanyo Biomedical, USA
Hybex Microsample Incubator	SciGene., GeneWorks, Australia
Heraeus Multifuge 3S+ Centrifuge	Thermo Fisher Scientific, Australia
Illumina MiSeq™	Illumina Australia Pty Ltd., Australia
Invitrogen DynaMag™ - 96 side skirted magnetic particle concentrator	ThermoFisher Scientific, Australia
Mini PROTEAN 3 Casting apparatus	Bio-Rad Laboratories, USA
Mini PROTEAN 3 Cell tank	Bio-Rad Laboratories, USA
MiSeq® Reagent Kit v3 600 cycles MS-102-3003	Illumina Australia Pty Ltd., Australia

NanoDrop ND-1000 Spectrophotometer	NanoDrop, USA
PCR Workstation, Aura PCR Bioair, PC1000	Bio-Cabinets Australia, Australia
RNase/DNase-free 0.2ml 8-tube strips	SOPHiA GENETICS, Switzerland
Single Channel Pipettes, Eppendorf	Eppendorf, Germany
Qubit™ 2.0 Fluorometer	Invitrogen., Life Technologies Australia
UCSC In-silico PCR program	https://genome.ucsc.edu/cgi-bin/hgPcr

CHAPTER 3

Tumour Sequencing as a Pathway to Streamlined Diagnosis of Hereditary PC/PGL

CHAPTER 3. Tumour sequencing as a pathway to streamlined diagnosis of hereditary PC/PGL

3.1 Introduction

With the advent of Next Generation Sequencing (NGS), Sanger sequencing has been surpassed by multi-gene targeted panel testing. Guidelines for multi-gene panel testing for hereditary PC/PGL via NGS categories have been published. The 2017 consensus statement [72] curated driver genes into three suggested panels; 'basic', 'extended', and 'comprehensive'. The 'basic panel' being comprised of genes extensively validated in the literature as being associated with familial disease with syndromic features and were as follows: *VHL, SDHB, SDHD, SDHC, SDHA, RET, NF1, TMEM127, MAX,* and *FH*. The 'extended panel' contains other susceptibility genes which had been proven to be functionally important, however were found at low frequencies (i.e. in <1% of hereditary PC/PGL) and included the genes *EGLN1/PHD2, EPAS1, KIFB, MET,* and *SDHAF2*. Lastly, the 'comprehensive' panel incorporated additional genes which had limited evidence due to the low number of cases. The inclusion of these specific genes was modelled on the gold standard ranking database of disease-causing variants, ClinVar [https://www.ncbi.nlm.nih.gov/clinvar/]. ClinVar is a public archive reporting the relationship among human variations and phenotypes curated by the National Centre for Biotechnology Information. Genes within the basic and extended panel were being utilised in routine clinical practice.

Within Australia, the traditional approach to investigating patients suspected of having a hereditary endocrine tumour syndrome was via testing of blood-derived germline/constitutional DNA after genetic counselling in outpatient Familial Cancer Services (FCS). Referral by the Endocrinologist or Endocrine Surgeon to the Cancer Geneticist often occurred months following tumour resection. This approach capitalised on the expert knowledge and skills within FCS which can be summarised as a three-step process: 1) referral to the FCS for genetic counselling and blood sampling, 2) molecular analysis, and 3) return visit to discuss the genetic test results. We proposed through integration of two advances in the field of cancer genetics, namely tumour sequencing and 'mainstreaming', genetic testing for hereditary endocrine syndromes could be optimised and streamlined using DNA derived from tumour tissue (somatic DNA) for diagnostic testing rather than the traditional approach outlined above. In Australia, mainstreaming referred to situations where non-genetic specialists arranged tumour-blood sequencing following informed consent.

3.2 Hypothesis

Using patients with the highly heritable tumours PC/PGL this Chapter addressed the hypothesis that hereditary endocrine tumour syndromes could be more efficiently diagnosed by genomic testing of paired blood-tumour derived DNA compared against the current standard method of blood testing only (Figure 3.1). We proposed that modern DNA sequencing techniques, NGS would provide more time-

efficient testing of paired tumour-blood DNA (and positive results validated against blood-derived DNA, both obtained at the time of surgery), followed by a single visit to the FCS to discuss genetic test results. Further, molecular analysis of PC/PGL tumour tissue would provide insights into sporadic causes of these rare tumours and identify potential treatment targets.

i. Current approach to genetic testing for hereditary cancer syndrome

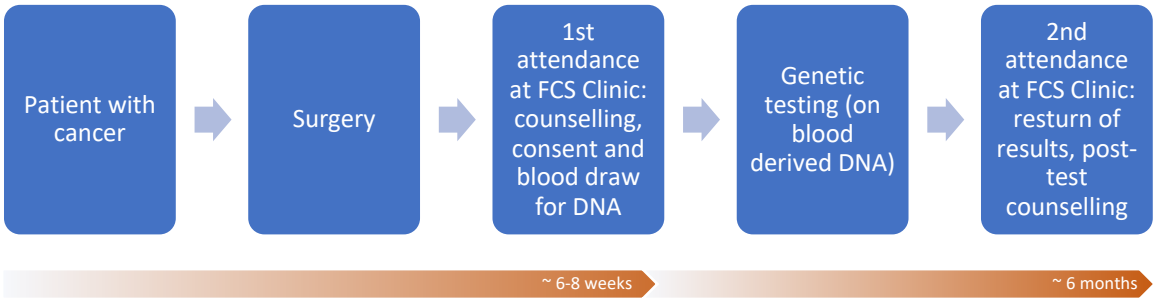

ii. Proposed new approach

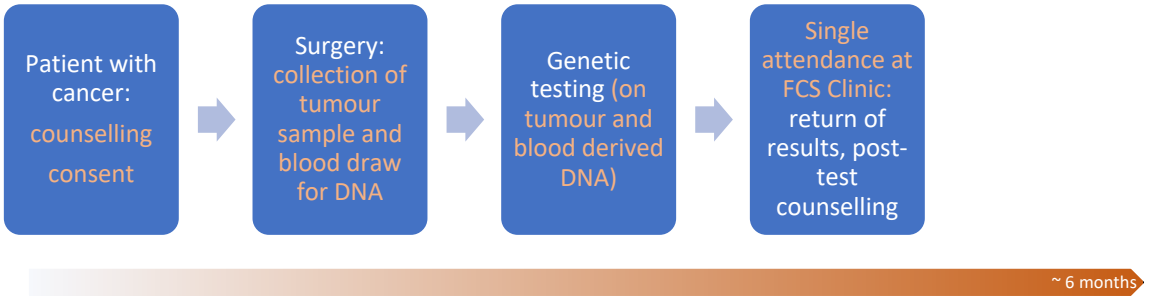

Figure 3.1. Current versus proposed new approach to genetic testing for hereditary PC/PGL
Current (i) and proposed new approach (ii) to genetic testing for hereditary PC/PGL. By avoiding the need for an Familial Cancer Service clinic visit to obtain blood for DNA, we anticipated a significant reduction in the time of return of test results without compromising stakeholder acceptance or accuracy of results.

3.3 Aims

Phase 1: In-laboratory validation of tumour sequencing using NGS

To validate tumour-based genetic testing for hereditary PC/PGL syndromes using fresh-frozen tumour tissue from patients who were known carriers of a germline variant.

i. Primary outcome: sensitivity of NGS to detect germline variants in PC/PGL tumour tissue (i.e. confirmation of the identical variant within the tumour tissue that had already been identified on germline testing)

ii. Secondary outcomes
    a. Quality control
        i. Depth: number of reads per target region
        ii. Coverage: proportion of DNA target that had adequate sequence
        iii. Inter-assay reliability
    b. Classification of additional variants discovered through paired blood-tumour molecular analysis through NGS

Phase 2: Timeliness of the proposed prospective application of paired tumour-blood sequencing using NGS

To assess the timeliness of the proposed prospective approach compared to current standard of care.

i. Primary outcome: compare time to diagnosis of the tumour-based sequencing model of care (*t*T) to current standard of care (*t*S).
ii. Secondary outcomes: report the germline and somatic findings of paired blood-tumour molecular analysis through NGS

3.4 Methodology

This project was divided into two cohorts, phase 1 and phase 2, with recruitment between 2019 and 2021 through Royal North Shore Hospital (RNSH), Sydney. Phase 1 involved in-laboratory validation of tumour sequencing via NGS, comprised of validating NGS with a MiSeq Illumina platform; Phase 2, comprised of assessment of the timeliness of the prospective application of paired tumour-blood sequencing via NGS. For phase 1, appropriate patients were identified through the Cancer Genetics Diagnostic Laboratory (CGDL) and tumour samples were obtained from the Kolling Institute Tumour Bank, Kolling Institute, RNSH, Sydney. For phase 2, patients were recruited through the RNSH outpatient clinic with written consent.

3.4.1 Phase 1: In-laboratory validation of tumour sequencing using NGS

3.4.1.1 DNA extraction

Fresh frozen PC/PGL samples from 20 patients with known germline (n = 18) or somatic (n = 2) variants were obtained from the Kolling Institute Tumour Bank. DNA was extracted from tissue using DNeasy Blood and Tissue DNA Extraction Kit (Qiagen, Germany), in accordance with the manufacturer's protocol. This method is described in full in Chapter 2.

3.4.1.2 Library preparation and NGS

Library preparation and sequencing was performed by Dr Catherine Luxford (Senior Scientific Officer, CGDL Kolling Institute, RNSH, Sydney). The methodology is outlined in full in Chapter 2, however in summary, NGS was performed using a custom gene panel (Custom 46 gene Solution by SOPHIA GENETICS pre-validated capture kit, Switzerland) encompassing the protein-coding regions of genes associated with hereditary PC/PGL syndromes (describe in full in Chapter 2). DNA libraries were prepared and sequenced on the MiSeq platform (Illumina) and FASTQ files were generated. Sequencing reads were aligned to the human genome (hg38) via Smith-Waterman algorithm, variant calling was performed via Genome-Analysis Toolkit[160], and processed by the MiSeq Reporter (v.5, 2017). VCF files were generated and annotated with functional consequences to variant calls performed using ANNOVAR [161]. Integrative Genomics Viewer open source software was used to visualise genomic data [162].

3.4.1.3 Bioinformatic analysis

Bioinformatic analysis of the annotated output was performed using the following filtering steps; 1) PC/PGL predisposition gene selected; *MAX, RET, SDHA, SDHB, SDHC, SDHD, TMEM127* and *VHL*, 2) region selected; upstream, splicing, exonic, intronic (3'-UTR/5'-UTR-removed), 3) mutation type selected; frameshift, indel, non-frameshift indel, non-synonymous SNV, stop-gain, '.' (synonymous removed), 4) read depth: ≥ 100 selected, and 5) minor allele frequency < 0.001 and those not reported in ExAC (https://exac.broadinstitute.org/) [now called the Genome Aggregation Database, gnomAD (https://gnomad.broadinstitute.org/)].

Sensitivity was calculated as the true positive value divided by the true positive plus false negative value x 100 (i.e. confirmation of the identical pathogenic variant within the tumour tissue that had already been identified on germline testing). Coverage was estimated using the Lander/Waterman equation (C=LN/G) where C stands for the coverage, G the haploid genome length, L the read length, and N the number of reads [163]. The depth of coverage (number of reads at each reference base position) was reported in ANNOVAR. PC/PGL samples were re-run to determine inter-assay reliability, which was calculated as the true positive values divided by the true positive plus false negative values x 100.

3.4.2 Phase 2: Timeliness of the proposed prospective application of paired tumour-blood sequencing using NGS

Patients were identified by relevant specialists (Endocrinologists and Endocrine Surgeons) within RNSH, Sydney. To be eligible, patients must have had:

1. A diagnosis of a paraganglioma at any age OR diagnosis of bilateral phaeochromocytoma at any age OR a diagnosis of a single phaeochromocytoma under the age of 50 plus high-risk features (family history of PC/PGL, multifocal disease, malignant disease, or abnormal IHC);
   AND
2. Not previously undergone genetic testing for, or have a known family history of, hereditary PC/PGL;
   AND
3. Been awaiting surgical resection of PC/PGL at RNSH;
   AND
4. Provided written informed consent.

Paired tumour-blood samples were collected during admission for PC/PGL resection. Samples were immediately stored at -80°C until required. DNA was extracted using DNeasy Blood and Tissue Extraction Kit (Qiagen, Germany), as described in full in Chapter 2. NGS sequencing was performed as outlined previously in Phase 1. Variants were filtered using an extended panel of germline and somatic PC/PGL susceptibility genes including *ATRX, EGNL1, EPAS1, GOT2, FH, KIF1B, MAX, MET, NF1, RET, SDHA, SDHAF2, SDHB, SDHC, SDHD, TERT, TMEM127, VHL*; otherwise, the steps replicated those outlined in Phase 1. Variants were categorised either as germline/constitutional if present in DNA isolated from whole blood and tumour, and somatic if present in tumour alone. Germline and somatic variants were classified as per the American College of Medical Genetics (ACMG) guidelines into benign, likely benign, variant of uncertain significance (VUS), likely pathogenic or pathogenic [66].

The timeliness of the new approach was compared to the current standard of care;

- New approach (*t*T); time from surgery to genetic diagnosis using tumour DNA (time from surgery to tumour-blood storage plus library preparation to result)
- Standard care (*t*S)): time from surgery to genetic diagnosis via standard FCS clinic (time from surgery to FCS review plus molecular analysis to result) was determined from a cohort of patients who had undergone surgery, genetics assessment, and molecular analysis through the current approach to genetic testing for hereditary PC/PGL (standard care) at RNSH between 2019-2020.

3.4.3 Statistical analysis

Descriptive statistics were used to describe the cohort. Mean, median and range were calculated for numerical values. Categorical variables were compared using Fisher's exact test. A p-value of < 0.05

was set for significance for all analyses. Cox proportional hazards test and Kaplan Meier analysis of *t*T vs *t*S (i.e. hazard ratio and time to "positive" diagnosis using either approach) was performed. Statistical analyses were performed using GraphPad Prism 8 (version 8.4.3, June 2020).

3.3 Results

3.5.1 Phase 1: In-laboratory validation of tumour sequencing using NGS

3.5.1.1 Primary outcome

Filtering steps with corresponding number of variants identified are summarised in Table 3.2. There were 21 variants detected in the 20 PC/PGL tumour samples, summarised in Table 3.3. Seventeen were germline and four were somatic. Following variant analysis, 19 were classified as true positive and one false negative, giving a sensitivity of 95%. The variant which was not detected on NGS was subsequently identified as an *SDHB* large-scale deletion (NM_003000.3(*SDHB*):c.1-?_72+?del). This tumour sample showed loss of SDHB staining on immunohistochemistry which had prompted further investigation with multiplex ligation dependant probe amplification (MLPA).

Table 3.1 Phase 1 filtering steps with corresponding number of variants identified in 20 PC/PGL samples

Bio-informatics output filtering steps	Variants (n)
Total variants detected	1039
Number of variants in PC/PGL susceptibility genes *MAX, RET, SDHA, SDHB, SDHC, SDHD, TMEM127, VHL*	252
Region upstream, splicing, exonic, intronic	251
Select frameshift deletion/insertion, non-frameshift deletion/insertion, nonsynonymous SNV, stop-gain, '.'	66
Select read depth ≥100	66
ExAC_ALL values ≤ 0.001, and those not reported in ExAC	21

Abbreviations: PC, phaeochromocytoma; PGL, paraganglioma; SNV, single nucleotide variant.

Table 3.2 Phase 1 variants detected in PC/PGL tissue samples via NGS.

Sample ID	T (%)	Variant (G/S)	ACMG	Depth	VAF	ExAC	Match +
AP 1.18	-	*SDHB* c.72+1G>T (G)	P	688	0.56	N/R	✓
AP 1.21	60	*TMEM127* c.532_533ins TCGCCGTTAGCTTCT, p.Tyr178delins (G)	P	638	0.42	N/R	✓
AP 1.22	40	*VHL* c.470C>T, p.Thr157Ile (G)	P	589	0.67	N/R	✓
AP 1.23	80	*VHL* c.250G>C, p.Val84Leu (G)	P	480	0.48	N/R	✓
AP 1.25	60	*VHL* c.492G>C, p.Gln164His (G)	LP	653	0.72	N/R	✓
AP 1.26	70	*VHL* c.250G>T, p.Val84Leu (G)	P	643	0.61	N/R	✓
AP 1.28	45	*VHL* c.481C>T, p.Arg161* (G)	P	532	0.55	N/R	✓
AP 1.33	-	*SDHB* c.88delC, p.Gln30fs (G)	P	332	0.62	< 0.01	✓
AP 1.5	60	*RET* c.1900T>C, p.Cys634Arg (G)	P	907	0.48	< 0.01	✓
AP 1.6	-	*RET* c.1901G>C, p.Cys634Tyr (G)	P	1093	0.55	N/R	✓
AP 1.7	90	*RET* c.2753T>C, p.Met918Thr (G)	P	856	0.54	N/R	✓
AP 1.9	70	*RET* c.1901G>A, p.Cys634Tyr (G)	P	839	0.48	N/R	✓
AP 1.12	55	*RET* c.2372A>G, p.Tyr791Phe (G)	LB	783	0.50	N/R	✓
		VHL c.326T>G, p.Ile109Asn (S)	P	248	0.58	N/R	
AP 1.13	10	*SDHA* c.91C>T, p.Arg31* (G)	P	756	0.48	< 0.01	✓
		SDHA c.455A>C, p.Glu152Ala (S)	P	768	0.13	N/R	
AP 1.14	15	*SDHA* c.1597C>G, p.Gln533Glu (G)	VUS	723	0.45	N/R	✓
AP 1.15	-	-	-	-	-	-	✗
AP 1.16	60	SDHB c.79C>T, p.Arg27Ter* (G)	P	382	0.68	< 0.01	✓
AP 1.17	50	SDHB c.268C>T, p.Arg90Ter* (G)	P	541	0.63	< 0.01	✓
Som 1-1	-	EPAS1 c.1589C>T, p.Tyr532Cys (S)	P	867	0.47	< 0.01	✓
Som 1-2	-	FH c.1517A>G, p.Met506Val (S)	P	216	0.88	< 0.01	✓

Abbreviations: ID, identification; T (%), tumour percentage composition; G, germline; s, somatic; SDHB, succinate dehydrogenase subunit B; TMEM127, transmembrane protein 127; VHL, von Hippel Lindau; RET, rearranged during transfection; SDHA, succinate dehydrogenase complex flavoprotein subunit A; EPAS1, endothelial PAS domain protein 1; FH, fumarate hydratase; ACMG; American College of Medical Genetics, pathogenic; LP; likely pathogenic, VUS; variant of uncertain significance. VAF; variant allele frequency, +; matches previously identified germline varian

3.5.1.2 Secondary outcomes

Quality control

The depth of coverage was achieved for each of the variants (depth > 100). There was no inter-assay variability with all variants detected on the initial run identified again in the second run.

Classification of additional variants discovered through paired blood-tumour molecular analysis through NGS

Two somatic variants were detected on tumour sequencing; *VHL* and *SDHA*

VHL

The tumour sample AP 1.12 was resected from a patient who had had a previously identified 'likely benign' germline *RET* variant. The tumour DNA was found to harbour a somatic *VHL* pathogenic variant [NM_000551.3(*VHL*):c.326T>G (p.Ile109Asn)] representing the driver mutation in this individual. This missense variant was located in exon 1 in a well-established functional domain without benign variation (PM1). MetaRNN 0.878, drawing from multiple *in silico* tools, provided computational evidence to support a deleterious effect on the gene (PP3). This variant was not found in population databases including gnomAD or 1000 Genomes [https://www.internationalgenome.org/] (PM2). This variant was reported in somatic databases (COSMIC) as having been identified in malignant phaeochromocytoma and clear cell renal cell carcinoma (PS1). As per somatic variant classification criteria this variant was classified as 'likely pathogenic'.

SDHA

The tumour sample AP 1.13 was resected from a patient historically identified to harbour an *SDHA* GPV (*SDHA* c.91-C>T) [NM_004168.3(*SDHA*):c.91C>T (p.Arg31*)] variant. The tumour DNA was found to harbour an additional somatic *SDHA* pathogenic variant (*SDHA* c.455A>C) [NM_004168.3(*SDHA*):c.455A>C (p.Glu152Ala)] representing the 'second hit' in this tumour sample. This missense variant located in exon 4 was predicted to effect splicing (scSNV-ASA = 0.99995) with a deleterious effect on the gene function by nonsense-mediated decay of protein product, where LOF in *SDHA* was known to cause disease (PP3). This variant was not found in population databases including gnomAD or 1000 genomes (PM2). Missense variants in this gene currently have a low rate of benign variation and were a common mechanism of disease (PP2). This variant had not been reported in somatic databases (COSMIC). As per somatic variant classification criteria this variant was classified as 'pathogenic'.

3.5.2 Phase 2: Timeliness of the proposed prospective application of paired tumour-blood sequencing using NGS

3.5.2.1 Primary outcome

Ten patients were recruited to the prospective phase of this study comparing the timeliness of the proposed new approach of tumour-blood sequencing via NGS to the current standard of care. The median time from surgery to DNA extraction (with the patient being reviewed within the FCS for genetic counselling within this time) was 4 months followed by 2 months for molecular analysis and variant interpretation. In total, the median time from surgery to a genetic diagnosis via standard care (*t*S) was 6 months (Figure 3.2a). The median time from surgery to DNA extraction was 0.25 months followed by 1.5 months for molecular analysis and variant interpretation. In total the median time from surgery to a genetic diagnosis via the proposed paired tumour-blood sequencing using NGS was 1.67 months (*t*T)(Figure 3.2b)

Figure 3.2a Median time from surgery to genetic diagnosis.

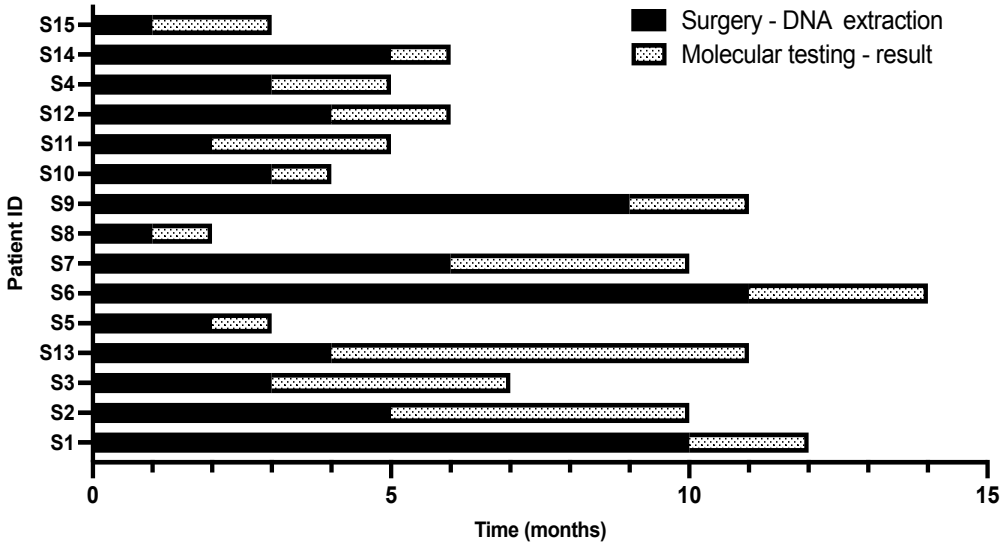

Figure 3.2a: Median time from surgery to genetic diagnosis using standard of care. *Median time from surgery to DNA extraction was 4 months followed by 2 months for molecular analysis and variant interpretation. In total, the time from surgery to a genetic diagnosis via standard care (tS) was 6 months*

Figure 3.2b. Median time from surgery to genetic diagnosis via the proposed paired tumour-blood sequencing using NGS

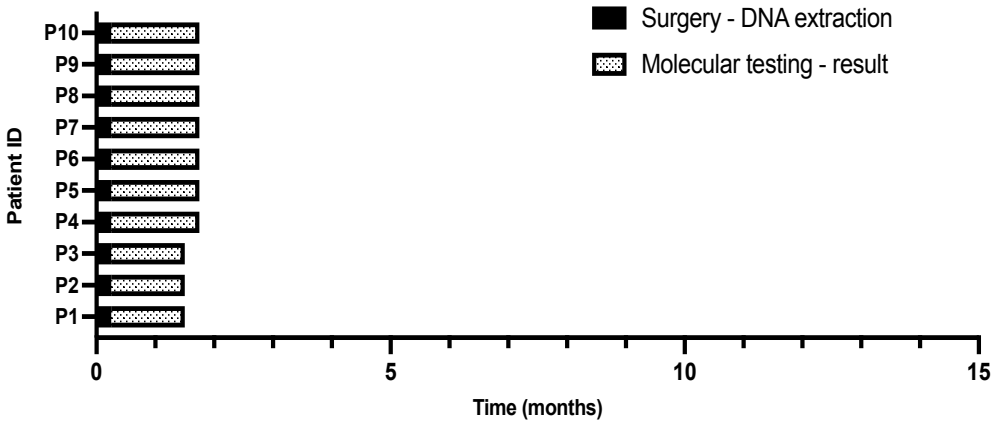

Figure 3.2b. Median time from surgery to genetic diagnosis via the proposed paired tumour-blood sequencing using NGS. The median time from surgery to DNA extraction was 0.25 months followed by 1.5 months for molecular analysis and variant interpretation. In total the median time from surgery to a genetic diagnosis via the proposed paired tumour-blood sequencing using NGS was 1.67 months (tT)

Kaplan-Meier analysis was used to compare the probability of a genetic test result over time between patients undergoing paired tumour-blood sequencing using NGS and standard of care. As above the median time from surgery to a genetic diagnosis was 1.67 months (*t*S) *versus* 6 months (*t*T)[HR 0.25 (95% CI 0.9-0.72)], $p < 0.0001$)(Figure 3.3).

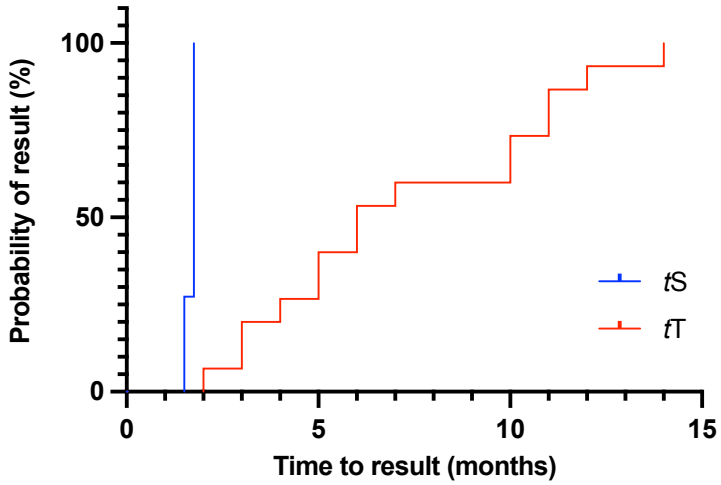

Figure 3.3 Kaplan Meier analysis of *t*S to *t*T) Median time from surgery to a genetic diagnosis was 1.67 months (tS) versus 6 months (tT)[HR 0.25 (95% CI 0.9-0.72)], p < 0.0001).

3.5.2.2 Secondary outcome

Secondary outcome was the reporting of the germline and somatic findings of paired blood-tumour DNA molecular analysis through NGS. Ten patients were recruited to the prospective phase of this study with basic demographics and phenotypic features summarised in Table 3.3 and filtering steps replicated those outlined in phase 1 and summarised in Table 3.4. .

Table 3.3 Phase 2 basic demographics and phenotypic features of patients

	Total	**Sporadic**	**Germline**	**Unknown**
Number of patients	10	4	4	2
Age at diagnosis (year), median (IQR)	53 (29-62)	59 (16-64)	43 (27-63)	55 (51-60)
GPV		*VHL, RET, MEN1, SDHD*	*MERTK, FH, SDHB*	-
Tumour details, n (%)				
PC	5	3	1	1
PGL	5	1	3	1
Tumour behaviour, n (%)				
Recurrent	1	-	1	-
Metastatic	3	-	3	-

Abbreviations: GPV, germline pathogenic variant; PC, phaeochromocytoma; PGL; paraganglioma

Table 3.4 Phase 2 filtering steps with corresponding number of variants identified in 10 PC/PGL samples

Bio-informatics output filtering steps	Variants (n)
Number of variants in PPGL susceptibility genes *ATRX, DNMT3A, EGLN1, EGLN2, EPAS1, IDH, GOT2, FH, KIF1B, MAX, MET, MDH2, MERTK, MEN1, H3F3A, NF1, RET, SDHA, SDHAF2, SDHB, SDHC, SDHD, SLC25A11, TERT, TMEM127, VHL*	626
Region upstream, splicing, exonic, intronic	624
Select frameshift deletion/insertion, non-frameshift deletion/insertion, nonsynonymous SNV, stop-gain, '.'	249
Select read depth ≥100	246
ExAC_ALL values ≤ 0.001, and those not reported in ExAC	45 (47*)

Abbreviations: PC, phaeochromocytoma; PGL, paraganglioma; SNV, single nucleotide variant.
* if depth < 100

A germline or somatic driver PV was identified in eight PC/PGL samples using the 46 gene panel; four harboured a germline pathogenic variant (*SDHB* (2), *VHL*, *FH,* and *MERTK*), two of which also harboured an *SDHA* somatic variant, and four somatic (*MEN1*, *VHL*, *RET,* and, *SDHD*)(Table 3.5). A driver PV was not identified in two samples.

3.5.2.2.1 Variant curation of germline pathogenic variants

MERTK

A *MERTK* GPV [NM_006343.3(*MERTK*):c.291delA (p.Lys97Asnfs*7)] was detected in a 33F with a unilateral PC (Pt.1). This loss of function frame-shift (null) variant located in exon 2 was predicted to cause nonsense-mediated decay with LOF being a known mechanism of disease (PVS1). This variant was not found in population databases including gnomAD or 1000 genomes (PM2). This variant was reported in germline database (ClinVar) as pathogenic (PP5), although associated with non-malignancy (retinitis pigmentosa) (PP5). Thus removing PP5 from the criteria as per ACMG criteria this variant was classified as 'likely pathogenic.'

SDHB

Two patients harboured *SDHB* GPVs. Loss of immunohistochemistry staining (LOS) for SDHB (although one tumour sample expressed equivocal loss of SDHB staining or diminished staining) with retained staining of SDHA was observed in both of these PGL samples.

A rare *SDHB* variant [NM_003000.2(*SDHB*):c.587G>A (p.Cys196Tyr)] was detected in a 67F with recurrent retroperitoneal PGLwith lymph node metastases (Pt.3). This missense variant was located in exon 6, a region of the *SDHB* containing a critical well established functional domain and without benign variation (PM1). Alternative variants at the same amino acid residue had been determined to be pathogenic (PM5). MetaRNN 0.992, drawing from multiple *in silico* tools, provided computational evidence of pathogenicity (PP3). This variant was not found in population databases including gnomAD or 1000 genomes (PM2). This variant was reported in germline database (ClinVar) as pathogenic (PP5). As per ACMG criteria this variant was classified as 'pathogenic'.

A pathogenic SNV was not identified in a 26M with a metastatic retroperitoneal PGL (Pt.4) with SDHB LOS on IHC. Further investigations using MLPA were performed which identified a heterozygous gross deletion of the genomic region encompassing the full coding sequence of the *SDHB*.

FH

An *FH* GPV ([NM_000143.3(*FH*):c.222A>T (p.Arg74Ser)] was identified in a 53F with metastatic PGL. This missense variant was located in exon 2 and was predicted to result in an Arginine to a Serine change in the protein product. This change was located in a critical/well established functional domain without benign variation (PM1). Alternative variants at the same amino acid residue have been determined to be pathogenic (PM5). MetaRNN 0.992, drawing from multiple *in silico* tools, provided computational evidence of pathogenicity (PP3). This variant was reported in germline database (ClinVar) as pathogenic (PP5). This rare variant was not found in population databases including gnomAD or 1000 genomes (PM2). As per ACMG criteria this variant was classified as 'pathogenic'.

3.5.2.2.2 Variant curation of somatic pathogenic variants

VHL

A *VHL* SPV [NM_000551.3(*VHL*):c.361G>A (p.Asp121Asn)] was identified in a 16M with a unilateral PC. This variant was located in exon 2 containing a critical/well established functional domain without benign variation (PM1). Alternative variants at the same amino acid residue had been determined to be pathogenic (PM5). MetaRNN 0.989, drawing from multiple *in silico* tools, provides computational evidence of a pathogenicity (PP3). This variant was not reported in somatic databases (COSMIC, CIVic, ICGC) although was reported in germline database (ClinVar) as pathogenic (PP5). This rare variant

was not found in population databases including gnomAD or 1000 genomes (PM2). As per somatic variant classification criteria this variant was classified as 'pathogenic.'

SDHD

A *SDHD* SPV [NM_003003.3(*SDHD*):c.155C>G (p.Ser52*)] was identified in 64F with a unilateral PC (Pt.8). This missense variant in exon 2 of the *SDHD* gene results from a C to G substitution at nucleotide position 155. This was predicted to change the amino acid from a serine to stop codon. This null variant (nonsense) in *SDHD* was predicted to cause NMD with loss of function being a known mechanism of disease (PVS1). Another variant in the same codon predicted to result in a premature stop signal [NM_003003.3(*SDHD*):c.155C>A (p.Ser52*)] was reported in a patient with multifocal PC/PGL[164] (PM5). This rare variant was not found in population databases including gnomAD or 1000 genomes (PM2). As per somatic variant classification criteria this variant was classified as 'pathogenic.'

RET

A *RET* SPV [NM_020975.4(*RET*):c.1902C>G (p.Cys634Trp)] was identified in a 59M with unilateral PC. This missense variant in exon 11 was predicted to cause a substitution of a cysteine to tryptophan within codon 634. This variant was located in a mutational hot spot (PM1). Alternative variants at the same amino acid residue had been determined to be pathogenic (PM5). MetaRNN 0.989, drawing from multiple *in silico* tools, provided computational evidence of a pathogenicity (PP3). This variant was reported in somatic databases (COSMIC, CIVic) to be associated with medullary thyroid cancer and classified in germline database (ClinVar) as pathogenic (PP5). This variant was absent in population databases including gnomAD or 1000 genomes or was very rare (PM2). As per somatic variant classification criteria this variant was classified as 'pathogenic.'

.

MEN1

A novel *MEN1* SPV [NM_000244(*MEN1*):c.1621C>T (p.Gln541*)] was identified in a 57F with a unilateral PC with metastatic disease to the retroperitoneal lymph nodes. This highly truncating, nonsense variant located in exon 10 was predicted to affect one functional domain where loss of function is a known mechanism of disease (PVS1). This variant was not found in population databases including gnomAD or 1000 genomes or was very rare (PM2). This variant was present in somatic databases (COSMIC, CIVic) and had been reported in current literature to occur in patients with other endocrine neoplasia including parathyroid adenoma and pancreatic acinar carcinoma [165] (PP5). As per somatic variant classification criteria this variant was classified as 'pathogenic.'

Table 3.5 Phase 2 phenotypic, immunohistochemical and outcomes of molecular analysis

	ID	Phenotype	IHC	%	Germline /Somatic	VAF (B/T)	ACMG classification	Database
Germline	**Pt.1**	33F, unilateral PC	SDHB+ SDHA+	80%	***MERTK*(NM_00634)c.291_292del:p.K97fs (G)** ***SDHA* (NM_004168) c.1556T>C:p.M519T (S)** *SDHA* (NM_004168) c.424A>G:p.M142V (S) *SDHA* (NM_004168) c.442G>A:p.A148T (S) *SDHA* (NM_004168) c.448G>A:p.V150M (S) *SDHA* (NM_004168) c.1591G>T:p.V531L (S) *H3F3A* (NM_002107) c.173C>T:p.S58F (S) *H3F3A* (NM_002107) c.176C>G:p.T59S (S) *H3F3A* (NM_002107) c.179A>G:p.E60G (S) *ATRX* (NM_000489) c.2450A>C:p.Y817S (S)	**0.48/0.47**	**Pathogenic (PVS1, PM2)** **LP (PP3, PM2, PP2)** VUS (PP3, PM2, PP2) VUS (PM2, PP2, BP4) VUS (PP3, PM2, PP2) VUS (PM2, PP2) VUS (PM2, PP2, PP3) VUS (PM2, PP2) VUS (PM2, PP2, PP3) VUS (PM2, BP1)	ClinVar: Path COS.: liver
	Pt.2	53F, metastatic PGL	FH -	40%	***FH* (NM_000143) c.222A>T:p.R74S (G)** *SDHC* (NM_001035511 NM_003001?) c.424G>A:p.A142T (G)	**0.5/0.45**	**Pathogenic (PP3, PM1, PM5, PM2, PP5)** Benign (BP6, BS1, BS2, BP4, BP1, BP3)	Clinvar: VUS/LP
	Pt.3	67F, retroperitoneal PGL (rec), LN mets	SDHB ~. SDHA+	80%	***SDHB* (NM_003000) c.587G>A:p.C196Y (G^{+})** *MET* (NM_001127500) c.504G>T:p.E168D (G*) *KIF1B* (NM_183416) c.997G>A:p.D333N (S) *IDH2* (NM_001290114) c.757G>T:p.G253W (S)	**0.48/0.75**	**Pathogenic (PP5, PM1, PM5, PP#, PM2)** Benign (BS1, BS2, BP4, BP6, PP5) VUS (PM2, PP2, PP3) VUS (PP3, PM2)	ClinVar: Path

	Pt.4	26M, retroperitoneal PGL, metastatic	SDHB - SDHA +	-	***SDHA* (NM_004168) c.1064+1G>A (S)** *SDHA* (NM_004168) c.1799G>A:p.R600Q (G) *ATRX* (NM_138270) c.2178G>C:p.L726F (G)	**0.29**	**LP (PVS1, PM2)** VUS (PM2, PP2) LB (BP4, BP1, PM2)	COS: melanoma
Somatic	**Pt.5**	F PC unifocal, metastatic	SDHA+ SDHB+ FH +		***MEN1* (NM_000244) c.1621C>T:p.Q541X(S)** ATRX (NM_138270) c.226T>A:p.S76T (G)	**0.56**	**LP (PVS1, PM2)** LB (BP1, BP4, PM2)	COS: N/R
	Pt.6	16M, unilateral PC	SDHA+ SDHB+	68%	***VHL* (NM_000551) c.361G>A:p.D121N (S)** *RET* (NM_020975) c.1946C>T:p.S649L (G)	**0.367**	**LP (PM1, PM5, PP3, PP5, PM2)** LB (BS3, BP6, PM2)	- COS: N/R
	Pt.7	59M, unilateral PC	SDHA+ SDHB+	60%	***RET* (NM 020630) c.1902C>G:p.Cys634Trp (S)** HIF1A (NM_001243084) c.1849G>A:p.A617T	**0.17**	**Pathogenic (PP5, PM1, PM5, PP3, PM2)** Benign (BS1, BP4, PM1)	COS: MTC
	Pt.8	64F, unilateral PGL	SDHB - * SDHA +	25%	***SDHD* (NM_003002) c.155C>G:p.S52* (S)**	**0.377**	**LP (PVS1, PM2)**	COS:N/R
PV not identified	**Pt.9**	60M, Abdominal PGL	SDHA + SDHB + FH +	-	FH (NM_000143) c.1433_1434insAAA:p.N478delinsKN (G) MERTK (NM_006343) c.1998G>T:p.K666N (G)		LB (BS1, BS2, BP6, PM4, PP%) VUS (PM1, PM2)	
	Pt.10	51M, unilateral PC	SDHA+ SDHB+	-	No variants of uncertain significance (VUS)/likely pathogenic/pathogenic variants detected			

	FH +

Abbreviations: PV, pathogenic variant; PC, phaeochromocytoma; PGL, paraganglioma; IHC, immunohistochemistry; %, percentage tumour composition; G, germline; S, somatic; VAF, variant allele frequency; ACMG, American College of Medical Genetics; LP, likely pathogenic; LB, likely benign; VUS, variant of uncertain significance; COS, cosmic database of somatic mutations.

Pathogenic and likely pathogenic variants highlighted in bold.

+ somatic variant detected when depth set to < 100

** cytoplasmic blush

3.6 Discussion

This chapter established that paired tumour-blood sequencing at the time of primary PC/PGL resection via NGS was a sensitive tool to detect germline PV within tumour and resulted in the more timely delivery of a genetic test result, compared with the current standard of carediagnostic process of sequential Sanger sequencing (1.67 months vs 7.2 months, p <0.0001). Further, performing tumour analysis as part of routine care provided insights into PC/PGL biology and, where a somatic pathogenic variant was detected, that result definitively identified that disease as sporadic.

The inception of tumour sequencing was in the establishment of 'precision oncology'. That is, investigating molecular changes from tumour-derived DNA may have diagnostic, prognostic, or therapeutic implications for the patient [166]. The incidental discovery of a GPV carried broader consequences for the individual due to the associated multifocal, recurrent and metastatic tumours being key features of hereditary tumour syndromes. Further, GPV in germline cancer susceptibility genes typically follow autosomal dominant patterns of inheritance with a 50% chance that immediate (first degree) blood relatives may have inherited the disease-causing variant.

Germline sequencing has traditionally been performed on peripherally-drawn leucocytes from whole blood of patients who meet 'genetic testing criteria' compiled by professional organisations [167, 168] [169]. Criteria for genetic testing are drawn from clinical aspects of the individual and family, including age at tumour diagnosis, tumour histology, and the pattern of disease in relatives. It has been proposed that this traditional approach misses clinically relevant germline mutations leading to a transition towards routine tumour-blood sequencing in many realms of cancer care [170]. In a cohort of adult patients with advanced cancer (comprising of prostate pancreatic, breast, and renal cancers), actionable germline findings were identified in 17.5% of patients by paired blood-tumour sequencing, of which 55.5% would have been missed if traditional criteria were applied [171]. However these findings were biased given the aggressive nature of the cancer included in the study and further studies are required to establish the utility in early-stage cancer.

Tumour sequencing not only provides insights into tumorigenesis, but also can be used for confirmation of pathogenicity through analysis for loss of heterozygosity (LOH). According to Knudson's two hit hypothesis 'inactivation of both alleles of a cancer susceptibility gene is necessary for tumour development'[143]. NGS output reported variant allele frequency (VAF) which could be used to differentiate between somatic and germline variants [172]. VAF represented the fraction of variant sequencing reads within a genetic locus and provided insights in to tumour heterogeneity. Tumours which arise in patients with GPVs often lose the wild-type allele through additional somatic variants or copy number changes known as loss of heterozygosity (LOH) [172]. Thus, the VAF of heterozygous

germline variants were characteristically between 40-60% in the blood and over 50% in the tumour, and with a low VAF within the tumour interpreted as being representative of the presence of a somatic variant. However, this approach is not failproof with many factors affecting VAF including increased copy number, gene deletions, gene re-arrangements, translocations, and promotor hypermethylation [172].

Further pitfalls of NGS which may result in the detection of false positives include the 'field effect', where inclusion of DNA isolated from samples containing high levels of non-cancerous tissue from regions surrounding the tumour impacts the detection of low VAF within the tumour due to the presence of variants from normal cells. This highlights the importance of assessing tumour percentage composition of the sample to be analysed prior to DNA extraction and sequencing. False positives in DNA extracted from peripheral whole blood may also occur through clonal haematopoiesis of indeterminate potential (CHIP). CHIP is the detection of clonally expanded stem cells, a common age-related phenomenon which can also be induced by chemotherapy, whereby haematopoietic stem cells acquire leukemogenic variants in a sub-population of white blood cells [173].

Taking the above caveats of NGS into consideration, the benefits included a greater number of genes being testing in conjunction, and fruitful insights on PC/PGL. Within our cohort 40% of patients harboured a GPV of which two patients harboured *SDHB* (including an *SDHB* deletion), another *FH*, and another a potential *MERTK* variant. This reflected the unique nature of PC/PGL possessing a high heritability rate with over 30% occurring as part of a hereditary syndrome, most frequently von Hippel Lindau disease *(VHL*) and familial phaeochromocytoma-paraganglioma 4 (*SDHB*) [174].

This study also highlighted two important features of *SDHB* GPV; the usefulness of SDHB immunohistochemistry (IHC) and the occurrence of *SDHB* large deletions [175] [176] . *SDHB*-, *SDHC*, and *SDHD*-mutated PC/PGL displayed SDHB immunonegativity and SDHA immunoreactivity, whereas *SDHA*-mutated PC/PGL showed immunonegativity for both. The sensitivity of SDHB IHC has been previously reported to be as high as 90% for SDHx mutated cases and 93% for non-SDHx mutated cases [175]. Thus, this simple laboratory technique could be used to guide genetic testing where panel sequencing is not routinely performed and as a prompt to proceed with MLPA if an *SDHB* GPV was not detected on NGS. Large deletions are reported in several hereditary PC/PGL syndromes including *MAX* (10%), *SDHA* (1 reported), *SDHB* (5-15%), *SDHD* (5-10%), and *VHL* [176] highlighting the importance of MLPA to detect abnormal copy numbers at an exon and gene levels. SDHA and SDHB IHC should also be considered as functional evidence of pathogenicity of a variant and be used in variant classification (PS3 strong evidence of pathogenicity, well-established *in vitro* or *in vivo* functional studies supportive of a damaging effect on the gene or gene product) as per ACMG guidelines [66].

FH GPV have been reported in approximately 1% of PC/PGL and often in the absence of a family history or syndromic features [114]. The median age of diagnosis at diagnosis of PC/PGL has been reported to be 55y (30-77y), with 50% occurring within the adrenal, and 25% demonstrating metastatic disease [114, 115]. *FH* GPV are traditionally associated with hereditary leiomyomatosis and renal cell carcinoma (HLRCC), an autosomal dominant syndrome predisposing patients to a high lifetime risk of cutaneous leiomyoma (76-100%), uterine leiomyoma (80%), and HLRCC-associated RCC [177]. Loss of staining for FH on IHC in RCC carries a high probability of a germline cause, whereas uterine leiomyomas, particularly single and occurring at an older age are less unlikely [178, 179]. The former appears to apply for FH-deficient PC/PGL with over 85% of tumours with LOS for FH harbouring a *FH* germline pathogenic variant [115]. Genotype-phenotype correlations have been proposed with missense variants driving the development of PC with an absence of HLRCC-associated tumours, and truncating variants causing the typical spectrum of disease [115].

Mer proto-oncogene tyrosine kinase (*MERTK*) is a member of the MER/AXL/TYRO3 receptor tyrosine kinase receptor that has been shown to activate the MAPK/ERK, PIK3CA, and AKT pathways. *MERTK* contains 19 exons which encode a long tyrosine kinase receptor protein, similar to *RET* and *MET*, comprised of an extracellular component (two immunoglobulin-like and fibronectin type III domains) and intracellular tyrosine kinase domains [176]. *MERTK* was first reported to occur in PC by Toledo *et al*., in 2016 in a patient with an MEN2 syndrome-like phenotype (with medullary thyroid cancer and metastatic PC/PGL)[180]. *MERTK* PVs have since also been identified in sporadic PC/PGL [74]. A GPV in *MERTK* was detected in a 32F with unilateral phaeochromocytoma. Although this variant (NM_006343.3(*MERTK*):c.291delA (p.Lys97Asnfs*7) was deemed to meet ACMG criteria as 'pathogenic', further analyses were performed. Upon removal of the 'PP5' criterion, as this variant had not been previously described in association with PC/PGL, this variant still satisfied the classification as 'likely pathogenic'. This classification was attributed to the null variant being predicted to produce a significantly truncated protein leading to its undergoing nonsense-mediated decay, and also the variant being rare/absent in population databases. As stated above, *MERTK* variants are currently incredibly rare, and to date none had been associated with PC/PGL. Due to these facts, when coupled with the absence of data from functional assessment/s of the effect/s on the protein, and absence of segregation of the variant with disease, the variant was subsequently regarded in this study as being of 'uncertain significance.

The landscape of somatic PV in PC/PGL continues to evolve. Comprehensive molecular analysis of 173 tumour samples from The Cancer Genome Atlas (TCGA; https://www.cancer.gov/ccg/research/genome-sequencing/tcga) provided estimates of the prevalence of somatic pathogenic variants (SPV): 39% harboured a SPV, predominantly *HRAS* (10%), *NF1* (9%), *EPAS1* (5%), and *RET* (3%) [181]. Recently a large cohort of 183 PC/PGL tumour samples were

identified as containing a SPV in 31.7% with the following frequencies; *NF1* 14%, *VHL* 6.6%, *HRAS* 5.5%, and *RET* 4.4% [69]. Also Winzler *et al.,* identified SPV in 18% of PC/PGL, with the genes being most commonly involved including *NF1* (7%), *VHL* (5%), *HRAS* (4%), *EPAS1* (4%), and *RET* (3%) [182]. A key finding from ~~all~~ these studies was that the somatic variants in *HRAS, EPAS1, FGFR3*, and *MAML3* fusions were mutually exclusive from GPVs in other genes; and that PVs in *NF1*, *VHL*, and *RET* needed to be confirmed as sporadic, mosaic, or heritable by analysis of germline DNA.

Interestingly, a somatic *VHL* PV was detected within our cohort. This finding raised the possibility for mosaicism, known to occur with *VHL* and, infrequently, with *SDHB* [71, 183]. Spontaneous post-zygotic pathogenic variants arising in genetically distinct cell linages has been shown to result in mosaicism [184], Generalised mosaicism arising from early post-zygotic alteration and results in the affected cells being dispersed through all tissue types. Somatic alterations occurring later in embryogenesis result in only the progeny cells from the affected lineage carrying the genetic alteration. The advent of NGS has allowed detection of low-level mosaicism within the germline of affected tissues with a VAF below 10%. Although 20% of cases have been reported to be *de novo* it has since been recognised that approximately 5% of VHL disease cases are considered to have arisen due to mosaicism [185]. Reanalysis of the parents of patients with presumed sporadic VHL disease with no documented family history revealed mosaicism in 4.8% [186]. Of note, mosaicism in *SDHB* has been reported in a single case with recurrent paraganglioma with LOS for SDHB whereby an *SDHB* variant was detected with a VAF of 15% in the blood and 42% in the tumour [183]. Thus it would be important to consider mosaicism when a molecular diagnosis could not made. There are several points of interest with post-zygotic mosaicism; tissue affected will vary between patients, and if germ cells carry the PV children are at a 50% chance of inheriting VHL from their mosaic parent; thus testing the parent of a presumed *de novo* patient should be considered to assess for mosaicism [186].

The role of *MEN1* in hereditary Multiple Endocrine Neoplasia type 1 syndrome has been well established, however the function of this gene in sporadic endocrine tumorigenesis is a currently emerging area of research. The majority of GPV in *MEN1* have been previously identified as producing nonsense or frameshifts, duplications, or insertions, resulting in the loss of function of the MENIN protein. Allelic deletions of the *MEN1* locus on chromosome 11q13 and PV within the gene have both been described in typical MEN1-type sporadic tumours including pancreatic neuroendocrine tumours and parathyroid adenoma [187]. Although rare, occurring in < 2% of patient with MEN1 syndrome, phaeochromocytoma has also been reported [188]. This finding was of particular interest to this study, as the variant identified within this study cohort NM_000244(*MEN1*):c.1621C>T (p.Gln541*) had not been previously reported in the somatic variant databases used for variant classification in this study.

Further somatic variants were identified in *SDHB*, *SDHD,* and *SDHA*. *SDHB* and *SDHD* somatic variants are currently exceptionally rare with only a few cases being reported. The *SDHB* variant NM_003000(*SDHB*):c.299C>T (p.Ser100Phe) was reported in a 25 year old with a bladder paraganglioma [133]. The known pathogenic *SDHD* variant NM_003002(*SDHD*):c.242C>T (p.Pro81Leu) had been described in a 42 year old female with a phaeochromocytoma; this variant has been acknowledged to cause hereditary disease [132]. Two novel somatic *SDHA* variants were detected in our cohort, one in sporadic disease and the other co-occurring with a *MERTK* GPV. Of note both PC/PGL demonstrated retained SDHA/SDHB staining on IHC, which did not support classification of these variants as pathogenic, although sensitivity was reported to be 75% [175]. Somatic *SDHA* PV have previously been reported with GIST (n=8), RCC (n=2) , and pituitary adenoma (n=1) [189]. Interestingly, a challenge with optimal surveillance for patients found to harbour an *SDHA* GPV has been identified. These *SDHA* GPV which have been identified in 10% of patients with PC/PGL have been determined to have a low lifetime penetrance, with a lifetime risk in non-probands to be 10-13% [189].

Limitations

This chapter does not explore the practicalities of the clinical integration of 'mainstreaming' into genetic testing for hereditary endocrine neoplasia, and this requires careful planning. Aspects to be addressed regarding the uptake of this approach includes a discussion with key stakeholders, particularly non-genetic clinicians, who will be involved in performing pre-test counselling and ordering the genetic test. This could comprise of educational sessions regarding hereditary endocrine syndromes and steps on how to complete of the NSW health genetic testing consent form. There would be ongoing support from genetic specialists, when required. Pre-test counselling provided by genetic experts is unique and highly specialised, and creating an abridged version which could be completed by a clinician without this training, and with time constraints, can be seen as a key challenge. It would be vital to include clinician and patient feedback when extending this study to identity the effectiveness and/or barriers to the uptake of this approach

3.7 Conclusion

In conclusion, this chapter has demonstrated the transition from routine clinical care towards blood-tumour DNA paired molecular analysis via NGS provided a highly sensitive sequencing technique with rapid return of results. Application of this model of care would be of benefit to both patients and the healthcare system. A comparatively lengthy wait for results can cause undue anxiety for the patients and their families whereby the weight of harbouring a hereditary endocrine neoplasia syndrome can also be challenging, given the implications for the individual and to their direct relatives due to the autosomal dominant pattern of inheritance of these pathogenic variants. It was proposed from the

findings of this project that patients attend the FCS for a single visit to discuss the outcome of genetic testing, effectively halving the number of clinic visits. The flow-on effects of adoption of these findings in clinical practice would include lessening the number of clinic visits, reduction of patient anxiety, alleviating pressure of long clinic waitlists, and allowing improvement in the reallocation of limited clinical resources to those with the highest need.

CHAPTER 4

Utility of RNA Sequencing to Assist in Re-classification of *TMEM127* Germline Variants of Uncertain Significance

CHAPTER 4. Utility of RNA sequencing to assist in re-classification of *TMEM127* germline variants of unknown significance detected in patients diagnosed with phaeochromocytoma or paraganglioma

4.1 Introduction

4.1.1 Transmembrane protein 127

The transmembrane protein 127 (*TMEM127*) gene, located on chromosome 2q11, is highly conserved across many species and expressed in a broad range of human tissues [190]. *TMEM127* encodes a protein of 238-amino acids which contains four transmembrane domains. Although the specific function of the protein product (TMEM127) has not been fully elucidated to date, the location in the plasma membrane endosomes, the Golgi apparatus, and lysosomes [126, 191], together with an association with endocytosis suggest a role in cellular protein trafficking [190]. Furthermore, *in vivo* studies support a role in nutrient sensing, as well as in regulating glucose and insulin sensitivity, underscoring its potential importance in regulating metabolism [192]. Wild-type TMEM127 protein co-localise with the aforementioned cellular structures with a punctate appearance whereas cells containing *TMEM127* variants which disrupt the transmembrane domains have been shown to display a characteristic diffuse cytoplasmic distribution [190, 191].

4.1.2 Proposed role of TMEM127 as a negative regulator of mTOR via mTORC1

Transcription signature analysis using micro-array expression profiling has shown that the *TMEM127*-mutant tumour signature was enriched for kinase receptors including those for IGF-1, PDGF, insulin and EGF [190]. The behaviour of these mutated TMEM127 has been described as most similar to *NF1*-mutant tumours, particularly in the hyperphosphorylation of mammalian target of rapamycin (mTOR) pathway targets [190].

The mammalian target of rapamycin (mTOR) has been identified as a target of several kinase receptor pathways and often deregulated in malignancy [193]. mTOR belongs to the phosphoinositide 3-kinase-Akt (PI3K-AKT) related kinase family, responding to growth factors, amino acids, and oxidative stress [194, 195]. Operative mTOR has been shown to be comprised of two functionally distinct complexes, mTORC1 and mTORC2. mTORC1 positively regulates cell growth and proliferation through promotion of anabolic processes (biosynthesis of proteins, lipids and organelles) and restriction of catabolic processes (i.e. autophagy) [193]. mTORC1 regulates growth through the translation of eukaryotic translation initiation factor 4E binding protein 1 (4EBP1) and ribosomal S6 kinase 1(S6K1) [194]. In contrast the role of mTORC2 was less well understood, however had been demonstrated to play a role in cell survival, metabolism, and proliferation [193]. Studies have shown that mTORC2

directly phosphorylated Akt at key sites which was required for Akt activation in response to growth factor signalling [194].

The demonstrated interaction between mTOR and TMEM127 was suggestive that TMEM127 plays a role as a negative regulator of mTORC1 signalling; *TMEM127* knockdown experiments have demonstrated increased phosphorylation of 4EBP1 and overexpression leading to reduced mTORC1 activity [190]. However, in the same studies, TMEM127 did not affect AKT15 phosphorylation, which was indicative that mTORC2, a substrate of AKT15, was not influenced by TMEM127 levels.

4.1.3 TMEM127 germline pathogenic variants and phaeochromocytoma and paraganglioma

TMEM127 germline pathogenic variants (PV) have been recognised as typical tumour suppressors, with the loss of heterozygosity demonstrated in PC/PGL in keeping with the two-hit model of tumorigenesis [190, 196]. There is an autosomal dominant pattern of inheritance [190]. *TMEM127* has been implicated in hereditary PC/PGL as the underlying driver in 2% of cases presenting with PC. To date, 111 unique variants have been identified occurring throughout the exon coding regions of the gene. Variants resulted more often in loss-of-function (including nonsense, splice site, frameshift, and start-stop variants) (n=66) than non-truncated forms (missense or in-frame deletions) (n=42)(p=0.03). Over 60% of these variants have been detected only once, and most non-truncated variants are found within the transmembrane domain, which comprises a third of the protein's sequence. An emerging genotype-phenotype correlation suggests that truncating variants are more common in patients with PGL or renal cell carcinoma than in those presenting solely with PC (35.8% vs 93%, $p < 0.001$) [127].

Patients harbouring a *TMEM127* germline PV predominantly present with phaeochromocytoma (85.5%) with a median age of diagnosis at 45 y (range 21-84 y) with a female preponderance (2:1 ratio) [127]. Multifocality was common with 33% of patients developing multiple tumours (usually bilateral PC), however, metastatic disease was less frequent. *TMEM127*-mutated PC/PGL were typically associated with a “mixed” biochemical phenotype, producing epinephrine and norepinephrine. Penetrance of *TMEM127* germline PVs is estimated to be lower than many other PC/PGL driver genes with one estimate of 30% by age 65 y [197]. As such the absence of family history for PC/PGL is not uncommon, being reported in only 25% of kindreds [196, 198]. PGL occur less frequently and clear cell renal cell carcinoma has been reported in 5.4% of cases [126, 199, 200]. The phenotype of a unifocal PC/PGL occurring later in life with no family history can cause erroneous misclassification into sporadic disease if germline molecular analysis is not pursued.

4.1.4 Current challenges with TMEM127 variant classification

Interpreting *TMEM127* variants has presented unique challenges. The American College of Medical Genetics (ACMG) had established standardised guidelines in 2015 for sequence variant interpretation, facilitating the categorization of variants as 'pathogenic,' 'likely pathogenic,' 'of uncertain significance,' 'likely benign', and 'benign' [66]. Correct classification was crucial for the management of affected patients and their families, as those patients with a *TMEM127* pathogenic variant require ongoing surveillance for recurrent PC/PGL. Furthermore, the relatives would require genetic counselling to assess the benefits of predictive testing. Variants of uncertain significance (VUS) were particularly problematic; as molecular impacts were not well understood, often producing insufficient or conflicting evidence to allow definitive classification as either benign or pathogenic, thus being uninformative for clinical decision making. The rarity of *TMEM127* associated PC/PGL and the fact that many variants were unique, combined with the complex molecular functions of TMEM127 protein, complicated the determination of variant pathogenicity. Despite efforts by expert groups to reclassify *TMEM127* variants using clinical and experimental data for functional evidence, the pathogenicity of over 30% of variants remained classified as having uncertain significance [127].

4.1.4 Emerging evidence supporting the role of RNA sequencing in variant curation

The advent of RNA sequencing (RNA-seq) via high throughput next-generation sequencing (NGS) of complementary DNA (cDNA) had revolutionised transcriptomics. This approach using short read cDNA sequencing allowed the delivery of comprehensive quantitative analysis of gene expression, alternative splicing and allele-specific expression [199, 201]. Deep profiling of the transcriptome provided insights into the molecular biology of tumours through the identification of differential gene transcript expression. Recent application of RNA-seq in hereditary cancer syndromes, outside of endocrine neoplasia, resulted in a 9.1% relative increase in the detection of pathogenic variants in one cohort and clarification of the pathogenicity in 88% of inconclusive cases in another [202, 203].

The challenge of managing patients without a clear molecular diagnosis due to *TMEM127* variants classified as 'of uncertain significance' is not to be underestimated. The ACMG guidelines recognised appropriately validated *in vivo* or *in vitro* functional studies as providing strong evidence (PS3/BS3) for variant interpretation [66]. However to date, despite the potential, RNA-seq had not yet routinely applied to determining the pathogenicity of *TMEM127* variants of uncertain significance. In this Chapter, it was proposed that RNA sequencing of tumour samples containing *TMEM127* variants classified as 'of uncertain significance' could contribute evidence that would facilitate reclassification into one of the more definitive categories.

4.2 Hypotheses

In this chapter it was hypothesised that sequencing of PC/PGL derived RNA from patients harbouring a *TMEM127* VUS had the potential to assist in variant classification through review of

i) *TMEM127* transcript expression levels
ii) Differential gene expression
iii) Variant allele frequency and copy number variation
iv) Splice site analysis

4.3 Aim

The aim of this chapter was to establish the role of RNA sequencing in variant classification.

4.3 Materials and methodology

4.3.1 Cohort selection, phenotypic features and germline molecular analysis

Appropriate cases were identified through a database search of the Cancer Genetics Diagnostic Laboratory (CGDL), Royal North Shore Hospital, Sydney, Australia. Search criteria included the histopathological diagnosis of phaeochromocytoma or paraganglioma with subsequent identification of the patient as harbouring a germline *TMEM127* variant ('pathogenic', 'likely pathogenic', or 'uncertain significance'). Two control PC/PGL tumour samples were included in these experiments, one from a patient identified as harbouring a germline *SDHB* pathogenic variant and another from a sporadic patient where no germline pathogenic variant had been detected. Phenotypic features for patients found to harbour a germline *TMEM127* variant included patient age, gender, hormone secretion, tumour location (phaeochromocytoma, thoracoabdominal or head/neck paraganglioma). Molecular features including variant details as per Human Genome Variant Society nomenclature, variant location relating to the four TMEM127 4 transmembrane regions, loss of heterozygosity (LOH) on germline analysis and variant pathogenicity determined by ACMG criteria (with the assistance of Varsome[204] and expert opinion within the CGDL), and ClinVar classification [https://www.ncbi.nlm.nih.gov/clinvar/]. *TMEM127* variant location was generated using cBioPortal Mutation Mapper [205].

4.3.2 RNA extraction

Formalin fixed paraffin embedded tissue sections (10 μx 4) were obtained from the relevant Anatomical Pathology departments throughout Sydney. RNA extraction was performed at the Westmead Institute of Medical Research, Sydney, as per established protocol using the RNeasy extraction kit (Qiagen, Germany). RNA was quantified (ng/μL) using the Qubit 4 Fluorometer (ThermoFisher) using the RNA broad range assay (Qubit RNA broad range assay kit).

Various markers of RNA quality and integrity (including RNA yield, integrity, size distribution, DV200) were assessed using the Agilent 2100 bioanalyzer. The RNA integrity number (RIN) was measured for each RNA extraction. RIN compared the ratio between isolated 18sRNA and 28s rRNA, with scoring of the ratios as a measure of RNA degradation using a numbering system of 1-10 (with 1 displaying the highest levels and 10 the lowest levels of RNA degradation). The DV200 was an assessment of the percentage of RNA fragments > 200 nucleotides, as the size distribution of the RNA varies greatly among the samples. A DV200 provided measurement as to the likelihood of whether high-quality RNA sequencing libraries could be prepared from poor quality FFPE; with DV_{200} > 70% being deemed as having high quality potential, 50-70% (medium quality), 30-50% (low quality), and < 30% as being too degraded.

4.3.3 RNA sequencing

RNA sequencing (RNA-seq) is a powerful method for qualitative and quantitative analysis of the transcriptome and was used for differential gene expression, detection of alternate splicing, and characterisation of novel transcripts. RNA sequencing was undertaken at the Australian Genome Research Facility (AGRF).

Library preparation was performed using Illumina's TruSeq stranded RNA sample preparation kit (TruSeq RNA Library Prep Kit v2) and protocol as this procedure had been documented as providing efficient whole transcriptome analysis across samples that had been historically difficult to analyse (of particular relevance to this study, with FFPE samples). Processing included the following steps.

1. cDNA Synthesis
    a. Purification of mRNA (via oligo(dT) beads)
    b. Fragmentation of mRNA with divalent cations and heat
    c. First strand cDNA synthesis (randomly primed)
    d. Second strand cDNA synthesis
2. cDNA library preparation
    a. DNA fragment end repair (blunt ending of DNA fragments)
    b. 3'-Adenylation of DNA fragments
    c. Sequencing adapter ligation (utilizing T-A pairing of adapter and DNA fragments)
3. Amplification of library via PCR

RNA whole transcriptome sequencing (TruSeq 50M paired end reads) was undertaken by AGRF using their in-house Illumina NovaSeq X Plus system. Image analysis was performed in real time by the NovaSeq Control Software (v1.7.5) and Real Time Analysis (v3.4.4), running on the instrument computer. Illumina DRAGEN BCL Convert 07.021.609.3.9.3 pipeline was used to generate the

sequence data in standard FASTQ format. Read depth was defined as the target number of sequence reads obtained for each sample. The cleaned sequence reads were aligned against the *Pinctada maxima* genome. The STAR aligner (v2.5.3a) was used to map reads to the genomic sequences. Transcripts were assembled with the StringTie tool (v2.1.4) utilising the aligned reads and reference annotation-based assembly option (RABT).

4.3.4 RNA sequencing bioinformatic analysis

Comprehensive bioinformatics was performed in tripartite collaboration between myself, Mr Matthew Andrews (bioinformatician, AGRF) and Dr Aidan Flynn (University of Melbourne).

4.3.4.1 TMEM127 expression levels

The default Trimmed Mean of M-values (TMM) normalisation method of edgeR (v.3.38.4) was used to normalise the counts between samples controlling for library size bias and to compare counts across sample groups.

4.3.4.2 Differential gene expression

EdgeR (v.3.38.4) was used to perform differential expression analysis to detect and quantify gene expression data (measured counts of reads mapped for each gene). A generalised linear model was then used to quantify the differential expression between the groups. Significant differentially expressed genes were defined as those with a false discovery rate (FDR of < 0.05, and summarised in a heatmap to display the top 50 differentially ranked genes. A multidimensional Scaling (MDS) plot was generated which indicated the distance between samples corresponding to the leading log-fold change between each pair of RNAseq samples whereby samples with similar expression profiles cluster together.

RNA sequencing data from these samples with *TMEM127* variants was then compared with RNA sequencing output of a bespoke PC/PGL dataset. The PC/PGL dataset comprised of by data from The Cancer Genome Atlas Program (187 PC/PGL samples or which 120 harboured germline PV), local Australian samples (42 PC/PGL samples of which 30 harboured known germline PV) and the A5 Alliance Project (98 PC/PGL samples, of which all harboured germline PV). Samples were grouped according to their underlying driver germline PV into 8 sub-types reflecting the key transcription pathways. Finally, Uniform Manifold Approximation and Projection (UMAP) algorithm was used for dimension reduction.

4.3.4.3 Copy number analysis

Variant calling was performed using Illumina DRAGEN software (version 07.021.645.4.0.3) RNA Somatic variant calling pipeline, against RefSeq human (GRCh38.p13) genome reference dataset

including the alternate contigs. Hard-filtered VCF files were passed to downstream CNV analyses using R package 'RNAseqCNV' (v1.2.2). The data from these analyses produced the depths and minor allele frequencies (MAF) of each variant, filtered out the low quality and/or low depth variant calls, and generated a set of CNV plots for each sample. Plots were subsequently created per-chromosome to visualise the P and Q arms and to assess the results for partial gain/loss. The majority of samples were examined using a minimum read depth of 15 with the exception of samples deemed to have low quality RNA metrics. Low quality samples were analysed with the depth threshold set at 6 to generate output. An estimation table was generated with alterations as estimated by Random Forest model.

4.3.4.3 Splice site analysis

Alternative splicing patterns of *TMEM127* were investigated in the sample V-PH-83T. StringTie results generated in the previous analysis were subset to only include *TMEM127* transcripts. The Gene Transfer Format file was uploaded for visualisation to IGV (v2.17.2) [206].

4.4 Results

4.4.1 Phenotypic features and molecular analysis

Phenotypic features and molecular analysis of the seven patients found to harbour a *TMEM127* variant are summarised in Table 4.1. The median age at diagnosis was determined to be 49 y (range 37-57 y). Four patients presented with PC (one with bilateral disease), one with an abdominal PGL and a gastric carcinoid, and two further with both PC and PGL (one abdominal and the other head and neck). Sequencing identified eight unique *TMEM127* germline variants within the seven patients; two *TMEM127* variants within a single PC sample (VPH-84T). Using ACMG guidelines two variants were classed as pathogenic (VPH-81T and VPH-84T) and the remaining five variants classified as VUS. Two samples were used as controls, one from a patient with an *SHDB* pathogenic variant and the other a presumed sporadic case. Overall, within this cohort, four variants were located within the transmembrane domains, two before TM1, one after TM1 (Figure 4.1).

Table 4.1. Phenotypic features, molecular analysis and variant classification of patients harbouring a *TMEM127* (NM_017849) variant

Sample ID	Age, y (F/M)	PC/PGL	Hormone secretion	Variant	TM domain	LOH **	Pathogenicity ^	ClinVar
VPH-80T	52F	PC (U)	**Met. 2968 nmol/24hr** **Nor. 4317 nmol/24hr** **Dop. 2906 nmol/24hr**	*TMEM12T* c.424_426delACC (p.Thr142del)	TM3	No	VUS (3P-0B) PM4, PM2	Not reported
VPH-81T	53F	PC (B)	**Nor. 8.7 (<0.9)** **Met. 19 (< 0.4)**	*TMEM127* c.117_120delGTCT p.Ile41Arg*39	TM1	N/A	P (16P-0B) PVS1, PP5	Pathogenic
VPH-82T	57M	PC/PGL	**Noradr. 3540 umol/24hr** **Adr. 591 nmol/24h** Dop. 3070 nmol/24hr	*TMEM127* c.50G>T, p.Ser17Ile	No	No	LB (1P-3B) BP4, BP1, PM2	VUS
VPH-83T	45F	PGL *	Not tested	*TMEM127* c.410-6T>G, p.?	No	N/A	LB (0P-6B) BS1, BP4	VUS
VPH-84T	51F	PC (U)	**'Elevated urinary adrenaline and metanephrine levels'**	*TMEM127* c.82G>T, p.Glu28*	No	Yes	P (10P-0B) PVS1, PP5)	Pathogenic
				TMEM127 c.121A>T, p.Ile41Phe	TM1	Yes	VUS (2P-1B) PP3, BP1	Uncertain significance
VPH-85-T	49F	PC (U)	Normet. 1940 pmol/L Met. 1070 pmol/L	*TMEM127* c.176G>A, p.Gly59Asp	No	N/A	VUS	Not reported

VPH-86T	37F	PC (B), HNPGL	**Met. 37.3 umol/24hr** **Nor. 12.6 umol/24hr** Dop. 1.59umol/24hr	*TMEM127* TCGCCGTTAGCTTCT p.Tyr178Phefs*67	c.532_533ins	TM4	Yes	VUS (PM4, PM2)	Not reported

Abbreviations: F; female, M, male, PC; phaeochromocytoma, PGL; paraganglioma, HNPGL; head and neck paraganglioma. U; unilateral, B; bilateral. Met; metanephrine, Nor; normetanephrine, Dop; dopamine, Norad; noradrenaline, Adr; adrenaline, TM; transmembrane domain location, LOH; loss of heterozygosity, N/A; not assessed, LP; likely pathogenic, VUS; variant of uncertain significance.

Bold = elevated catecholamine

* also presented with gastric carcinoid

** LOH identified on Next Generation Sequencing

^ As per ACMG criteria curated from Varsome and expert opinion within the CGDL, Sydney.

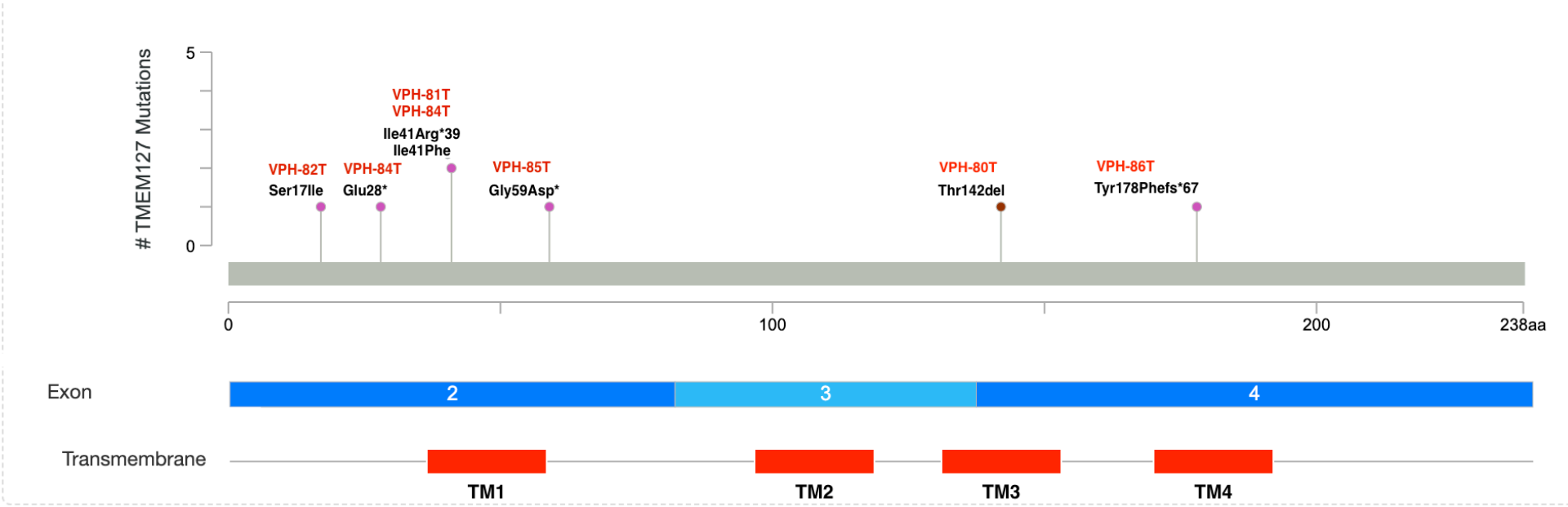

Figure 4.1 Variant location within the TMEM127 (NM_017849) gene: TMEM127 (NM_017849) variant (protein change) locations within the gene and the relationship to the four transmembrane (TM) domain amino acid locations (TM1 30-53, TM2 95-116, TM3 129-150, TM4 170-193). Corresponding sample ID codes are highlighted in red above the protein changes. Splice site variant not depicted in this image.

4.4.2 RNA extraction

RNA quality was low for all FFPE samples but high for the single fresh frozen tumour sample (VPH-88T). RIN measurements for the RNA isolated from all FFPE samples ranged from 1-3 (Table 4.2), and with an absence of 18S and 28S peak on electropherograms being indicative of highly degraded RNA (Appendix 1). Conversely, RIN was high for the fresh frozen tumour sample at 8.8 with a clear peak at 18S and 28S on the electropherogram indicating high quality RNA. DV 200 was below threshold at < 30% with severely degraded RNA in two samples (VPH-81T and VPH-86T). It is well recognised that extracting high-quality RNA from FFPE tissue samples is challenging due to the extensive crosslinking and degradation caused by formalin fixation [207, 208]. Fresh frozen tissues are often preferred as they more readily produce higher quality RNA, thus the RNA assessments of the FFPE and fresh frozen samples used in this study were similar to published findings [208].

4.4.3 RNA sequencing

Mapping rates were between 78-88%, as expected for human samples, apart from the two previously identified as highly degraded samples (VPH-81T and VPH-86T). These two samples were excluded from subsequent analysis.

Table 4.2. RNA extraction from FFPE and fresh frozen PC/PGL tumour tissue

RNA Storage (Temp): -80°C RNA Extraction Method: Qiagen RNeasy FFPE Kit / RNeasy Plus Mini RNA Quantification Method: Qubit RNA BR assay Kit

Sample ID	Sample Type	Amount 10µm section	Elution vol. (µL)	Final vol. (µL)	Spectro conc. (ng/µL)	A260 /280	A260/ 230	Qubit (ng/µL)	TapeStation conc. (ng/µL)	RIN	Yield (µg)	DV200 (% fragments > 200bp)
VPH-80T	FFPE section	2	18	14	175.3	1.85	1.97	108	85.2	2.3	1.5	53.93%
VPH-81T	FFPE section	2	18	14	16.3	1.52	0.98	13.5	1.9	2.1	0.2	21.31%
VPH-82T	FFPE section	2	18	14	336.3	1.91	2.02	279	169.6	2	3.9	49.71%
VPH-83T	FFPE section	2	18	14	94.7	1.83	1.68	89.6	29	3	1.3	33.82%
VPH-84T	FFPE section	2	18	15	-	-	-	34.3	22.2	2.3	0.5	52.53%
VPH-85T	FFPE	2	20	14	351	1.9	1.85	246	124	2.4	3.4	67.14%
VPH-86T	FFPE section	2	18	15	-	-	-	204	45.4	2	3.1	30.52%
VPH-87T (*SDHB*)	FFPE section	2	18	15	-	-	-	216	88.8	2.5	3.2	60.91%

VPH-88T (sporadic)	FFT	2	20	15	178.4	2.07	2.03	178	114		8.8	2.7	80.8%

Abbreviations: RNA, ribonucleic acid; FFPE, formalin fixed paraffin embedded; RIN, RNA integrity number.

4.4.5 RNA-Seq analyses: TMEM127 expression levels

TMM was used to measure *TMEM127* transcription (Table 4.3). TMM was low (~50%) for two samples: VPH-84T (PV, TMM 39.26) and VPH-80T (VUS, TMM 54.68). Conversely TMM for the other samples were all >100, similar to the TMM of the *SDHB* sample (VPH-87T) and sporadic (VPH-88T). When TMM read counts were compared between VPH-84T/VPH-80T and the other samples, there was a significant difference (46.97 *versus* 132.9, *p* 0.011).

Table 4.3 *TMEM127* expression levels

	VPH-80T	**V-PH-82T**	**V-PH-83T**	**VPH-84T**	**VPH-85T**	**VPH-87T**	**VPH-88T**
ACMG criteria	**VUS**	**VUS**	**VUS**	**PV**	**VUS**	***SDHB***	**(sporadic)**
Raw	657	1714	3024	633	1494	2051	5190
FPKM	9.12	18.36	29.56	6.86	20.50	19.59	18.52
TMM	54.68	107.66	169.90	39.26	110.07	119.87	157.18

Abbreviations: ACMG, American College of Medical Genetics. FPKM; fragments per kilobase, TMM; trimmed mean of M values.

4.4.6 RNA-Seq analyses: differential gene expression

MDS plot grouped three samples with similar expression profiles: the two samples with low TMM read counts (VPH-80T and VPH-84T) and a third sample (VPH-85T)(Figure 4.2a). Differentially expressed genes between this '*TMEM127* cluster' and the rest included signatures in the kinase signalling pathway (*RET*), adrenal medulla (*PNMT*) and steroidogenesis (*CYP11B1, CYP17A1, CYP11B2, STAR*)(Figure 4.2b).

We then compared RNA sequencing data from these samples with *TMEM127* variants to a bespoke dataset of PC/PGL classified according to their underlying driver germline PV into 8 previously validated sub-types reflecting the key transcription pathways. Using UMAP for dimension reduction, this showed clustering of these three samples (VPH-80T, VPH-84T and VPH-85T) towards the border of the kinase and cortical admixture group (Figure 4.2c). Interestingly, the remainder of the VUS clustered with the Receptor Tyrosine Kinase group. *SDHB* clustered appropriately with the SDHx group.

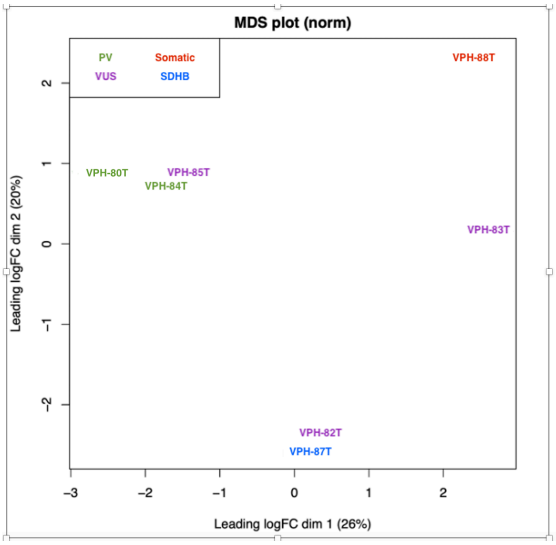

Figure 4.2a RNA sequencing *TMEM127* MDS plot

MDS plot with each dimension representing similarities/differences between samples calculated as the leading fold change based on RNA sequencing differential gene expression analysis. The two samples with low TMM read counts (VPH-80T and VPH-84T) and a third sample (VPH-85T) show similar expression profiles. Labelling; green, pathogenic variant; purple, VUS; red, somatic; blue, SDHB

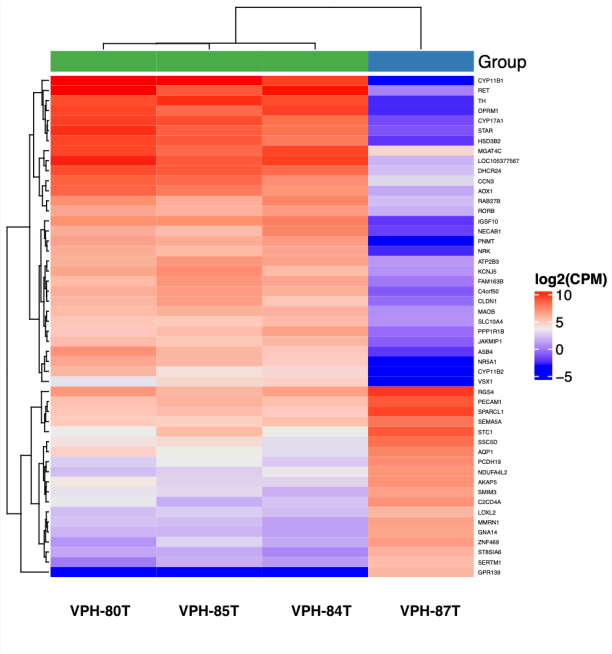

Figure 4.2b RNA sequencing *TMEM127* heat-map of differentially expressed genes

Gene expression heatmap comparing samples which clustered together on MDS plot (VPH-80T, VPH-84T and VPH-85T) with the control samples harbouring an SDHB pathogenic variant (VPH-87T). Relevant differentially expressed genes (FDR < 0.05) within the 'TMEM127 cluster' included RET, PNMT, CYP11B1, CYP17A1, CYP11B2 and STAR.

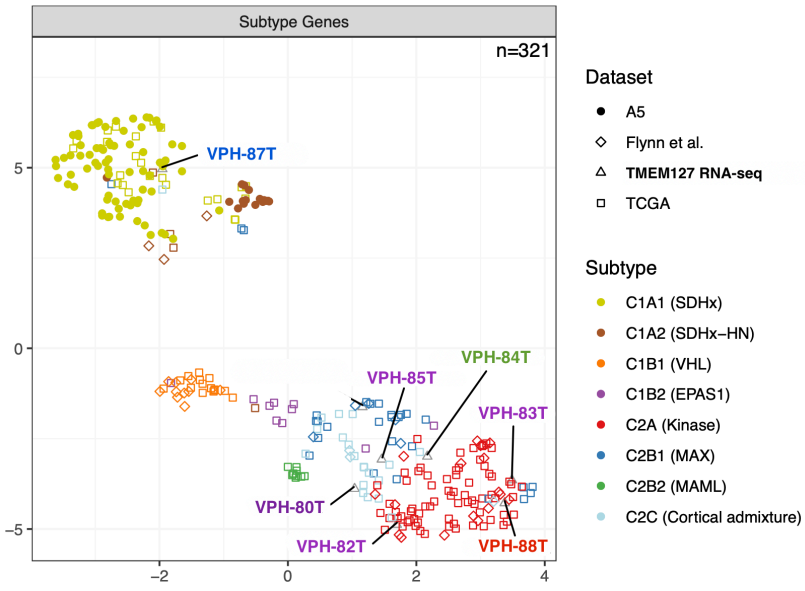

Figure 4.2c RNA sequencing *TMEM127* UMAP. UMAP plot generated to demonstrate similarities/differences in differential gene expression between our cohort of PC/PGL and a bespoke set of PC/PGL. This showed clustering of the same three samples together as previously demonstrated on MDS plot (VPH-80T, VPH-84T and VPH-85T) located towards the border of the kinase and cortical admixture group. Labelling; green, pathogenic variant; purple, VUS; red, somatic; blue, SDHB.

4.4.7 RNA-Seq analyses: Copy number analysis and LOH

There were no gross CNV abnormalities detected in chromosome 2 in any of the samples (Table 4.4). When looking specifically at the sample harbouring the established pathogenic variant (VPH-84T) whilst there was no evidence of CNV at a chromosome level (Appendix 2a) reviewing the arm level figures showed a reduced MAF (Appendix 3a). Similarly for the potential PV (VPH-80T) again whilst there was no evidence of CNV at the chromosome level (Appendix 2b) reviewing the arm level figure again showed a reduced MAF (Appendix 3b). These changes were not seen in any further samples.

Table 4. Summary of CNV abnormalities detected in RNA-sequencing samples

sample	gender	Ch	alterations
VPH-80T	female	46	?1p, ?2q, ?10q, ?13, ?14, ?16, ?18p, ?Xq
VPH-82T	male	46	?1p-, ?3q, ?4p, ?5p, ?6p, ?11p+, ?14, ?22
VPH-83T	female	46	1p-, ?4q-, ?6p+, 8p-, 11q+, ?17q, 18p-, ?21+, ?22
VPH-84T	female	46	1p-, ?21-
VPH-85T	female	46	?1p-, ?3q-, ?7p, 17p-
VPH-87T (SDHB)	male	46	?1p-, ?11p, 18p-
VPH-88T (sporadic)	female	46	1p-, 3q-, 17p-, ?Xp

Abbreviations; Gain: Ch, chromosome; gain; "+"; loss: "-"; double gain (and higher); "++"; double loss; "--". 'p' and 'q' specify the chromosomal arms. '?' signifies low confidence CNV calls

4.4.8 RNA-Seq analyses: Alternative splicing

Sample VPH-83T, from a 45F with an aortocaval PGL and gastric carcinoid, harboured a germline variant NM_017849.4 (*TMEM127*)c.410-6T>G. This single nucleotide substitution at the -6 position in intron 3 was currently classified to have no effect on the canonical acceptor splice site. This variant has not been reported in population databases (LOVD) although has been reported in ClinVar (two submissions) and has been classified as having 'conflicting classifications of pathogenicity' (ClinVar ID: 801731, VUS). *In silico* splicing prediction tool (SpliceAI, MaxEnt, NNSPLICE and SSF) predict this variant to not significantly affect the canonical acceptor splice site. In the absence of RNA studies this variant was classified as a VUS.

Studies performed in this chapter, specifically on the RNA extracted from the tumour sample harbouring the germline splice site variant NM_017849.4(*TMEM127*):c.410-6T>G and two assemblies were generated (30458.1 and 30458.2). Surprisingly we did not identify the variant at the -6 position of intron 3 (Figure 4.3) reported in the germline whereby the acceptor sequence of intron 3 showed the nucleotide at the -6 position aligning with the reference sequence TTgatcctctg, rather than the expected change detected on germline sequencing of TTgatccgctg (where lowercase represents the intron and red the nucleotide of interest). However, an alternative splice site was identified in the second assembly (30458.2) in exon two (Figure 4.4). The implications of this finding warrant further investigation.

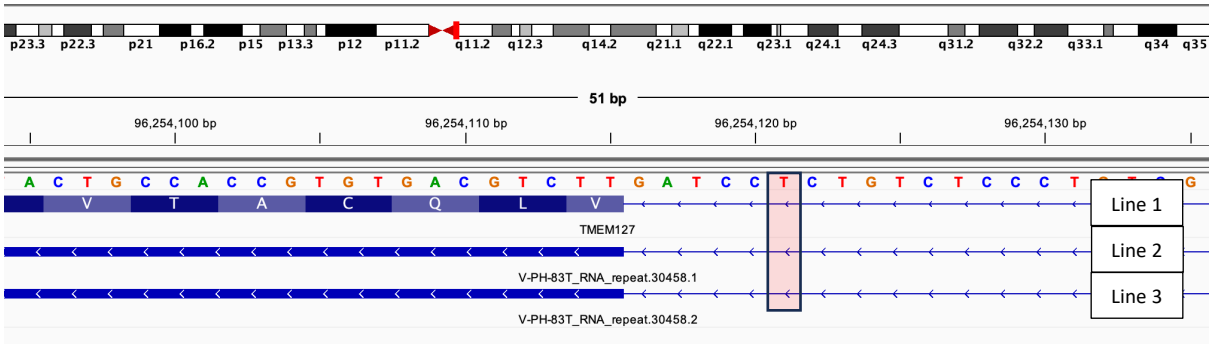

Figure 4.3. RNA sequencing of sample VPH-83T intron 3 splice site. RNA sequencing output visualised on IGV showing the reference sequence (RefSeq, NCBI) of TMEM127 (line 1) and the two TMEM127 assemblies generated from sequencing RNA extracted from the VPH-83T sample (30458.1 and 30458.2). The acceptor sequences of intron 3 (line 2 and line 3) in the lower window show the -6 position aligning with the reference sequence.

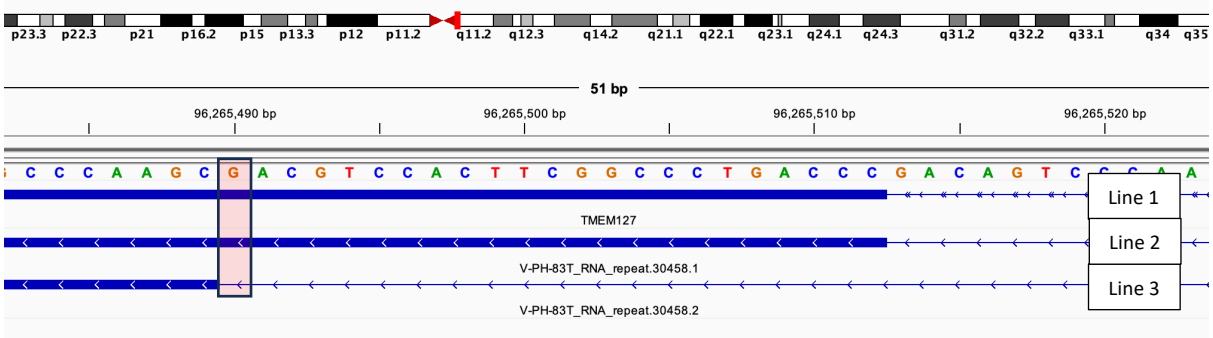

Figure 4.4 RNA sequencing of VPH-83T alternative splice site exon 2. RNA sequencing output visualised on IGV showing the reference sequence of TMEM127 (line 1) and the two TMEM127 assemblies generated from sequencing RNA extracted from the VPH-83T sample (30458.1 and 30458.2). Image showing the alternative splice site in the second assembly (30458.2) in exon two.

4.5 Discussion

Within this chapter it was proposed that integration of RNA sequencing data could complement current variant curation techniques. These studies have demonstrated that whole transcriptome analyses can provide functional characterisation and quantification of transcript gene expression, as well as differential gene expression, copy number analyses, and interrogation of alternative splice sites, particularly in the classification of the pathogenicity of a cohort of rare *TMEM127* germline variants.

Reduced *TMEM127* gene expression, and consequently reduced TMEM127 protein function, was found to be readily assessed through several approaches. Whilst genes harbouring nonsense variants are well known to result in loss of protein function through non-sense mediated decay (ultimately resulting in degraded transcripts), splice site and non-coding variants in regulatory regions (i.e. promotors, enhancers, large deletions) have also been found to produce aberrant protein expression [209]. Several normalisation methods including RPKM, FPKM and TMM were performed. Whilst RPKM has been calculated for single-end RNA-seq, where each read corresponds to a single fragment sequence, FPKM has been used in pair-end sequencing (as each fragment will have two reads) [210]. This was the approach adopted in this study and thus was used when comparing regions within a single sample. The TMM approach calculated the fold changes and absolute expression levels relative to a reference sample, and was deemed to have shown most utility when comparing expression levels across different groups [211].

Using TMM we were able to demonstrate significantly reduced expression in two samples; one within a sample from a patient harbouring an established *TMEM127* germline PV (p.Glu28*) and another from a patient harbouring a *TMEM127* VUS (p.Thr142del). These study findings were in agreement with previous functional analyses measuring TMEM127 transcription levels using real time PCR, which had shown a four-fold decrease in the expression of *TMEM127* in samples with *TMEM127* PVs compared to those from non-*TMEM127* variants from varied genetic backgrounds [190].

MDS analysis identified three samples, including VPH-84T associated with a *TMEM127* germline PV [NM_017849(*TMEM127*): p.Glu28*) and VPH-80T and VPH-85T associated with *TMEM127* VUS ([NM_017849(*TMEM127*):c.424_426delACC*), [NM_017849(*TMEM127*):c.176G>A]) which we will term the ‘TMEM127 Cluster’. Differential expression identified this ‘TMEM127 Cluster’ to show upregulated expression of genes associated with kinase signalling pathway and adrenal medulla (*RET*, *PNMT*) and some genes involved in steroidogenesis, a key role of the adrenal cortex (*CYP11B1, CYP17A1, CYP11B2, STAR*). *PNMT*, the gene which encodes the enzyme that converts norepinephrine to epinephrine, has been reported by others to be most highly expressed in the kinase signalling subtype [67]. If validated as a functional assay (ACMG guidelines code PS3), these RNA-seq data would

upgrade the *TMEM127* variants p.Gly59Asp (in VPH-80T) and p.Thr142del (in VPH-85T) from VUS to likely pathogenic.

Recently, cortical admixture has been considered a contaminating artefact of sample preparation, however it is notable samples containing *TMEM127* PVs are seemingly over-represented in the cortical admixture cluster (C2C). Whether this proves a *bona fide* phenotypic marker for *TMEM127* PVs requires further study. Previous studies using mRNA methylation analysis of the cortical admixture subtype of PC/PGL found these tumours exhibited the PC/PGL methylation profile, rather than that of normal adrenal cortex, suggesting cortical admixture tumours are not defined by adrenal cortex molecular features [67]. Similar to *TMEM127,* another germline PV which causes alterations in the kinase signalling pathway and predisposes patients to phaeochromocytoma and paraganglioma is *MYC-associated factor X (MAX).* Intriguingly germline pathogenic variants in *MAX* has also occurred in the cortical admixture sub-type [67].

Splicing is the removal of introns from the pre-mRNA primary transcript. All introns contain two highly conserved dinucleotides and splice site variants affect splicing donor (+1 and +2) or acceptor (-1 and -2) sites at the exon-intron boundary. The nucleotide sequences at the donor and acceptor sites are GT and AG, respectively, and are required to interact with the U2 spliceosome to facilitate the generation of wild-type transcripts [212, 213]. Aberrant splicing is well known cause of gene dysfunction, particularly splice site variants occurring at the exon-intron boundary, known as 'canonical splice site' variants with predicted loss of function [66]. Variants occurring in the sites can easily be predicted to result in pathogenicity. Variants occurring in the 'near splice' region [214], within 100 base pairs of exon-intron boundaries, and deep intronic variants are more recently being recognised to also disrupt splicing [215]. Within this study, the germline *TMEM127* PV intronic variant (NM_017849.4 (*TMEM127*) c.410-6T>G) identified in a 45F with an aortocaval PGL and gastric carcinoid, was not detected on RNA-seq. However, an alternative splice site was detected in exon two. These findings warrant further investigation.

4.6 Conclusion

RNA-seq shows promise as a functional assay to validate *TMEM127* variant classification. This chapter highlights several approaches using RNA-seq and, if validated, would upgrade two *TMEM127* variants of uncertain significance to likely pathogenetic. The implications of this change in classification would be two-fold; for the patient, ongoing surveillance would be appropriate, due to the multifocal nature PC in patients harbouring a *TMEM127* PV. Further, immediate relatives should be referred to a FCS for genetic counselling and consideration for genetic testing, due to the autosomal dominant nature of *TMEM127*.

CHAPTER 5

Multiple Endocrine Tumours Associated with Germline MAX Pathogenic Variants: Multiple Endocrine Neoplasia Type 5?

CHAPTER 5. Multiple Endocrine Tumours Associated with Germline *MAX* Pathogenic Variants: Multiple Endocrine Neoplasia Type 5?

Rare molecular causes of PC/PGL pose a challenge to clinicians regarding surveillance recommendations; at what age to commence, how frequent, which organs to review. This chapter reports multifocal PC/PGL and other endocrine and non-endocrine tumours occurring in a patient harbouring germline pathogenic variant in *MYC-associated factor X* (*MAX*), and was included in a larger published case series proposing this genetic subtype be termed Multiple Endocrine Neoplasia Syndrome Type 5.

5.1 Introduction

MYC-associated factor X (*MAX*), was first associated with hereditary PPGL in 2011 [121]. MAX is a transcription factor and an essential component of the MYC/MAX/MXD1 axis, such that MYC-MAX heterodimers activate, and MAX-MXD1 [and other MXD family members] heterodimers repress, transcription through the same E-box DNA recognition sequences [216]. The resultant equilibrium regulates cell proliferation, differentiation, angiogenesis and apoptosis. MYC is a key oncogene, with overexpression evident in many tumour types, including neuroblastoma (specifically by *MYCN* amplification)[217] and *MAX*-associated PC/PGL [121]. *MAX* pathogenic variants (PV) that prevent homo- or heterodimerisation lead to a loss of repression and overactive MYC signalling, as MYC can function - at least in part - independently of MAX [218]. Thus the major role of MAX in the MYC/MAX/MXD1 axis is as a tumour-suppressor gene [216] and it has been suggested this axis may represent a convergent pathway for upstream PVs in other PC/PGL susceptibility genes [219].

Germline PC/PGL-associated *MAX* variants have been identified in all five exons and include nonsense and missense variants as well as large deletions [121, 123, 220, 221]. In common with *SDHD*- and *SDHAF2*-associated PC/PGL [90, 96] a parent-of origin effect due to paternal uniparental disomy has been reported in some families [121, 123, 217, 222]. *MAX*-associated PC/PGL are often bilateral at presentation; and metastatic and/or asynchronous disease is common [123, 220, 223]. Whilst MAX-associated PC are classified as Cluster 2 PC/PGL (i.e., affecting the tyrosine kinase pathway) which typically show an adrenergic catecholamine secretory pattern, these tumours may show a mixed noradrenergic/adrenergic phenotype [123, 219].

In 2014 a family with a *MAX* PV with PC and other neural crest tumours was reported [224] and it was suggested that *MAX* PVs might cause a novel form of multiple endocrine neoplasia (MEN). Petignot *et al*. recently published a family with an intragenic exon 3 deletion, in whom the affected father manifested PC and a macroprolactinoma [222]; a low grade pancreatic neuroendocrine tumour was

identified in his son which on biopsy demonstrated loss of MAX nuclear staining and loss-of-heterozygosity [LOH] due to uniparental disomy. The authors similarly suggested *MAX* PVs as the cause of a novel MEN syndrome.

Here we present clinical, genetic, and immunohistochemical studies of an individual with a pathogenic germline *MAX* variant, associated with multifocal PC/PGL and other endocrine and non-endocrine tumours. In concordance with the suggestion of Petignot *et al*.[222], the evidence suggests that *MAX* should be considered a new cause of a unique multiple endocrine neoplasia (MEN) syndrome.

5.2 Materials and methods

5.2.1 Phenotyping

Clinical history was obtained from participating individuals and their treating physicians. Radiological and biochemical assessments were as per clinical need.

5.2.2 MAX Germline genetic analysis

Genomic DNA was extracted from blood, using Qiagen DNAeasy extraction kits (Qiagen, Germany) as outline in detail in Chapter 2. Panel sequencing was performed on germline DNA using a customised amplicon panel targeting PC/PGL genes. DNA libraries were prepared and sequenced on a MiSeq platform according to the manufacturer's instructions (Illumina). FASTQ files (containing reads and their base call quality scores) were generated for each sample; and alignment of reads (banded Smith-Waterman algorithm) and variant calling (GATK) was processed by MiSeq Reporter (version 2.0, Illumina). Annotation of functional consequences to variant calls was performed using ANNOVAR (v. July 2013). Visualisation of reads was performed using IGV (v2.1) [225]. Variants were analysed using *in silico* tools (Provean [226], Mutation Taster [227]) and classified according to ACMG criteria [66].

5.2.3 MAX Immunohistochemistry

Immunohistochemistry assessing MAX expression was performed by Professor Anthony Gill (Anatomical Pathology Department, Royal North Shore Hospital, Sydney) on FFPE tissue sections from parathyroid adenoma and lung adenocarcinoma using a commercially available rabbit anti-MAX1 polyclonal antibody C-17 (cat no: sc-197, Santa Cruz Biotechnology) at a dilution of 1 in 1000 after heat induced epitope retrieval in alkaline solution for 30 minutes at 97° C. Methodology is described in full in Chapter 2.

5.3 Results

5.3.1 Clinical details

This family's pedigree is presented in Figure 5.1. The proband (II.1) presented aged 21 y, with headaches, palpitations, diaphoresis and severe hypertension (blood pressure 280/180 mmHg). Bilateral PC were resected, with biochemical and clinical resolution. At age 34 y she represented with a large (80 x 50 mm) moderately differentiated (Grade 2) rib chondrosarcoma, successfully resected. Incidentally, an asymptomatic micro-prolactinoma (7 x 8 mm) was detected; this has remained stable in size and secretion over many years without dopamine agonist therapy. At age 60 y she developed primary hyperparathyroidism. Multiple lesions were evident preoperatively; histopathology of the three resected glands showed multiglandular parathyroid adenomas. At age 64 y, routine CT surveillance of the chondrosarcoma incidentally identified four spiculated ill-defined pulmonary lesions, with biopsy demonstrating well-differentiated lung adenocarcinoma. Fluorodeoxyglucose (FDG)-PET showed mild avidity of all opacities in keeping with the well-differentiated lesion. However, ^{68}Ga-DOTATATE-PET showed intense uptake in a soft tissue density adjacent to the crus of the right hemidiaphragm and a non-enlarged left abdominal para-aortic lymph node, with mild uptake in the pulmonary lesions, interpreted as metastatic PC (Figure 5.2). Plasma metanephrine and normetanephrine levels were normal.

The proband's deceased half-sister (II.2) had breast carcinoma and pancreatic carcinoma. Neither of these tumors were accessible for assessment and no germline DNA was available. No other family history was available.

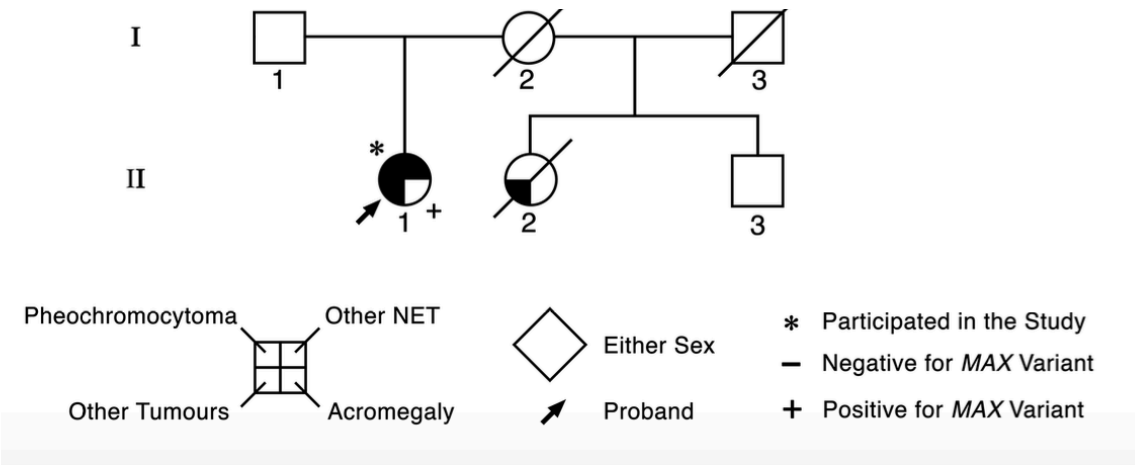

Figure 5.1 Pedigree of the *MAX* kindred. The proband (II.1) was affected with bilateral phaeochromocytoma (subsequently metastatic), pituitary micro-prolactinoma primary hyperparathyroidism (multi-glandular), chondrosarcoma and lung adenocarcinoma. The proband's sister (II.2) was diagnosed with breast and pancreatic cancer.

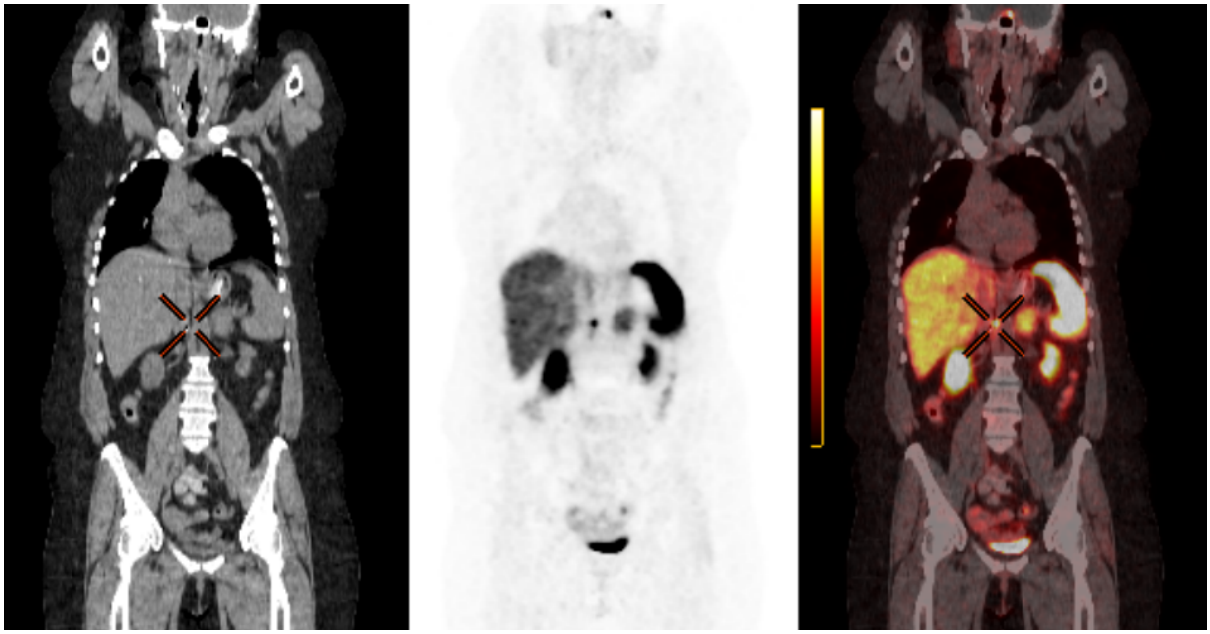

Figure 5.2 Functional imaging of the proband harbouring the MAX pathogenic variant. ^{68}Ga-DOTATATE PET for individual II.1 demonstrating metastatic disease with intense uptake localised to an abdominal para-aortic lymph node (cross-hairs).

5.3.2 Genetic testing

A novel heterozygous *MAX* variant (NM_002382.4: c.22G>T, p.Glu8*) was identified, not previously reported in population (gnomAD [228], 1000Genomes [229]) or variant (ClinVar [153]), HGMD databases)(Figure 5.3). The nonsense variant, early in exon 1, is most likely to cause nonsense-mediated decay, or, possibly, an extremely truncated protein (and as such was classified as 'disease causing' by Mutation Taster; PolyPhen and SIFT do not calculate scores for STOP variants). The variant fulfilled ACMG criteria as 'likely pathogenic'.

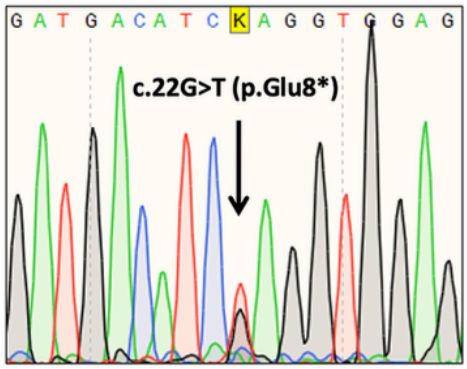

Figure 5.3 Electropherogram showing the *MAX* variant (NM_002382.4: c.22G>T, p.Glu8*)

5.3.4 MAX1 Tissue Immunohistochemistry

MAX1 immunohistochemistry was attempted on parathyroid and lung carcinoma FFPE samples but was considered uninterpretable (no staining in neoplastic cells or internal positive controls).

5.4 Discussion

This chapter describes a patient with a *MAX* PV, who developed bilateral PC (with metastatic disease detected many decades later) and multiple other endocrine and non-endocrine tumours. This patient demonstrated the highest number of tumours types (five) yet associated with *MAX* which emphasises the diverse tumour spectrum associated with *MAX* PV. The proband initially presented with PC at a young age with metastatic disease only detected decades later. Additionally, of the endocrine tumours, both PC and parathyroid adenoma were multifocal in nature. Her sister (II.2, now deceased) had two carcinomas. The absence of a family history of PC/PGL in this case is not surprising; a previous study of individuals with germline *MAX* PV and PC reported a family history of PC/PGL in only 37% [123]. Our data and other reports argue strongly that *MAX* is not only a PC/PGL-driver gene, but more broadly is a novel cause of MEN.

Co-occurrence of PC/PGL with pituitary neuroendocrine tumour (pituitary adenoma), coined the '3PA syndrome', was initially associated with pathogenic *SDHx* PVs [230], which remain the commonest cause of familial 3PAs (62.5-75% of cases) and of 3PAs overall (61.3%). Pituitary tumors in 3PAs are typically functional: a recent review of all 82 3PAs published case reports reported 17 prolactinomas, seven cases with acromegaly, and one case with combined prolactin/GH excess in the 31 individuals with identified germline PVs (including some with *MAX* variants), with 13 prolactinomas and 21 acromegaly cases in 51 individuals without an identified germline PVs [230]. Other PC/PGL genes are also associated with the 3PAs, including *MEN1* and *MAX*.

Our individual presented with PC and pituitary disease (a micro-prolactinoma) adding to a growing number of individuals previously identified with the 3PAs and germline *MAX* PVs. Seven individuals with a germline *MAX* variant, PC/PGL, and a pituitary neuroendocrine tumour (pituitary adenoma) have been reported (Table 5.1), six of whom had functional pituitary tumours (four prolactinomas, two somatotrophinomas)[221, 231, 232]; one study did not comment on secretory status [123]. Most were managed medically; tumour tissue from the single pituitary tumour resected surgically was unavailable for immunohistochemistry (IHC) or *MAX* sequencing. Thus, although a direct role of *MAX* in these pituitary neuroendocrine tumours remains conjectural, these cases suggest *MAX* may be a *bona fide* multiple endocrine neoplasia susceptibility gene.

Other endocrine tumours have also been reported in individuals with germline *MAX* PVs and PC, including ganglioneuroma [233], ganglioneuroblastoma [234], adrenomedullary hyperplasia [235], pancreatic neuroendocrine tumours [222], and parathyroid adenomas [123, 231], as have non-endocrine tumours including renal oncocytomas [123, 233], renal carcinomas[123, 199], breast carcinomas[123] and squamous cell tumours[123]. Somatic *MAX* variants have also been reported, in lung[236] [237] and endometrial cancer [238].

This case was included with another family (from Prof Emma Duncan) in a joint publication [239]. Our cases extended the phenotype associated with germline *MAX* PVs to include ganglioneuroma, neuroblastoma, composite PC/PGL tumors, chondrosarcoma, lung adenocarcinomas, pituitary adenoma and parathyroid adenomas. Ganglioneuroma and neuroblastoma share an embryological origin with PC and PGL, arising from neural crest cells which migrate to form the adrenal medulla and paraganglia [240]. We demonstrated loss of MAX immunohistochemistry in the neuroblastoma and most ganglion cells of the ganglioneuroma, though not loss-of-heterozygosity in the shards from the FFPE tumor blocks. This is the first time a neuroblastoma has been reported associated with a *MAX* PV. Neuroblastoma cause 15% of all paediatric cancer deaths [241]. In a cohort of 372 neuroblastoma tumors, LOH of chromosome 14q was observed in 22%, and specifically loss at 14q23, which locus contains *MAX* [31]. Notably, LOH at this site strongly correlated with LOH of 11q also, which was observed in the PC of an individual described in our publication. Somatic amplification and over-expression of *MYCN* (negatively regulated by MAX) is one of the most important and well established prognostic features of aggressive stage 4 neuroblastoma [217] and higher MAX expression correlates with more favourable neuroblastoma patient outcomes [242]. Our data suggests that germline PVs in *MAX* should be assessed in children with neuroblastoma.

We also reported a composite PC/ganglioneuroma. Thirty-five composite PC/PGL tumors have been reported previously, with germline PC/PGL driver genes *NF1*[243], *RET*[244, 245], *VHL* [246], and, most recently, *MAX* [234]; in the last case, the affected individual manifest a ganglioneuroblastoma, a composite PC/ganglioneuroma, bilateral and metastatic PC and a PGL.

MAX acts as a classic tumor suppressor gene, with somatic loss of the wild-type allele. Interestingly, of tumor suppressor genes that predispose to hereditary PC/PGL, *MAX* is one of the least tolerant to loss-of-function (LOF); in gnomAD [228], its probability of being LOF intolerant (pLI) is 0.83 (the closer pLI is to 1.0, the less tolerant the gene is to LOF), compared to pLI scores of 0.9 for *NF1*, 0.08 for *VHL*, 0 for *SDHA*, *SDHB*, *SDHC* and *SDHD*, 0.09 for *FH*, and 0.01 for *TMEM127*. Collectively, we interpret these data as being consistent with *MAX* having high penetrance for PC and may also explain the observed moderate penetrance for non-PC/PGL tumors as well.

Our families received clinical care over many decades and at many institutions, resulting in a lack of uniformity of biochemical and radiological testing and in availability of tumor tissue for this study. Pituitary imaging was ad hoc, according to clinical indication, rather than systematically assessed. We acknowledge also that we have not demonstrated LOH in the non-PC tumors reported here, due to lack of access to tumor samples, and/or poorly preserved specimens.

Our data, along with the recent papers of Pozza *et al.[234]* and Petignot *et al*.[222], are consistent with *MAX* as a novel MEN gene, encompassing a phenotype including classic MEN endocrinopathies (PC/PGL, pituitary and parathyroid disease) in addition to non-endocrine tumors, particularly those of neural crest origin. Our families highlight the requirement for lifelong surveillance in subjects with pathogenic *MAX* variants, for bilateral and/or metastatic PC, pituitary adenomas, and other endocrine and non-endocrine neoplasms. We recommend all individuals identified with pathogenic *MAX* variants should have a comprehensive baseline evaluation for PC/PGL, pituitary and parathyroid disease, including biochemical assessment (plasma or urinary metanephrines, pituitary profile and serum calcium/PTH) together with imaging (e.g. MRI from pituitary to pelvis and/or DOTATATE- or DOPA-PET). The timing and extent of follow-up assessments is evolving but should take account of a predilection for bilateral and/or metastatic pheochromocytoma.

5.5 Conclusion

This chapter describes a patient with germline *MAX* PV associated with multifocal PC/PGL and other endocrine and non-endocrine tumours. This case was combined with another Australian family for a publication in the *Journal of Endocrinology and Metabolism*, proposing this genetic subtype be termed Multiple Endocrine Neoplasia Syndrome Type 5. Our suggestion was subsequently endorsed by the WHO Blue Book on Endocrine Pathology. Patients with MEN5 should have routine surveillance for PC (often bilateral) and pituitary tumours. Further interrogation and collation of the phenotype of additional cases of patients with MEN5 will provide insights into the frequency of endocrine neoplasia and the development of a cost-effective surveillance protocol.

In keeping with a focus on rarer genetic subtypes of PC/PGL, the next chapter will describe somatic *EPAS1*.

Table 5.1. **Non-Pheochromocytoma/Paraganglioma Tumours Associated with Germline *MAX* Variants**

Publication	Gender	PC/PGL presentation	Age*	Subsequent PC/PGL	Other diagnoses and/or comments	Variant
Burnichon *et al.*	M	Bilateral PC	18	(not reported)	Primary hyperparathyroidism (age at diagnosis not given)	c.223C>T (p.Arg75*)
	M	Bilateral PC	24	(not reported)	C-cell hyperplasia (age at diagnosis not given)	c.97C>T (p.Arg33*)
	M	Unilateral PC	38	(not reported)	Squamous cell carcinoma of the tongue (age at diagnosis not given)	c.97C>T (p.Arg33*)
	F	Bilateral PC, four thoracoabdominal PGL	43	(not reported)	Breast carcinoma, renal oncocytoma (age at diagnoses not given)	c.73C>T (p.Arg25Trp)
	F	Unilateral PC	57	(not reported)	Renal carcinoma (age at diagnosis not given)	c.103C>T (p.Arg35Cys)
	M	Multiple PC	57	(not reported)	Pituitary neuroendocrine tumour (pituitary adenoma): size, secretory behaviour and age at diagnosis not given	c.220A>G (p. Met74Val)
Korpershoek *et al.*	M	Bilateral PC	28	Recurrent PC, diagnosed at age 46 years, initially thought unilateral, however, unilateral adrenalectomy non-curative; metastatic composite	Ganglioneuroma as part of composite metastatic tumour, diagnosed aged 47 years (also had beta thalassemia, sibling of individual below)	Complex *MAX* deletions and rearrangement (large (445kb) deletion encompassing *MAX* promoter areas and exons 1 and 2, and *FUT9*; 62bp intronic

				PC/ganglioneuroma tumor diagnosed at age 47 years.		deletion; 113 bp region duplicated and translocated in deleted region).
	M	Bilateral PC	45	No	Renal oncocytoma diagnosed contemporaneously with bilateral PC (n.b.: negative MAX staining on immunohistochemistry), erythrocytosis, (also had beta thalassemia, no *JAK2* mutation identified).	As above
Rozko *et al.*	F	Bilateral PC	49	No	Pituitary neuroendocrine tumour (macroprolactinoma) presented aged 49 (four months before PC diagnosis). Mild primary hyperparathyroidism (resolved following resection of PC).	c.296-1G>T (disrupting a canonical splice site acceptor site)
Daly *et al.*	M	Bilateral PC	22	Metastatic PC	Pituitary neuroendocrine tumour (GH-secreting macroadenoma), diagnosed aged 16 years.	Exon 1-3 del
	M	Unilateral PC	32	Recurrence of unilateral PC, diagnosed age 50	Pituitary neuroendocrine tumour (microprolactinoma), diagnosed aged 49 years	Exon 3 del

	F	Bilateral PC	35	No	Pituitary neuroendocrine tumour (GH-secreting macroadenoma), diagnosed aged 26 years; papillary thyroid cancer, diagnosed aged 35 years (n.b.: PTC heterozygous for *MAX* deletion and positive MAX staining on IHC; PCs homozygous for *MAX* deletion with negative MAX IHC)	Exon 4 del
Kobza *et al.*	F	Bilateral PC	39	Contralateral PC, diagnosed at age 50 years	Pituitary neuroendocrine tumour (microprolactinoma), diagnosed at age 33	c.171 +2T>A
Petignot *et al.*	M	(no PPGL to date)			Pancreatic neuroendocrine tumour (no functional information), diagnosed age 32	Intragenic exon 3 deletion
Pozza *et al.*	F	Composite PC-ganglioneuroblastoma;	15	PGL, diagnosed at age 20 years; contralateral PC, diagnosed at age 28 years.	Ganglioneuroblastoma diagnosed at age 11 months (including lymph node metastases); ganglioneuroblastoma re-presented as part of composite tumour with PC, at age 15 years.	c.299G>C (p.Arg100Pro)
Seabrook *et al.*	M	Bilateral PC	21	Recurrent unilateral PC at age 24 years; bilateral lesions medial to renal hilum (reported as PC) at age	Acromegaly with pituitary changes "consistent with but not diagnostic of somatotrophinoma" contemporaneously with first presentation with PC	c.200C>A (p.Ala67Asp)

			42 years; metastatic abdominal disease diagnosed aged 61 years.		
M	To date, not evident	-		Paravertebral ganglioneuroma, diagnosed aged 5 years	c.200C>A, (p.Ala67Asp)
M	To date, not evident	-		Abdominal neuroblastoma, diagnosed aged 8 months	c.200C>A (p.Ala67Asp)
F	Bilateral PC	21	Metastatic PC, diagnosed aged 64 years	Pituitary neuroendocrine tumour (micro-prolactinoma), diagnosed aged 34 years; thoracic chondrosarcoma, diagnosed aged 34 years; multifocal parathyroid adenomas, diagnosed aged 60 years; multifocal lung adenocarcinoma, diagnosed aged 64 years.	c.22G>T (p.Glu8*)

*age at time of first diagnosis of pheochromocytoma/paraganglioma biochemically, radiologically and/or histologically, rather than at symptom onset.Abbrevs: M, male. F, female. PC, pheochromocytoma. PGL, paraganglioma. IHC, immunohistochemistry. NMD, nonsense mediated decay. KB, kilobase. BP, base pair.

CHAPTER 6

Somatic *EPAS1* Pathogenic Variants in the Development of Sporadic PC/PGL

CHAPTER 6. Somatic *EPAS1* pathogenic variants in the development of sporadic phaeochromocytoma

6.1 *EPAS1* somatic mosaicism; a 10 year update since the discovery of Pacak-Zhuang Syndrome

6.1.1 Introduction

As with germline PV in hereditary PC/PGL, somatic PV occur within the molecularly defined groups based on transcription signalling pathways; pseudohypoxia, kinase signalling, Wnt-altered, and cortical admixture [67]. Somatic pathogenic variants (PV) have been identified in up to 37% of PC/PGL; most frequently within the following genes *NF1*, *RET*, *HRAS,* and *EPAS1*, of which the last two genes occur in sporadic disease exclusively [69, 70]. HIF-2α, the final protein produced in the pseudohypoxia pathway, is encoded by endothelial PAS domain-containing protein 1 *(EPAS1*) [247]. *EPAS1* (OMIM: 603349) is a 16 exon gene located at 2p21. HIF-2α, along with additional HIF transcription factors, play an essential role in the cellular response to fluctuating intracellular oxygen levels [248, 249]. In normoxia, alpha subunit hydroxylation by prolyl hydroxylase occurs at two proline residues, Pro405 and Pro531, leading to ubiquination by the VHL protein and subsequent proteosomal degradation.

Gain-of-function *EPAS1* somatic PVs have been identified as occurring in two hotspots, located on exon 9 and exon 12, and cause disruption of the aforementioned primary hydroxylation sites required for HIF-2α proteasomal degradation. Subsequent inappropriate accumulation of HIF-2α has been shown to promote the transcription of genes involved in cell proliferation, angiogenesis and metastasis. *EPAS1* gain of function somatic PV have been reported as frequent drivers of disease, accounting for up to 8% of PC/PGL based on molecular characterisation of a large volume of tumours [67, 250]. Post-zygotic mosaicism has been identified as occurring in a subset of these patients which manifests phenotypically with PC/PGL, polycythaemia and somatostatinoma, eponymously named Pacak-Zhuang syndrome in 2012 [247].

6.1.2 HIF-2α normal function

HIF proteins are highly conserved transcription factors composed of 2 sub-units, HIF-alpha (HIF-α) and HIF-beta (HIF-β) [251]. The beta sub-unit is constitutively expressed whereas the alpha sub-unit is inducible by hypoxia. HIF-α exists as three isoforms; HIF-1α, HIF-2α and HIF-3α [252]. HIF-1α and HIF-2α have been extensively researched, with the former having been identified as being expressed in all cells, and the latter preferentially expressed in endothelium, kidney, heart, and tissues of neural crest origin [249]. It has been observed that HIF-1α is activated during short periods of severe hypoxia (O_2 < 1%), whereas the HIF-2α is activated under mild, prolonged hypoxia (O_2 1-5%) [137]. Healthy

replicating cells respond to increased oxygen requirements through the stabilisation of HIF-α which heterodimerizes with HIF-β and binds to target genes at hypoxia-responsive elements (HREs) and activates transcription [249]. Genes, and the respective protein products, regulated by HIF2-α are extensive and include *SLC2A1* (GLUT1), *VEGFA* (VEGFA), *EPO* (erythropoietin), and *TGF-α/β* (TGFα/β), among many others. Each gene identified to date has been shown to be involved in the response to hypoxia including glucose transport, angiogenesis, erythropoiesis, cell cycle proliferation and cell proliferation and differentiation [251]. HIF-α is regulated by the binding of prolyl hydroxylase (PHD) enzymes to two proline residues to the oxygen-dependant degradation domain [253]. Under normoxic conditions proline hydroxylation by PHD allows for HIFα recognition by the VHL-E3 ligase protein complex, targeting HIF-α for ubiquitin-mediated proteolysis in a continuous process [249]. Factor inhibiting HIF (FIH) has also been demonstrated to play a role through hydroxylation of an asparagine residue causing inhibition of binding with the transcription-dependant p300/CREB-binding protein [254].

6.1.3 HIF-2α and tumorigenesis

Hypoxia (resulting from increased cell division and disordered blood flow) and pseudohypoxia (whereby oxygen is present although unable to be utilised due to intracellular defects) in solid tumours is well recognised.[255] HIFs, including HIF-α, form part of the adaptive response of cancer cells to this hypoxic environment. The effects of accumulated HIF-α has been implicated in multiple 'hallmarks of cancer', including inducing angiogenesis, activating invasion and metastases, deregulating cellular energetics, and sustaining proliferative signalling [248, 256]. Oxygen-independent oncogenic pathways include both growth factor stimulation, and loss of function PV within cancer susceptibility genes. Increased expression of HIF-α has been detected in a variation of malignancies, most notably clear cell renal cell carcinoma, as well as pancreatic, lung, glioblastoma, and neuroblastoma, and is correlated with a negative prognosis resulting from aggressive and treatment-refractory tumours [257-259].

6.1.4 HIF-2α and PC/PGL

Whilst HIF-1α has been reported to be found in most cell types, HIF-2α has been found to be restricted to a small number of cell types, including neural crest cells [258]. Animal embryos have shown strong expression of HIF-2α in sympathoadrenal derivates of the neural crest with evidence supporting a function in carotid body development and catecholamine biosynthesis [260] [261]. It follows that EPAS1 expression also correlated with chromaffin cell differentiation in humans with HIF2α being the main isoform expressed in catecholamine secreting cells and hypoxia-induced stimulation of secretion of catecholamines [258]. The link between PC/PGL and hypoxic syndromes has been previously demonstrated, including cases which have been reported with cyanotic congenital heart disease and *EPAS1* SPV, being the driver in 80% of cases of PC/PGL [262]. Cases of sickle cell disease, an inherited

haemoglobinopathy whereby the oxygen carrying protein haemoglobin in red blood cells is impaired resulting in chronic anaemia, has also been demonstrated to be associated with early onset PC/PGL harbouring *EPAS1* SPV [263, 264]. Similarly, high altitude has also been identified as being a risk factor for PC/PGL [265]. The proposed unifying mechanism being that chronic hypoxia prompts the oncogenic mechanism of *EPAS1*-mutated chromaffin cells with positive selection for mutated *EPAS1* clones [263].

HIF-2α stabilisation has been marked as a critical step in the development of neural crest tumours [137]. HIF-α dysregulation within PC/PGL is unique being driven by aberrations within the pseudo-hypoxia (Cluster 1b) pathway inclusive of the gene encoding HIF-2α, *EPAS1*. Loss of function PV along this intracellular cascade, most notably *SDHA-D, SDHAF2, FH, EGLN1,* and *VHL* (Figure 6.1) result in HIF-2α stabilisation and neuroendocrine cell tumorigenesis [251, 253]. *SDHA-D* (collectively referred to as *SDHx*) are four genes encoding the mitochondrial succinate dehydrogenase enzymes; succinate dehydrogenase A-D. These enzymes play a key role in the citric acid cycle and the respiratory electron transport chain. Pathogenic variants within the *SDHx* genes impair the oxidation of succinate to fumarate resulting in accumulation of succinate and reactive oxygen species which impair prolyl hydroxylases and thus HIFα hydroxylation [259, 266]. PV in the homotetramer fumarate hydratase (encoded by the gene *FH*) disrupts the catalysation of fumarate to malate with subsequent increased intracellular levels of fumarate [267]. Prolyl-4-hydroxylase domain proteins (PHD 1-3) are three independent cytoplasmic dioxygenases that convent α-ketoglutarate to succinate and hydroxylate key proline residues within the oxygen-dependant degradation domain of the HIF-α sub-unit [268]. PHD2 (encoded by the gene *EGLN1*) is particularly crucial in the pseudohypoxia pathway in mammalian cells [269]. As mentioned above, PHD2 enzyme hydroxylates two conserved proline residues, Pro405 and Pro531, on HIF-2α permitting recognition and binding to the VHL protein [269]. *PHD2* PV disrupt this critical binding site. Lastly, *VHL* PV mutations result in failure of the VHL protein to recognise the hydroxylated HIFα protein targeted for degradation with resultant HIF-2α accumulation in VHL-related tumours [269].

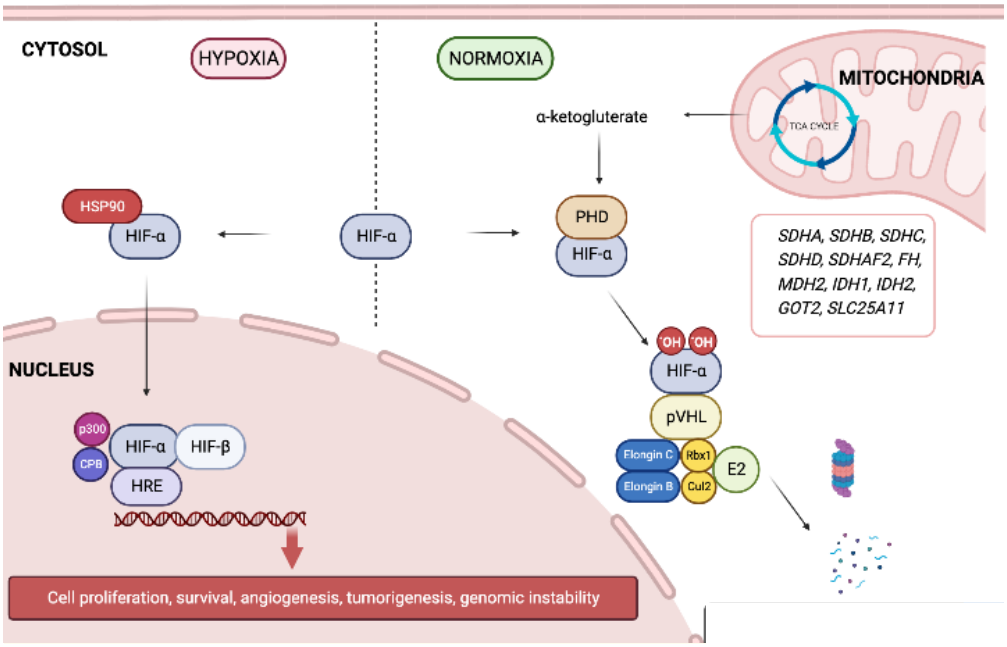

Figure 6.1 HIF-α regulation under normoxic and hypoxic conditions.

Abbreviations: CBP, cAMP-response element-binding protein; Cul2, cullin 2; E2, E2 ubiquitin-conjugating enzyme; HIF = hypoxia inducible factor; HRE, hypoxia-responsive elements; HSP90, heat shock protein 90; p300, histone acetyltransferase p300; PHD, prolyl hydroxylase domain protein; pVHL, von Hippel-Lindau protein; Rbx1 = ring box protein 1; SDH, succinate dehydrogenase; SSAT2 = spermidine/spermine N1-acetyltransferase 2; UQ, ubiquitin. Image adapted from Jochmanova et al.[251]

HIF accumulation has also been identified in PC/PGL driven by PVs within the kinase signalling pathway (Cluster 2). *RET* and *NF1* both cause dysregulation of the Ras pathway resulting in activation of MAPK, PI3K and mTORC pathways. *NF1* (encoding NF1, a GTPase activating protein) and the oncogene *RET* (encoding the RET tyrosine kinase receptor) both result in activation of Ras culminating in the phosphorylation of HIF-1α by extracellular signal-regulated kinase (ERK) and induction of *VEGF* [270]. Although currently their mode of action has not been elucidated, *TMEM127* and *MAX* appear to cause HIF-1α accumulation due to mTORC activation [251, 271].

6.1.5 HIF-2α functional studies

An array of functional studies has established the pathogenic role of *EPAS1* PV in PC/PGL. Studies examining the immunohistochemical staining of PC/PGL for HIF-1α and HIF-2α have been published. The findings have shown the presence of HIF-2α and absence of HIF-1α expression in PC/PGL tumour specimens [247, 272]. Gene expression analysis has demonstrated increased *EPAS1* mRNA levels similar to those found in SDHx- and VHL-mutated tumours supporting a key role within the

pseudohypoxia pathway [138]. Experiments investigating HIF2-α protein half-life within PC/PGL, calculated by cyclohexamine assay, have shown that mutants forms of HIF2-α protein were four- to six-fold more stable than wild type HIF-2α [247]. The same group also demonstrated decreased affinity of HIF-2α to the VHL protein and decreased Pro531 hydroxylation through immunoprecipitation and peptide binding assay [247, 272]. Finally, the effect of HIF-2α stabilisation has been demonstrated by several groups, with increased up-regulation of HIF-2α target genes within mutant *EPAS1* PC/PGL tumours with increased mRNA levels of *EDN1*, *EPO*, *VEGF*, *GNA14*, and *GLUT1* [247, 272].

6.1.6 Somatic and germline HIF-2α

EPAS1 has been identified as one of the most frequently occurring somatic events in the development of PC/PGL, reportedly being the driver in 5-8% of PC/PGL based on molecular profiling of large numbers of PC/PGL [67, 250]. A proportion of patients have also been reported to have developed somatostatinoma and polycythaemia resulting from post-zygotic mosaicism [273]. As with other somatic PV in PC/PGL *EPAS1* variants occur independently of other PC/PGL susceptibility genes. Approximately 90% of *EPAS1* variants have been reported within a hotspot region between the amino acids Leu529 and Ser544 located on exon 12, with a minor proportion occurring within exon 9 [274]. PV within these two exons disrupt the Pro405 and Pro531 residues, the key prolyl hydroxylation sites, and nearby amino acids (i.e. Ala530, Asn539, Tyr532) impairing recognition of the hydroxylation domain by PHD2 [138]. Pathogenic variants described to date have been primarily missense, insertions, and deletions. Copy number alteration, with the exclusive gain of chromosome 2p, has been demonstrated in *EPAS1* PC/PGL [138, 253]. Interestingly, with the identification of two heterozygous *EPAS1* SPV occurring in *cis* having been sequenced in the same tumour, this finding has been proposed to also result in stabilisation of HIF-2α [253].

There are few cases of PC/PGL developing in the context of an underlying *EPAS1* germline PV.[275] Although several cases have been described with the variant NM_001430.5(*EPAS1*):c.1121T>A (p.Phe374Tyr), the pathogenicity of the variant has not been established [253, 275]. The germline PV variant in *EPAS1* exon 9 (EPAS1 Phe374Tyr) was identified in a patient with congenital polycythaemia who subsequently developed PC/PGL. However, this variant is not located within the typical hot-spot region and there was no LOH or alternative somatic *EPAS1* mutation within the tumour, suggesting this variant may be predisposing rather than causative [275]. A further three germline *EPAS1* pathogenic variants were reported by Dwight et. al [NM_001430.5(*EPAS1*):c.739C>A (p.Arg247Ser), :c.1121T>A (p.Phe374Tyr), and :c.2353C>A (p.Pro785Thr)] which were demonstrated to share some functional aberrations similar to the SPV NM_001430.5(*EPAS1*):c.1591C>A (p.Pro531Thr) suggesting a co-pathogenic role [276].

6.1.2 Aim

The aim of this chapter is to summarise the current body of literature describing the phenotypic presentation of patients assessed for Pacak-Zhuang syndrome resulting from *EPAS1* somatic pathogenic variants, and from these findings propose recommendations for surveillance.

6.1.3 Methodology

PubMed searches were performed spanning 2012-2023. 'Title-abstract' search terms were as follows; (*pheochromocytoma OR paraganglioma) AND (HIF2alpha OR EPAS1 OR Pacak-Zhuang Syndrome*). Manual review of each paper was undertaken to collate relevant articles reporting cases with PC/PGL and *EPAS1* somatic PV. Cases with *EPAS1* germline PV were excluded. Data collected included age of primary PC/PGL diagnoses, PC/PGL location (adrenal, abdominal, thoracic, head and neck), and focality (unifocal, multifocal), tumour behaviour (recurrent or metastatic), hormone secretion, functional imaging, associated diagnoses (somatostatinoma, polycythaemia, erythrocytosis, ocular manifestations, other tumours), and results from molecular analyses.

Clinical features were compared using Fisher exact test for categorical variables and Mann-Whitney U-test for continuous variables. A p value of ≤ 0.05 was considered statistically significant.

6.1.4 Results

Pub-Med searches identified 3737 journal articles, of which 10 publications described the phenotype Pacak-Zhuang syndrome with PC/PGL and one additional tumour due to *EPAS1* somatic PV with a total of 30 cases (Table 6.1). There was a significant female preponderance of 26F:4M.

The mean age of primary PC/PGL diagnosis was 27 y (range 8 -78 y). The mean age at diagnosis in males was younger than females 13y versus 29 y ($p = < 0.01$) (Figure 6.2). Primary tumours comprised of PC (n=5), PGL (n=15) or PC/PGL co-occurring (n=10). The percentages of patients that presented with unifocal disease and with multifocal disease were 43% (n=13) and 56% (n=17) respectively. No statistically significant association between unifocal or multifocal disease was observed based on the site of primary tumour development; PC (all 5 unifocal) compared with PGL (8 unifocal *versus* 7 multifocal) ($p = 0.12$). Of the 29 patients reported to have had longitudinal follow up, 69% (n=20) developed recurrent disease with recurrence more likely to have occurred in patients with PC (n=8) compared with PGL (n=12) (89% *versus* 60%; $p = 0.02$). Of the 20 patients with longitudinal follow up, 25% (n=5) were diagnosed with metastatic disease which occurred exclusively in patients with PGL (n=7) compared with PC (n=0) (100% *versus* 0%; $p \leq 0.01$). PC/PGL were purely noradrenergic (n=20) or co-secreting adrenaline and/or dopamine (n=6), and the remainder non-functioning (n=3). Functional imaging was determined to be comprised of ^{123}I-MIBG, F-DOPA, ^{18}FDG-PET and ^{68}Ga DOTATATE.

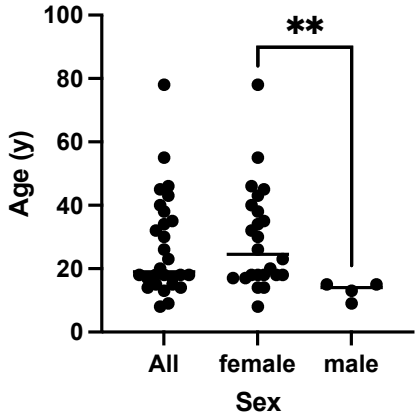

Figure 6.2: Mean at diagnosis of primary PC/PGL of patients with Pacak-Zhuang syndrome Scatterplot showing age (*y*-axis) and patients grouped into all (female and male), and divided into sex (*x*-axis). The mean age at diagnosis for all patients was 27 y (range 8 -78 y). The mean age at diagnosis in males was younger than females (13y versus 29 y, $p = < 0.01$)

Of the 18 cases investigated for somatostatinoma 72% (n=13) were identified. The mean age of diagnosis was 30 y (range 18-59 y) (Figure 6.3). The mean age at diagnosis in females was 31 y (range 18 – 59 y) compared with a single male patient, aged 19 y. Where specified, all tumours were reported to be located within the duodenum (n=7) with some co-occurring in the pancreas (n=3). Multifocal (n=8) and metastatic disease (n=2) were also described, with 9 being identified as hormone secreting (defined as a somatostatin level > 53pg/ml), with the remaining cases being diagnosed on histopathology following biopsy or resection.

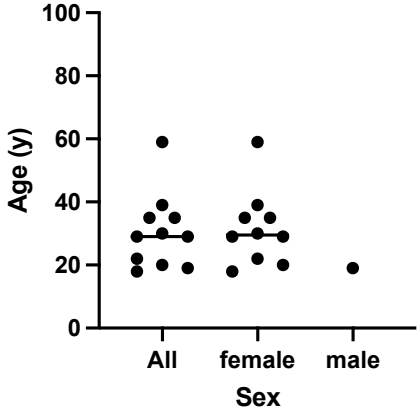

Figure 6.3: Mean at diagnosis of somatostatinoma of patients with Pacak-Zhuang syndrome. Scatterplot showing age (*y*-axis) and patients grouped into all (female and male), and divided into sex (*x*-axis). The mean age at diagnosis for all patients was 30 y (range 18- 59 y). The mean age at diagnosis in females was 31 y (range 18 – 59 y) compared with a single male patient, aged 19 y.

Non-endocrine manifestations of Pacak-Zhuang syndrome

There were 30 cases investigated for polycythaemia, 76% (n=29) were identified, of which 70% (n=21) were diagnosed under the age of 10 y and frequently at birth. When assessed, eye manifestations were frequently detected (particularly optic disc fibrosis). Further tumours detected included BCC (n=1), parotid adenoma (n=1), and uterine myoma (n=1), intraosseous haemangioma (n=1).

Molecular findings

Within the defined cohort of 30 patients there were 13 unique variants (11 missense, 2 in-frame deletions). All occurred within Exon 12. *EPAS1* c. 1589C>T (occurring seven times) followed by *EPAS1* c. 1591C>T, c.1586T>C, c.1588G>A (each occurring four times), *EPAS1* c.1615G>A (occurring 3 times) and the remainder only once.

Table 6.1 Publications describing the phenotype of patients diagnosed with Pacak-Zhuang syndrome

Author	PC/PGL						Ery.	Somatostatinoma			Ocular	Other tumours	*EPAS1* Variant	Exon
	Age (rec.)	M/F	Location	U/MF	Hor.	Rec./ Met.		Age	Location	U/ MF				
Abdallah, 2016 [277]	32	F	PGL	U	Nor.	U	No	-	-	-	-	No	c.1589C>T p.Ala530Val	12
Abdallah, 2020 [278]	15	M	PC, PGL	MF	Nor.	Rec	2y	19y		No	ODF	No	c.1591C>T, p.Pro531Ser	12
Buffet, 2014	45 (59)	F	PC	U	Nor.	Rec	16y	59y	duodenal	No	-	No	c.1586T>C p.Leu529Pro	12
[279]	9	M	PGL	U	NF	-	2y	-	-	-	-	IOH	c.1625T>C p.Leu542Pro	12
Comino-Mendez, 2013	18 (22, 26)	F	PC, PGL	MF	Nor, Dop	Rec.	1 y	-	-	-	-	-	c.1588G>A p.Ala530Thr	12
[138]	40	F	PC (bilat.) PGL	MF	Nor, Adr	-	No	-	-	-	-	BCC	c.1589C>T p.Ala530Val	12
	13 (22, 23)	M	PC, PGL	MF	NF	Rec.	7y	-	-	-	-	Parotid adenoma	c.1591C>T p.Pro531Ser	12

	18 (20)	F	PC, PGL	MF	NF	Rec.	1y	-	-	-	-	-	c.1592C>T p.Pro531Leu	12
	46	F	PC	U	-	-	No	-	-	-	-	-	c.1599_1604 del p.Ile533_Pro 534del	12
	43	F	PC	U	Nor., Adr	-	No	-	-	-	-	Uterine myoma	c.1600_1608 del p.Pro534_As p53del	12
	78	F	PGL	U	-	-	No	-	-	-	-	-	c.1615G>T p.Asp539Tyr	12
Darr, 2016 [280]	18 (21, 24)	F	PC, PGL	MF	Nor.	Rec.	<1*	22 y	Duodenal (pancreatic)	MF	ODF *	-	c.1589C>T p.Ala530Val	12
	35 (36, 38, 44)	F	PGL	U	Nor.	Rec.	7y	35 y	Duodenal	MF	ODF	-	c.1595A>C p.Tyr532Cys	12
	14 (23, 29, 31, 33)	F	PGL	U	Nor., Adr	Rec.	< 1*	29y	Duodenal (pancreatic) Metastatic	MF	ODF*	-	c.1588G>A, p.Ala530Thr	12
	17	F	PGL	MF	Nor.	-	5y	-	-		ODF*	-	c.1586T>C	12

	(20, 22, 25, 28)												p.Leu529Pro	
	8 (11)	F	PGL	U	Nor.	Rec. Met.	< 1*	-			ODF*	-	c.1615G>A p.Asp539Asn	12
	38 (39, 40)	F	PGL	MF	Nor., Adr.	Rec. Met.	2y	39 y	Pancreatic, duodenal Metastatic	MF	ODF	-	c.1615G>A p.Asp539Asn	12
	15 (17)	M	PC, PGL	MF	Nor.	Rec.	2y	-	-		ODF*	-	c.1591C>T p.Pro531Ser	12
Pacak, 2013 [247]	23	F	PGL	MF	Nor.	-	< 1*	29y	-	MF	-		c.1588G>A p.Ala530Thr	12
	26 (36)	F	PGL	U	Nor.	Rec. Met.	7y	35 y	-	MF	-		c.1595A>G p.Tyr532Cys	12
	18 (20)	F	PC, PGL	MF	Nor.	Rec.	< 1*	18y	-		ODF#		c.1589C>T p.Ala530Val	12
	17 (20)	F	PGL	MF	Nor.	Rec. Met.	5y	20y	-	MF	ODF#		c.1586T>C p.Leu529Pro	12
Pang, 2019	34 (39)	F	PC	U	Nor.	Rec.	30y	No	-	-	-		c.1589C>T p.Ala530Val	12

	30 (31)	F	PC, PGL	MF	Nor., Dop.	Rec.	30y	No	-	-	RH		c.1591C>T p.Pro531Ser	12
	55 (58)	F	PGL	MF	Nor.	Rec.	30y	No	-	-	ODF		c.1615G>A p.Asp539Asn	12
Taieb, 2013 [281]	20 (25, 27, 32)	F	PC	U	Nor.	Rec	< 1 y*	No	-	-	-		c.1589C>T p.Ala530Val	12
Yang, 2013	-	F	PGL	MF	Nor.	-	5 y	Yes					c.1586T>C p.Leu529Pro	12
[272]	-	F	PGL	MF	Nor.		7 y	Yes					c.1595A>G p.Ala530Glu	12
Zhuang, 2012 [273]	14 y (15, 23, 24, 27)	F	PGL	U	Nor.	Rec., Met.	Infancy	30 y	Duodenal	MF	ODF #	-	c.1588G>A p.Ala530Thr	12
	18 y (20)	F	PC, PGL	MF	Nor.	Rec.	Infancy	No	-	-	-	-	c.1589C>T p.Ala530Val	12

Abbreviations: PC, phaeochromocytoma; PGL, paraganglioma; U, unifocal; MF multifocal, Hor, hormone secretion; Nor., noradrenaline; Adr., adrenaline; dop, dopamine; OH, intra-osseuous haemangioma, RH; retinal haemangioma; BCC, basal cell carcinoma

*# from Pacak 2014 ocular manifestations paper; * from birth*

6.1.5 Discussion

Somatic post-zygotic mosaicism of *EPAS1* occurring in early embryogenesis underlies the development of multiple endocrine and non-endocrine manifestations within this non-familial disease [273]. The co-occurrence of PC/PGL, somatostatinoma and/or polycythaemia driven by mosaic somatic *EPAS1* was eponymously named Pacak-Zhuang Syndrome in 2012 [273]. Identification of mosaicism was substantiated in a study reported by Buffet *et al.* that quantified *EPAS1* in tissue [279]. This particular study found the variants to be present at low frequency in leucocytes (3.33%) and buccal cells (8.96%), yet high in paraganglioma cells (21.13%) whilst being absent in patient's relatives. It has been proposed that this variant allele frequency may correlate with the severity of the phenotype however others hypothesised that the earlier the development of the *EPAS1* PV, the more extensive the phenotype [280]. A further alternative to this hypothesis was that tissue specific variations in HIF-2α regulation may underly the phenotypic tumorigenesis, as described in von Hippel-Lindau disease [282]. A reason for the female bias is yet to be determined and may relate to hormone and gender-dependant copy number variations and signalling pathways relating to HIF2-alpha stability, with a functional oestrogen responsive element having been subsequently identified in the first intron of *EPAS1* [281, 283, 284].

'Syndromic' features of Pacak-Zhuang Syndrome

EPAS1 and PC/PGL

Findings detailed in this chapter have highlighted the early onset of PC/PGL (mean age at diagnosis of PC/PGL 27 y, range 8 - 78 y) in Pacak-Zhuang syndrome, with males being diagnosed at a significantly younger age (18 y versus 31 y; $p < 0.01$). Multifocal disease at diagnosis of primary PC/PGL was also common, occurring in 41% of patients, and recurrence was high at 69%, being more likely to develop in patients with PC as the primary tumour. Regardless, prognosis was found to be very good with patients undergoing long-term follow up of metastatic disease not reported to require cytotoxic chemotherapy [285]. Hormone secretion was typically noradrenergic with some PC/PGL co-secreting dopamine or adrenaline. This finding reflected the poorly differentiated nature of cluster 1-mutated PC/PGL, with low expression of the phenylethanolamine N-methyltransferase (the enzyme required for the methylation of noradrenaline to adrenaline) in PC/PGL harbouring *EPAS1* [253, 286]. This review also emphasises the variation of functional imaging utilised, including ^{123}I-MIBG, F-DOPA, ^{18}FDG-PET, and ^{68}Ga DOTATATE, with more than one modality frequently used. Although drawn from a small cohort, others have reported 18F-DOPA PET/CT was suggestive of being superior functional imaging of choice with a greater overall sensitivity [280]. This finding differed from the use of Ga68 DOTATATE, which has been previously described as being superior in functional imaging of cases found to contain variants in *SDHB* [280].

EPAS1 and duodenal somatostatinoma

Somatostatinoma, a rare neuro-endocrine tumour accounting for < 1% of GI tract NETS [287], was identified in 69% of patients with Pacak-Zhuang syndrome at a mean age of 30 y (range 18-59 y). All somatostatinoma were reported to have developed within the duodenum, with only a small proportion co-occurring within the pancreas. Phenotypically this mimics that seen in hereditary endocrine syndromes including multiple endocrine neoplasia type 1 (MEN1) syndrome and VHL disease who typically develop somatostatinoma in the third decade of life, have a lower risk of malignancy and predominantly duodenal location (with the exception of VHL where neuro-endocrine tumours typically develop in the pancreas) [165, 288]. Although Darr *et al*. [280] reported somatostatinoma occurred exclusively in women, a subsequent case has now been reported in a male [278]. Disease behaviour of somatostatinoma reported in this study differs significantly from sporadic disease whereby the mean age at diagnosis is 50-55 y, there is an approximately equal sex ratio, and were found to predominantly to have arisen within the pancreas [289, 290]. Hormone secretion is known to cause somatostatinoma syndrome resulting in abdominal pain, gall stones, weight loss, diabetes/glucose intolerance and diarrhoea/steathorrhoea [290]. Due to the high association with malignant disease in sporadic somatostatinoma, early detection is essential with resection of lesions > 1cm [280, 289]. It is yet to be decided if this management approach is also required in somatostatinoma developing within Pacak-Zhuang syndrome.

EPAS1 and polycythaemia

Polycythaemia is defined as an elevated haemoglobin concentration due to an increase in red blood cell mass resulting from increased production of erythropoietin [291]. Primary polycythaemia is characterised by the increased proliferation of erythroid progenitor cells from an intrinsic cellular defect, such as a *JAK2* PV [292]. Secondary polycythaemia is a physiologically normal response to tissue hypoxia (i.e. chronic lung disease, high altitude) or inappropriate secretion of erythropoietin (drug-induced, tumours producing excess erythropoietin, end-stage renal disease). Rarely germline PVs in genes within the aforementioned pseudohypoxia pathway have been linked with polycythaemia. Specifically the homozygous *VHL* c.598C>T variant causing Chuvash congenital polycythaemia and a case of a heterozygous germline *EGLN1* PV presenting with both congenital polycythaemia and paraganglioma [268, 293]. Germline *EPAS1* PV have been associated with hereditary polycythaemia although the association with PC/PGL is unclear, and with the pathogenicity of the variants in the few cases described with PC/PGL remaining uncertain to date [268, 294, 295]. In Pacak-Zhuang syndrome it was initially hypothesised that polycythaemia developed due to the up-regulation of hypoxia-induced genes by PC/PGL, as normalisation of erythropoietin was demonstrated following PC/PGL removal

[247]. However, the subsequent finding of polycythaemia in infancy, preceding the development of PC/PGL, confounded this theory. It has since been suggested that the erythrocytosis may be driven by more neural crest cells also harbouring an *EPAS1* PV, with the same embryological origins, distributed throughout the gastro-intestinal tract and nervous system [294]. Alternatively mosaicism involving the erythropoietin-producing renal interstitial cells has also been proposed [285]. Together, these findings are suggestive of dual pathways in the aetiology of polycythaemia in Pacak-Zhuang syndrome including a paraneoplastic phenomenon and HIF-2α stabilisation outside of neuro-endocrine tissue.

EPAS1 and retinal abnormalities

The most infrequently reported feature, albeit also the least screened for, are ocular manifestations. Pacak et al. were the first to report ocular manifestation of Pacak-Zhuang Syndrome [296]. Bilateral dilated capillaries and fibrosis overlying the optic disc were features frequently identified. Their study reported that two patients required anti-vascular endothelial growth factor agents for the management of complications including macula oedema and hard exudate. Following this finding further studies were published where ophthalmological reviews had been undertaken, detecting optic disc fibrosis in all [280]. Mechanisms proposed for the development of these ocular findings in Pacak-Zhuang syndrome included the shared neural crest origins of the retina or as a result of the potent angiogenic effect that erythropeitin has on the retina [296].

EPAS1 and other tumours

The occurrence of vascular malformations was first reported by Darr. *et al.* in 2016 where cystic lesions and haemangioma were detected in 57% of patients (n=4) [280]. Further, a series of sporadic central nervous system haemangioblastomas were found to harbour somatic EPAS1 pathogenic variants [281]. Following evidence that HIF-2α regulates the development of the arterial and venous system, radiological investigation by Rosenblum *et al.* for vascular malformations was undertaken on a cohort of patients with a history of PC/PGL known to harbour somatic *EPAS1* PVs [297]. This study found (in addition to congenital malformations of the eye as described above), a range of changes including intracranial venous and cavernous, and extrinsic and intrinsic spinal venous modifications.

Suggested screening

This study highlights the importance of PC/PGL tumour sequencing whereby identification of a somatic *EPAS1* PV alters patient management. Although it was unclear what proportion of patients harbouring a somatic *EPAS1* PV would be found to have Pacak-Zhuang syndrome~~,~~ due to somatic mosaicism, the almost universal finding of polycythaemia makes this diagnosis straightforward to investigate. The benefit of establishing a diagnosis of Pacak-Zhuang syndrome has implications for screening, with the

aim to detect tumours early. A surveillance protocol which reflects the phenotype including the age of onset of features, rate of progression, risk of multifocality or metastases would be appropriate. Although the number of current cases was comparatively small several recommendations were drawn from the above findings:

1) **commence screening for PC/PGL from age 8 y:** annual plasma or urinary metanephrines, 2 yearly anatomical imaging (CT/MRI); consider functional imaging with 18-F-DOPA PET/CT at baseline, 3-5 yearly, or if metastatic disease suspected

2) **commence screening for NET from age 20 y:** annual somatostatin levels; anatomical and functional imaging to align with PC/PGL screening

3) **screen for polycythaemia at diagnosis**: baseline haemoglobin, haematocrit

4) **screen for ocular manifestations at diagnosis:** baseline retinal imaging

Imaging modalities with radiation exposure (i.e CT) should not be used for lifelong surveillance, especially in childhood. We acknowledge that access to F-DOPA PET/CT may be limited to specific nuclear medicine departments in major tertiary hospitals.

Although not demonstrated, constitutional mosaicism should also be considered, as well as investigations for polycythaemia should be considered for offspring of patients diagnosed with Pacak-Zhuang syndrome.

Treatment

The other key motivation to investigate for a somatic *EPAS* is treatment-focussed. The recently developed HIF2-α inhibitor, belzutifan, is a selective small-molecule inhibitor of hypoxia inducible factor 2a. This targeted therapy was first demonstrated to be highly effective in patients with clear cell renal cell carcinoma [298]. Kahmihara *et al.* recently reported a response to belzutifan therapy in a 17 year-old patient with Pacak-Zhuang syndrome diagnosed with both severe polycythaemia and a noradrenergic multifocal paraganglioma [299]. There was a rapid biochemical response within several weeks of the initiation of belzutifan treatment, with a fall in biochemical markers (normetanephrine, chromogranin A and haemoglobin), a tumour response on anatomical and function imaging, and clinical improvement. High efficacy has been demonstrated on a larger scale in renal cell carcinoma (RCC) resulting from *VHL* pathogenic variant (resulting in the constitutive activation of HIF2a) [298]. In this phase 2 trial of patients with stable RCC nearly half had an objective response to treatment as assessed by RECIST 1.1 with only low-grade adverse events reported. Interestingly, responses to belzutifan treatment was also found in pancreatic NET, central nervous system haemangioblastoma and retinal angioma.

6.1.6 Conclusion

In conclusion, this comprehensive review of cases reported as having Pacak-Zhuang syndrome provides further insight into the phenotype confirming early onset of PC/PGL and somatostatinoma compared with sporadic disease, multifocality and metastases, and a female preponderance (however with an earlier age of tumour development in males). Surveillance recommendations aim to detect neuroendocrine tumours early to allow prompt intervention. Although not hereditary *per se*, clinicians should consider referring patients for genetic counselling to discuss the potential for constitutional mosaicism.

6.2 Molecular analysis for somatic *EPAS1* pathogenic variants in a cohort of patients with apparently sporadic phaeochromocytoma and phaeochromocytoma

6.2.1 Introduction

As outlined in detail in Chapter 6.1, HIF-2α, the final protein produced in the pseudohypoxia pathway, is encoded by the gene endothelial PAS domain-containing protein 1(*EPAS1)* [138]. Somatic gain of function *EPAS1* (OMIM: 603349) pathogenic variants (PV) have been identified as a frequent event implicated in the development of sporadic PC/PGL, occurring in 6-12% of patients who develop these rare neuroendocrine tumours. *EPAS1* PV occur in two hotspots located on exon 9 and exon 12 with resultant disruption of the primary hydroxylation sites required for HIF-2α proteasomal degradation [67, 253]. Subsequent inappropriate accumulation of HIF-2α has been shown to promote the transcription of genes involved in cell proliferation, angiogenesis and metastasis. Somatic post-zygotic mosaicism of *EPAS1* PV has manifested phenotypically with PC/PGL, polycythaemia, and somatostatinoma, and was eponymously named Pacak-Zhuang syndrome in 2012 [273].

6.2.2. Hypothesis

In this chapter it was hypothesised that sequencing of tumour-derived DNA extracted from patients diagnosed with apparently sporadic PC/PGL would uncover a cohort harbouring a somatic *EPAS1* PV. Further investigation for clinical features of Pacak-Zhuang syndrome would provide additional insights into the phenotype of this rare disease.

6.2.3 Aim

The aims of this chapter were to

1. Establish the prevalence of *EPAS1* PV in a cohort of patients with apparently sporadic PC/PGL
2. Undertake screening for features of Pacak-Zhuang syndrome in patients found to harbour a somatic *EPAS1* PV

6.2.4 Materials and methods

6.2.4.1 Cohort selection

'Apparently sporadic' cases of PC/PGL were identified through searches of databases within the Cancer Genetics Diagnostic Laboratory (CGDL), Kolling Institute, Royal North Shore Hospital (RNSH), Sydney, Australia. This laboratory is well renowned for its specialty expertise in genetic testing of patients with hereditary PC/PGL and receives a large volume of referrals. Apparently sporadic cases

were defined as patients with a PC/PGL resected and who had undergone genetic testing for a panel of genes known to be implicated in hereditary disease. This panel included (although was not limited to) *SDHB*, *SDHD*, *RET*, and *VHL*. Patients that had been identified as having apparently sporadic disease were then matched to fresh frozen PC/PGL tissue samples stored within the Kolling Institute Tumour Bank (KITB), Kolling Institute, RNSH, Sydney. Tumour sections weighing between 10-25mg were obtained from the KITB and stored at -80°C.

6.2.4.2 DNA extraction and sequencing

DNA was extracted from the PC/PGL tumour samples as per the established protocol using the DNEasy extraction kit (Qiagen, Germany) and *EPAS1* exon 12 cDNA was amplified by polymerase chain reaction as described in detail in Chapter 2. DNA sequencing was undertaken at the Australian Genome Research Facility (AGRF) and the .ab1 files containing the DNA sequence electropherograms were generated. Electropherograms were viewed on 4Peaks (v 1.8).

6.2.4.3 Patient screening for Pacak Zhuang syndrome

Patients found to harbour somatic *EPAS1* PV were recruited into the 'patient screening element' of the study and underwent assessment for features of Pacak-Zhuang syndrome. Assessment comprised of recording medical history and relevant investigations (including any pathology and imaging). Medical history included details of the diagnosis of PC/PGL (age at diagnosis, PC/PGL location, hormone secretion, PC/PGL behaviour [multifocal, metastatic]), presence of a specific history of polycythaemia, somatostatinoma, or vision impairment, and further diagnoses. Investigations included blood testing (plasma metanephrine / normetanephrine / 3-methoxy-tyramine, full blood counts [haemoglobin, haematocrit, erythropoietin], and somatostatin) and imaging (MRI, base of skull to coccyx).

6.2.5 Results

6.2.5.1 DNA extraction and sequencing

For this study, 62 apparently sporadic cases were identified within the KITB and samples obtained. DNA extraction, PCR and sequencing was successful in 59 of the cases. Of note, the somatic *EPAS1* PV (*EPAS1* [NM_001430.5] c.1589C>T, p.A530V) was identified (and confirmed by visual examination of the electropherograms) within 2 (designated patient A and patient B) of these 59 samples (3.4%)(Figure 6.4). This variant was located within the previously described *EPAS1* exon 12 hotspot.

Patient A **Patient B**

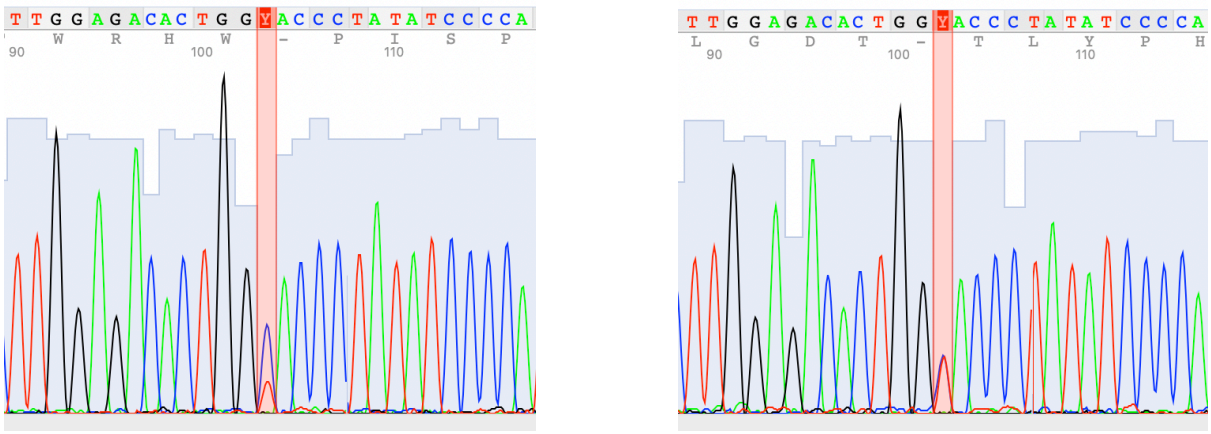

Figure 6.4 Electropherogram demonstrating the *EPAS1* PV identified in patient A and B. *Electropherogram demonstrating the substitution of the nucleotide C>T in codon 530 with resultant protein change from alanine to valine.*

6.2.5.2 Patient screening for Pacak-Zhuang syndrome

The clinical phenotype at baseline for each patient is outlined below and summarised in Table 6.2.

Patient A:

Patient A presented aged 22 y with hypertension and diaphoresis leading to a diagnosis of right sided phaeochromocytoma. There was no family history of endocrine neoplasia. Urinary catecholamines were reported to be 'elevated' (unfortunately the specific levels measured were unable to be sourced for this study). Haemoglobin and haematocrit were reported as normal. Computed tomography (CT) abdomen scanning results identified a 6 cm right adrenal mass. Following alpha-blockade with phenoxybenzamine the phaeochromocytoma was resected laparoscopically.

Histopathological analyses had identified a phaeochromocytoma (morcellated) with typical histological features and with no evidence of capsular invasion. Immunohistochemistry showed the normal/retained pattern of staining for both SDHA and SDHB proteins.

Now aged 30 y, the patient had not undergone biochemical or radiological surveillance since his primary surgery. At that time, there were no reported symptoms consistent with a functional PC/PGL or somatostatinoma, nor was there any reported history of polycythaemia or vision impairment.

The patient subsequently moved overseas, and was lost to follow-up. Unfortunately no further investigations being able to be pursued with regards to this study.

Patient B:

Patient B presented aged 64 y with two incidentally diagnosed multi-focal lesions on CT following a motor vehicle accident. CT reported a 20mm right retroperitoneal mass in the aortocaval region and a 20mm heterogenous, well-circumscribed, soft tissue lesion in the retroperitoneum adjacent to the aorta. The patient underwent laparoscopic surgery for excision of both tumours. Patient B also had a past medical history of ischaemic heart disease having suffered an acute myocardial infarction aged 55 y. Haemoglobin and haematocrit were reported as normal.

Histopathology of both tumours revealed typical histological features of paraganglioma, with prominent nested and trabecular architecture, and with the presence of sustentacular cells. The cells showed moderate pleomorphism with ovoid nuclei, prominent nucleoli and plentiful amphophilic cytoplasm. No soft tissue invasion was seen. A foci of lympho-vascular invasion was seen adjacent to the pre-aortic tumour. Immunohistochemistry of both tumours showed the normal/retained pattern of staining, with the cells staining positive for chromogranin A, positive for synaptophysin, and positive for SDHA, SDHB, and FH.

Now aged 72, COVID restrictions prevented further investigations being pursued. However, at that time Patient B reported to be in good health, undergoing regular investigations for recurrence of PC/PGL, and with no symptoms of a functional somatostatinoma.

Table 6.2 Clinical details of patient A and B found to harbour a somatic *EPAS1* PV

		Patient A	Patient B
Clinical	**BP (mmHg)**	165/71	137/67
	HR (bpm)	64	70
Catecholamines			
24hr Ur	**Noradrenaline**	'Elevated'	N/A
	Adrenaline	'Elevated'	N/A
Plasma	**Metanephrine**	Normal	0.29 nmol/L (rr < 0.4) (post-op)
	Normetanephrine	Normal	0.83 nmol/L (rr < 0.83) (post-op)
FBC	**Hb**	149 g/L	125 g/L
	Haematocrit	0.43 L/L	0.37 L/L

Abbreviations: BP, blood pressure; HR, heart rate; Ur, urinary; FBC, full blood count. N/A, not available.

6.2.6 Discussion

These investigations presented within this chapter into the prevalence of *EPAS1* PV within a cohort of 62 apparently sporadic cases of PC/PGL at RNSH have determined that somatic *EPAS1* PV were present at 3.4%. Interestingly, this finding was lower than published findings, where somatic *EPAS1* PV have been reported to account for between 5-8% of all PC/PGL [67, 253]. The difference in proportion of *EPAS1* PV in PC/PGL between this study and those previously reported levels can be explained in part as arising from the following study limitations; due to the rarity of the tumour type, and relatively small size of this cohort. Within this study the investigations were limited to a small hotspot section of the *EPAS1* gene sequence, and as such the possibility of the presence of other genetic variations in *EPAS1* was not tested or examined further in this study.

Unfortunately, at the time of analyses, neither of the patients identified in this study as having PC/PGL carrying *EPAS1* PV proceeded with further formal surveillance to assess for clinical features of Pacak-Zhuang syndrome. Regardless, records showed haemoglobin and haematocrit measurements were within the normal range, excluding the clinical diagnosis of polycythaemia. Further, neither patient had reported symptoms of a somatostatinoma (abdominal pain, diabetes, gall stones or diarrhoea) nor were duodenal or pancreatic masses identified when each patient underwent diagnostic work-up of their PC/PGL.

Conclusion

The identification of the presence of somatic *EPAS1* PV in 2 out of 62 patients with PC/PGL is a crucial discovery regarding the genetic landscape of their tumours, and may have revealed the genetic driver of their PC/PGL disease. Such information would be important for patient management. In the absence at the time of analyses of any report of the aforementioned features of Pacak-Zhuang syndrome, the likelihood of Pacak-Zhuang syndrome in these two patients would appear to be low. Regardless, identification of a somatic aetiology in these PC/PGL would preclude further investigation for germline drivers of disease and allow such patients to be provided with reassurance that there would be no underlying hereditary risk.

CHAPTER 7

Genotype-phenotype Correlations in Paediatric and Adolescent PC/PGL: a cross sectional study

CHAPTER 7. Genotype-phenotype correlations in paediatric and adolescent phaeochromocytoma and paraganglioma: a cross sectional study

7.1 Introduction

The likelihood of detecting a germline pathogenic variant in patients diagnosed with PC/PGL is much higher earlier in life with a prevalence of 80% in paediatric cohorts, compared with 30% in adulthood [300]. The rare nature of these tumours has made it challenging to establish genotype-phenotype correlations and disease frequency. The objective of this study was to review the clinical features, outcome of genetic analysis and tumour immunohistochemistry of patients diagnosed with PC/PGL aged 0-21 years old who were assessed within Familial Cancer Services within New South Wales (NSW) and the Australian Capital Territory (ACT), Australia. We determined the prevalence of germline pathogenic variants within this cohort and established the incidence of this rare disease within Australia.

7.2 Methodology

A detailed chart review was conducted on patients who attended FCS in NSW and ACT (Sydney, Newcastle, Wollongong and Canberra) between 1992 and November 2019. Patients were identified through a state-wide online genetic database ('TrakGene'), used by these FCS to record patient demographics, clinical information, pedigrees and genetic test results. Search criteria entered in to TrakGene comprised the terms 'diagnosis' PLUS 'phaeochromocytoma' OR 'paraganglioma' OR 'adrenal cancer' AND age of diagnosis as '≤ 21'. Those with 'adrenal cancer' were reviewed in more detail and excluded if not phaeochromocytoma or paraganglioma. Medical records were then also reviewed.

7.2.2 Basic demographics and clinical features

Basic demographics, clinical features (gender, age of diagnosis, symptoms at presentation, family history) and tumour characteristics (hormone secretion, tumour behaviour [solitary, recurrent, multifocal, malignant; synchronous, metachronous] tumour location (adrenal, extra-adrenal [abdominal, thoracic, head or neck]) and immunohistochemistry were recorded.

PC/PGL diagnosis and anatomical location was confirmed with histopathology reports for surgically resected tumours, or anatomical and functional imaging if the tumour was inoperable. Multifocal PC/PGL was defined as > 1 PC/PGL at the time of primary PC/PGL diagnosis. Recurrent PC/PGL was defined as the diagnosis of a new PC/PGL more than six months after the primary diagnosis. Metastatic

disease was defined as the presence of chromaffin tissue in an organ where this tissue is usually absent (i.e. lymph nodes, lungs, bone, or liver). Synchronous metastasis was defined as metastasis present at the time of diagnosis (or within six months), and metachronous as a new metastatic lesion diagnosed more than six months later.

7.2.3 Genetic testing

The outcome of genetic testing was classified as 'apparently sporadic' or 'hereditary' based on the absence or presence of a germline pathogenic variant. Variants were recorded as per Human Genome Variation Society sequence variant nomenclature and pathogenicity classified per ACMG criteria as 'pathogenic', 'likely pathogenic', 'of uncertain significance', 'likely benign' or 'benign'. Genetic testing was either a 'mutation search' in the proband or a 'predictive test' in relatives. Whether the PC/PGL was identified at initial screening or as part of ongoing surveillance was documented for individuals undergoing predictive testing.

Genetic testing was performed on leukocyte DNA extracted from peripherally collected EDTA-anticoagulated blood or buccal swabs. Testing was performed at National Association of Testing Authorities accredited laboratories. Samples were tested via Sanger sequencing and/or Next-Generation Sequencing. Multiplex ligation probe amplification (MLPA) was also performed to assess for large deletions, where appropriate.

7.2.4 Hormone secretion

Plasma normetanephrine, metanephrine and 3-methoxytyramine were measured by liquid chromatography-mass spectrometry. Laboratory specific normal ranges were as follows: plasma normetanephrine < 540 (age 2-14 years), < 550 (age 14-20 years), < 560 pmol/L (20-23 years), plasma metanephrine < 447 pmol/L (age > 2 years). Results within reference range were recorded as 'normal' and where information was unavailable, data were recorded as not available (N/A).

7.2.5 Statistical analyses

We analysed data using STATA 14.0 (StataCorp, College Station, TX, USA). Descriptive analyses were used to describe the study population (frequency, percentages). Median and range were calculated for numerical variables, and groups were compared using the Mann-Whitney test. Categorical variables were compared using Fisher's exact test. A two-tailed test with a 5% significance level was used for all statistical analyses.

Incidence rate was calculated using both NSW and ACT statewide data with the numerator being new cases of PC/PGL diagnosed in patients born after 1992 and the denominator being the total person-time of observation while at risk during the study (using live births) over the study period of 1992-2019. Trend analyses were conducted to compare changes over time (frequency of PC/PGL tumour diagnoses and frequency of genetic testing for causes of hereditary PC/PGL). The prevalence was defined as the total number diagnosed with hereditary disease divided by the total number of individuals diagnosed with PC/PGL.

7.3 Results

30 patients diagnosed with PC/PGL aged 21 years and under years underwent genetic testing within FCS between 1992-2019. 15 of the 30 patients were born after 1992 and were used to calculate the incidence rate.

7.3.1 Basic demographics and clinical features

The median age at primary PC/PGL diagnosis was 13 years (range 4-21 years) (Table 7.1). Gender was equally distributed between males (n=15) and females (n=15). Symptoms were documented in 17 patients' medical records and were primarily attributed to catecholamine excess. Hypertension was reported most frequently in 13 (76%) of patients, followed by headaches, diaphoresis and abdominal pain. The two patients who presented with symptoms of mass effect had both developed parasympathetic head and neck paraganglioma.

TABLE 7.1: Basic demographics and clinical details of paediatric and adolescent patients diagnosed with PC/PGL

	Overall (n)	Apparently sporadic (n)	Hereditary (n)	P value	Germline Mutation			
					SDHB	***VHL***	***MAX***	**P value**
Age at PC/PGL diagnosis (years)								
Overall								
Median (min-max)	13y (4-21)	13y (9-15)	13y (4-21)	0.36*	15y (7-21)	10y (4-19)	21y	0.12+
MS median age (min-max)	13.5y (7-21)	13y (9-15)	14y (7-21)	0.12*	19y (7-21)	13y (7-19)	-	
PT median age (min-max)	10y (4-19)	-	10 (4-19)	0.16#	13.5y (9-17)	5.5y (4-19)	-	
Gender M:F (% male)	15:15 (50%)	2:4 (33%)	13:11 (46%)		8:4 (67%)	5:6 (45%)	0:1 (-)	
Symptoms (n)								
Hypertension	76% (13/17)	33% (1/3)	86% (12/14)					
Headaches	12% (2/17)	33% (1/3)	7 % (1/14)					
Diaphoresis, flushing	12% (2/17)	- (0/3)	14 % (2/14)					
Palpitations	6% (1/17)	- (0/3)	7% (1/14)					
Abdominal pain	12% (2/17)	- (0/3)	14 % (2/14)					
Mass	12% (2/17)	33% (1/3)	7 % (1/14)					
Other	12% (2/17)	- (0/3)	14 % (2/14)					
Genetic testing (n)	30	20% (6/30)	80% (24/30)		50% (12/24)	46% (11/24)	4% (1/24)	

MS (Proband):PT	22:8	7:0	15:8		8:4	7:4	1:0	
Family history (n)								
No family hx		100% (6/6)	37.5% (9/24)	0.02*	42% (5/12)	27% (3/11)	100%	0.67[+]
Family history		-	62.5% (15/24)		58% (7/12)	82% (8/11)	(1/1)	
1 relative with syndromic tumours		-	60% (9/15)		86% (6/7)	37% (3/8)	-	
≥ 2 relatives with syndromic tumours		-	40% (6/15)		14% (1/7)	63% (5/8)	-	

*Abbreviations: MS; mutation search. PT; predictive test, *****; comparing apparently sporadic and hereditary, [#] comparing MS and PT, [+]; comparing SDHB and VHL*

7.3.2 Genetic testing

The prevalence of a pathogenic germline variant was 80% (24/30) of which 96% (23/24) were pseudohypoxia pathway genes (Cluster 1) (*SDHB* [n = 12] and *VHL* [n = 11] and one was a novel *MAX* variant (Cluster 2)(Table 7.1). All 12 *SDHB* pathogenic variants were unique including six missense, one frameshift, one deletion, one duplication and three nonsense pathogenic variants. There were nine unique *VHL* pathogenic variants, all missense.

Genetic testing did not identify a germline cause in 20% (6/30) patients (termed 'apparently sporadic' hereafter). There was no family history of PC/PGL or tumours associated with hereditary syndromes predisposing to PC/PGL in these individuals. Within this group of apparently sporadic patients all had undergone molecular analysis for at least *VHL, SDHB, SDHD* and *RET;* two patients had undergone extended panel testing including *VHL*, *RET, SDHA*, *SDHB, SDHC*, *SDHD*, *SDHAF2, MAX*, *FH* and *TMEM127* (Table 7.2).

There was no difference in age of diagnosis of primary PC/PGL between cases of apparently sporadic *versus* hereditary disease (13 years [range: 9-15 years] *vs.* 13 years [range: 4-21 years], p = 0.36), between those diagnosed with *VHL versus SDHB* (10 years [range: 4-19 years] *vs* 15 years [range: 7-21], $p = 0.12$) or those undergoing a mutation search *versus* predictive test (13.5 years [years 7-21] *vs.* 10 years [range: 4-19 years], $p = 0.16$) (Table 1; Figure 7.1).

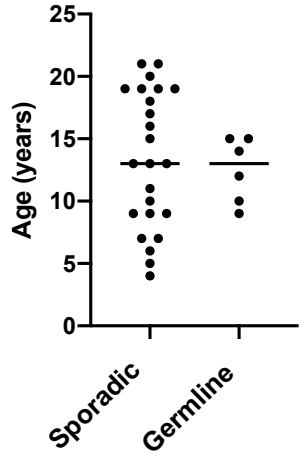

A

Figure 7.1.a Age at development of PC/PGL (sporadic versus hereditary). Scatterplot comparing age of development of primary PC/PGL between hereditary and apparently sporadic PC/PGL. The median age was the same at 13 years [range: 9-15 years] *vs.* 13 years [range: 4-21 years], p = 0.36), with the earliest age of PC/PGL at 4 years in hereditary PC/PGL compared with 9 years in apparently sporadic.

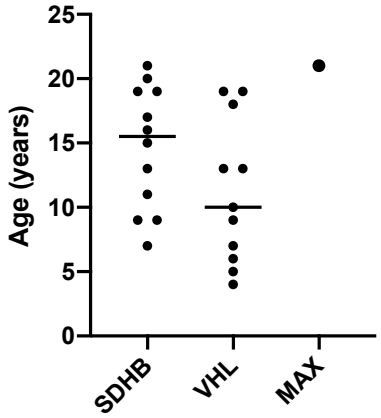

Figure 7.1.b Age at development of PC/PGL (genotypes). Scatterplot comparing age of development of primary PC/PGL between each genotype. The median age of PC/PGL diagnosis in those with *VHL* was 10 years [range: 4-19 years] *versus* 15 years [range: 7-21] in those with *SDHB, p* = 0.12. The single *MAX* case was diagnosed at 21 y.

Table 7.2. Clinical details SDHB immunonegative participants

	Primary tumour location	Family history	SDHA/SDHB immuno-histochemistry	Genes tested	
Patient 1	Carotid PGL	No	Positive / Negative	NGS	EPAS1, FH, IDH1, KIF1B, MAX, MDH2, NF1, RET, SDHA, SDHAF2, SDHB, SDHC, SDHD, TMEM127, VHL*
				MLPA	SDHB, SDHC, SDHD
Patient 2	Abdominal (retroperitoneal) PGL with lypmh node metastases.	No	Positive/ Negative	NGS	ATRX, DNMT3A, EGLN1-3, EPAS1, FH, H3F3A, GOT2, HIF1A, HIF3A, IDH1, IDH2, IDH3B, KIF1B, ETFRF1, MAX, MDH1, MDH2, MERKT, MET, MGA, MYCT1, NF1, SDHA, SDHB, SDHC,SDHD, SDHAF1, SDHAF2, SIRT3, SLC5A11, TMEM127, VHL
				MLPA	SDHB, SDHC, VHL

Abbreviations: NGS; next generation sequencing. MLPA; Multiplex Ligation Dependant Probe Amplification

7.3.3 Mutation search and predictive testing

In all, 73% (22/30) of patients were probands and thus had undergone genetic testing for a panel of genes known as a 'mutation search' (Table 7.1). 27% (8/30) of patients had a known family history of a pathogenic variant and thus underwent 'predictive testing' for the previously identified pathogenic variant only. The ratio of predictive test to mutation search performed in those subsequently diagnosed with *VHL* and *SDHB* were similar (8:4;7:4).

Family history

Patients harbouring a pathogenic variant often presented with a family history; those with apparently sporadic disease did not (62.5% *versus* 0%, p=0.02)(Table 7.1). At the time of data collection 82% (8/11) of patients with VHL syndrome had a family history of syndromic tumours (reported either at the time of genetic testing or prospectively), 33% (3/8) had a single affected relative and 63% (5/8) had ≥ two affected relatives. Only three patients with VHL disease had no known family history of syndromic tumours. 58% (7/12) of *SDHB* pathogenic variant carriers had a family history of syndromic features, of which 86% (6/7) had a single affected relative only. Where the family history was known, all affected individuals with *VHL* had a first-degree relative affected compared with *SDHB* where affected relatives were either 2nd degree or more distantly related.

7.3.4 PC/PGL tumour characteristics in adolescent and paediatric patients.

Of the 12 patients harbouring an *SDHB* pathogenic variant, 75% (9/12) had been diagnosed with PGL (four abdominal PGL, three bladder PGL and two head and neck PGL) and 25% (3/12) were PC (Table 7.3). All 11/11 patients harbouring a *VHL* pathogenic variant were diagnosed with PC compared with 3/12 patients with *SDHB* pathogenic variants (100% *versus* 25%, $p = < 0.01$). 17% (5/30) of patients had developed > 1 primary PC/PGL at diagnosis, all occurring in those harbouring a germline pathogenic variant. The *MAX* case presented with bilateral pheochromocytoma.

TABLE 7.3.PC/PGL tumour characteristics in paediatric and adolescent patients

	Overall (*n*)	**Genetic analysis**			**Germline Mutation**			
		Sporadic	**Hereditary**	***p*-value**	***SDHB***	***VHL***	***MAX***	***p-value***
Primary tumour								
PC (adrenal)	63% (19/30)	67% (4/6)	62.5% (15/24)	0.38*	25% (3/12)	100%	100% (1/1)	$< 0.01^{+}$
PGL (extra-adrenal)	37% (11/30)	33% (2/6)	37.5% (9/24)		75% (9/12)	(11/11)	-	
						-		
Hormone secretion (% functional)	70% (12/17)	60% (3/5)	75% (9/12)	1.0^{*}	50% (2/4)	71% (5/7)	100% (1/1)	0.57^{+}
Multifocal								
Total multifocal	43% (13/30)	16% (1/6)	50% (12/24)	0.19*	33% (4/12)	63% (7/11)		0.22^{+}
> 1 PC/PGL at diagnosis	17% (5/30)	- (0/6)	21% (5/24)	0.55*	- (0/12)	36% (4/11)	100% (1/1)	0.03^{+}
Recurrent primary PC/PGL	42% (8/19)	20% (1/5)	50% (7/14)	0.34*	50% (4/8)	60% (3/5)	- (0/1)	1.0^{+}
Total metastatic	27% (8/30)	17% (1/6)	29% (7/24)	1*	42% (4/12)	27% (2/11)	100% (1/1)	0.64^{+}
Synchronous	7% (2/30)	- (0/6)	8.3% (2/24)	1*	59% (1/12)	18% (1/11)	- (0/1)	1^{+}
Metachronous	26% (5/19)	- (0/5)	36% (7/14)	0.11*	38% (4/8)	20% (2/5)	100%(1/1)	1^{+}
Site of metastases								
Lymph node	50% (3/6)	-	50% (3/6)		2/4 (50%)	1/1 (100%)	1/1 (100%)	
Lung	16% (1/6)	-	16% (1/6)		-	-	-	

Bone	33% (2/6)	-	33% (2/6)		2/4 (50%)	-	-	
Liver	-	-	-		-	-	-	
IHC (+/-)								
SDHA+/SDHB+ (no LOS)	20% (2/10)	33% (1/3)	14% (1/7)	0.4*	-	100% (1/1)	ND	0.14^{+}
SDHA+/SDHB-	80% (8/10)	75% (2/3)	86% (6/7)		100% (6/6)	-		
SDHA-/SDHB -	-	-	-		-	-		

Abbreviations: LOS, loss of staining; ND, not done; *, comparing sporadic and hereditary; $^{+}$, comparing *SDHB* and *VHL*

Hormone secretion

Catecholamines, or the metabolites of, were available in 57% (17/30) of patients of which 70% (12/17) were elevated ('functional')(Table 7.3). All patients with elevated catecholamines were symptomatic. 3/5 patients within the apparently sporadic disease and 9/12 in the hereditary group were functional (60% *versus* 75%, p = 1.0). 2/4 patients harbouring an *SDHB* pathogenic variant and 5/7 patients harbouring a *VHL* pathogenic variant developed functional PC/PGL (50% *versus* 71%, p = 0.57). All but one patient (16/17) displayed a purely noradrenergic phenotype, with a single VHL patient having mixed hormone secretion (Figure 7.2).

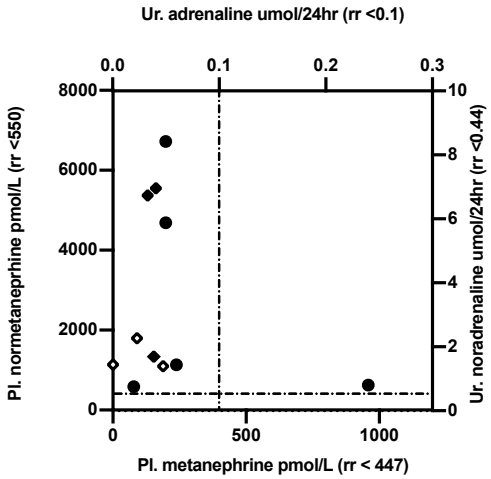

Figure 7.2: Catecholamine secretion. Catecholamine secretion of each individual with functional PC/PGL. The y-axis is shows results of biochemical testing for plasma normetanephrine (marked as ♦) or urinary noradrenaline (marked as •) . The x-axis shows the corresponding plasma metanephrine (marked as ♦) or urinary adrenaline (marked as •). The dotted line delineates between the normal range (below for normetanephrine, noradrenaline; left for metanephrine, adrenaline) and elevated (above for normetanephrine, noradrenaline; right for metanephrine, adrenaline). Filled symbols represent GMD (•), empty symbols represent patients with apparently sporadic disease (o).

Longitudinal data

Longitudinal data following the primary diagnosis of PC/PGL were available for 19 patients (63%), with surveillance data on participants that were ≥ five years from primary tumour diagnosis (n=13/19, 68%), ≥ 10 years (n= 5/19, 26%) and ≥ 20 years (n=1/19, 5%). Of these participants, all but one patient remained alive. The mean follow-up time was nine years (range 1-47 years). The deceased patient diagnosed with VHL, had developed bilateral phaeochromocytoma and succumbed to metastatic pancreatic NET.

Recurrence

42% (8/19) of patients developed recurrent disease (i.e. a second primary PC/PGL greater than 6 months following initial PC/PGL diagnosis)(Table 7.3). This occurred in 7/14 patients with hereditary disease (4/8 patients with *SDHB* and 3/5 patients with *VHL* [50% versus 60%, $p = 1.0$]) and 1/6 patients with apparently sporadic disease (20% versus 50% $p = 0.34$). Of the eight patients who developed recurrent disease, four patients developed recurrent disease within the first 5 years (all harbouring a germline pathogenic variant) and seven within the first decade. A single patient, with VHL Syndrome, developed a second primary PC in the contralateral adrenal gland 26 years after initial diagnosis. One patient with apparently sporadic disease developed recurrent disease (PGL six years later, at age 15y) and another metastatic PC/PGL to lymph nodes soon after primary PC/PGL diagnosis.

Multifocality

Overall, 43%(13/30) of patients developed multifocal disease with either > 1 PC/PGL at diagnosis or recurrent primary PC/PGL (Table 7.3). Multifocality occurred in 1/6 patients with apparently sporadic disease and 12/24 hereditary (16% *versus* 50%, $p = 0.19$). 4/12 patients with *SDHB* developed multifocal disease compared with 7/11 patients with *VHL* (33% versus 63%, $p = 0.22$). 4/11 patients with *VHL* presented with multifocal disease at the time of primary PC/PGL diagnosis (i.e. bilateral PC) compared with no patients (0/12) with *SDHB* (36% versus 0%, $p = 0.03$).

Metastasis – synchronous and metachronous

Twenty seven % (8/30) of patients developed metastatic disease which occurred in only a single patient with sporadic disease (Table 7.3). In 2/8(25%) of patients, metastases were present at diagnosis (synchronous). Metastatic disease developed in 4/12 with *SDHB* and 2/11 with *VHL* (42% versus 27%, $p = 0.64$), and the single patient with *MAX*. Metastatic deposits developed in lymph nodes (50%) followed by bone (33%) and then lung (16%).

IHC

Immunohistochemical staining for SDHA and SDHB was performed on 10 tumours (Table 3). There was loss of expression of SDHB by immunohistochemistry (termed *SDH deficiency*) and retained expression of SDHA in all PC/PGL from patients with *SDHB* (n=6). The single PC/PGL from a patient with *VHL* which had undergone IHC staining demonstrated immunopositivity for both SDHA and SDHB. Interestingly, 2/3 (67%) of the apparently sporadic cases were SDH deficient (with retained SDHA staining) despite the absence of a germline *SDHB* pathogenic variant, which included analysis for large scale deletions. One patient was diagnosed with metastases soon after the diagnosis of primary PC/PGL, the other had no evidence of recurrent or metastatic disease (Table 7.2).

7.3.5 Incidence and trend analysis

The incidence rate of paediatric PC/PGL was 0.45 cases per million person years within NSW/ACT. Over the study period both diagnosis of primary PC/PGL and undertaking of genetic testing for hereditary causes of PC/PGL within NSW/ACT increased steadily over time (Figure 7.3). There was a two-fold increase in diagnosis of primary PC/PGL from a mean of 2.5 cases per decade between 1970-1989 up to 5.25 cases per decade between 2000-2019. There was a 5-fold increase in genetic testing from a mean of 1.5 cases between 1990-1999 up to 7.5 cases per decade from 2010-2019.

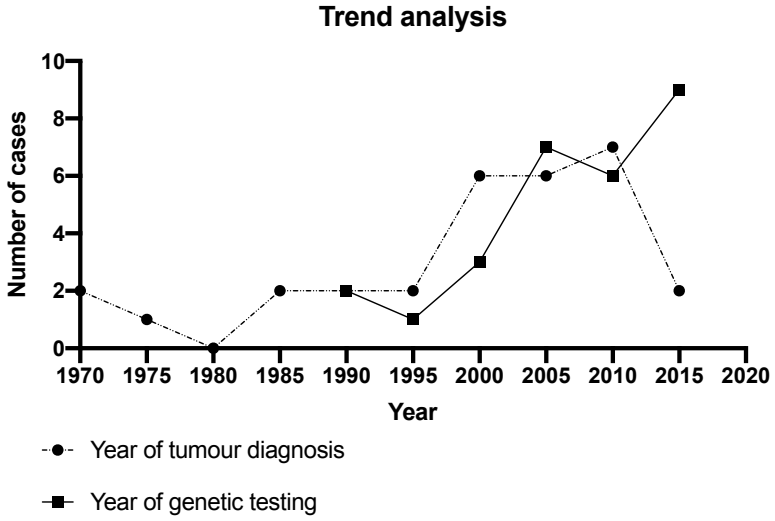

Figure 7.3: NSW/ACT Trend Analysis. The y-axis shows the number of paediatric or adolescent cases diagnosed with primary PC/PGL (represented as —) or cases who have undergone genetic testing for hereditary PC/PGL (represented as ---). The x-axis shows the year of diagnosis grouped into five yearly intervals, commencing at 1970-1974 inclusive. The earliest diagnosis of primary PC/PGL was 1970, with two cases, and peaked in 2010-2014 at 7 cases. Genetic testing for hereditary PC/PGL through FCS was first recorded in the time period of 1990-1995, with 2 cases, and has peaked in 2015-2019 with 9 cases.

7.4 Discussion

This chapter reports the diagnosis of PC/PGL in subjects aged 21 years and under in NSW and ACT, Australia, from 1992-2019. The incidence rate of 0.45 cases per million person years falls within the range of that published in the literature of 0.1-0.5 cases per million [301, 302]. This estimation, at the upper range of that reported elsewhere, reflects the high awareness of hereditary causes of PC/PGL by clinicians within the Australian public health service and streamlined referral pathways between endocrinologists and cancer geneticists. As awareness of hereditary causes of PC/PGL increased, the frequency of paediatric and adolescent patients who underwent genetic testing increased 5-fold over the study period (1.5 cases per decade to 7.5 cases per decade).

The prevalence of a germline pathogenic variant in patients diagnosed with PC/PGL in childhood or adolescence was 80%. Driver pathogenic variants predominantly occurred in the pseudohypoxia pathway (Cluster 1) with *SDHB* and *VHL* being most frequently implicated, occurring in 40% and 37% of cases, respectively. Our findings are similar to those reported elsewhere; four large retrospective cohort studies also identified hereditary disease in 77-83% with pathogenic variants primarily occurring in *VHL* (21-51%) and *SDHB* (15-39.1%) [303-305]. The prevalence of pathogenic variants occurring within the pseudohypoxia pathway is reported to be 1.9 fold higher ($p < 0.0001$) in children whereas pathogenic variants occurring in the kinase signaling pathway was 3 fold higher ($p < 0.0008$) in adults [305]. This emphasises that aberrations in the pseudo-hypoxic pathway are the predominant molecular mechanisms in the development PC/PGLs in younger patients. Paediatric PC/PGLs are uncommonly associated with *SDHD* or *NF1* and rarely occur due to *RET*, *SDHA*, *SDHC*, *FH, MAX* and *TMEM127* pathogenic variants.

Within our cohort tumour location was genotype specific. *VHL* carriers presented exclusively with PC and *SDHB* predominantly PGL (100% vs. 25%, $p < 0.01$). The frequency of PGL versus PC within paediatric patients reported elsewhere reflects this genotype-phenotype correlation. PGL were more commonly reported by Pamporaki *et al.* (with a higher proportion of *SDHB* carriers) [305], but less commonly reported by Bausch *et al.* (with a higher proportion of *VHL* carriers)[220]. Two patients harbouring *SDHB* pathogenic variants in our study were diagnosed with urinary bladder PGL. This is a rare occurrence accounting for less than 6% of PGL and 0.06% of all bladder tumours [306]. However, 60% of bladder PGLs are associated with a germline pathogenic variant, most frequently detected in patients with *SDHB* (51.7%) and should therefore prompt genetic testing regardless of age [21]. Symptoms specific for bladder PGL (pertinent for the paediatrician) include haematuria, voiding headaches and post-micturition syncope, or may present silently [307].

Due to the autosomal dominant pattern of inheritance of germline pathogenic variants in genes causing hereditary PC/PGL syndromes we found patients harbouring a pathogenic variant often presented with a family history of syndromic tumours. The presence of a family history was not significantly different between *VHL* and *SDHB* (82% *versus* 58%, $p = 0.67$). This is consistent with a previous study finding a family history in 66% of patients harbouring *VHL* pathogenic variants (unless *de novo*) and in 36.4% of patients with *SDHB* pathogenic variants [305].

Within our cohort, 43% of patients developed multifocal disease (defined as > PC/PGL at diagnosis or recurrent primary PC/PGL). Those harbouring a *VHL* pathogenic variant were more likely to have developed multifocal disease at the time of diagnosis compared with *SDHB* (36% vs 0%, $p = 0.03$). Multifocality as a feature of hereditary PC/PGL is also reported elsewhere; overall approximately 10% of paediatric patients present with bilateral PC and 17% with multifocal PGL at diagnosis usually associated with hereditary disease [308]. Longitudinal follow up of paediatric patients by Bausch *et al.* found 50% of patients will develop a second PC/PGL by 30 years following their primary PC/PGL diagnosis [303].

Metastatic spread occurred in 17% of patients with apparently sporadic and 29% of patients with hereditary disease. In previous studies, metastases have been described in 9-12% of children with PC/PGL and are more frequently metachronous rather than synchronous [220, 302]. Some studies have found *SDHB* pathogenic variants to be strongly associated with metastatic disease in paediatric PC/PGL patients [309]. In a large cohort study exploring *SDHB* pathogenic variant carriers in paediatric patients, metastatic disease was reported in 70% of cases with a median age at diagnosis of 13 years [300]. Although referral bias of more aggressive disease to this tertiary care centre may be a factor. Regardless, even with metastatic spread overall prognosis is relatively good with survival rates at 5-, 10-, 20-years being 100%, 97.14% and 77.71%, respectively [308].

Therefore, three key features need to be considered in the follow-up of paediatric patients with hereditary PC/PGL: 1) that there is an increased risk of multiple PC/PGL at diagnosis; 2) that there is a lifelong risk of developing a second PC/PGL; and 3) that there is a lifelong risk of metastatic disease. Genotype specific surveillance protocols for carriers of these gene pathogenic variants reflect these hallmarks of tumour behaviour in addition to phenotypic features such as the youngest reported age of occurrence, age specific risk of PC/PGL, location of primary tumour development (PC vs PGL), tumour growth rate and potential clinical impact of tumour progression.

Predictive testing should be offered to all immediate blood relatives of patients harbouring a pathogenic variant, including siblings. Early diagnosis of a germline cause of PC/PGL translates into increased surveillance and thus improved clinical outcomes through the adoption of a structured surveillance regimen [310] with surveillance detected PC/PGL being smaller and associated with a reduced risk of metastatic disease and lower mortality [311]. The childhood penetrance of PC/PGL in VHL Syndrome is 14% with the youngest age of diagnosis 2 years. Thus, current surveillance guidelines for carriers of a *VHL* pathogenic variant recommend clinical and biochemical testing for PC/PGL from age two years and anatomical imaging with annual MRI from age ten years, in accordance with imaging guidelines for renal cell carcinoma (RCC) and pancreatic neuroendocrine tumours [304]. The childhood penetrance of PC/PGL in *SDHB* pathogenic variant carriers is 0%, 0.3%, 1.2% and 2.2% at age 5, 10, 16 and 18 years respectively, with the earliest age of diagnosis 6 years [99]. It follows that clinical and biochemical surveillance with blood pressure monitoring and plasma metanephrines is recommended to commence from age 6 years.

In light of the high occurrence of germline driver pathogenic variants in PC/PGL, molecular testing for hereditary causes of PC/PGL should occur in all children. More than 20 germline predisposition genes have been identified in PC/PGL [78], of which 15 genes have been extensively validated as being associated with familial disease [72]. Panel testing via Next Generation Sequencing is now the mainstay of genetic testing and has been widely incorporated into clinical practice. The Consensus Statement on Next-Generation-Sequencing of hereditary PC/PGL was published in 2017 and has been widely incorporated into clinical practice and includes sequencing of the following genes; *EGLN1/PHD2, EPAS1, FH, KIF1B, MAX, MET, NF1* (not always tested due to reliable clinical features)*, RET, SDHB, SDHD, SDHC, SDHA, SDHAF2, TMEM127, VHL* [72]. 'Mainstreaming' is a further advance in the approach to genetic testing for hereditary cancer syndromes. This is a paradigm shift away from somatic sequencing requested by oncologists to detect therapeutic targets or prognostication followed (often months later) by germline sequencing performed separately by cancer geneticists through FCS. Mainstreaming involves tumour-normal sequencing (paired somatic and germline testing) of patients with solid tumours requested by the oncologist, with subsequent referral to FCS if a germline pathogenic variant is detected. Benefits of this approach include verification of somatic and germline driver variants and rationalisation of referrals to FCS.

Immunohistochemistry of phaeochromocytoma or paraganglioma tissue for loss of staining for SDHA and SDHB is a useful adjunct to molecular analysis. The usefulness of this test is particularly pertinent when immediate access to genetic testing is unavailable. *SDHB*-, *SDHC*- and *SDHD*-mutated tumours demonstrate loss of staining for SDHB whereas SDHA mutated tumours demonstrate loss of staining

for both SDHB and SDHA [312]. The mean sensitivity of this tool has been reported to be 94.23% and specificity 84.35% [313].

Two patients in this study presented in early adolescence with SDH deficient paraganglioma with no pathogenic variants identified despite extensive molecular genetic testing (Table 7.3). NGS included sequencing for the novel deep intronic *SDHC* variant identified by others [314] and MLPA. It is reasonable to assign these patients a presumptive diagnosis of Carney Triad. Although initially defined clinically as the co-occurrence of SDH deficient paraganglioma, gastrointestinal stromal tumour (GIST) and pulmonary chondroma, according to the recent WHO 2022 classification of endocrine neoplasia, the term 'Carney Triad' is now appropriate for patients with syndromic SDH deficient neoplasia where currently available testing techniques have failed to identify a pathogenic germline variant [315]. Most patients with Carney Triad will have syndromic but not hereditary disease due to post-zygotic mosaic epimutation (promoter hypermethylation) of *SDHC* (not tested for in this series), although some may be caused by pathogenic variants not detected by current methods. Using this revised definition of Carney triad, unless somatic only biallelic mutations are demonstrated (a rarity in the SDH genes), the diagnosis of even a single SDH deficient neoplasm at any age (but particularly in childhood) should lead to a presumptive diagnosis of germline *SDH* pathogenic variant or Carney Triad and lifelong surveillance for syndromic manifestations [315].

Limitations

As with previous reports of paediatric PC/PGL limitations include the small number of patients and incomplete follow-up. Not all patients underwent testing for the full panel of germline driver pathogenic variants, particularly as genetic testing of many of these individuals was either prior to discovery of the PC/PGL candidate genes or prior to the implementation of NGS. This is particularly pertinent for the six apparently sporadic cases; only two have undergone extensive panel testing (Table 7.3) with the remainder having been sequenced for *SDHB, SDHD, VHL* and *RET* only. The prevalence of germline pathogenic variants in our study may therefore be an underestimate. Lastly, this is a highly select population potentially affected by referral bias, with patients reporting a family history of endocrine neoplasia being more likely to be referred to FCS for genetic testing.

7.5 Conclusion

This chapter presents Australian data on the prevalence of germline pathogenic variants in paediatric and adolescent patients presenting with PC/PGL, particularly *VHL* or *SDHB*. These patients carry a high likelihood of developing aggressive features with clinical implications, including multifocal or recurrent disease. Findings presented in this study highlight the importance for general physicians to

refer paediatric patients diagnosed with PC/PGL to familial cancer services for family counselling and genetic testing. Further, where a pathogenic variant is detected paediatric patients should be referred to specialty services for comprehensive work-up to detect bilateral, multifocal or metastatic disease and long term follow up.

CHAPTER 8.

Moderating Impact of Somatic Mitochondrial Variants PC/PGL

CHAPTER 8. Moderating impact of mitochondrial variants PC/PGL

8.1 Introduction

8.1.1 Normal mitochondrial function

Human mitochondria are located within all nucleated cells and are essential for energy generation. Within mitochondria, electrons move along the electron transport resulting in production of adenosine triphosphate (ATP).[316] ATP is the primary cellular energy source and is essential for all biochemical processes. This metabolic process is known as oxidative phosphorylation (OXPHOS). The 90 individual protein sub-units which make up the electron transport chain form four complexes embedded in the inner-membrane of the mitochondria (complex I-IV) and ATP synthase (complex V) (Figure 8.1). Most protein subunits are encoded by genes within mitochondrial DNA (mtDNA), although some have been identified as being nuclear encoded. Although the contribution of these proteins is small when compared to the whole cellular proteins, the proteins encoded by the mitochondrial genes remain essential components of the electron transport chain.[317, 318]

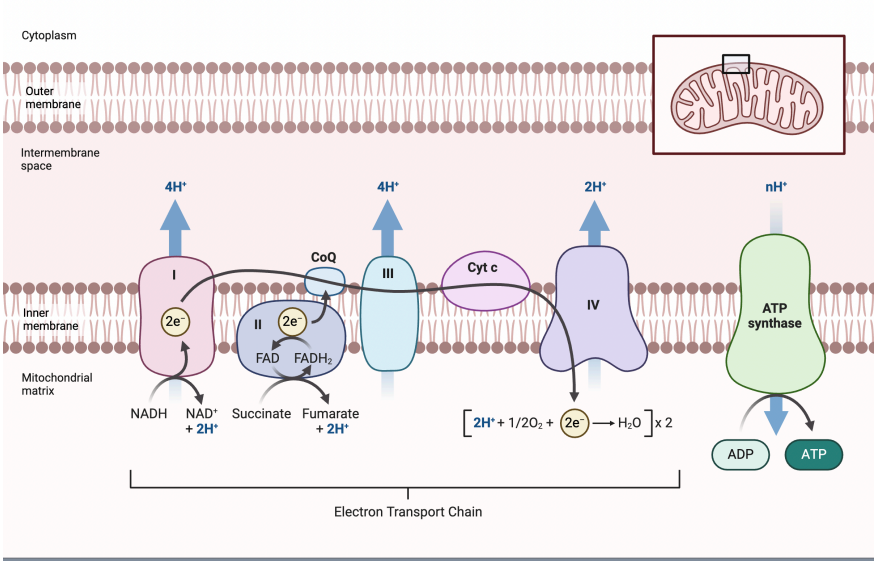

Figure 8.1 Electron transport chain. This image depicts the electron transport chain, a series of protein complexes (embedded in the inner mitochondrial membrane) and other molecules involved in electron transfer from electron donors to acceptors (via redox reactions) and drives the synthesis of ATP. Image adapted from Gammage *et al.* [317]

8.1.1 Mitochondrial DNA structure

mtDNA is 16.6 kb intron-free double stranded circular DNA coding for 11 mRNAs, 22 transfer RNAs and two ribosomal RNAs (Figure 8.2) [319]. mtDNA is divided into a 'light strand', rich in pyrimidine bases (C and T), and the 'heavy strand', rich in purine bases (G and A). Coding regions are predominantly located on the heavy strand. mRNA is translated into 13 poly-peptide sub-units contributing to mitochondrial complex I (encoded by the genes *ND1, ND2, ND3, ND4, ND4L, ND5*), mitochondrial complex III (encoded by *cytochrome b, [CYTB])*, mitochondrial complex IV (encoded by *CO1, CO2,* and *CO3*), and mitochondrial complex V (encoded by *ATPase 6 [ATP6]* and *ATPase 8 [ATP8]*). Complex II has been shown to be entirely encoded from genes within the nuclear genome. The displacement loop is a 1.1 kb triple stranded non-coding region involved in regulation and transcription of DNA.

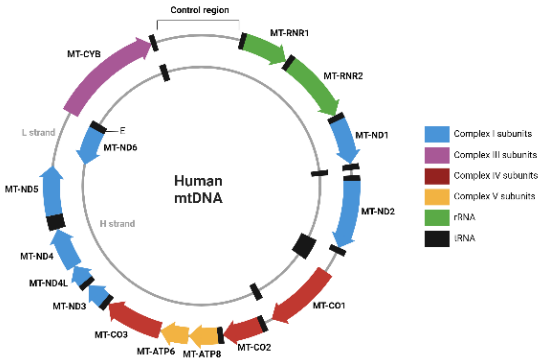

Figure 8.2 Human mitochondrial DNA. Figure depicts annotated features of human mtDNA showing mtRNA (blue, pink, red, yellow), tRNA (black) and and rRNA (green) with the inner heavy strand (H-strand) and out light strant (L-strand). Imaged adapted from Gammage et al [317].

mtDNA is polyploid with each mitochondria containing 1-10 copies of mitochondrial DNA [320]. As cells contain hundreds of mitochondria, the overall number of copies of mtDNA per cell can be thousands. Homoplasmy and heteroplasmy describe the phenomena whereby all copies of the mitochondrial genome are identical (the former) or a mixture of genotypes (the latter), meaning mtDNA within a single cell may carry variable proportions of mutant *versus* wild-type genomes [317]. A 'threshold' effect exists in that a certain cellular burden of mutated mtDNA must be reached before respiratory failure and cellular dysfunction ensues [321]. This 'threshold' appears to be lower in tissues reliant on oxidative phosphorylation for energy production. Among other variables, the degree of heteroplasmy has often been correlated with the severity of diseases associated with germline mtDNA

mutations; for instance, mutation heteroplasmy ranging between 60-80% typically translates into mild juvenile or adult onset disease, whereas heteroplasmy > 90% leading to severely impaired mitochondrial function often causes early onset and more severe disease [322],[323].

8.1.2 Mitochondrial disease in humans

There is a wide range of clinical expression of mitochondrial disease (MD), particularly within organs relying on aerobic metabolism with the neurological system being preferentially affected [324]. MD is known to be compromised of myopathies, encephalomyopathies, and multisystemic diseases arising due to mitochondrial or nuclear DNA errors. Features of mitochondrial disease include a history of maternal inheritance and unique patterns of disease, such as multiple organ involvement (deafness and diabetes), combinations of disease (stroke, migraine, seizures, ataxia), as well as abnormal biochemical findings (lactic acidaemia in children, abnormal muscle biopsy) [324]. Well described mitochondrial disease syndromes include Leber Hereditary Optic Neuropathy, Kearns-Sayre syndrome (progressive myopathy, ophthalmoplegia, cardiomyopathy), MELAS (myopathy, encephalopathy, lactic acidosis, stroke-like syndrome), and Leigh syndrome (encephalopathy, lactic acidosis).

8.1.3 Mitochondrial dysfunction in human cancer

The intrinsic link between malignancy and mitochondrial dysfunction has been identified as arising from one of the eight hallmarks of cancer, namely deregulation of cellular energetics [325]. mtDNA is highly modified with somatic mutations having been identified in 50% of tumours associated with mitochondrial disease [326]. A persisting conundrum is the mechanism by which mtDNA variants confer a selective advantage to cancer cells whilst concurrently impairing OXPHOS [327]. Further, establishing mitochondrial variants as *bona fide* 'driver' variants which advance tumour survival, rather than 'passenger' variants, remains challenging. The problem of defining the role of mitochondrial variants in carcinogenesis can be attributed to the large number of variants being identified, coupled with unclear mechanisms of pathogenicity (with an absence of tools for functional interrogation of mitochondrial variants), and historically absent/rare data sets.

Recently, two comprehensive studies utilised whole-genome sequencing from the International Cancer Genome Consortium (ICGC)/Pan-Cancer Analysis of Whole Genomes (PCAWG)[328] and the Cancer Genome Atlas (TCGA)[329] to elucidate the role of mitochondrial mutations in human cancer. Three key points were identified from these extensive datasets. Firstly, somatic mtDNA pathogenic variants are common, reflecting the high mtDNA background mutation rate (up to 17-fold) when compared to that of nuclear DNA. Secondly, cancer mt DNA often shows strand specific mutations (with

predominance of C>T in the heavy strand and T>C in the light strand) [326]. This pattern is inconsistent with mutational patterns seen in oxidative damage and suggests replication-coupled mutational processes being the dominant cause of somatic mtDNA mutations in malignancy [328]. Thirdly, the frequency and type of mutations (i.e. truncating/non-truncating) was found to be lineage specific. In particular, colorectal, thyroid and some types of renal cancer (chromophobe, papillary renal cell carcinoma) were shown to be enriched with respect to truncating variants in contrast with haematological malignancies which have been described as carrying a low somatic mutational burden [328, 329].

8.1.4 Relationship between mitochondrial genes and SDHB

As outlined in Chapter 1 the SDHx proteins, encoded by the nuclear genome, form the respiratory enzyme complex II. Complex II is well characterised as a key component of the electron transport chain. Of relevance to this chapter, complex II also participates in the Kreb's tricarboxylic acid cycle, where SDHx converts succinate to fumarate with immediate subsequent conversion (by fumarate hydratase) of fumarate to malate [259]. Germline pathogenic variants (PVs) in *SDHx*, in particular *SDHB*, result in dysfunction of this complex and accumulation of succinate [330], which in turn triggers pseudohypoxia whereby succinate inhibits alpha-ketoglutarate-dependant enzymes such as PHD with the downstream consequence of HIF-α stabilisation [259]. It has been proposed oxidative damage from accumulation of reactive oxygen species may be the origin of somatic mtDNA mutations [331].

Currently, there are no validated histopathological or molecular features to predict tumour behaviour in *SDHB* mutated PC/PGL. Iidentification of somatic mtDNA variants which affect tumour biology would not only provide insights into tumour biology, but also patient management. This chapter describes the occurrence of somatic mtDNA PVs in PC/PGL, which has not previously been investigated, and assessed for a relationship between somatic mtDNA PV and disease behaviour.

8.2 Hypotheses

In this chapter it was hypothesised that:

i. There would be clustering of somatic mtDNA PV type (nonsense *versus* missense) within complex specific coding regions.
ii. Genotype-phenotype correlations would exist between somatic mtDNA PV type (nonsense *versus* missense) and disease behaviour (age at diagnosis of primary PC/PGL, benign versus metastatic disease, primary PC/PGL size).

iii. PVs within *ATRX* and *TERT*, which are genes associated with telomere maintenance and established disease modifiers, would also impact on disease behaviour in patients harbouring somatic mtDNA PVs.

8.3 Aim

The aims of the studies reported in this chapter were:

i. Describe the occurrence of somatic mtDNA PV in PC/PGL
ii. Assess for genotype-phenotype correlations between somatic mtDNA PV and disease behaviour
iii. Assess the impact of further genes associated with disease behaviour (*ATRX* and *TERT*)

8.4 Materials and methodology

8.4.1 Cohort selection and phenotypic features

The cohort selected for this study comprised of 99 matched fresh-frozen PC/PGL tumour-blood samples collected from 84 individuals harbouring a germline *SDHB* PV recruited in the international multi-centre A5 SDHB Genomics Study; synoptic details of this study led by Professor Karel Pacak (NIH), A/Professor Richard Tothill (University of Melbourne) and Professor Roderick Clifton-Bligh (University of Sydney) are available at https://medicine.unimelb.edu.au/research-groups/clinical-pathology-research/rare-disease-oncogenomics/a5-sdhb-genomics-study. It is important to note the first papers arising from this study are yet to be published and involve a large international study team. The author was kindly granted access to the whole genome sequencing data by A/Prof Tothill and Dr Aidan Flynn (University of Melbourne) and with permission from the A5 SDHB study team for the sole purpose of analysing mtDNA variants. Corresponding phenotypic information which had been collected as part of the A5 Genomics Study (including age, gender, tumour status [primary, recurrent, metastatic], tumour location [adrenal, extra-adrenal: abdominal, thoracic, head and neck], tumour size [< or ≥ 5cm] and whether metastatic [yes, no]) was collated for this the cohort investigated in this chapter.

8.4.2 Whole genome sequencing and output generation.

Whole genome sequencing was performed as part of the A5 SDHB Genomics Study on paired blood-tumour PC/PGL samples and sequencing output was run through a mitochondrial bio-informatics pipeline – known as '*Mity*' - a highly sensitive mitochondrial variant analysis pipeline developed by Dr Ryan Davis and collaborators within the Neurobiology Research Group, Kolling Institute, University

of Sydney. The *Mity* programme was used for detection and interpretation of heteroplasmic SNVs and INDELs discovered within the mitochondrial genome extracted from WGS data.[332] *Mity* created a comprehensively annotated mitochondrial variant list from analysis of BAM files to call, filter and normalise mitochondrial SNVs and INDELS. Data was aligned to GRCh37 + decoy (hs37d5) reference genome using BWA-MEM. Variants were tiered by VAF to aid prioritisation: tier 1, VAF ≥0.01; tier 2, VAF <0.01 with 10 supporting reads; and tier 3, remaining variants.

8.4.3 Filtering of WGS mitochondrial output

Variants within protein-coding regions were selected; complex I (ND1-ND6), complex III (CYTB), complex IV (CO1-CO3), and complex V (ATP6/ATP8). Variants in the hypermutated and control region and rRNA (*RNR1, RNR2)* were excluded. Tier 1 (VAF ≥ 0.01 was selected). Minimum read depth was set at > 100. Population allele frequency was set to < 0.001. 'Non-synonymous' variants were selected and 'synonymous' variants excluded. Samples were then filtered into somatic (observed in PC/PGL only) or germline (occurring simultaneously in both the tumour and blood), with germline variants excluded from further analysis.

8.4.4 Variant interpretation

Variants identified were subsequently classified into three sub-groups; high impact, moderate impact, and variants of uncertain significance (VUS) as outlined below. For the purposes of this chapter, high and moderate impact variants were assessed collectively as 'pathogenic'.

Filtered variants were further analysed through two *in silico* tools: the MSeqDR mvTool[333] which was a programme to predict protein consequences and Ensembl Variant Effect Predictor[334] which was used to sort variants into classification groups: 'low' (variant assumed to be mostly harmless or unlikely to change protein behaviour), 'moderate' (a non-disruptive variant that might change protein effectiveness), or 'high' (variant has been determined to have a disruptive impact on the protein, resulting in protein truncation, loss of function or triggering nonsense-mediated decay).

Moderate impact variants were further sub-classified using APOGEE (a machine learning algorithm used to estimate the deleteriousness of mitochondrial non-synonymous genome variations) which sorted moderate impact variants into pathogenic or VUS groupings. APOGEE assessed with high confidence the functional impact of human mitochondrial non-synonymous genome variants and and was demonstrated to outperform existing *in silico* tools [335]. Those variants classified as 'pathogenic'

remained in the 'moderate impact' group where-as those classified as 'neutral' consequently re-classified as VUS.

Variants identified underwent further investigations utilizing various mitochondrial somatic variant cancer databases,including the International Cancer Genome Consortium (ICGC),[336] the Catalogue of Somatic Mutation in Cancer (COSMIC),[274], and MitoMap,[274] a compendium of human mitochondrial disease.

8.4.5 mtDNA somatic variants and disease behaviour.

High and moderate impact (pathogenic) mitochondrial variants were grouped into the following complex coding regions – complex I, complex III, complex IV and complex V. Somatic mtDNA PV were linked to corresponding phenotypic information and comparisons were made to interrogate the frequency of somatic mtDNA PV in PC/PGL, association between variants and disease behaviour (age at diagnosis of primary PC/PGL, tumour location, benign versus metastatic and primary tumour size)

8.4.6 Calculation of tumour mutational burden of mitochondrial somatic pathogenic variants

For this study tumour mutational burden (TMB) of somatic mtDNA PV was calculated as total number of somatic mutations identified within PC/PGL divided by total genomic length sequenced in PC/PGL (in Mb s^{-1}). TMB was calculated for different cohorts with somatic mtDNA PV grouped by complex, high impact and disease behaviour. Groups were compared using the R package epitools (v 0.5-10.1, October 2022) to calculate the 95% Poisson's exact confidence intervals for rates, using the total number of mutations as the count of events, and the genomic length sequenced in Mb as the time at risk.

8.4.7 Impact of genes involved in telomere maintenance on disease behaviour

The frequency of genes PV in genes associated with telomere maintenance (*ATRX* and *TERT*) was assessed, including analysis for an association with PC/PGL disease behaviour (primary, recurrent or metastatic disease)

8.4.8 Statistical analysis

Descriptive statistics were used to describe the cohort. Mean, median and range were calculated for numerical values and groups compared using the Mann-Whitney *t*-test. Categorical variables were compared using Fisher's exact test. A p-value of < 0.05 was set for significance for all analyses. Statistical analyses were performed using GraphPad Prism 8 (version 8.4.3, June 2020).

8.5 Results

8.5.1 Phenotypic features

Selected phenotypic data was made available to the author by the A5 SDHB Study team. The cohort comprised of 99 paired tumour-blood samples from 84 individuals (i.e. there were multiple samples from some patients) diagnosed with a PC/PGL and known to harbour a germline *SDHB* PV (Table 8.1). There were 36 unique *SDHB* PV identified: 10 frameshift, 9 non-sense and 17 missense variants. Mean age of diagnosis of PC/PGL was 32 y (range 9-76 y) with a slight male preponderance (female 44%: male 56%).

Of the 99 PC/PGL tumour samples, 74 were primary, 6 recurrent and 19 metastatic PC/PGL. Of 74 primary tumour samples, 5 (7%) were PC and 69 (93%) were paraganglioma; 59 abdominal, 5 thoracic, and 14 head and neck. Primary PC/PGL had metastasised in 23 (31%); 15 were synchronous and eight metachronous metastases. Tumour size was recorded in 69 primary PC/PGL of which 39 (56%) were < 5cm and 30 (44%) ≥ 5cm.

Table. 8.1 Clinical characteristics of 99 *SDHB* PC/PGL including tumour location, behaviour and size.

Baseline characteristics	***Total (n)***	**Cases**
Mean age at diagnosis, y (range)	99	32 (9-76)
F:M		44:56
Tumour type (n, %)	**99**	
Primary		74 (75%)
Recurrent		6 (6%)
Metastatic		19 (19%)
Tumour location of primary PC/PGL (n, %)	**74**	
Phaeochromocytoma		5 (7%)
Paraganglioma		69 (93%)
Abdominal		50 (73%)
Thoracic		5 (7%)
Head and Neck		14 (20%)
Tumour behaviour of primary PC/PGL (n, %)	**74**	
Non-metastatic		51 (69%)
Metastatic		23 (31%)
Synchronous		15
Metachronous		8
Tumour size of primary PC/PGL (n, %)	**69**	
< 5cm		39 (56%)
≥ 5cm		30 (44%)

Abbreviations: F, female; M, male; PC, phaeochromocytoma; PGL, paraganglioma

8.5.2 Filtering of WGS mitochondrial output

The annotated mitochondrial variant list generated from *mity* was filtered and summarised in Table 8.2.

Table 8.2. Filtering steps of annotated mitochondrial variants

Filtering step	Number of variants identified (n)
Variant output	208385
Protein coding	195376
Tier 1 (variant allele frequency ≥ 0.01)	3558
Read depth > 100	3551
Population allele frequency < 0.001	1224
Non-synonymous	1072
Unique variants	207
Somatic	114
Germline	172

8.5.3 Mitochondrial somatic variants

There were 114 unique somatic mtDNA variants identified from analyses of this study cohort as detailed above. Specifically, 40 variants were pathogenic (15 high impact, 25 moderate impact) and 74 variants of uncertain significance (Figure 8.3). Of samples harbouring a somatic mtDNA PV, the median heteroplasmy was 0.02 (IQR 0.01-0.06) (Figure 8.2a) and median age at diagnosis of primary PC/PGL was 38 y (IQR 27-59 y)(Figure 8.2b).

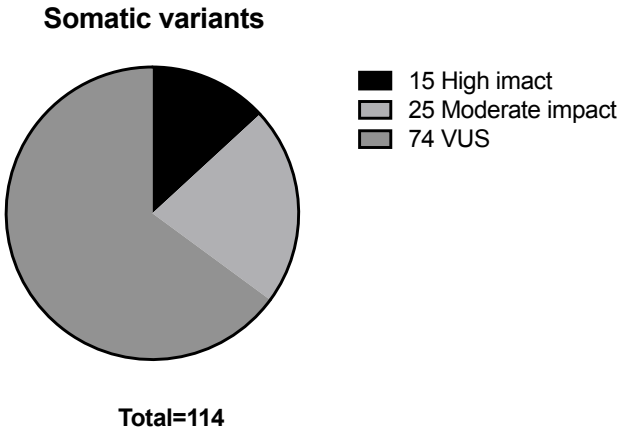

Figure 8.3 Somatic mtDNA variant type. 114 unique somatic mtDNA variants were detected of which 40 were pathogenic (15 high impact, 25 moderate impact) and 74 variants of uncertain significance.

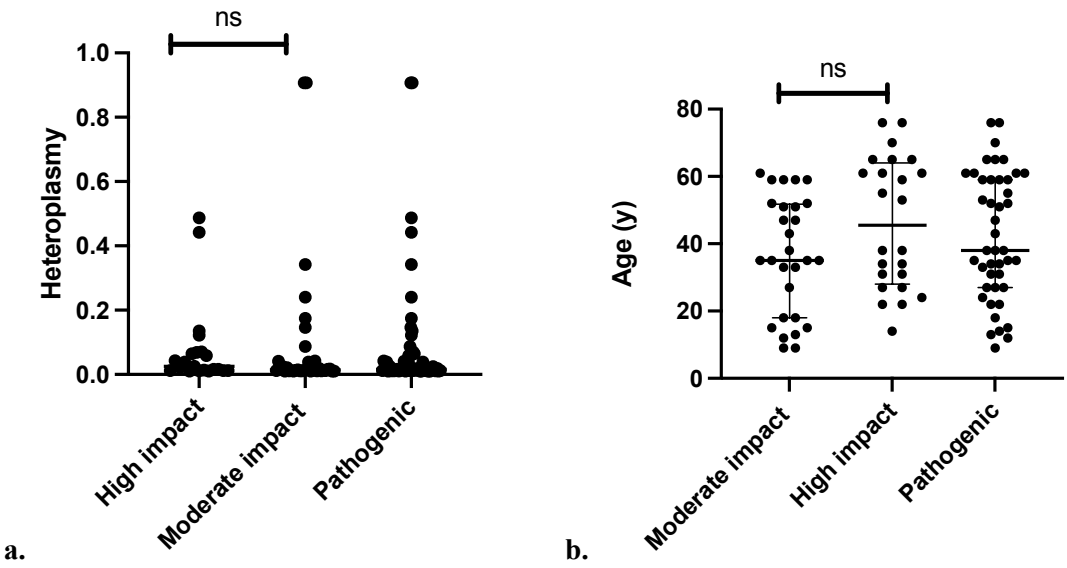

Figure 8.4 Somatic mtDNA variants, variant heteroplasmy (A) and age at diagnosis of primary PC/PGL (B). Fig. 8.2a: pie chart displaying the spectrum of mtDNA variants including high impact (n=15), moderate impact (n=25) and VUS (n=75). Fig. 8.2b: somatic mtDNA PV variant heteroplasmy with a median of 0.02 (IQR 0.01-0.06) with no difference in heteroplasmy between high impact and moderate impact (0.02 *versus* 0.014, $p = 0.21$). Fig. 8.1c: age at diagnosis of primary PC/PGL where the median age was 38 y (IQR 27-59) with no difference between age at diagnosis between high impact and moderate impact somatic mtDNA variants (45 y versus 35 y, $p = 0.6$)

8.5.4 Complex location of unique somatic mtDNA PV

Of the 40 unique somatic mtDNA PV, variants occurred predominantly in complex I (n=25) compared to the remaining complexes combined (n=15) (63% *versus* 37%, $p = 0.04$); 5 (12%) in complex II, 10 in complex III (25%) and no variants detected in complex IV (Figure 8.2).

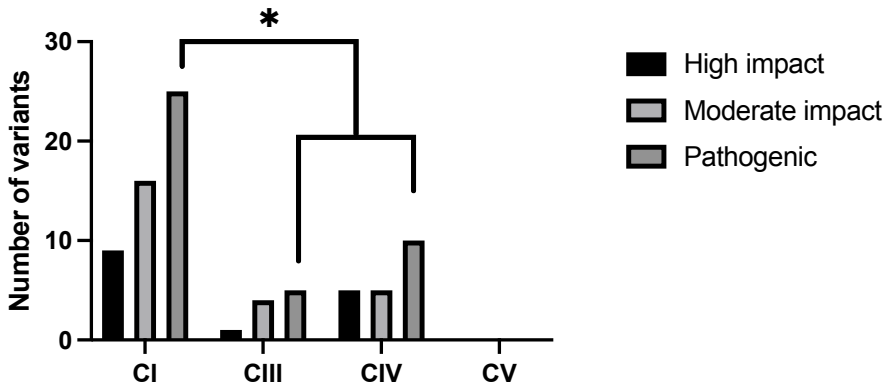

Figure 8.5 Complex location of unique somatic mtDNA PVs. Bar chart displaying the number of somatic mtDNA variants indentified within each of the four mitochondrial complex coding regions; complex I, complex III, complex IV and complex V. PV were found to occur more frequently in complex I compared to the remaining complexes combined (63% *versus* 37%, $p = 0.04$)

8.5.5 Frequency of pathogenic variants in PC/PGL

The frequency of somatic mtDNA PV was greater in recurrent/metastatic compared with primary PC/PGL (84% *versus* 49%, p=0.002)(Table 8.2). Similarly, the frequency of somatic mtDNA PV in complex I was greater in recurrent/metastatic PC/PGL compared with primary PC/PGL (57% *versus* 38%, $p = 0.05$). Conversely, high impact somatic mtDNA PVs occurred more frequently in primary compared with recurrent/metastatic PC/PGL (21% versus 7%, $p = 0.02$). Similarly, the frequency of high impact somatic mtDNA PV occurring in complex I was greater in primary compared with recurrent/metastatic PC/PGL (15% versus 4%, $p = 0.05$).

Table 8.3 Frequency of somatic mtDNA pathogenic variants in PC/PGL

	Total	**PV**	**CI**	**CIII-CV**
Primary PC/PGL, n (%)	74	36/74 (49%)	28/74 (38%)	8/74 (11%)
High impact		16/74 (21%)	11/74 (15%)	5/74 (7%)
Metastatic/recurrent, *n* (%)	25	21/25 (84%)	14/25 (57%)	7/25 (28%)
High impact		5/74 (7%)	3/74 (4%)	2/74 (3%)
***p* -value**		0.002	0.05	0.05

8.5.6 Comparing high impact and moderate impact somatic mtDNA pathogenic variants

High impact

Of 15 unique high impact somatic mtDNA variants all were found to be truncating variants; ten stop-gain and five frameshifts. Variants occurred predominantly in complex I (9 [60%]) with the remaining variants being 1 in complex III genes (7%) and 5 (33%) in complex III genes (Figure 8.5). There were no high impact variants found within complex V in our study cohort. Median heteroplasmy was 0.02 (0.01 to 0.48)(Figure 8.4, Table 8.4). 12 variants were identified in singleton tumours only and three variants were recurrent; one in two PC/PGL, one in three PC/PGL, and one in four PC/PGL

Twenty-one PC/PGLs contained high impact somatic mtDNA PV with two high impact variants co-occurring in a single sample. Sixteen of these PC/PGLs with high impact variants were primary (of which 6 went on to metastasise), three were recurrent and two were metastatic. All these primary tumours were PGL with a median age of diagnosis 45 y (range 14-62 y)(Figure 8.4, Table 8.4). Of 16 primary PGL 10 were < 5 cm; 5 PC/PGL ≥ 5 cm (one unknown).

Four high risk somatic pathogenic variants were found to have been previously reported in somatic cancer databases; pancreatic cancer endocrine neoplasm (m.12806G>A, m.15240G>A, ICGC PAEN-AU:1/52), cervical squamous cell carcinoma (m.13267G>A ICGC CESC-US:1/194), ovarian cancer (m.13366G>A, ICGC OV-AU:1/93. No variants were described in mitochondrial disease at the time of conducting these analyses.

Moderate impact

There were 25 unique moderate impact somatic mtDNA PV identified; 16 (64%) occurred in complex I, 4 (16%) in complex III, 5 (20%) in complex IV and none in complex V.(Figure 8.5) Median variant heteroplasmy was 0.02 (range 0.01-0.89) (Figure 8.4). There were 22 variants occurring within in a single PC/PGL and only three were recurrent; one in two PC/PGL, one in three PC/PGL and one in 12 PC/PGL.

Thirty-nine PC/PGL tumour samples contained moderate impact mtDNA PV. Twenty-two were primary PC/PGL (of which 10 went on to metastasise), four were recurrent and 13 were metastatic. Primary tumours were predominantly extra-adrenal (20 PGL versus two PC) with median age of diagnosis 35 y (range 9-52 y)(Figure 8.1c, Table 8.3). Of the 22 primary PC/PGL 10 were < 5 cm; 12 PC/PGL ≥ 5 cm (two unknown).

Five moderate risk somatic variants were reported in somatic cancer databases; thyroid cancer (m.14849T>C, ICGC THCA-CN:1/50), ovarian cancer (m.6261G>A), lung adenocarcinoma (m.13052G>A, COSM6188323), melanoma (m.15807C>T, MELA-AU:1/183), pancreatic cancer (m.15092G>A, PACA-AU:1/391). Four variants were also described in mitochondrial disease; EXIT (m.14849T>C), LHON (m.6261G>A), Leigh disease (m.10158T>C) and MELAS (m.15092G>A).

Comparing disease behaviour between high impact and moderate impact mitochondrial somatic variants

Comparing high and moderate impact somatic mtDNA PVs there was no difference in median heteroplasmy, age of primary PC/PGL diagnosis, tumour behaviour, tumour location or tumour size (Table 8.4).

Table 8.4. Frequency of somatic mtDNA high and moderate impact variants in primary PC/PGL.

	Het. (range)	**Age at dx, median (range)**	**Tumour behaviour**		**Tumour location**		**Tumour size**	
			Benign	Mal.	PC	PGL	<5cm	≥ 5cm
High impact	0.02 (0.01-0.48)	45y (14-62)	10	6	0	16	10	5
Mod. impact	0.014 (0.01-0.91)	35 years (9-52)	12	10	2	20	10	12
***p* - value**	0.21	0.06	0.5		0.5		0.3	

8.5.7 Tumour mutational burden in primary PC/PGL

TMB in primary PC/PGL per complex

Within primary PC/PGL, the total TMB of truncating PVs was 19/Mb and missense PVs 24/Mb. The TMB of truncating mtDNA PV divided into complex was 23/Mb in CI, 12/Mb in complex III, and 18/Mb in CV and 0/Mb in complex V (Table 8.5). There was no statistically significant difference between the groups.

The TMB of missense mtDNA PV divided into complexes was 36/Mb in CI, 0.3/Mb in complex III, and 9//Mb in CV and 0Mt/Mb in complex V (Table 8.5). There was a trend towards statistical significance difference between CI and CV ($p = 0.049$).

Table 8.5. Tumour mutational burden of somatic mtDNA PV in primary PC/PGL per complex.

	TMB (Mut/Mb)	
	Truncating variant	Missense variants
Total	19 (95% CI 11-31)	24 (95% CI 14-37)
CI	23 (95% CI 12-42)	36 (95% CI 21-58)
CIII	12 (95% CI 0.3-66)	0.3 (95% CI 0.3-66)
CIV	18 (95% CI 5-46)	9 (95% CI 1-32)
CV	-	-

Abbreviations: TMB Mut/Mb; Tumour mutational burden (mutations/megabase), CI; complex I, CIII; complex three, CIV; complex four; C5, complex five.

TMB per disease behaviour

The TMB of truncating somatic mtDNA PV in primary PC/PGL was 19/Mb, recurrent 5/Mb and metastatic 5/Mb, with a statistically significant difference in TMB between primary *versus* recurrent ($p = < 0.01$), and primary *versus* metastatic ($p = < 0.01$). The TMB of missense somatic mtDNA PV in primary PC/PGL was 19/Mb, recurrent 3/Mb, and metastatic 10/Mb, with a statistically significant difference in TMB between primary and recurrent PC/PGL ($p<0.01$)

Table 8.6. Tumour mutational burden of somatic mtDNA PV in primary PC/PGL per disease behaviour.

	TMB (Mut/Mb)	
	Truncating variants	Missense variants
Primary PC/PGL	19 (95% CI 10-26)	17 (95% CI 10-26)
Recurrent PC/PGL	5 (95% CI 0.5-8)	3 (95% CI 0.5-7.8)
Metastatic PC/PGL	5 (95% CI 1 – 10)	10 (95% CI 4 – 17)

Abbreviations: TMB Mut/Mb; PC, phaeochromocytoma; PGL, paraganglioma

8.5.8 Impact of genes involved in telomere maintenance on disease behaviour

In total 30% of samples harboured an ATRX or TERT PV (n=30) and 70% were wild-type (n=69). *ATRX* or *TERT* PVs occurred more frequently in samples harbouring a mtDNA somatic PV compared with samples with no mtDNA somatic PV (41% versus 22%, $p = 0.04$). Within patients harbouring a somatic mtDNA PV, an *ATRX* or *TERT* PV occurred less frequently in patients diagnosed with primary PC/PGL compared with patients diagnosed with recurrent or metastatic PC/PGL (30% *versus* 80%, $p = < 0.01$).

8.6 Discussion

By sequencing the mitochondrial genome of tumours from patients with PC/PGL associated with germline *SDHB* PVs, this study was able to identify a unique pattern of high impact (truncating) variants.

We confirmed heteroplasmy of somatic mtDNA somatic PVs in PC/PGL was low (median heteroplasmy 0.02, IQR 0.01-0.06). These findings align with TCGA published data that have shown somatic mtDNA variants to be predominantly heteroplasmic with only 8% reaching homoplasmy [328]. This previously published cohort showed 85% of heteroplasmic samples had a VAF lower than 0.66 (mean 0.2, median 0.045). It was hypothesised low heteroplasmy allows mitochondria to retain functioning wild-type mtDNA for oxidative phosphorylation [326, 328]. Others found frameshift indels and non-sense variants exhibit lower heteroplasmy than missense variants, implying highly disruptive variants are under negative selection pressure [328]. In contrast, data presented in this chapter did not find a difference in heteroplasmy between truncating *vs* missense variants albeit with relatively low numbers.

The analysis performed within this chapter identified truncating somatic mtDNA PV occurred most frequently in complex I (63% *versus* 37%, $p = 0.04$). There were no pathogenic variants detected in complex V. Truncating variants have previously been reported to be present at 2-fold greater numbers in complex I relative to other complexes. These findings imply positive selective pressure for truncating variants within the first electron acceptor along the electron transport chain [329]. Although not further analysed in this study, it was of interest to note that truncating PV have been reported by others to arise repeatedly at specific genomic loci, analogous to nuclear-DNA somatic cancer hot-spots [329]. In a previous study, six homopolymeric repeat loci (*ND1* m.3566–3571, *ND4* m.10947–10952, *ND4* m.11032–11038 *ND4* m.11867–11872, *ND5* m.12385–12390 and *ND5* m.12418–12425 occurred

exclusively in complex I and accounted for 40% of all truncating variants within this complex detected throughout tissue lineages [329]. Whilst none of these variants were identified in our PC/PGL cohort we did find two recurring truncating variants, also located in complex I: MT-ND2 m.4611-4618del (n=3) and MT ND1 m.3678T>G (n=4).

In contrast to the frequent occurrence of variants in complex I, complex V variants were rare. It could be proposed this phenomenon may represent some form of locus-specific alterations in cellular fitness. An absence of mtDNA somatic PV in complex V has been commonly reported in previous publications [317, 326, 329]. This implies impairment of the final complex of the ETC with impairment of ATP synthesis has significantly detrimental functional consequences, which are not tolerated, and thus are under negative selection.

Somatic mtDNA PV were most frequent in metastatic/recurrent PC/PGL (84%) however, when restricting analysis to complex I, the frequency was greatest in primary PC/PGL (20%). Gorelick et. al. calculated the rate of truncating variant throughout various tumour types, being lowest in soft tissue sarcoma and glioma (range 2-5%) and highest in renal cell carcinoma, colorectal cancer and thyroid cancer (20-30%) [329]. Our findings therefore report PC/PGL to have a relatively high frequency of somatic mtDNA PV compared to other tumour types.

Complex I is the largest coding region of the mitochondrial genome and calculating TMB therefore more accurately represents the burden of PVs between complexes. Within this study, the TMB was greatest in complex I for both missense and truncating variants (23 mut./Mb and 36 mut./Mb). Similarly, the TMB of truncating PV of various tumours calculated from the TCGA/PCAWG ranged between 11-12 mutation / Mb with a significantly greater burden in complex I. mtDNA also has the distinctive insult of exposure to radical oxygen produced by the respiratory transport chain [317]. However, recent evidence questioned the role of oxidative stress as a driver of mtDNA mutations with superoxide, the proximal radical oxygen species generated in the respiratory chain being shown to be an inefficient DNA modifier [317]. Further, mutational signatures support somatic substitutions are unlikely to be secondary to reactive oxygen species, which is characterised by G:C > T:A transversion resulting from guanine oxidation [326]. Similarly mtDNA mutations signatures differed from those seen secondary to carcinogens such as smoking and UV light [328]. mtDNA showed extreme replicational mtDNA strand bias which were consistent between malignancies. C:G>T:A and T:A > C:G were the most frequent signatures at 58.3 and 34.2% [328]. Proposed mechanisms are mitochondrial specific and include endogenous mtDNA polymerase replication errors being preferentially generation. Interrogation of

whether truncating PVs across different tissue lineages resulted in similar functional consequences was assessed through gene expression analysis [329]. Upregulation of genes associated with OXPHOS, which appeared to be more commonly associated with higher VAF truncating variants, was suggestive of a dosage effect. Downregulation of genes which relate to innate immune pathways, including TNF-alpha, was also differentially expressed. It is proposed upregulation of OXPHOS genes in the context of truncating PV is a compensatory mechanism with the aim of maintaining mitochondrial respiration, a vital process in malignancy.

Surprisingly, the median age at diagnosis of primary PC/PGL in patients harbouring a somatic mtDNA PV in this study (38 y) is higher than the average age of diagnosis of *SDHB* related PC/PGL at 29 y, implying a less aggressive phenotype. A similar finding was reported in colorectal cancer whereby presence of truncating and non-truncating mtDNA variants were associated with superior clinical outcomes [329]. These finding imply a potential survival advantage for patients harbouring a somatic mtDNA PV whereby a change from oxidative phosphorylation to an alternative method of energy production, such as aerobic glycolysis, occurs. And, along with kidney, colorectal and thyroid cancer, the resulting aberrations with alteration in NAD+: NADH which occurs with complex I dysfunction can be tolerated more-so than in other tumour types.

The finding of an association between the occurrence of somatic mtDNA PV and variants associated with *ATRX* and *TERT* in this study was novel. We found *ATRX/TERT* PV occurred more frequently in samples harbouring a mtDNA somatic PV compared with samples with no mtDNA somatic PV, and, within patient harbouring a somatic mtDNA PV, *ATRX/TERT* PV occurred more frequently in patients with recurrent or metastatic PC/PGL. *ATRX* and *TERT* are both involved in telomere maintenance through different mechanisms. Telomerase activation is common in malignancy, driven by somatic telomerase reverse transcriptase (*TERT*) alterations, including *TERT* promotor mutations or *TERT* amplification [337, 338]. TERT has also been shown to localise to the mitochondria and play a role in mtDNA metabolism [339]. Alternative lengthening of telomeres (a homologous recombination based process involved in maintaining telomere length) has been linked with inactivating pathogenic variants in *ATRX* [340]. The apparent co-occurrence of again uncovers a potential relationship between mtDNA somatic PVs and the nuclear DNA.

A key limitation of this study was the exclusion of mitochondrial RNAs. Higher tRNA, rRNA and mRNA aberrations have been reported in tumours than normal cells with a greater proportion in metastatic and recurrent tumours [341].

8.7 Conclusion

This is the first description of somatic mtDNA variants in tumours already harbouring severe deficiency of mitochondrial respiration – namely biallelic *SDHB* inactivation resulting in impaired Krebs cycle and ETC. The data presented herein confirmed somatic mtDNA PVs occurred more often in complex I, with relatively low heteroplasmy; and high/moderate impact mtDNA variants were more frequent in recurrent/metastatic PC/PGL and those associated with *TERT* or *ATRX* mutations. Overall, these findings suggest an important role for mtDNA variation in the genesis of aggressive and/or metastatic PC/PGL and raise the intriguing possibility pre-existing SDH deficiency creates specific vulnerabilities to further impairment in the ETC. Further correlation with phenotype is warranted, including survival analysis.

CHAPTER 9

Efficacy of Radionuclide Therapy in the Treatment of Inoperable or Metastatic PC/PGL

Chapter 9: Efficacy of radionuclide therapy using ^{131}Iodine meta-iodobenzylguanidine (I-131-MIBG) or ^{177}Lutetium-[DOTA,Tyr^{3}]octreotate (^{177}Lu-DOTATATE or Lu-177-Octreotate) for the treatment of inoperable or metastatic phaeochromocytoma and paraganglioma.

9.1 Introduction

Metastatic PC/PGL is defined as the presence of chromaffin tissue in an organ where this tissue is usually absent [342]. Overall 15-17% of PC/PGL metastasize [30] developing more frequently in patients with thoraco-abdominal paraganglioma (15-35%) compared with PC (5-20%) [23]. Common metastatic sites include lymph nodes, bone, lung and liver [343]. Malignancy is diagnosed predominantly between age 42-48 y [29, 343, 344]. On average diagnosis is made 6 years following primary PC/PGL diagnosis, although cases have been reported to occur many decades later [343, 345]. Historically, reports have been published detailing survival following diagnosis of PC/PGL, and metastatic PC/PGL has been confirmed as having poorer prognoses. Factors which correlate with shorter survival include male sex, older age at diagnosis of primary PC/PGL, and tumour-specific features (including but not limited to large primary tumour size, thoraco-abdominal PGL, presence of synchronous metastases) [343, 346]. Of relevance to this study, presence of an underlying germline pathogenic variant, particularly in *SDHB,* is another key risk factor for metastatic PC/PGL, and thus poorer outcomes [347]. With advances in early diagnosis and treatment, the 5- and 10-year overall survival rates have improved dramatically and are currently reported as 85.4% and 72.5%, respectively [343].

Treatment of inoperable and/or metastatic disease remains challenging. The rare nature of PC/PGL has hindered large prospective clinical trials. Cytotoxic chemotherapy remains first line of therapy for patients with rapidly progressing PC/PGL, particularly in those patients with a high visceral burden [13]. Meta-analyses of the efficacy of cytotoxic chemotherapy have reported a disease control rate (DCR) of 55% and overall response rate (ORR) of 41% [348]. A Phase II clinical trial into the efficacy of the tyrosine kinase inhibitor (TKI) Sunitinib reported an DCR of 35.9% over 12 months and a progression free survival of 8.9 months compared to 3.6 months in the placebo group [349]. Treatment with TKI is currently reserved for patients with slowly or moderately progressive PC/PGL who have been categorised as unsuitable for previous routine therapies [13]. For slow-to-moderate growing PC/PGL, targeted radionuclide therapy has recently come to be considered the first line treatment regime [13]. Two radiopharmaceutical therapies currently available for treating inoperable recurrent or metastatic PC/PGL are iodine-131 metaiodobenzylguanine (I-131 MIBG) and Lutetium-177-DOTA-

octreotate (Lu-177-DOTATATE)[13]. Both deliver β-emitting ionising radiation causing cytocidal DNA damage [350, 351].

MIBG is structurally similar to noradrenaline, and has been shown to act as a substrate for the noradrenaline reuptake transporter, present on the cell surfaces of approximately 60% of PC/PGL, and to be subsequently stored within intra-cellular neurosecretory granules.[352] MIBG radiolabelled with ^{131}I, abbreviated I-131 MIBG, has been proven to have a favourable safety profile and has been used to treat inoperable and/or metastatic PC/PGL for many decades [350, 353]. Recently, high-specific-activity I-131 MIBG has been developed. This formulation is almost entirely radiolabelled delivering a much higher dose of targeted radiation with fewer side effects [354].

Lu-177-DOTATATE, a form of Peptide Receptor Radionuclide Therapy (PRRT), comprises the chelator 1,4,7,10-tetraazacyclododecane-1,4,7,10-tetraacetic acid (DOTA)-peptide and SSTR analogue tyrosine-octreotate radiolabelled with lutetium-177. The NETTER1 trial in mid-gut neuroendocrine tumors found a high response rate with Lu-177-DOTATATE and reported prolonged progression-free survival when compared with high dose long-acting slow release octreotide acetate [355]. Following these findings PRRT was approved in the United States in 2018 for treatment of somatostatin receptor (SSTR)-positive gastro-enteropancreatic neuroendocrine tumours. As PC/PGLs have also been shown to express SSTR, it followed that PRRT be considered as a therapeutic option for the treatment of inoperable or metastatic disease.

The rare nature of PC/PGL has impeded rigorous analyses of efficacy of targeted radionuclide therapies. The aim of this chapter was to assess efficacy and toxicity of I-131 MIBG and Lu-177-DOTATATE in treating patients with PC/PGL within a single centre.

9.2 Aims

The aims of this chapter were to;

i) Assess for treatment response (overall response rate, disease control rate) to radionuclide therapy (I-131 MIBG or Lu-177-DOTATATE) by measuring three variables; clinical, hormonal and radiological response
ii) Perform survival analyses (progression free survival, overall survival)
iii) Grade toxicity as per the Common Terminology Criteria for Adverse Events

9.3 Materials and methods

This retrospective audit was comprised of the review of clinical notes and investigation results (biochemical and radiological) of patients who received systemic radiopharmaceutical therapy at Royal North Shore Hospital (RNSH), Sydney, Australia, for treatment of inoperable or metastatic PC/PGL (2007-2021). Patients with follow-up data of less than three months were excluded from this review.

9.3.1 Treatment eligibility

Patient eligibility for I-131 MIBG and Lu-177-DOTATATE aligned with the recommendations outlined in the 'EANM procedure guidelines for I-131-meta-iodobenzylguanine therapy' [356] and the 'NSW Lutate therapy referral and protocol'[357], respectively. Patients were required to meet all suitability criteria with no contraindications. Lu-177-DOTATATE therapy was approved by the RNSH Neuroendocrine Tumour Multidisciplinary Team and by the Special Access Scheme of the Therapeutic Goods Administration. I-131 MIBG and Lu-177-DOTATATE were procured from recognised radiopharmaceutical suppliers. The therapies were administered as per local protocol, briefly summarised as treatment with I-131 MIBG as a single dose and/or Lu-177-DOTATATE as four cycles over 8 weeks (range 6-12 weeks).

9.3.2 Patient recruitment

Patients were identified by searching the RNSH Nuclear Medicine Department database for treatment-naïve individuals with a diagnosis of PC/PGL who had undergone treatment with I-131 MIBG and/or Lu-177-DOTATATE. Data collected included age, gender, location of primary PC/PGL (adrenal, pelvic, abdominal, thoracic, mediastinal, head and neck), age at diagnosis of primary PC/PGL, years from diagnosis of primary PC/PGL to diagnosis of inoperable and/or metastatic PC/PGL, and metastatic site (lymph nodes, liver, lung, bone). Outcome of molecular analyses were recorded.

9.3.3 Response analysis

Response was assessed using three variables; clinical, hormonal and radiological. Measurements were taken three months following the first treatment with radionuclide therapy (R1). Clinical and functional response was classified using adapted response criteria and anatomical response as per RECIST 1.1 (Table 9.1). Response analyses included disease control rates (DCR, stable disease, partial responses, and complete responses) and overall response rates (ORR, those with partial responses, and complete responses).

Table 9.1. Clinical, functional and radiological response criteria for patient receiving radionuclide therapy

Response	Clinical *		Functional	Radiological (RECIST 1.1)
	Symptomatic	ARS		
Complete response	Complete resolution of symptoms	Normalisation of previously elevated score	Normalisation of previously elevated levels	Disappearance of all target lesions
Partial response	Decrease in intensity and/or frequency of symptoms	Reduction by > 20%	Reduction by > 20%	≥ 30% decrease in the sum of diameters of target lesion
Stable disease	No change in symptoms	Not decreased by > 20% OR increased by > 20%	Not decreased by > 20% (or increased by > 20%	Neither PR nor PD
Progressive disease	Increase in severity and/or frequency of symptoms	Increased by > 20%	Increased by > 20%	≥ 20% increase of at least 5mm in the sum of diameters of target lesions OR the appearance of new lesions

*Abbreviations: ARS, anti-hypertensive response score; * Composite clinical response ('best response')*

Clinical response

Symptoms of catecholamine excess, systolic blood pressure and changes in blood pressure (BP) medications were used to assess clinical response. Given the variation in individual BP medications, an antihypertensive response score (ARS) was calculated whereby 1 point = standard dose, ± 0.5 point = increase/decrease by half standard dose, ± 2 = double/half standard dose, etc (Table 9.2). Percentage change in ARS was calculated. Symptomatic response and ARS were combined to give a composite clinical response capturing data on the best/worst response of either variable.

Table 9.2: Standard doses of anti-hypertensive medications

Medication	Standard Dose
Phenoxybenzamine	10mg OD
Irbesartan	75mg OD
Propranolol	10mg OD
Metoprolol	25mg OD
Labetalol	100mg OD

Abbreviations: OD, once daily

Functional response

Catecholamines and their metabolites were recorded with lab specific ranges (REF). Percentage response for each individual was calculated as an average between noradrenaline/adrenaline or normetanephrine/metanephrine.

Radiological response

Radiological response was assessed for both I-131 MIBG and Lu-177-DOTATATE as per RECIST 1.1 criteria [358].

9.3.4 Survival analysis

Survival analysis included progression free survival (PFS, time from administration of radionuclide therapy to the time of objective tumour progression) and overall survival (OS, time from administration

of radionuclide therapy to death from any cause). Survival outcomes were censored at time of last follow-up where relevant.

9.3.5 Toxicity

Haematological and renal toxicity were graded as per the Common Terminology Criteria for Adverse Events (CTCAE) 5.0 (November, 2017) [359]

9.3.6 Statistical analyses

Statistical analyses presented from data obtain from this study were performed using GraphPad Prism 8 (version 8.4.3, June 2020). Continuous variables were expressed as the median and interquartile range and the means of two groups were compared using the Mann-Whitney *U*-test. Categorical variables were expressed as numbers and percentages and differences between groups were compared using Fisher's exact test. Survival analyses of the PFS and OS were assessed using Kaplan-Meier analyses and comparisons performed using a log-rank test incorporating the Mantel-Cox method. Statistical significance was set at $p<0.05$.

9.4 Results

9.4.1 Baseline characteristics

Sixteen patients received systemic radionuclide therapy for metastatic or inoperable PC/PGL and met criteria for inclusion in this study (Table 9.3). Three patients were subsequently excluded from the analyses; two were lost to follow up and the third received a partial dosing (only two doses of Lu-177-DOTATATE) and was removed from the study cohort.

Gender was identified as being unequally distributed with a greater proportion of males (11M:5F). Nine patients were diagnosed with PC and seven with PGL (five with head and neck tumours, one mediastinal, one pelvic (bladder)). Metastatic sites included bone (n=12), lymph nodes (n=5), liver (n=6), lung (n=5), prostate (n=1). Median age of primary tumour diagnosis was 45 y (IQR 17-80). There were no statistically significant differences in age between those receiving I-131 MIBG (median 41.5 y, IQR 23-54.5) and Lu-177-DOTATATE (median 44 y, IQR 23-54.4) (p=0.96). Median time from primary PC/PGL diagnosis to the diagnosis of inoperable or metastatic disease for all patients receiving radionuclide therapy was 7 y (IQR 2.5-13) (Figure 9.1). There were no statistically significant differences in the median time from primary PC/PGL diagnosis to the diagnosis of inoperable or

metastatic disease in those patients receiving I-131-MIBG (median 9.5 y, IQR 5.5-17) and Lu-177-DOTA-octreotate (median 4.0 y, IQR 2.0-11) (p=0.2).

Ten patients (62%) were identified as harbouring pathogenic germline variants (Table 9.3). Six patients had apparently sporadic disease, five patients were without a germline mutation being detected and one patient who did not undergo genetic testing.

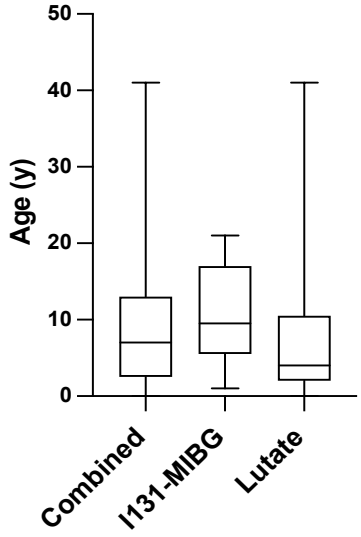

Figure 9.1 Time from primary PC/PGL diagnosis to inoperable recurrent or metastatic disease. Box and whisker plot showing the time from primary PC/PGL diagnosis to the diagnosis of inoperable or metastatic disease. For all patients median 7 y (IQR 2.5-13), those receiving PRRT (median 4 y, IQR 2.0-11) and those receiving I-131 MIBG (median 9.5 y, IQR 5.5-17) (p=0.2).

Table 9.3. Baseline characteristics of patients diagnosed with inoperable or metastatic PC/PGL

	Total	I-131-MIBG	Lu-177-DOTATATE	*p* -value
No of patients	16	8	8	0.96
Median age at dx	45 y (IQR 17-80 y)	41.5 y (IQR 23-54.5 y)	44 y (IQR 23-54.4 y)	
M: F	11:5	7:1	4:4	
Symptomatic, n (%)				0.58
Yes	11/16 (69%)	5/8 (62%)	6/8 (75%)	
No	5/16 (31%)	3/8 (38%)	2/8 (25%)	
Tumour loc. , n (%)				0.011
PC	9/16 (56%)	7/8 (88%)	2/8 (25%)	
PGL	7/16 (44%)	1/8 (12%)	6/8 (75%)	
abdominal	1/7	-	1/8	
thoracic	1/7	-	1/8	
H+N	5/7	1/8	4/8	
Hormone secreting, n (%)	11/16 (89%)	7/8 (88%)	4/8 (50%)	0.10
Indication, n (%)				
Inoperable	2/16 (12%)	-	2/8 (25%)	0.13
Metastatic	14/16 (88%)	8/8 (100%)	6/8 (75%)	
Molecular analysis				
GPV	10/16 (62%)	4/8 (50%)	6/8 (75%)	0.3

	RET (2)*, NF1, VHL*	*SDHB* (2), S*DHC, SDHD* (2), *NF1*

Abbreviations: F, female. M, male. PC, phaeochromocytoma. PGL, paraganglioma. H+N; head and neck. GPV; germline pathogenic variant

9.4.2 Systemic therapy

Of the sixteen patients reviewed at R1, eight (8/16, 50%) received I-131 MIBG and eight (8/16, 50%) Lu-177-DOTATATE. Two patients (2/16, 12%) qualified for systemic therapy based on recurrence of local disease which was inoperable, with the remaining fourteen patients (14/16, 88%) qualifying due to the presence of metastatic disease. Three patients concomitantly received radio-sensitising cytotoxic chemotherapy. The median time from diagnosis of inoperable recurrent or metastatic disease to administration of treatment was 12.4 months (IQR 3.2 – 23 months) (Figure 9.2). This period of time was found to be statistically significantly shorter in those patients who received I-131 MIBG (11 m, IQR 2-12) *versus* Lu-177-DOTATATE (23 months, IQR 2-12 months) (p=0.04).

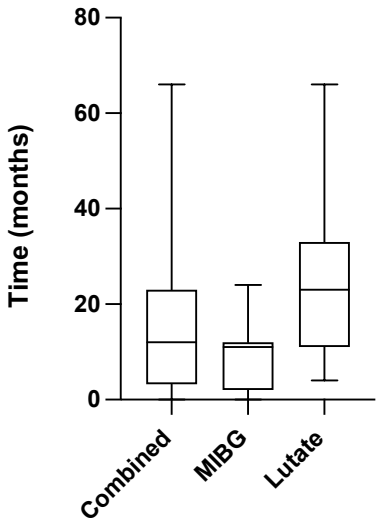

Figure 9.2. Time from diagnosis of inoperable recurrent or metastatic PC/PGL to administration of systemic radionuclide therapy Box and whisker plot showing the time from diagnosis of inoperable recurrent or metastatic PC/PGL to administration of systemic radionuclide therapy. For all patients median 12.4 months (IQR 3.2-23 months), those receiving PRRT (median 23 months, IQR 11-33 months) and those receiving I-131 MIBG (median 11 months, IQR 2-12 months) (p=0.04).

Longitudinal data was available for ≥ 12 months in fourteen patients, ≥ 3 years in seven patients and ≥ 5 years in three patients. All but two patients (6/8, 75%) who received I-131 MIBG as primary therapy progressed to require two or more additional treatments with radionuclide therapy (all participants had received additional doses of I-131 MIBG and one also received Lu-177-DOTATATE). Three patients (3/8, 37%) who received Lu-177-DOTATATE as the primary therapy progressed to require one

additional radionuclide therapy (two received further treatment with Lu-177-DOTATATE and one treated with I-131 MIBG). The number of additional doses with I-131 MIBG ranged from one to seven, and cycles with Lu-177-DOTATATE ranged between one to two. During follow-up, one patient was administered the RET-selective inhibitor Selpercatinib and another the multi-kinase inhibitor Lenvatinib.

9.4.3 Response to radionuclide therapy

Clinical response

Symptoms attributable to catecholamine excess were present in twelve patients and symptomatic response at R1 was documented in nine patients (Table 9.4). Common symptoms described were headaches (n=5), pain (n=5), sweatiness (n=4) and palpitations (n=4). Following radionuclide therapy, there was CR in six (6/9, 67%), PR in two (2/9, 22%) and SD in one (1/9, 11%). No patients reported worsening of symptoms. One patient receiving I-131 MIBG showed SD (1/3, 33%) and the remaining CR (2/3, 67%). All patients receiving Lu-177-DOTATATE showed a response, with a CR in four patients (4/6, 66%) and PR in two patients (2/6, 64%).

Of the eight patients identified as undertaking treatment with blood pressure medications recorded pre-treatment and at R1, one patient demonstrated CR (1/8, 12.5%), three PR (3/8, 37.5%), three SD (3/8, 37.5%) and one PD (1/8, 12.5%) on ARS. A single patient administered I-131 MIBG demonstrated progressive disease, with one showing CR (1/6, 17%), two PR (2/6, 33%), two SD (2/6, 33%) and one PD (1/6, 17%). One patient administered Lu-177-DOTATATE showed SD (1/2, 50%) and the other PR (1/2, 50%).

Composite symptomatic response (combining symptomatic response and ARS) showed predominantly CR (7/12, 58%) followed by PR (3/12, 25%), SD (1/12, 8%) and PD (1/8, 12.5%). In patients receiving I-131 MIBG a CR was seen in three patients (3/6, 50%), PR in one (1/6, 16%), SD in one (1/6, 16%) and PD in one (1/6, 16%). All patients receiving Lu-177-DOTATATE responded with a CR seen in four patients (4/7, 67%), PR in two (2/6, 33%).

Table 9.4. Clinical response to radionuclide therapy

Response	I-131 MIBG	Lu-177-DOTATATE	*p*-value	Combined
Symptomatic				
CR	2/3 (67%)	4/6 (66%)	1.0	6/9 (67%)
PR	0/3 (-)	2/6 (64%)	0.3	2/9 (22%)
SD	1/3 (33%)	0/6 (-)	0.1	1/9 (11%)
PD	0/3 (-)	0/6 (-)	1.0	0/9 (-)
ARS				
CR	1/6 (17%)	0/2 (-)	0.5	1/8 (12%)
PR	2/6 (33%),	1/2 (50%)	0.6	3/8 (38%)
SD	2/6 (33%)	1/2 (50%)	0.6	3/8 (38%)
PD	1/6 (17%)	0/2 (-)	0.5	1/8 (12%)
Composite *				
CR	3/6 (50%)	4/6 (67%)	0.5	7/12 (58%)
PR	1/6 (16%)	2/6 (33%)	0.5	3/12 (25%)
SD	1/6 (16%)	0/6 (-)	0.3	1/12 (8.5%)
PD	1/6 (16%)	0/6 (-)	0.3	1/12 (8.5%)

Abbreviations: CR; complete response, PR; partial response, SD; stable disease, PD; progressive disease, ARS; antihypertensive response score, *; Composite clinical response ('best response' between symptomatic and ARS)

Prior to therapy two patients recorded an AHA SBP of 'normal', five were 'elevated', four 'stage 1', six 'stage 2' and one 'crisis'. Following systemic therapy three patients fell to within normal range, two 'elevated', four 'stage 1', two stage 2 and none 'crisis'. Overall, the median SBP fell by 6mmHg (from 133mmHg [IQR 124.5-145.5] to 127mmHg [IQR 112.5-130.8] at R1 (p=0.05) (Figure 9.3). There was a fall of 11mmHg (from 134mmgHg to 123mmHg at R1, p=0.09) in participants receiving Lu-177-DOTA-octreotate and 2mmHg (from 132mmHg to 130mmHg at R1, p=0.38) for those receiving I-131-MIBG

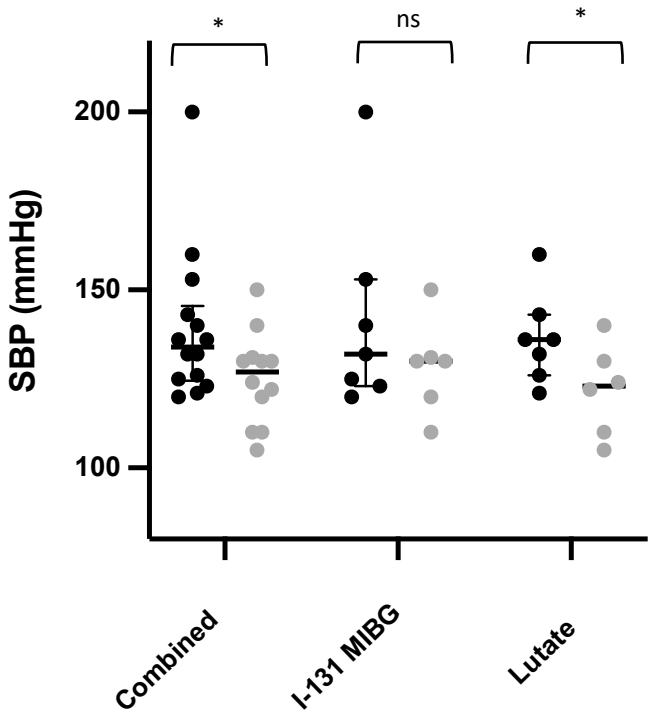

Figure 9.3 Systolic blood pressure response to radionuclide therapy. Scatterplot demonstrating systolic blood pressure (SBP) at baseline and at the time of initial review (black dot) following systemic radionuclide therapy (grey dot). The median SBP fell from 133mmHg (IQR 124.5-145.5) at baseline to 127mmHg (IQR 112.5-130.8) at R1 (p=0.05). The median SBP in patients receiving I-131 MIBG reduced from 132mmHg to 130mmHg (p=0.38) and in those receiving Lu-177-DOTATATE 134mmgHg to 123mmHg (p=0.04)

Functional response

Eleven PC/PGL were functioning (11/16, 68%) with either elevated plasma and/or urinary catecholamines or metanephrines (Table 9.5). R1 measurements were available for all patients. Overall one patient demonstrated CR (1/11, 9%), four PR (4/11, 36%), six SD (6/11, 54%) and no patients with progressive disease. Patients administered I-131 MIBG predominantly demonstrated stable disease in five (5/7, 71%) with two patients exhibited a partial response (2/7, 29%); One patient administered Lu-177-DOTATATE demonstrated SD (1/4, 25%), two with PR (2/4, 50%) and one with a CR (1/4, 25%).

Table 9.5. Functional response to radionuclide therapy

RESPONSE	I-131 MIBG	Lu-177-DOTATATE	*p*-value	Combined
Functional				
CR	0/7 (-)	1/4 (25%)	0.16	1/11 (9%)
PR	2/7 (29%)	2/4 (50%)	0.5	4/11 (36%)
SD	5/7 (71%)	1/4 (25%)	0.1	6/11 (54%)
PD	0/7 (-)	0/4 (-)	-	0/11 (-)

Abbreviations: CR; complete response, PR; partial response, SD; stable disease, PD; progressive disease, ARS; antihypertensive response score.

Radiological response

Pre-treatment and R1 images were available for assessment as per RECIST 1.1 criteria in thirteen patients (six who received I-131 MIBG, seven who received Lu-177-DOTATATE) (Table 9.6). One patient demonstrated a PR (1/13, 8%), twelve patients SD (12/13, 92%) and no patients demonstrated CR or PD. One patient receiving I-131 MIBG showed a PR (1/6, 17%) and five SD (5/6, 83%). All patients receiving Lu-177-DOTATATE showed SD (7/7, 100%).

Table 9.6. Radiological response to radionuclide therapy

RESPONSE	I-131 MIBG	Lu-177-DOTATATE	*p*-value	Combined
RECIST 1.1				
CR	0/6 (-)	0/7 (-)	-	0/12 (-)
PR	1/6 (17%)	0/7 (-)	0.26	1/13 (8%)
SD	5/6 (83%)	7/7 (100%)	0.16	12/13 (92%)
PD	0/6 (-)	0/7 (-)	-	0/13 (-)

Abbreviations: CR; complete response, PR; partial response, SD; stable disease, PD; progressive disease, ARS; antihypertensive response score.

Data was available for fourteen patients following all treatments with systemic radionuclide therapy at final follow up (seven I-131-MIBG; seven Lu-177-DOTA-octreotate). Nine patients (9/14, 65%) demonstrated SD, two PR (2/14, 14%) and three PD (3/14, 21%) as per RECIST 1.1 criteria. Of those who received I-131-MIBG as primary therapy, three demonstrated SD (3/7, 43%), two PR (2/7, 28.5%)

and two PD (2/7, 28.5%) compared with those who received Lu-177-DOTATATE as the primary therapy whereby most patients continued to demonstrate SD (6/7, 86%) and the remainder PD (1/7, 14%).

9.4.4 Disease control rate and overall response, comparing I-131 MIBG and Lu-177 DOTATATE

DCR for 'composite' clinical, functional, and radiological variables at R1 was 92% (12/13), 100% (9/9) and 100% (13/13) respectively (Table 7). Comparing I-131 MIBG and Lu-177-DOTATATE, DCR for clinical response was 83% (5/6) *versus* 100% (7/7), functional response 100% (7/7) *versus* 100% (2//2), and radiological response 100% (6/6) *versus* 100% (7/7) respectively.

ORR for 'composite' clinical, functional and radiological parameters at R1 was 83% (10/12), 45% (5/11) and 8% (1/13) respectively (Table 8). Comparing I-131 MIBG and Lu-177-DOTATATE, ORR at R1 for 'composite' clinical response was 67% (4/6) *versus* 100% (7/7), functional response 28% (2/7) *versus* 75% (3/4), and radiological response 17% (1/6) *versus* 0% (0/7) respectively.

Table 9.7. 7. Disease control rate and overall response rate to radionuclide therapy

	RESPONSE	I-131 MIBG	Lu-177-DOTATATE	*p*-value	Combined
Disease control rate	Clinical	5/6 (83%)	6/6 (100%)	0.29	11/12 (92%)
	Functional	7/7 (100%)	4/4 (100%)	-	11/11 (100%)
	Radiological	6/6 (100%)	7/7 (100%)	-	13/13 (100%)
Overall response rate	Clinical	4/6 67%)	6/6 (100%)	0.12	10/12 (83%)
	Functional	2/7 (28%)	3/4 (75%)	0.13	5/11 (45%)
	Radiological	1/6 (17%)	0/7 (-)	0.26	1/13 (8%)

Abbreviations: CR; complete response, PR; partial response, SD; stable disease, PD; progressive disease, ARS; antihypertensive response score.

9.4.5 Progression free survival and overall survival

The median period of follow up was 31 months (range 8-184 months) and longer for those receiving I-131 MIBG (median 84 months, range 9-184 months) compared with those who received Lu-177-DOTATATE (median 23 months, range 8-76 months). Median PFS (defined as progression in any clinical, functional, or radiological variable) for I-131 MIBG was 16 months (range 5-24 months) compared with 27 months (range 3-40 months) in those receiving Lu-177-DOTATATE (HR 1.6, 95% CI 0.43-6.12, p=0.4) (Figure 9.3a). Of the eleven patients who progressed, five developed increased catecholamine secretion and the remainder exhibited tumour progression radiologically. Median OS for I-131 MIBG and Lu-177-DOTA-octreotate was not reached in this study cohort (Figure 9.3b). Two of seventeen patients with longitudinal data unfortunately died from their disease.

Figure 9.3 Survival analysis of patients receiving radionuclide therapy

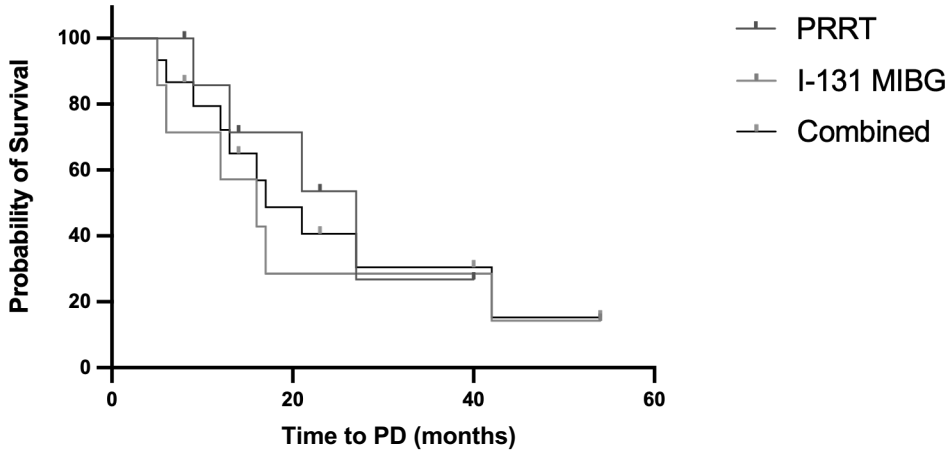

A. Progression free survival

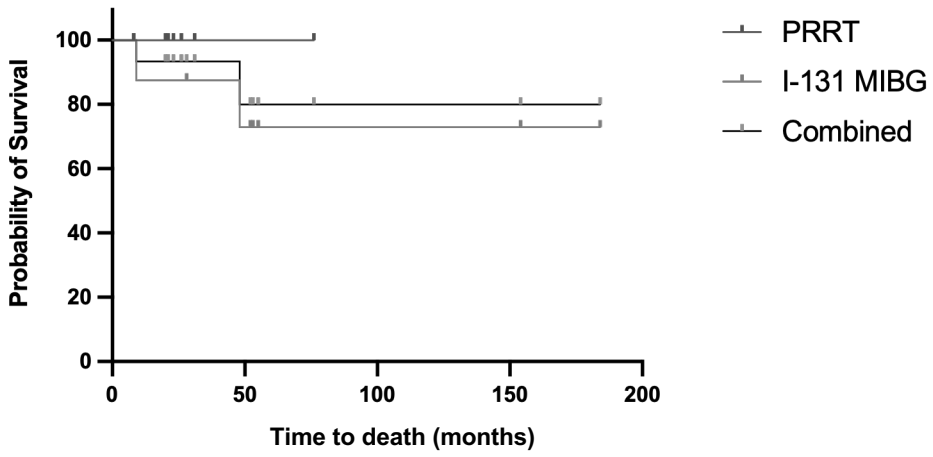

B. Overall survival

9.4.6 Correlation between response, progression free survival and overall survival

There was no correlation between clinical, functional, or radiological parameters at R1 and 'poor responders' (defined as those who died within 24 months of treatment) and 'good responders' (defined as those who survived past 60 months). The single patient with PD on ARS progressed rapidly and subsequently died within 12 months. This individual demonstrated stable disease radiologically at R1. Of note, the patient's disease was advanced at diagnosis and was associated with markedly elevated catecholamines. Interestingly, the three patients with the longest periods of survival (76, 154 and 184 months) demonstrated favourable response at R1 with none of those patients showing progressive disease on any variable (clinical, functional, or radiological).

There appeared to be no correlation between genotype and response to therapy. Review of PFS demonstrated that patients who were yet to progress harboured germline variants; *SDHB* (n=2), *SDHD* (n=1), *NF1* (n=1) and *RET* (n=1). Of this group, all but one had recently received Lu-177-DOTATATE and all had received comparatively shorter periods of follow up.

9.4.7 Toxicity

Six patients developed haematological toxicity post-therapy, which resolved in all within 12 months (Table 9.8). Four patients who received I-131 MIBG; one with neutropenia (grade 1) and four with thrombocytopaenia (grade 1-4). Two patients who received Lu-177-DOTATATE; two with anaemia (grade 1), one with neutropenia (grade 2), and one with thrombocytopaenia (grade 2). Three patients with pre-existing renal impairment developed transient falls in eGFR which subsequently returned to baseline/normal levels.

Table 9.8 Toxicity from radionuclide therapy. Graded as per Common Terminology Criteria for Adverse Events (CTCAE) 5.0 criteria.

	I131-MIBG	Lu-177-DOTATATE	Combined
Hb	-	2/8 (25%)	2/16 (12%)
G1	-	-	-
G2-4			
Neutrophils	1/8 (12%)	1/8 (12%)	2/16 (12%)
G1	-	-	-
G2	-	-	-
G3-4			
Plt	2/8 (25%)	1/8 (12%)	3/16 (18%)
G1	-	-	-
G2-3	1/8 (12%)	-	1/16 (6%)
G4			
eGFR	6/8 (75%)	7/8 (88%)	13/16 (82%)
> 90	2/8 (25%)*	1/8 (12%) **	3/16 (18%)
stage II	-	-	-
stage III	-	-	-
stage IV	-	-	-
stage V			

Abbreviations: Hb, haemoglobin; Plt, platelets; eGFR, estimated glomerular filtration rate.

9.5 Discussion

The analyses presented in this chapter have been undertaken to demonstrate differences in the efficacy between I-131 MIBG and Lu-177-DOTATATE within a cohort of patients receiving targeted radionuclide therapy for inoperable and/or metastatic PC/PGL. The investigations found that the two treatment groups were comparable with no statistically significant differences in either the age at diagnosis of PC/PGL and time to development of metastatic or inoperable PC/PGL. The median time from diagnosis of inoperable recurrent or metastatic disease to administration of radionuclide therapy was significantly shorter in those patients who received I-131 MIBG (11 *months*, IQR 2-12) *versus* Lu-177-DOTATATE (23 months, IQR 2-12) (p=0.04). This finding may reflect a paradigm shift with the adoption of close surveillance of stable PC/PGL over treatment. Radionuclide therapy was mostly administered for metastatic disease, rather than recurrent/inoperable PC/PGL. A germline pathogenic variant was detected in 62% of patients, much higher than the 30% predicted on population studies.[67]

This finding likely reflected the nature of hereditary PC/PGL syndromes (particularly *VHL*, *SDHB, SDHD* and *RET*) driving multifocal, recurrent, or metastatic disease [90, 108, 119, 288].

This study demonstrated radionuclide therapy is effective in alleviating symptoms. In patients receiving radionuclide therapy the symptomatic DCR was 100% (100% I-131 MIBG; 100% Lu-177-DOTATATE) and ORR 89% (67% I-131 MIBG; 100% Lu-177-DOTATATE). This high degree of symptomatic response to I-131 MIBG has been reported by others, with 75%-86% of patients experiencing an improvement or near resolution in symptoms, including pain, fatigue, anorexia, sweating and palpitations [360, 361]. Similarly, a meta-analysis on PRRT described a clinical response (defined as improvement in 'tumour related symptoms') in 61% of patients [362]. Alleviation of symptomatic response translates into improved quality of life; Yadav. *et al. [363]* illustrated this response in patients using receiving PRRT using Karnofsky Performance Status. This common tool is used to measure the ability of cancer patients to carry out daily tasks, and most patients reported an improvement in general wellbeing, social contact, and food intake.

Increased cardiovascular risk associated with PC/PGL arises from the acute and chronic effects of catecholamine secretion [42]. Paroxysms of hypertension and arrhythmia may precipitate acute myocardial infarction or stroke [364, 365]. Long term cardiac and metabolic complications arise including persistent hypertension, cardiomyopathy, arrhythmias and impaired glycaemic control [366]. Resection of PC/PGL reduces cardiovascular risk to that of the general population, emphasising the importance of the control of blood pressure and catecholamine secretion [367]. The investigations presented in this chapter have demonstrated a statistically significant fall in systemic blood pressure following initial treatment (from 133mmHg [IQR 124.5-145.5] to 127mmHg [IQR 112.5-130.8] (p=0.05) and a reduction in blood pressure medications (defined as 'anti-hypertensive response score'). Approximately 50% of the patients within our cohort required a reduction in dose/s of anti-hypertensive medication with an 87% DCR (83% I-131 MIBG; 100% Lu-177-DOTATATE) and 50% ORR (50% I-131 MIBG; 50% Lu-177-DOTATATE). Similarly, 25% of patients who received at least a single dose of HSA-I-131 MIBG reached the primary endpoint of ≥ 50% reduction in baseline anti-hypertensive medication [354]. These findings were in agreement with those published by Kong *et. al.* who had reported Lu-177-DOTATATE treatment had achieved a reduction in anti-hypertension medication in 36% [62].

Results presented in this chapter demonstrated a fall in catecholamine secretion with a DCR of 100% (100% I-131 MIBG; 100% Lu-177-DOTATATE) and ORR 45% (28% I-131 MIBG; 75% Lu-177-

DOTATATE). Although no patients demonstrated progressive disease with either therapy, the ORR in those patients receiving Lu-177-DOTA-octreotate was greater than in the subgroup treated with I-131 MIBG. This study design differed from those undertaken by others previously, in particular where chromogranin A, a non-specific marker of neuroendocrine tumours, had been measured to assess response to I-131 MIBG. This study collected cohort data on hormone secretion profiles that were specific for PC/PGL (catecholamines and their metabolites). Such specificity of neuroendocrine tumour biomarker data made direct comparisons with other more generic cancer-associated biomarker data sets previously published difficult. Regardless, meta-analyses of patients administered I-131 MIBG measured a higher ORR of 51% [63]. Normalisation or a decrease in normetanephrine levels has also been reported in response to PRRT [29, 62, 368] with a biochemical response seen in 64% (95% CI: 11%-96%), defined as any measurable decline in tumour marker [362].

This study found the effect of radionuclide therapy on tumour size to be less dramatic when compared with a clinical and functional response; ORR 8% (17% I-131 MIBG; 0% Lu-177-DOTATATE) however a high DCR of 100% (100% I-131 MIBG; 100% Lu-177-DOTATATE). This outcome reflected the predominance of stable disease seen in most patients receiving I-131 MIBG and all patients treated with Lu-177-DOTATATE. The findings on structural response were comparable with a meta-analysis of low specificity I-131 MIBG demonstrating a radiological DCR of 82% [63]. HSA-I 131MIBG, currently unavailable in Australia, demonstrated superior tumour response with a DCR of 92% (stable disease in 69%; partial response 23%) as per RECIST 1.1 [65]. A systematic review and meta-analysis on the use of PRRT in the management of advanced PC/PGL found a DCR of 84% (95% CI :77-89%) and ORR of 25% (95% CI 19-32%) [362]. A key limitation of this meta-analysis was the use of different anatomical response criteria highlighting the importance of standardised response criteria.

The median PFS of our cohort was 17 months (16.5 months in patients receiving I-131 MIBG versus 27 months in patients receiving Lu-177-DOTATATE, p=0.46), with OS not being reached in either cohort subgroup. Studies have reported significant variability in survival analyses in patients treated with I-131 MIBG, with a median PFS of 17.5-24 months [369-371] and median OS of 16-50 months [369, 370, 372]. Median OS of those who received the newly developed HSA-I-131-MIBG was 36.7 months (CI 29.9–49.1 months), although there was a large contrast between those who received a single therapeutic dose (18 months, CI: 4–31 months) compared with those who received two therapeutic doses (44 months, CI 32–60 months) [65]. Satapathy *et al*.[362], found the pooled estimate of the median PFS in those receiving PRRT was 37.1 months (95% CI: 32.1-42.0 months) and the mean OS

was 54.5 months (95% CI: 42.5-66.5 months) To date, only a single study has been performed directly comparing I-131 MIBG with PRRT in patients with metastatic/progressive PC/PGL and that study found a significantly increased response to treatment (defined as non-progressive disease) in the latter (62.5 *versus* 100%, p=0.013) [373].

Radionuclide therapy was tolerated well in both cohort subgroups with no patients developing long term haematological or renal toxicity. Toxicity findings in the cohort were consistent with previous studies. I-131 MIBG is associated with haematological toxicity, particularly thrombocytopenia [63, 374, 375]. Complications from low specificity I-131 MIBG are dose dependent and generally minor if < 8GBq administered, even with repeated treatments [375]. Patients administered high dose I-131 MIBG (up to 43GBq, median 444MBq/kg) were at risk of serious haematological toxicity (grade 3-4 neutropenia in 87% and thrombocytopenia in 83%), acute respiratory distress syndrome, acute hypertension and hypogonadism [374]. Meta-analysis of toxicity from PRRT in the treatment of PC/PGL found severe neutropenia (grade 3-4) occurred in 3%, thrombocytopenia in 9%, lymphopenia in 11% and nephrotoxicity in 4% of patients [362]. Myelosuppression was reversible with few patients requiring intervention and a mean time to normalisation of 12 months [376].

Clinical or histopathological features to guide clinicians' choice of radionuclide therapy are yet to be defined with the findings from small studies yet to be replicated. High dose I-131 MIBG has been shown to produce a greater response in patients harbouring *SDHB* mutations compared to non-*SDHB* carriers, although this was not predictive of progression free or overall survival [374]. A Ki67 index of < 15% was found to be associated with longer OS and PFS [377] and linear regression analysis found a baseline SUV_{max} of > 21 on Ga68-DOTATATE to be a positive predictor of early response in patients administered PRRT [64]. Another group found PC was a negative predictor of response to PRRT, potentially due to loss of the SSTR or the de-differentiated nature of the tumour [373]. Jha *et al.*[65] proposed a personalised stepwise approach whereby patients with avidity on both I-123 MIBG and SSTR imaging who develop disease progression be administered radionuclide therapy based on the toxicity profile of each therapy. HSA-I-131-MIBG could be more appropriate in young adults, patients with elevated catecholamine, or those with lower burdens of bone metastases. Conversely Lu-177-DOTATATE could be preferred for treatment of older patients, patients who have previously received cytotoxic therapies, those with pre-existing cytopenias, or those exhibiting low bone marrow reserve or a high burden of bone metastases.

Limitations

The small number of patients within this cohort was a limitation to the study. Significant variability in cumulative dose of radionuclide therapy at the time of analysis was a major limitation when comparing the findings arising from this study with those of previously published analyses. This retrospective investigation measured treatment response and survival outcomes following the first dose of I-131-MIBG or Lu-177-DOTATATE in treatment naïve patients. In other studies, the numbers of doses of I-131 MIBG administered ranged from 1-12 with a cumulative dose of 70-2322mCi and Lu-177-DOTATATE 1-8 cycles with a median cumulative dose of 22GBq. The heterogeneity between cohorts was augmented by unavoidable differences in the pre-therapy baseline study populations who were likely to have undergone surgery, systemic therapy (cytotoxic chemotherapy or TKI), and/or external beam radiotherapy.

9.6 Conclusion

Study of this retrospective cohort has been shown the utility of I-131 MIBG and Lu-177-DOTATATE in the management of locally recurrent and/or metastatic PC/PGL. These findings were consistent with an emerging consensus that radionuclide therapy is more effective at clinical and biochemical responses than for radiological responses. Further studies are needed to optimize patient selection for these therapies, and to identify chemotherapy co-treatments to enhance treatment efficacy.

CHAPTER 10.

Conclusion and Future Directions

CHAPTER 10. Conclusion and Future Directions

10.1 Overview

Phaeochromocytoma (PC) and paraganglioma (PGL) are rare neuroendocrine tumours that arise in the adrenal medulla and sympathetic/parasympathetic ganglia, respectively. Morbidity and mortality arises from catecholamine secretion and/or mass effect from location tumour invasion or metastases. PC/PGL have a diverse molecular background with somatic and germline pathogenic variants being grouped predominantly into Cluster 1 and Cluster 2 transcription pathways. Due to the high proportion of patients found to harbour an underlying germline pathogenic variant (over 30% of patients diagnosed with PC/PGL), genetic testing is recommended for all patients diagnosed with a PC/PGL due to the implications for the individual and their family. For the individual, hereditary PC/PGL syndromes are often associated with multi-focal and recurrent PC/PGL, and other tumours types (i.e. medullary thyroid cancer in Multiple Endocrine Neoplasia type 2A), with evidence routine surveillance detects tumours early and improves survival. For immediate relatives, there is a 50% chance a pathogenic variant is present in these individuals due to the autosomal dominant nature of these hereditary genes.

Precision medicine, the delivery of health care specific to the individual patient, has advanced the field of oncology with emergence of comprehensive molecular analysis of germline and somatic tissue. This has been achieved through developing sequencing techniques, including massively parallel sequencing, which are able to investigate multiple genes in tandem in a highly sensitive manner. Although of great value, the large volume of data produced from this approach requires careful curation to determine variant pathogenicity.

With the goal of applying precision medicine to patients diagnosed with PC/PGL, studies within this thesis have sought to expand on current knowledge of underlying molecular mechanisms driving PC/PGL, thus allowing patient management to be personalised. In Chapter 3 and Chapter 4, two genetic testing techniques, Next Generation Sequencing (NGS) and RNA-sequencing. (RNA-Seq), were used for diagnosis. In Chapters 5, 6 and 7 the phenotype of two rare genes implicated in PC/PGL (*MYC-associated factor X [MAX]* and *endothelial PAS-domain containing protein 1 [EPAS1]*) and genotype-phenotype correlations in paediatric PC/PGL were expanded, thus guiding surveillance for these cohorts of patients. In Chapter 8, the impact of somatic mitochondrial variants on disease behaviour in patients harbouring a germline *succinate dehydrogenase subunit B (SDHB)* pathogenic variant was interrogated. Finally, in Chapter 9, the efficacy of radionuclide therapy in treating metastatic or inoperable PC/PGL was assessed.

10.1.2 Tumour sequencing as a pathway to streamlined diagnosis of hereditary PC/PGL

MPS, including NGS, has revolutionised somatic and germline genetic testing. Germline multi-gene panel testing is now standard of care for patients who present with a personal or family history of malignancy associated with hereditary predisposition. Within Australia, investigation of patients for hereditary PC/PGL using paired blood-tumour testing using NGS is novel where current standard of care via testing of blood-derived germline/constitutional DNA after genetic counselling in outpatient Familial Cancer Services (FCS).

Chapter 3 validated paired tumour-blood genetic testing for hereditary PC/PGL using NGS followed by review of the timeliness of this proposed new approach when compared to the current standard of care. Phase 1 comprised of in-laboratory validation of PC/PGL tumour sequencing via NGS using fresh frozen PC/PGL samples from 20 patients with known germline (n = 18) or somatic (n = 2) variants. Phase 2 assessed the timeliness of prospective application of paired tumour-blood sequencing via NGS and curation of germline and somatic variants. This approach was found to be highly sensitive (sensitivity 95%) with a single variant not detected being a large scale deletion, which was subsequently identified on multiplex-ligation dependant probe amplification. Phase 2 showed the proposed approach to be significantly more timely, with median time from surgery to genetic diagnosis being 1.67 months compared with 6 months from standard care [HR 0.25 (95% CI 0.9-0.72)], $p < 0.0001$). Another advantage of tumour sequencing (compared with blood alone) was illuminating sporadic causes in three of eight cases, thus proving a molecular diagnosis and preventing further interrogation for germline causes.

10.1.3 Utility of RNA sequencing to assist in re-classifying germline *TMEM127* variants of uncertain significance.

A key challenge arising from NGS is variant curation. Variants of uncertain significance (VUS) pose a management conundrum as there is insufficient or conflicting evidence to allow definitive classification of the variant as either benign or pathogenic. The rarity of *Transmembrane protein 127 (TMEM127)* associated PC/PGL and high occurrence of unique variants (i.e. variants only identified on a single occasion), combined with complex molecular functions of TMEM127 protein, have complicated determination of variant pathogenicity. The relevance of reclassifying a VUS into either a pathogenic or benign variant (if there is supportive evidence) has great relevance for the patient; germline *TMEM127* PVs are often associated with multifocal disease and lifelong surveillance would be

required. Further, due to the autosomal dominant nature of *TMEM127* there is a 50% chance the PV will also be inherited.

RNA sequencing studies in Chapter 4 present a novel approach to using this modality of molecular analysis as a functional tool for variant curation. As per the American College of Medical Genetics guidelines, 'PS3' provides strong support of towards a pathogenic impact. RNA-Seq was used to assess *TMEM127* expression, differential gene expression, variant allele frequency and copy number analysis, and alternative splicing. Particularly through differential gene expression, we were able to identify a 'TMEM127 cluster' which showed up-regulated expression of genes associated with the kinase signalling pathway. If validated, RNA seq could upgrade two of the *TMEM127* variants described herein from VUS to likely pathogenic, thus triggering recommendations for lifelong surveillance for recurrent PC/PGL and relatives be referred for genetic counselling to consider predictive testing. Further, *TMEM127* PV are seemingly over-represented in the cortical admixture phenotype (similar to another kinase signalling pathway gene implicated in hereditary PC/PGL, *MAX*). It is unknown whether this proves a *bona fide* phenotypic marker for *TMEM127* PV or simply represents contaminating artefact from sample preparation.

10.1.4 Establishing the phenotype of rare germline and somatic drivers of PC/PGL; Multiple endocrine tumours associated with germline *MAX*, somatic *EPAS1* in development of sporadic PC/PGL, genotype-phenotype correlations in paediatric and adolescent PC/PGL.

Syndrome-appropriate specific surveillance recommendations which balances early detection of tumours and, conversely, rationalises resources and avoid oversurveillance is essential. Rare hereditary diseases with incomplete penetrance pose a particular challenge. Chapter 5, 6 and 7 expanded what is currently known of these phenotypes and disease behaviour. Firstly, association of germline *MAX* PVs with multifocal PC/PGL with other endocrine and non-endocrine neoplasia was demonstrated. Together with a second kindred (included in a joint publication), these cases extended the phenotype to include ganglioneuroma, neuroblastoma, composite PC/PGL, chondrosarcoma, lung adenocarcinoma, pituitary adenoma and parathyroid adenoma. Secondly, comprehensive review of the literature explored the phenotype of somatic mosaic *EPAS1* PVs underlying Pacak-Zhuang syndrome. This review highlighted endocrine neoplasias occurred at an early age; mean age at diagnosis of PC/PGL was 27 y (range 8 – 78 y) with a younger at diagnosis in males *versus* females (18 y *vs*. 31 y, $p = < 0.01$) and a young age at diagnosis of somatostatinoma (30 y, range 18 – 59 y). Two somatic *EPAS1* PV were detected within a cohort of 'apparently sporadic' patients with PC/PGL, and although they were not able to be recruited for work-up for Pacak-Zhuang syndrome, this still identified a molecular mechanism for tumour

development in these two individuals. The COVID-19 pandemic was a limitation of further progression of this study. Lastly, Australian data was presented on the prevalence of germline PVs within paediatric and adolescent patients diagnosed with PC/PGL. We found a high prevalence of germline pathogenic variants, identified in 80% of patients, predominantly occurring within the pseudohypoxia pathway (*VHL* 40%; *SDHB* 37%). Multi-focal disease was common, developing in 43% of patients, as was malignancy, developing in 29% of patients. These findings highlight the high likelihood of aggressive disease and emphasise the importance not only of genetic testing in these individuals, but also lifelong surveillance required if a PV is detected.

10.1.5 Moderating impact of somatic mitochondrial variants in patients harbouring a germline *SDHB* pathogenic variant.

Human mitochondria are located within all nucleated cells and are essential for energy generation via ATP production, generated as electrons move along the electron transport chain embedded in the inner mitochondrial membrane through mitochondrial complexes I-V. All subunits, bar complex II, are encoded by the mitochondrial genome. We searched for a relationship between tumour behaviour and somatic mitochondrial PVs obtained from PC/PGL harbouring biallelic *SDHB* PVs resulting in electron chain and Krebs cycle dysfunction. We identified somatic mtDNA PVs occurred most frequently in complex I, with high/moderate impact PVs being associated with recurrent and metastatic disease and with pathogenic variants in telomere regulating genes (*ATRX* and *TERT*).

10.1.6 Efficacy of radionuclide therapy in treating inoperable or metastatic PC/PGL

Prior chapters of this thesis have explored the molecular features of PC/PGL. This final chapter aimed to address a key challenge in clinical care, namely treatment of these rare neuroendocrine tumours. An audit of patients receiving radionuclide therapy for treatment of metastatic and/or inoperable PC/PGL was undertaken to compare efficacy of I131-MIBG and Lu-177 DOTATATE. We demonstrated utility of these two treatments for alleviating symptoms with an ORR of 89%. There was a significant fall in systolic blood pressure as a response to treatment from 133mmHg to 127mmHg ($p = 0.05$) and 50% of patients required reduction in the dose of anti-hypertensive medication, reducing pill burden in these patients. There was a reduction in catecholamine secretion with a DCR of 100% and ORR of 45%. Tumour response, assess using RECIST 1.1 criteria, was less profound with an ORR of 8%, however a DCR of 100%. Toxicity was minimal and spontaneously resolved in all patients. Given the small numbers within this audit, due to the rarity of PC/PGL, conclusions between genotype and response

were unable to be drawn. These findings support the use of radionuclide therapy particularly for symptomatic control, blood pressure management and control of hormone secretion.

10.7 Future directions

Future directions will include expanding the studies described in this thesis. Due to rarity of PC/PGL, many conclusions drawn within each chapter are based on a small number of patients.

Following validation of paired-tumour blood sequencing as a highly sensitive and timely approach to diagnosing hereditary PC/PGL, this methodology could be adopted into clinical care. 'Mainstreaming' is a paradigm shift away from patients being assessed within Familial Cancer Services (FCS) by a Cancer Geneticist to consent and testing being organised by the treating clinician, followed by FCS review if a PV is found. Adopting this process by the referring clinician (e.g. Endocrinologist or Endocrine surgeon), who routinely meet with patients diagnosed with PC/PGL, would require education surrounding consent for genetic testing with feedback sought from relevant stakeholders regarding suitability of this approach. The uptake of NGS has identified rarer driver genes implicated in hereditary PC/PGL, however the implications of these PVs for patients is still emerging. RNA-sequencing showed promise as a functional tool to be incorporated into variant classification. This approach is novel, with RNA-seq in its infancy.

We were able to expand the phenotype in three rare scenarios in which PC/PGL develop; in patients harbouring a germline *MAX* PV. somatic *EPAS1* PV or children and adolescents diagnosed with PC/PGL. The infrequent occurrence, with case reports and small case series being studied, highlights the importance of international collaboration to collate cases of rare disease.

Radionuclide therapy (I131-MIBG and Lu-177 DOTATATE) is one systemic therapeutic option for PC/PGL, in addition to cytotoxic chemotherapy and tyrosine kinase inhibitors. Emerging therapies which target the underlying molecular mechanism of PC/PGL development are emerging and will further personalise patient management. Two such therapies include belzutifan and selpercatinib. Belzutifan, a selective HIF2α inhibitor, facilitates the degradation of HIF2α and subsequently prevents the up-regulation of hypoxia-related genes. This medication has proved effective on PG/PGL occurring in Pacak-Zhuang syndrome, caused by gain-of-function mutations in *EPAS1*, with symptomatic, hormonal and imaging response. It has been theorised that PC/PGL occurring in VHL syndrome, which is also characterised by HIF2α accumulation, should respond to belzutifan, given outcomes of a recent

phase 2 clinical trial of patients with renal cell carcinoma with pathogenic germline variants in *VHL* showing an ORR of 49% and PFS at 24 months of 96%. Selpercatinib, a multi-kinase inhibitor targeting the *RET* proto-oncogene responsible for Multiple Endocrine Neoplasia type 2A, has shown durable efficacy in medullary thyroid cancers. The efficacy of this therapy in *RET*-mutated PC/PGL is yet to be reported.

10.8 Overall conclusions

This thesis established the role of genetic profiling to develop precision management of patients diagnosed with PC/PGL. Studies described explored molecular analysis (NGS, RNA sequencing), expanded the phenotype of patients diagnosed with rare causes of PC/PGL, examined disease modifiers of PC/PGL and reviewed radionuclide therapy for inoperable and/or metastatic PC/PGL in an effort to personalising care for these individuals.

References

1. Carmichael, S.W. and Rochester, *The history of the adrenal medulla.* Rev Neurosci, 1989. **2**(2): p. 83-100.
2. Mete, O., et al., *Overview of the 2022 WHO Classification of Paragangliomas and Pheochromocytomas.* Endocrine Pathology, 2022. **33**(1): p. 90-114.
3. Moriguchi, T., et al., *Gata3 participates in a complex transcriptional feedback network to regulate sympathoadrenal differentiation.* Development, 2006. **133**(19): p. 3871-81.
4. La Rosa, S. and S. Uccella, *Classification of neuroendocrine neoplasms: lights and shadows.* Rev Endocr Metab Disord, 2021. **22**(3): p. 527-538.
5. Mete, O., et al., *MEN2 Syndrome-Related Medullary Thyroid Carcinoma with Focal Tyrosine Hydroxylase Expression: Does It Represent a Hybrid Cellular Phenotype or Functional State of Tumor Cells?* Endocr Pathol, 2017. **28**(4): p. 362-366.
6. Mamilla, D., et al., *Immunohistochemical distinction of paragangliomas from epithelial neuroendocrine tumors-gangliocytic duodenal and cauda equina paragangliomas align with epithelial neuroendocrine tumors.* Hum Pathol, 2020. **103**: p. 72-82.
7. Beard, C.M., et al., *Occurrence of pheochromocytoma in Rochester, Minnesota, 1950 through 1979.* Mayo Clin Proc, 1983. **58**(12): p. 802-4.
8. Sutton, M.G., S.G. Sheps, and J.T. Lie, *Prevalence of clinically unsuspected pheochromocytoma. Review of a 50-year autopsy series.* Mayo Clin Proc, 1981. **56**(6): p. 354-60.
9. Guerrero, M.A., et al., *Clinical spectrum of pheochromocytoma.* J Am Coll Surg, 2009. **209**(6): p. 727-32.
10. Stein, P.P. and H.R. Black, *A simplified diagnostic approach to pheochromocytoma. A review of the literature and report of one institution's experience.* Medicine (Baltimore), 1991. **70**(1): p. 46-66.
11. Nölting, S., et al., *Personalized Management of Pheochromocytoma and Paraganglioma.* Endocr Rev, 2022. **43**(2): p. 199-239.
12. Eisenhofer, G., C. Pamporaki, and J.W.M. Lenders, *Biochemical Assessment of Pheochromocytoma and Paraganglioma.* Endocr Rev, 2023. **44**(5): p. 862-909.
13. Taïeb, D., et al., *Management of phaeochromocytoma and paraganglioma in patients with germline SDHB pathogenic variants: an international expert Consensus statement.* Nature Reviews Endocrinology, 2024. **20**(3): p. 168-184.
14. van Duinen, N., et al., *Increased urinary excretion of 3-methoxytyramine in patients with head and neck paragangliomas.* J Clin Endocrinol Metab, 2010. **95**(1): p. 209-14.
15. Taïeb, D., et al., *Clinical consensus guideline on the management of phaeochromocytoma and paraganglioma in patients harbouring germline SDHD pathogenic variants.* Lancet Diabetes Endocrinol, 2023. **11**(5): p. 345-361.
16. Kruepunga, N., et al., *Development of the sympathetic trunks in human embryos.* J Anat, 2021. **239**(1): p. 32-45.
17. SF., G. *Developmental Biology: The Neural Crest.* 2000 [cited 2023; Available from: https://www.ncbi.nlm.nih.gov/books/NBK10065/.
18. Sucheston, M.E. and M.S. Cannon, *Development of zonular patterns in the human adrenal gland.* Journal of Morphology, 1968. **126**(4): p. 477-491.

19. Lips, C.J.M., et al., *Familial paragangliomas.* Hereditary Cancer in Clinical Practice, 2006. **4**(4): p. 169.
20. Lenders, J.W., et al., *Biochemical diagnosis of pheochromocytoma: which test is best?* Jama, 2002. **287**(11): p. 1427-34.
21. Martucci, V.L., et al., *Association of urinary bladder paragangliomas with germline mutations in the SDHB and VHL genes.* Urol Oncol, 2015. **33**(4): p. 167.e13-20.
22. *Succinate Dehydrogenase–Deficient Paraganglioma of the Prostate.* Annals of Internal Medicine: Clinical Cases, 2023. **2**(10): p. e230361.
23. Crona, J., D. Taïeb, and K. Pacak, *New Perspectives on Pheochromocytoma and Paraganglioma: Toward a Molecular Classification.* Endocr Rev, 2017. **38**(6): p. 489-515.
24. Eisenhofer, G., et al., *Plasma normetanephrine and metanephrine for detecting pheochromocytoma in von Hippel-Lindau disease and multiple endocrine neoplasia type 2.* N Engl J Med, 1999. **340**(24): p. 1872-9.
25. Perlman, R.L. and M. Chalfie, *Catecholamine release from the adrenal medulla.* Clin Endocrinol Metab, 1977. **6**(3): p. 551-76.
26. Peterson, C.T., M.G. Ziegler, and P.J. Mills, *Catecholamines and Catecholamine Receptors in Cardiovascular Behavioral Medicine*, in *Handbook of Cardiovascular Behavioral Medicine*, S.R. Waldstein, et al., Editors. 2022, Springer New York: New York, NY. p. 891-909.
27. Eisenhofer, G., C. Pamporaki, and J.W.M. Lenders, *Biochemical Assessment of Pheochromocytoma and Paraganglioma.* Endocrine Reviews, 2023. **44**(5): p. 862-909.
28. Laduron, P. and F. Belpaire, *Tissue fractionation and catecholamines. II. Intracellular distribution patterns of tyrosine hydroxylase, dopa decarboxylase, dopamine-beta-hydroxylase, phenylethanolamine N-methyltransferase and monoamine oxidase in adrenal medulla.* Biochem Pharmacol, 1968. **17**(7): p. 1127-40.
29. Amar, L., et al., *Succinate dehydrogenase B gene mutations predict survival in patients with malignant pheochromocytomas or paragangliomas.* J Clin Endocrinol Metab, 2007. **92**(10): p. 3822-8.
30. Ayala-Ramirez, M., et al., *Clinical risk factors for malignancy and overall survival in patients with pheochromocytomas and sympathetic paragangliomas: primary tumor size and primary tumor location as prognostic indicators.* J Clin Endocrinol Metab, 2011. **96**(3): p. 717-25.
31. Thompson, L.D., *Pheochromocytoma of the Adrenal gland Scaled Score (PASS) to separate benign from malignant neoplasms: a clinicopathologic and immunophenotypic study of 100 cases.* Am J Surg Pathol, 2002. **26**(5): p. 551-66.
32. Tavangar, S.M., et al., *Immunohistochemical expression of Ki67, c-erbB-2, and c-kit antigens in benign and malignant pheochromocytoma.* Pathol Res Pract, 2010. **206**(5): p. 305-9.
33. Manger, W.M. and R.W. Gifford, *Pheochromocytoma.* J Clin Hypertens (Greenwich), 2002. **4**(1): p. 62-72.
34. Neumann, H.P., et al., *Distinct clinical features of paraganglioma syndromes associated with SDHB and SDHD gene mutations.* Jama, 2004. **292**(8): p. 943-51.
35. Bravo, E.L. and R.W. Gifford, Jr., *Pheochromocytoma.* Endocrinol Metab Clin North Am, 1993. **22**(2): p. 329-41.

36. Bravo, E.L., *Pheochromocytoma: new concepts and future trends.* Kidney Int, 1991. **40**(3): p. 544-56.
37. Kassim, T.A., et al., *Catecholamine-induced cardiomyopathy.* Endocr Pract, 2008. **14**(9): p. 1137-49.
38. Sibal, L., et al., *Phaeochromocytomas presenting as acute crises after beta blockade therapy.* Clin Endocrinol (Oxf), 2006. **65**(2): p. 186-90.
39. Kopetschke, R., et al., *Frequent incidental discovery of phaeochromocytoma: data from a German cohort of 201 phaeochromocytoma.* Eur J Endocrinol, 2009. **161**(2): p. 355-61.
40. Griffin, T.P., et al., *Evaluating the optimum rest period prior to blood collection for fractionated plasma free metanephrines analysis.* Pract Lab Med, 2016. **5**: p. 39-46.
41. Zhang, L., et al., *Risk of complications after core needle biopsy in pheochromocytoma/paraganglioma.* Endocrine-Related Cancer, 2023. **30**(7): p. e220354.
42. Lenders, J.W.M., et al., *Pheochromocytoma and Paraganglioma: An Endocrine Society Clinical Practice Guideline.* The Journal of Clinical Endocrinology & Metabolism, 2014. **99**(6): p. 1915-1942.
43. Bravo, E.L., *Evolving concepts in the pathophysiology, diagnosis, and treatment of pheochromocytoma.* Endocr Rev, 1994. **15**(3): p. 356-68.
44. Northcutt, B.G., et al., *MDCT of adrenal masses: Can dual-phase enhancement patterns be used to differentiate adenoma and pheochromocytoma?* AJR Am J Roentgenol, 2013. **201**(4): p. 834-9.
45. Janssen, I., et al., *PET/CT comparing (68)Ga-DOTATATE and other radiopharmaceuticals and in comparison with CT/MRI for the localization of sporadic metastatic pheochromocytoma and paraganglioma.* Eur J Nucl Med Mol Imaging, 2016. **43**(10): p. 1784-91.
46. Björklund, P., K. Pacak, and J. Crona, *Precision medicine in pheochromocytoma and paraganglioma: current and future concepts.* J Intern Med, 2016. **280**(6): p. 559-573.
47. Kliewer, K.E., et al., *Paragangliomas: assessment of prognosis by histologic, immunohistochemical, and ultrastructural techniques.* Hum Pathol, 1989. **20**(1): p. 29-39.
48. Kliewer, K.E. and A.J. Cochran, *A review of the histology, ultrastructure, immunohistology, and molecular biology of extra-adrenal paragangliomas.* Arch Pathol Lab Med, 1989. **113**(11): p. 1209-18.
49. Stenström, G. and K. Swolin, *Pheochromocytoma in pregnancy. Experience of treatment with phenoxybenzamine in three patients.* Acta Obstet Gynecol Scand, 1985. **64**(4): p. 357-61.
50. Bihain, F., et al., *Robotic adrenalectomy in patients with pheochromocytoma: a systematic review.* Gland Surg, 2020. **9**(3): p. 844-848.
51. Walz, M.K., et al., *Laparoscopic and retroperitoneoscopic treatment of pheochromocytomas and retroperitoneal paragangliomas: results of 161 tumors in 126 patients.* World J Surg, 2006. **30**(5): p. 899-908.
52. Rafat, C., et al., *Peritoneal implantation of pheochromocytoma following tumor capsule rupture during surgery.* J Clin Endocrinol Metab, 2014. **99**(12): p. E2681-5.
53. Power, A.H., et al., *Impact of preoperative embolization on outcomes of carotid body tumor resections.* J Vasc Surg, 2012. **56**(4): p. 979-89.

54. Brown, M.L., et al., *Mediastinal paragangliomas: the mayo clinic experience.* Ann Thorac Surg, 2008. **86**(3): p. 946-51.
55. Strajina, V., et al., *Surgical Treatment of Malignant Pheochromocytoma and Paraganglioma: Retrospective Case Series.* Ann Surg Oncol, 2017. **24**(6): p. 1546-1550.
56. Noda, T., et al., *Successful outcome after resection of liver metastasis arising from an extraadrenal retroperitoneal paraganglioma that appeared 9 years after surgical excision of the primary lesion.* Int J Clin Oncol, 2009. **14**(5): p. 473-7.
57. Adjallé, R., et al., *Treatment of malignant pheochromocytoma.* Horm Metab Res, 2009. **41**(9): p. 687-96.
58. Breen, W., et al., *External beam radiation therapy for advanced/unresectable malignant paraganglioma and pheochromocytoma.* Adv Radiat Oncol, 2018. **3**(1): p. 25-29.
59. Li, G., et al., *Irradiation of glomus jugulare tumors: a historical perspective.* Neurosurg Focus, 2007. **23**(6): p. E13.
60. Bravo, E.L., S.R. Kalmadi, and I. Gill, *Clinical utility of temozolomide in the treatment of malignant paraganglioma: a preliminary report.* Horm Metab Res, 2009. **41**(9): p. 703-6.
61. Baudin, E., et al., *567O First international randomized study in malignant progressive pheochromocytoma and paragangliomas (FIRSTMAPPP): an academic double-blind trial investigating sunitinib.* Annals of Oncology, 2021. **32**: p. S621.
62. Kong, G., et al., *Efficacy of Peptide Receptor Radionuclide Therapy for Functional Metastatic Paraganglioma and Pheochromocytoma.* J Clin Endocrinol Metab, 2017. **102**(9): p. 3278-3287.
63. van Hulsteijn, L.T., et al., *131I-MIBG therapy for malignant paraganglioma and phaeochromocytoma: systematic review and meta-analysis.* Clinical Endocrinology, 2014. **80**(4): p. 487-501.
64. Jaiswal, S.K., et al., *177Lu-DOTATATE therapy in metastatic/inoperable pheochromocytoma-paraganglioma.* Endocr Connect, 2020. **9**(9): p. 864-873.
65. Jha, A., et al., *High-Specific-Activity-(131)I-MIBG versus (177)Lu-DOTATATE Targeted Radionuclide Therapy for Metastatic Pheochromocytoma and Paraganglioma.* Clin Cancer Res, 2021. **27**(11): p. 2989-2995.
66. Richards, S., et al., *Standards and guidelines for the interpretation of sequence variants: a joint consensus recommendation of the American College of Medical Genetics and Genomics and the Association for Molecular Pathology.* Genet Med, 2015. **17**(5): p. 405-24.
67. Fishbein, L., et al., *Comprehensive Molecular Characterization of Pheochromocytoma and Paraganglioma.* Cancer Cell, 2017. **31**(2): p. 181-193.
68. Lawrence, M.S., et al., *Mutational heterogeneity in cancer and the search for new cancer-associated genes.* Nature, 2013. **499**(7457): p. 214-218.
69. Currás-Freixes, M., et al., *PheoSeq: A Targeted Next-Generation Sequencing Assay for Pheochromocytoma and Paraganglioma Diagnostics.* J Mol Diagn, 2017. **19**(4): p. 575-588.
70. Ben Aim, L., et al., *Targeted next-generation sequencing detects rare genetic events in pheochromocytoma and paraganglioma.* J Med Genet, 2019. **56**(8): p. 513-520.

71. Coppin, L., et al., *VHL mosaicism can be detected by clinical next-generation sequencing and is not restricted to patients with a mild phenotype.* Eur J Hum Genet, 2014. **22**(9): p. 1149-52.
72. Toledo, R.A., et al., *Consensus Statement on next-generation-sequencing-based diagnostic testing of hereditary phaeochromocytomas and paragangliomas.* Nat Rev Endocrinol, 2017. **13**(4): p. 233-247.
73. Dahia, P.L., et al., *A HIF1alpha regulatory loop links hypoxia and mitochondrial signals in pheochromocytomas.* PLoS Genet, 2005. **1**(1): p. 72-80.
74. Dahia, P.L., *Pheochromocytoma and paraganglioma pathogenesis: learning from genetic heterogeneity.* Nat Rev Cancer, 2014. **14**(2): p. 108-19.
75. Zethoven, M., et al., *Single-nuclei and bulk-tissue gene-expression analysis of pheochromocytoma and paraganglioma links disease subtypes with tumor microenvironment.* Nature Communications, 2022. **13**(1): p. 6262.
76. Bezawork-Geleta, A., et al., *Mitochondrial Complex II: At the Crossroads.* Trends Biochem Sci, 2017. **42**(4): p. 312-325.
77. Pacak, K., et al., *New syndrome of paraganglioma and somatostatinoma associated with polycythemia.* Journal of clinical oncology, 2013. **31**(13): p. 1690.
78. Fishbein, L., et al., *Whole-exome sequencing identifies somatic ATRX mutations in pheochromocytomas and paragangliomas.* Nature communications, 2015. **6**(1): p. 6140.
79. Comino-Méndez, I., et al., *ATRX driver mutation in a composite malignant pheochromocytoma.* Cancer Genetics, 2016. **209**(6): p. 272-277.
80. Job, S., et al., *Telomerase activation and ATRX mutations are independent risk factors for metastatic pheochromocytoma and paraganglioma.* Clinical Cancer Research, 2019. **25**(2): p. 760-770.
81. Dwight, T., et al., *TERT structural rearrangements in metastatic pheochromocytomas.* Endocr Relat Cancer, 2018. **25**(1): p. 1-9.
82. Benn, D.E., B.G. Robinson, and R.J. Clifton-Bligh, *15 YEARS OF PARAGANGLIOMA: Clinical manifestations of paraganglioma syndromes types 1-5.* Endocr Relat Cancer, 2015. **22**(4): p. T91-103.
83. Else T, G.S., Fishbein L. . *Hereditary Paraganglioma-Pheochromocytoma Syndromes*. GeneReviews 2023 [cited 2024; Available from: https://www.ncbi.nlm.nih.gov/books/NBK1548/.
84. Latif, F., et al., *Identification of the von Hippel-Lindau disease tumor suppressor gene.* Science, 1993. **260**(5112): p. 1317-20.
85. Kaelin, W.G., Jr., *Molecular basis of the VHL hereditary cancer syndrome.* Nat Rev Cancer, 2002. **2**(9): p. 673-82.
86. Sgambati, M., et al., *Mosaicism in von Hippel–Lindau disease: lessons from kindreds with germline mutations identified in offspring with mosaic parents.* The American Journal of Human Genetics, 2000. **66**(1): p. 84-91.
87. Kim, W.Y. and W.G. Kaelin, *Role of VHL gene mutation in human cancer.* Journal of clinical oncology, 2004. **22**(24): p. 4991-5004.
88. Ong, K.R., et al., *Genotype–phenotype correlations in von Hippel-Lindau disease.* Human mutation, 2007. **28**(2): p. 143-149.
89. Walther, M.M., et al., *Clinical and genetic characterization of pheochromocytoma in von Hippel-Lindau families: comparison with sporadic pheochromocytoma gives*

insight into natural history of pheochromocytoma. J Urol, 1999. **162**(3 Pt 1): p. 659-64.
90. Baysal, B.E., et al., *Mutations in SDHD, a mitochondrial complex II gene, in hereditary paraganglioma.* Science, 2000. **287**(5454): p. 848-51.
91. Niemann, S. and U. Müller, *Mutations in SDHC cause autosomal dominant paraganglioma, type 3.* Nat Genet, 2000. **26**(3): p. 268-70.
92. Astuti, D., et al., *Gene mutations in the succinate dehydrogenase subunit SDHB cause susceptibility to familial pheochromocytoma and to familial paraganglioma.* Am J Hum Genet, 2001. **69**(1): p. 49-54.
93. Lee, S.C., et al., *Hereditary paraganglioma due to the SDHD M1I mutation in a second Chinese family: a founder effect?* Laryngoscope, 2003. **113**(6): p. 1055-8.
94. Astuti, D., et al., *Germline SDHD mutation in familial phaeochromocytoma.* Lancet, 2001. **357**(9263): p. 1181-2.
95. Benn, D.E., et al., *Clinical presentation and penetrance of pheochromocytoma/paraganglioma syndromes.* J Clin Endocrinol Metab, 2006. **91**(3): p. 827-36.
96. Bayley, J.P., et al., *SDHAF2 mutations in familial and sporadic paraganglioma and phaeochromocytoma.* Lancet Oncol, 2010. **11**(4): p. 366-72.
97. Welander, J., P. Söderkvist, and O. Gimm, *Genetics and clinical characteristics of hereditary pheochromocytomas and paragangliomas.* Endocr Relat Cancer, 2011. **18**(6): p. R253-76.
98. Lee, H., et al., *Risk of metastatic pheochromocytoma and paraganglioma in SDHx mutation carriers: a systematic review and updated meta-analysis.* J Med Genet, 2020. **57**(4): p. 217-225.
99. Wong, M.Y., et al., *Clinical Practice Guidance: Surveillance for phaeochromocytoma and paraganglioma in paediatric succinate dehydrogenase gene mutation carriers.* Clin Endocrinol (Oxf), 2019. **90**(4): p. 499-505.
100. Hensen, E.F., et al., *Mutations in SDHD are the major determinants of the clinical characteristics of Dutch head and neck paraganglioma patients.* Clin Endocrinol (Oxf), 2011. **75**(5): p. 650-5.
101. Kunst, H.P., et al., *SDHAF2 (PGL2-SDH5) and hereditary head and neck paraganglioma.* Clin Cancer Res, 2011. **17**(2): p. 247-54.
102. Peczkowska, M., et al., *Extra-adrenal and adrenal pheochromocytomas associated with a germline SDHC mutation.* Nat Clin Pract Endocrinol Metab, 2008. **4**(2): p. 111-5.
103. Else, T., et al., *The clinical phenotype of SDHC-associated hereditary paraganglioma syndrome (PGL3).* J Clin Endocrinol Metab, 2014. **99**(8): p. E1482-6.
104. Bickmann, J.K., et al., *Phenotypic variability and risk of malignancy in SDHC-linked paragangliomas: lessons from three unrelated cases with an identical germline mutation (p.Arg133*).* J Clin Endocrinol Metab, 2014. **99**(3): p. E489-96.
105. Williams, S.T., et al., *SDHC phaeochromocytoma and paraganglioma: A UK-wide case series.* Clin Endocrinol (Oxf), 2022. **96**(4): p. 499-512.
106. Srirangalingam, U., et al., *Clinical manifestations of familial paraganglioma and phaeochromocytomas in succinate dehydrogenase B (SDH-B) gene mutation carriers.* Clin Endocrinol (Oxf), 2008. **69**(4): p. 587-96.
107. Boedeker, C.C., et al., *Malignant head and neck paragangliomas in SDHB mutation carriers.* Otolaryngol Head Neck Surg, 2007. **137**(1): p. 126-9.

108. Andrews, K.A., et al., *Tumour risks and genotype-phenotype correlations associated with germline variants in succinate dehydrogenase subunit genes SDHB, SDHC and SDHD.* J Med Genet, 2018. **55**(6): p. 384-394.
109. Burnichon, N., et al., *SDHA is a tumor suppressor gene causing paraganglioma.* Hum Mol Genet, 2010. **19**(15): p. 3011-20.
110. Korpershoek, E., et al., *SDHA immunohistochemistry detects germline SDHA gene mutations in apparently sporadic paragangliomas and pheochromocytomas.* J Clin Endocrinol Metab, 2011. **96**(9): p. E1472-6.
111. Jha, A., et al., *Clinical, Diagnostic, and Treatment Characteristics of SDHA-Related Metastatic Pheochromocytoma and Paraganglioma.* Front Oncol, 2019. **9**: p. 53.
112. Benn, D.E., et al., *Bayesian approach to determining penetrance of pathogenic SDH variants.* J Med Genet, 2018. **55**(11): p. 729-734.
113. Pollard, P., et al., *Accumulation of Krebs cycle intermediates and over-expression of HIF1α in tumours which result from germline FH and SDH mutations.* Human molecular genetics, 2005. **14**(15): p. 2231-2239.
114. Castro-Vega, L.J., et al., *Germline mutations in FH confer predisposition to malignant pheochromocytomas and paragangliomas.* Hum Mol Genet, 2014. **23**(9): p. 2440-6.
115. Fuchs, T.L., et al., *A Clinicopathologic and Molecular Analysis of Fumarate Hydratase-deficient Pheochromocytoma and Paraganglioma.* Am J Surg Pathol, 2023. **47**(1): p. 25-36.
116. Gupta, G., K. Pacak, and A.A.S.C. on behalf of the, *Precision Medicine: An Update on Genotype/Biochemical Phenotype Relationships in Pheochromocytoma/Paraganglioma Patients.* Endocrine Practice, 2017. **23**(6): p. 690-704.
117. Wells, S.A., Jr., et al., *Revised American Thyroid Association guidelines for the management of medullary thyroid carcinoma.* Thyroid, 2015. **25**(6): p. 567-610.
118. Mulligan, L.M. and B.A. Ponder, *Genetic basis of endocrine disease: multiple endocrine neoplasia type 2.* J Clin Endocrinol Metab, 1995. **80**(7): p. 1989-95.
119. Elisei, R., et al., *Twenty-Five Years Experience on RET Genetic Screening on Hereditary MTC: An Update on The Prevalence of Germline RET Mutations.* Genes (Basel), 2019. **10**(9).
120. Seri, M., et al., *A Cys634Gly substitution of the RET proto-oncogene in a family with recurrence of multiple endocrine neoplasia type 2A and cutaneous lichen amyloidosis.* Clin Genet, 1997. **51**(2): p. 86-90.
121. Comino-Méndez, I., et al., *Exome sequencing identifies MAX mutations as a cause of hereditary pheochromocytoma.* Nat Genet, 2011. **43**(7): p. 663-7.
122. Meyer, N. and L.Z. Penn, *Reflecting on 25 years with MYC.* Nat Rev Cancer, 2008. **8**(12): p. 976-90.
123. Burnichon, N., et al., *MAX mutations cause hereditary and sporadic pheochromocytoma and paraganglioma.* Clin Cancer Res, 2012. **18**(10): p. 2828-37.
124. Steinman, J.R., et al., *A novel pathogenic variant in MAX-Associated pheochromocytoma.* Journal of Clinical and Translational Endocrinology: Case Reports, 2021. **22**: p. 100101.
125. Srikantan, S., et al., *The tumor suppressor TMEM127 regulates insulin sensitivity in a tissue-specific manner.* Nat Commun, 2019. **10**(1): p. 4720.

126. Qin, Y., et al., *The tumor susceptibility gene TMEM127 is mutated in renal cell carcinomas and modulates endolysosomal function.* Hum Mol Genet, 2014. **23**(9): p. 2428-39.
127. Armaiz-Pena, G., et al., *Genotype-Phenotype Features of Germline Variants of the TMEM127 Pheochromocytoma Susceptibility Gene: A 10-Year Update.* The Journal of Clinical Endocrinology & Metabolism, 2020. **106**(1): p. e350-e364.
128. Gutmann, D.H., et al., *Neurofibromatosis type 1.* Nat Rev Dis Primers, 2017. **3**: p. 17004.
129. Gottfried, O.N., D.H. Viskochil, and W.T. Couldwell, *Neurofibromatosis Type 1 and tumorigenesis: molecular mechanisms and therapeutic implications.* Neurosurg Focus, 2010. **28**(1): p. E8.
130. Napolitano, F., et al., *Genotype-Phenotype Correlations in Neurofibromatosis Type 1: Identification of Novel and Recurrent NF1 Gene Variants and Correlations with Neurocognitive Phenotype.* Genes (Basel), 2022. **13**(7).
131. Gruber, L.M., et al., *Pheochromocytoma and paraganglioma in patients with neurofibromatosis type 1.* Clin Endocrinol (Oxf), 2017. **86**(1): p. 141-149.
132. Gimm, O., et al., *Somatic and occult germ-line mutations in SDHD, a mitochondrial complex II gene, in nonfamilial pheochromocytoma.* Cancer Res, 2000. **60**(24): p. 6822-5.
133. van Nederveen, F.H., et al., *Somatic SDHB mutation in an extraadrenal pheochromocytoma.* N Engl J Med, 2007. **357**(3): p. 306-8.
134. Stenman, A., et al., *HRAS mutation prevalence and associated expression patterns in pheochromocytoma.* Genes, Chromosomes and Cancer, 2016. **55**(5): p. 452-459.
135. Greco, A., et al., *Chapter 16 - Thyroid Cancer*, in *Cancer Genomics*, G. Dellaire, J.N. Berman, and R.J. Arceci, Editors. 2014, Academic Press: Boston. p. 265-280.
136. Luchetti, A., et al., *Profiling of somatic mutations in phaeochromocytoma and paraganglioma by targeted next generation sequencing analysis.* Int J Endocrinol, 2015. **2015**: p. 138573.
137. Holmquist-Mengelbier, L., et al., *Recruitment of HIF-1alpha and HIF-2alpha to common target genes is differentially regulated in neuroblastoma: HIF-2alpha promotes an aggressive phenotype.* Cancer Cell, 2006. **10**(5): p. 413-23.
138. Comino-Méndez, I., et al., *Tumoral EPAS1 (HIF2A) mutations explain sporadic pheochromocytoma and paraganglioma in the absence of erythrocytosis.* Human Molecular Genetics, 2013. **22**(11): p. 2169-2176.
139. Comino-Méndez, I., et al., *Tumoral EPAS1 (HIF2A) mutations explain sporadic pheochromocytoma and paraganglioma in the absence of erythrocytosis.* Hum Mol Genet, 2013. **22**(11): p. 2169-76.
140. Alzofon, N., et al., *Mastermind Like Transcriptional Coactivator 3 (MAML3) Drives Neuroendocrine Tumor Progression.* Mol Cancer Res, 2021. **19**(9): p. 1476-1485.
141. Guo, A.-X., et al., *The role of CSDE1 in translational reprogramming and human diseases.* Cell Communication and Signaling, 2020. **18**: p. 1-12.
142. Nagy, R., K. Sweet, and C. Eng, *Highly penetrant hereditary cancer syndromes.* Oncogene, 2004. **23**(38): p. 6445-70.
143. Knudson, A.G., Jr., *Mutation and cancer: statistical study of retinoblastoma.* Proc Natl Acad Sci U S A, 1971. **68**(4): p. 820-3.

144. Weitzel, J.N., et al., *Genetics, genomics, and cancer risk assessment: State of the Art and Future Directions in the Era of Personalized Medicine.* CA Cancer J Clin, 2011. **61**(5): p. 327-59.
145. Rizzo, J.M. and M.J. Buck, *Key principles and clinical applications of "next-generation" DNA sequencing.* Cancer Prev Res (Phila), 2012. **5**(7): p. 887-900.
146. Gomes, A. and B. Korf, *Chapter 5 - Genetic Testing Techniques*, in *Pediatric Cancer Genetics*, N.H. Robin and M.B. Farmer, Editors. 2018, Elsevier. p. 47-64.
147. Susswein, L.R., et al., *Pathogenic and likely pathogenic variant prevalence among the first 10,000 patients referred for next-generation cancer panel testing.* Genet Med, 2016. **18**(8): p. 823-32.
148. Tsaousis, G.N., et al., *Analysis of hereditary cancer syndromes by using a panel of genes: novel and multiple pathogenic mutations.* BMC Cancer, 2019. **19**(1): p. 535.
149. Robson, M.E., et al., *American Society of Clinical Oncology Policy Statement Update: Genetic and Genomic Testing for Cancer Susceptibility.* J Clin Oncol, 2015. **33**(31): p. 3660-7.
150. Qin, D., *Next-generation sequencing and its clinical application.* Cancer Biol Med, 2019. **16**(1): p. 4-10.
151. Roy, S., et al., *Next-Generation Sequencing Informatics: Challenges and Strategies for Implementation in a Clinical Environment.* Arch Pathol Lab Med, 2016. **140**(9): p. 958-75.
152. Kadri, S., *Advances in next-generation sequencing bioinformatics for clinical diagnostics: Taking precision oncology to the next level.* Advances in Molecular Pathology, 2018. **1**(1): p. 149-166.
153. Landrum, M.J., et al., *ClinVar: improving access to variant interpretations and supporting evidence.* Nucleic Acids Res, 2018. **46**(D1): p. D1062-d1067.
154. Tate, J.G., et al., *COSMIC: the Catalogue Of Somatic Mutations In Cancer.* Nucleic Acids Research, 2018. **47**(D1): p. D941-D947.
155. Chan, W., et al., *Development and validation of next generation sequencing based 35-gene hereditary cancer panel.* Hereditary Cancer in Clinical Practice, 2020. **18**(1): p. 9.
156. *Breast Cancer Risk Genes — Association Analysis in More than 113,000 Women.* New England Journal of Medicine, 2021. **384**(5): p. 428-439.
157. Australasia, H.G.S.o. *HGSA Policies and Position Statements*. 2014 [cited 2024; Available from: https://www.hgsa.org.au//Web/Consumer-resources/Policies-Position-Statements.aspx.
158. Wang, K., M. Li, and H. Hakonarson, *ANNOVAR: functional annotation of genetic variants from high-throughput sequencing data.* Nucleic Acids Res, 2010. **38**(16): p. e164.
159. Poplin, R., et al., *Scaling accurate genetic variant discovery to tens of thousands of samples.* bioRxiv, 2018: p. 201178.
160. McKenna, A., et al., *The Genome Analysis Toolkit: a MapReduce framework for analyzing next-generation DNA sequencing data.* Genome Res, 2010. **20**(9): p. 1297-303.
161. Cibulskis, K., et al., *Sensitive detection of somatic point mutations in impure and heterogeneous cancer samples.* Nat Biotechnol, 2013. **31**(3): p. 213-9.
162. Robinson, J.T., et al., *Integrative genomics viewer.* Nat Biotechnol, 2011. **29**(1): p. 24-6.

163. Lander, E.S. and M.S. Waterman, *Genomic mapping by fingerprinting random clones: a mathematical analysis.* Genomics, 1988. **2**(3): p. 231-9.
164. Burnichon, N., et al., *The succinate dehydrogenase genetic testing in a large prospective series of patients with paragangliomas.* J Clin Endocrinol Metab, 2009. **94**(8): p. 2817-27.
165. Wautot, V., et al., *Germline mutation profile of MEN1 in multiple endocrine neoplasia type 1: search for correlation between phenotype and the functional domains of the MEN1 protein.* Hum Mutat, 2002. **20**(1): p. 35-47.
166. Rose, M., et al., *PARP Inhibitors: Clinical Relevance, Mechanisms of Action and Tumor Resistance.* Front Cell Dev Biol, 2020. **8**: p. 564601.
167. Hampel, H., et al., *A practice guideline from the American College of Medical Genetics and Genomics and the National Society of Genetic Counselors: referral indications for cancer predisposition assessment.* Genet Med, 2015. **17**(1): p. 70-87.
168. Daly, M.B., et al., *Genetic/Familial High-Risk Assessment: Breast, Ovarian, and Pancreatic, Version 2.2021, NCCN Clinical Practice Guidelines in Oncology.* J Natl Compr Canc Netw, 2021. **19**(1): p. 77-102.
169. Gupta, S., et al., *NCCN Guidelines Insights: Genetic/Familial High-Risk Assessment: Colorectal, Version 3.2017.* J Natl Compr Canc Netw, 2017. **15**(12): p. 1465-1475.
170. Mandelker, D. and O. Ceyhan-Birsoy, *Evolving Significance of Tumor-Normal Sequencing in Cancer Care.* Trends Cancer, 2020. **6**(1): p. 31-39.
171. Mandelker, D., et al., *Mutation Detection in Patients With Advanced Cancer by Universal Sequencing of Cancer-Related Genes in Tumor and Normal DNA vs Guideline-Based Germline Testing.* Jama, 2017. **318**(9): p. 825-835.
172. Li, M.M., et al., *Points to consider for reporting of germline variation in patients undergoing tumor testing: a statement of the American College of Medical Genetics and Genomics (ACMG).* Genet Med, 2020. **22**(7): p. 1142-1148.
173. Uddin, M.d.M., et al., *Clonal hematopoiesis of indeterminate potential, DNA methylation, and risk for coronary artery disease.* Nature Communications, 2022. **13**(1): p. 5350.
174. Buffet, A., et al., *An overview of 20 years of genetic studies in pheochromocytoma and paraganglioma.* Best Pract Res Clin Endocrinol Metab, 2020. **34**(2): p. 101416.
175. Papathomas, T.G., et al., *SDHB/SDHA immunohistochemistry in pheochromocytomas and paragangliomas: a multicenter interobserver variation analysis using virtual microscopy: a Multinational Study of the European Network for the Study of Adrenal Tumors (ENS@T).* Modern Pathology, 2015. **28**(6): p. 807-821.
176. Toledo, R.A., *Genetics of Pheochromocytomas and Paragangliomas: An Overview on the Recently Implicated Genes MERTK, MET, Fibroblast Growth Factor Receptor 1, and H3F3A.* Endocrinol Metab Clin North Am, 2017. **46**(2): p. 459-489.
177. Muller, M., et al., *Reassessing the clinical spectrum associated with hereditary leiomyomatosis and renal cell carcinoma syndrome in French FH mutation carriers.* Clin Genet, 2017. **92**(6): p. 606-615.
178. Harrison, W.J., et al., *Fumarate Hydratase-deficient Uterine Leiomyomas Occur in Both the Syndromic and Sporadic Settings.* Am J Surg Pathol, 2016. **40**(5): p. 599-607.
179. Lau, H.D., et al., *A Clinicopathologic and Molecular Analysis of Fumarate Hydratase-deficient Renal Cell Carcinoma in 32 Patients.* Am J Surg Pathol, 2020. **44**(1): p. 98-110.

180. Toledo, R.A., et al., *Recurrent Mutations of Chromatin-Remodeling Genes and Kinase Receptors in Pheochromocytomas and Paragangliomas.* Clin Cancer Res, 2016. **22**(9): p. 2301-10.
181. Fishbein, L., et al., *Comprehensive Molecular Characterization of Pheochromocytoma and Paraganglioma.* Cancer Cell, 2017. **31**(2): p. 181-193.
182. Winzeler, B., et al., *Investigating the role of somatic sequencing platforms for phaeochromocytoma and paraganglioma in a large UK cohort.* Clin Endocrinol (Oxf), 2022. **97**(4): p. 448-459.
183. Cardot-Bauters, C., et al., *A Full Phenotype of Paraganglioma Linked to a Germline SDHB Mosaic Mutation.* The Journal of Clinical Endocrinology & Metabolism, 2019. **104**(8): p. 3362-3366.
184. Chen, J.L., et al., *Mosaicism in Tumor Suppressor Gene Syndromes: Prevalence, Diagnostic Strategies, and Transmission Risk.* Annual Review of Genomics and Human Genetics, 2022. **23**(1): p. 331-361.
185. Coppin, L., et al., *Optimization of Next-Generation Sequencing Technologies for von Hippel Lindau (VHL) Mosaic Mutation Detection and Development of Confirmation Methods.* J Mol Diagn, 2019. **21**(3): p. 462-470.
186. Sgambati, M.T., et al., *Mosaicism in von Hippel-Lindau disease: lessons from kindreds with germline mutations identified in offspring with mosaic parents.* Am J Hum Genet, 2000. **66**(1): p. 84-91.
187. Pannett, A.A.J. and R.V. Thakker, *Somatic Mutations in MEN Type 1 Tumors, Consistent with the Knudson "Two-Hit" Hypothesis.* The Journal of Clinical Endocrinology & Metabolism, 2001. **86**(9): p. 4371-4374.
188. Thakker, R.V., et al., *Clinical practice guidelines for multiple endocrine neoplasia type 1 (MEN1).* J Clin Endocrinol Metab, 2012. **97**(9): p. 2990-3011.
189. Casey, R.T., et al., *SDHA related tumorigenesis: a new case series and literature review for variant interpretation and pathogenicity.* Mol Genet Genomic Med, 2017. **5**(3): p. 237-250.
190. Qin, Y., et al., *Germline mutations in TMEM127 confer susceptibility to pheochromocytoma.* Nat Genet, 2010. **42**(3): p. 229-33.
191. Deng, Y., et al., *The TMEM127 human tumor suppressor is a component of the mTORC1 lysosomal nutrient-sensing complex.* Hum Mol Genet, 2018. **27**(10): p. 1794-1808.
192. Srikantan, S., et al., *The tumor suppressor TMEM127 regulates insulin sensitivity in a tissue-specific manner.* Nature Communications, 2019. **10**(1): p. 4720.
193. Laplante, M. and D.M. Sabatini, *mTOR signaling at a glance.* J Cell Sci, 2009. **122**(Pt 20): p. 3589-94.
194. Sabatini, D.M., *mTOR and cancer: insights into a complex relationship.* Nature Reviews Cancer, 2006. **6**(9): p. 729-734.
195. Peng, Y., et al., *PI3K/Akt/mTOR Pathway and Its Role in Cancer Therapeutics: Are We Making Headway?* Frontiers in Oncology, 2022. **12**.
196. Yao, L., et al., *Spectrum and prevalence of FP/TMEM127 gene mutations in pheochromocytomas and paragangliomas.* Jama, 2010. **304**(23): p. 2611-2619.
197. Toledo, S.P., et al., *Penetrance and clinical features of pheochromocytoma in a six-generation family carrying a germline TMEM127 mutation.* J Clin Endocrinol Metab, 2015. **100**(2): p. E308-18.

198. Abermil, N., et al., *TMEM127 screening in a large cohort of patients with pheochromocytoma and/or paraganglioma.* J Clin Endocrinol Metab, 2012. **97**(5): p. E805-9.
199. Casey, R.T., et al., *Clinical and Molecular Features of Renal and Pheochromocytoma/Paraganglioma Tumor Association Syndrome (RAPTAS): Case Series and Literature Review.* J Clin Endocrinol Metab, 2017. **102**(11): p. 4013-4022.
200. Hernandez, K.G., et al., *Familial pheochromocytoma and renal cell carcinoma syndrome: TMEM127 as a novel candidate gene for the association.* Virchows Arch, 2015. **466**(6): p. 727-32.
201. Conesa, A., et al., *A survey of best practices for RNA-seq data analysis.* Genome Biology, 2016. **17**(1): p. 13.
202. Karam, R., et al., *Assessment of Diagnostic Outcomes of RNA Genetic Testing for Hereditary Cancer.* JAMA Network Open, 2019. **2**(10): p. e1913900-e1913900.
203. Landrith, T., et al., *Splicing profile by capture RNA-seq identifies pathogenic germline variants in tumor suppressor genes.* NPJ Precis Oncol, 2020. **4**: p. 4.
204. Kopanos, C., et al., *VarSome: the human genomic variant search engine.* Bioinformatics, 2018. **35**(11): p. 1978-1980.
205. Cerami, E., et al., *The cBio cancer genomics portal: an open platform for exploring multidimensional cancer genomics data.* Cancer Discov, 2012. **2**(5): p. 401-4.
206. Robinson, J.T., et al., *igv.js: an embeddable JavaScript implementation of the Integrative Genomics Viewer (IGV).* Bioinformatics, 2022. **39**(1).
207. von Ahlfen, S., et al., *Determinants of RNA Quality from FFPE Samples.* PLOS ONE, 2007. **2**(12): p. e1261.
208. Penland, S.K., et al., *RNA expression analysis of formalin-fixed paraffin-embedded tumors.* Lab Invest, 2007. **87**(4): p. 383-91.
209. Ferraro, N.M., et al., *Transcriptomic signatures across human tissues identify functional rare genetic variation.* Science, 2020. **369**(6509).
210. Dillies, M.-A., et al., *A comprehensive evaluation of normalization methods for Illumina high-throughput RNA sequencing data analysis.* Briefings in Bioinformatics, 2012. **14**(6): p. 671-683.
211. Evans, C., J. Hardin, and D.M. Stoebel, *Selecting between-sample RNA-Seq normalization methods from the perspective of their assumptions.* Briefings in Bioinformatics, 2017. **19**(5): p. 776-792.
212. Krawczak, M., J. Reiss, and D.N. Cooper, *The mutational spectrum of single base-pair substitutions in mRNA splice junctions of human genes: causes and consequences.* Hum Genet, 1992. **90**(1-2): p. 41-54.
213. Burset, M., I.A. Seledtsov, and V.V. Solovyev, *Analysis of canonical and non-canonical splice sites in mammalian genomes.* Nucleic Acids Res, 2000. **28**(21): p. 4364-75.
214. Lord, J., et al., *Pathogenicity and selective constraint on variation near splice sites.* Genome Res, 2019. **29**(2): p. 159-170.
215. Blakes, A.J.M., et al., *A systematic analysis of splicing variants identifies new diagnoses in the 100,000 Genomes Project.* Genome Medicine, 2022. **14**(1): p. 79.
216. Cascón, A. and M. Robledo, *MAX and MYC: a heritable breakup.* Cancer Res, 2012. **72**(13): p. 3119-24.
217. Kohl, N.E., et al., *Transposition and amplification of oncogene-related sequences in human neuroblastomas.* Cell, 1983. **35**(2 Pt 1): p. 359-67.

218. Ribon, V., T. Leff, and A.R. Saltiel, *c-Myc does not require max for transcriptional activity in PC-12 cells.* Mol Cell Neurosci, 1994. **5**(3): p. 277-82.
219. Qin, N., et al., *Opposing effects of HIF1α and HIF2α on chromaffin cell phenotypic features and tumor cell proliferation: Insights from MYC-associated factor X.* Int J Cancer, 2014. **135**(9): p. 2054-64.
220. Bausch, B., et al., *Clinical Characterization of the Pheochromocytoma and Paraganglioma Susceptibility Genes SDHA, TMEM127, MAX, and SDHAF2 for Gene-Informed Prevention.* JAMA Oncol, 2017. **3**(9): p. 1204-1212.
221. Daly, A.F., et al., *Pheochromocytomas and pituitary adenomas in three patients with MAX exon deletions.* Endocr Relat Cancer, 2018. **25**(5): p. L37-l42.
222. Petignot, S., et al., *Pancreatic Neuroendocrine Neoplasm Associated with a Familial MAX Deletion.* Horm Metab Res, 2020. **52**(11): p. 784-787.
223. Shibata, M., et al., *Synchronous bilateral pheochromocytomas and paraganglioma with novel germline mutation in MAX: a case report.* Surg Case Rep, 2017. **3**(1): p. 131.
224. Hockings G, M.-L.A., Hockings N, et al., *A new pheochromocytoma syndrome: extending the phenotype associated with MAX mutations*, in *Annual Scientific Meeting of the Endocrine Society of Australia*. 2014: Melbourne, Australia. .
225. Robinson, J.T., et al., *Variant Review with the Integrative Genomics Viewer.* Cancer Research, 2017. **77**(21): p. e31-e34.
226. Choi, Y. and A.P. Chan, *PROVEAN web server: a tool to predict the functional effect of amino acid substitutions and indels.* Bioinformatics, 2015. **31**(16): p. 2745-7.
227. Schwarz, J.M., et al., *MutationTaster2: mutation prediction for the deep-sequencing age.* Nature Methods, 2014. **11**(4): p. 361-362.
228. Chen, S., et al., *A genomic mutational constraint map using variation in 76,156 human genomes.* Nature, 2024. **625**(7993): p. 92-100.
229. Auton, A., et al., *A global reference for human genetic variation.* Nature, 2015. **526**(7571): p. 68-74.
230. Xekouki, P., et al., *The 3PAs: An Update on the Association of Pheochromocytomas, Paragangliomas, and Pituitary Tumors.* Horm Metab Res, 2019. **51**(7): p. 419-436.
231. Roszko, K.L., et al., *Case Report of a Prolactinoma in a Patient With a Novel MAX Mutation and Bilateral Pheochromocytomas.* J Endocr Soc, 2017. **1**(11): p. 1401-1407.
232. Kobza, A.O., S. Dizon, and A. Arnaout, *Case Report of Bilateral Pheochromocytomas due to a Novel Max Mutation in a Patient Known to have a Pituitary Prolactinoma.* AACE Clinical Case Reports, 2018. **4**(6): p. e453-e456.
233. Korpershoek, E., et al., *Complex MAX Rearrangement in a Family With Malignant Pheochromocytoma, Renal Oncocytoma, and Erythrocytosis.* The Journal of Clinical Endocrinology & Metabolism, 2016. **101**(2): p. 453-460.
234. Pozza, C., et al., *A Novel MAX Gene Mutation Variant in a Patient With Multiple and "Composite" Neuroendocrine-Neuroblastic Tumors.* Front Endocrinol (Lausanne), 2020. **11**: p. 234.
235. Romanet, P., et al., *Pathological and Genetic Characterization of Bilateral Adrenomedullary Hyperplasia in a Patient with Germline MAX Mutation.* Endocr Pathol, 2017. **28**(4): p. 302-307.

236. Romero, O.A., et al., *MAX inactivation in small cell lung cancer disrupts MYC-SWI/SNF programs and is synthetic lethal with BRG1.* Cancer Discov, 2014. **4**(3): p. 292-303.
237. *Comprehensive molecular profiling of lung adenocarcinoma.* Nature, 2014. **511**(7511): p. 543-50.
238. Walker, C.J., et al., *MAX Mutations in Endometrial Cancer: Clinicopathologic Associations and Recurrent MAX p.His28Arg Functional Characterization.* J Natl Cancer Inst, 2018. **110**(5): p. 517-526.
239. Seabrook, A.J., et al., *Multiple Endocrine Tumors Associated with Germline MAX Mutations: Multiple Endocrine Neoplasia Type 5?* J Clin Endocrinol Metab, 2021. **106**(4): p. 1163-1182.
240. Shimada, H., et al., *Terminology and morphologic criteria of neuroblastic tumors: recommendations by the International Neuroblastoma Pathology Committee.* Cancer, 1999. **86**(2): p. 349-63.
241. Jiang, M., J. Stanke, and J.M. Lahti, *The connections between neural crest development and neuroblastoma.* Curr Top Dev Biol, 2011. **94**: p. 77-127.
242. Albanus, R.D.O., et al., *Reverse Engineering the Neuroblastoma Regulatory Network Uncovers MAX as One of the Master Regulators of Tumor Progression.* PLOS ONE, 2013. **8**(12): p. e82457.
243. Chetty, R. and J.D. Duhig, *Bilateral pheochromocytoma-ganglioneuroma of the adrenal in type 1 neurofibromatosis.* Am J Surg Pathol, 1993. **17**(8): p. 837-41.
244. Efared, B., et al., *Bilateral pheochromocytoma with ganglioneuroma component associated with multiple neuroendocrine neoplasia type 2A: a case report.* J Med Case Rep, 2017. **11**(1): p. 208.
245. Brady, S., et al., *Composite pheochromocytoma/ganglioneuroma of the adrenal gland associated with multiple endocrine neoplasia 2A: case report with immunohistochemical analysis.* Am J Surg Pathol, 1997. **21**(1): p. 102-8.
246. Bernini, G.P., et al., *Unique association of non-functioning pheochromocytoma, ganglioneuroma, adrenal cortical adenoma, hepatic and vertebral hemangiomas in a patient with a new intronic variant in the VHL gene.* J Endocrinol Invest, 2005. **28**(11): p. 1032-7.
247. Pacak, K., et al., *New syndrome of paraganglioma and somatostatinoma associated with polycythemia.* J Clin Oncol, 2013. **31**(13): p. 1690-8.
248. Semenza, G.L., *Hypoxia-inducible factors in physiology and medicine.* Cell, 2012. **148**(3): p. 399-408.
249. Kaelin, W.G., Jr. and P.J. Ratcliffe, *Oxygen sensing by metazoans: the central role of the HIF hydroxylase pathway.* Mol Cell, 2008. **30**(4): p. 393-402.
250. Ma, X., et al., *Mutational Profile and Potential Molecular Therapeutic Targets of Pheochromocytoma.* Front Endocrinol (Lausanne), 2022. **13**: p. 921645.
251. Jochmanová, I., et al., *Hypoxia-inducible factor signaling in pheochromocytoma: turning the rudder in the right direction.* J Natl Cancer Inst, 2013. **105**(17): p. 1270-83.
252. Schofield, C.J. and P.J. Ratcliffe, *Oxygen sensing by HIF hydroxylases.* Nature Reviews Molecular Cell Biology, 2004. **5**(5): p. 343-354.
253. Welander, J., et al., *Frequent EPAS1/HIF2α exons 9 and 12 mutations in non-familial pheochromocytoma.* Endocr Relat Cancer, 2014. **21**(3): p. 495-504.

254. Masson, N. and P.J. Ratcliffe, *Hypoxia signaling pathways in cancer metabolism: the importance of co-selecting interconnected physiological pathways.* Cancer Metab, 2014. **2**(1): p. 3.
255. Bertout, J.A., S.A. Patel, and M.C. Simon, *The impact of O2 availability on human cancer.* Nature Reviews Cancer, 2008. **8**(12): p. 967-975.
256. Liao, D. and R.S. Johnson, *Hypoxia: a key regulator of angiogenesis in cancer.* Cancer Metastasis Rev, 2007. **26**(2): p. 281-90.
257. Semenza, G.L., *Targeting HIF-1 for cancer therapy.* Nat Rev Cancer, 2003. **3**(10): p. 721-32.
258. Richter, S., et al., *Role of hypoxia and HIF2α in development of the sympathoadrenal cell lineage and chromaffin cell tumors with distinct catecholamine phenotypic features.* Adv Pharmacol, 2013. **68**: p. 285-317.
259. Selak, M.A., et al., *Succinate links TCA cycle dysfunction to oncogenesis by inhibiting HIF-alpha prolyl hydroxylase.* Cancer Cell, 2005. **7**(1): p. 77-85.
260. Favier, J., et al., *Cloning and expression pattern of EPAS1 in the chicken embryo. Colocalization with tyrosine hydroxylase.* FEBS Lett, 1999. **462**(1-2): p. 19-24.
261. Tian, H., et al., *The hypoxia-responsive transcription factor EPAS1 is essential for catecholamine homeostasis and protection against heart failure during embryonic development.* Genes Dev, 1998. **12**(21): p. 3320-4.
262. Vaidya, A., et al., *EPAS1 Mutations and Paragangliomas in Cyanotic Congenital Heart Disease.* N Engl J Med, 2018. **378**(13): p. 1259-1261.
263. White, G., et al., *Somatic EPAS1 Variants in Pheochromocytoma and Paraganglioma in Patients With Sickle Cell Disease.* J Clin Endocrinol Metab, 2023. **108**(12): p. 3302-3310.
264. Mancini, M., et al., *EPAS1-mutated paragangliomas associated with haemoglobin disorders.* British Journal of Haematology. **n/a**(n/a).
265. Astrom, K., et al., *Altitude is a phenotypic modifier in hereditary paraganglioma type 1: evidence for an oxygen-sensing defect.* Hum Genet, 2003. **113**(3): p. 228-37.
266. Pollard, P.J., et al., *Accumulation of Krebs cycle intermediates and over-expression of HIF1alpha in tumours which result from germline FH and SDH mutations.* Hum Mol Genet, 2005. **14**(15): p. 2231-9.
267. Clark, G.R., et al., *Germline FH Mutations Presenting With Pheochromocytoma.* The Journal of Clinical Endocrinology & Metabolism, 2014. **99**(10): p. E2046-E2050.
268. Ladroue, C., et al., *PHD2 mutation and congenital erythrocytosis with paraganglioma.* N Engl J Med, 2008. **359**(25): p. 2685-92.
269. Amorim-Pires, D., J. Peixoto, and J. Lima, *Hypoxia Pathway Mutations in Pheochromocytomas and Paragangliomas.* Cytogenet Genome Res, 2016. **150**(3-4): p. 227-241.
270. Lim, J.H., et al., *Ras-dependent induction of HIF-1alpha785 via the Raf/MEK/ERK pathway: a novel mechanism of Ras-mediated tumor promotion.* Oncogene, 2004. **23**(58): p. 9427-31.
271. Land, S.C. and A.R. Tee, *Hypoxia-inducible factor 1alpha is regulated by the mammalian target of rapamycin (mTOR) via an mTOR signaling motif.* J Biol Chem, 2007. **282**(28): p. 20534-43.
272. Yang, C., et al., *Novel HIF2A mutations disrupt oxygen sensing, leading to polycythemia, paragangliomas, and somatostatinomas.* Blood, 2013. **121**(13): p. 2563-6.

273. Zhuang, Z., et al., *Somatic HIF2A gain-of-function mutations in paraganglioma with polycythemia.* N Engl J Med, 2012. **367**(10): p. 922-30.
274. Tate, J.G., et al., *COSMIC: the Catalogue Of Somatic Mutations In Cancer.* Nucleic Acids Res, 2019. **47**(D1): p. D941-d947.
275. Lorenzo, F.R., et al., *A novel EPAS1/HIF2A germline mutation in a congenital polycythemia with paraganglioma.* J Mol Med (Berl), 2013. **91**(4): p. 507-12.
276. Dwight, T., et al., *Functional significance of germline EPAS1 variants.* Endocr Relat Cancer, 2021. **28**(2): p. 97-109.
277. Abdullah, A.E., et al., *Paraganglioma of the organ of Zuckerkandl associated with a somatic HIF2α mutation: A case report.* Oncol Lett, 2017. **13**(3): p. 1083-1086.
278. Abdallah, A., et al., *Clinical manifestations of Pacak-Zhuang syndrome in a male pediatric patient.* Pediatric Blood & Cancer, 2020. **67**(4): p. e28096.
279. Buffet, A., et al., *Mosaicism in HIF2A-related polycythemia-paraganglioma syndrome.* J Clin Endocrinol Metab, 2014. **99**(2): p. E369-73.
280. Därr, R., et al., *Novel insights into the polycythemia-paraganglioma-somatostatinoma syndrome.* Endocr Relat Cancer, 2016. **23**(12): p. 899-908.
281. Taïeb, D., et al., *First report of bilateral pheochromocytoma in the clinical spectrum of HIF2A-related polycythemia-paraganglioma syndrome.* J Clin Endocrinol Metab, 2013. **98**(5): p. E908-13.
282. Clifford, S.C., et al., *Contrasting effects on HIF-1α regulation by disease-causing pVHL mutations correlate with patterns of tumourigenesis in von Hippel-Lindau disease.* Human Molecular Genetics, 2001. **10**(10): p. 1029-1038.
283. Girirajan, S., et al., *Phenotypic Heterogeneity of Genomic Disorders and Rare Copy-Number Variants.* New England Journal of Medicine, 2012. **367**(14): p. 1321-1331.
284. Fuady, J.H., et al., *Estrogen-dependent downregulation of hypoxia-inducible factor (HIF)-2α in invasive breast cancer cells.* Oncotarget, 2016. **7**(21): p. 31153-65.
285. Haase, V.H., *Regulation of erythropoiesis by hypoxia-inducible factors.* Blood Rev, 2013. **27**(1): p. 41-53.
286. Eisenhofer, G., et al., *Distinct gene expression profiles in norepinephrine- and epinephrine-producing hereditary and sporadic pheochromocytomas: activation of hypoxia-driven angiogenic pathways in von Hippel-Lindau syndrome.* Endocr Relat Cancer, 2004. **11**(4): p. 897-911.
287. Delcore, R. and S.R. Friesen, *Gastrointestinal neuroendocrine tumors.* J Am Coll Surg, 1994. **178**(2): p. 187-211.
288. Blansfield, J.A., et al., *Clinical, genetic and radiographic analysis of 108 patients with von Hippel-Lindau disease (VHL) manifested by pancreatic neuroendocrine neoplasms (PNETs).* Surgery, 2007. **142**(6): p. 814-8; discussion 818.e1-2.
289. Doherty, G.M., *Rare endocrine tumours of the GI tract.* Best Pract Res Clin Gastroenterol, 2005. **19**(5): p. 807-17.
290. Harris, G.J., F. Tio, and A.B. Cruz, Jr., *Somatostatinoma: a case report and review of the literature.* J Surg Oncol, 1987. **36**(1): p. 8-16.
291. Raedler, L.A., *Diagnosis and Management of Polycythemia Vera: Proceedings from a Multidisciplinary Roundtable.* Am Health Drug Benefits, 2014. **7**(7 Suppl 3): p. S36-47.
292. Dos Santos, L.C., et al., *Cytogenetics, JAK2 and MPL mutations in polycythemia vera, primary myelofibrosis and essential thrombocythemia.* Rev Bras Hematol Hemoter, 2011. **33**(6): p. 417-24.

293. Ang, S.O., et al., *Disruption of oxygen homeostasis underlies congenital Chuvash polycythemia.* Nat Genet, 2002. **32**(4): p. 614-21.
294. Percy, M.J., et al., *A gain-of-function mutation in the HIF2A gene in familial erythrocytosis.* N Engl J Med, 2008. **358**(2): p. 162-8.
295. Gangat, N., et al., *Erythrocytosis associated with EPAS1(HIF2A), EGLN1(PHD2), VHL, EPOR or BPGM mutations: The Mayo Clinic experience.* Haematologica, 2022. **107**(5): p. 1201-1204.
296. Pacak, K., et al., *Ocular manifestations of hypoxia-inducible factor-2α paraganglioma-somatostatinoma-polycythemia syndrome.* Ophthalmology, 2014. **121**(11): p. 2291-3.
297. Rosenblum, J.S., et al., *Developmental vascular malformations in EPAS1 gain-of-function syndrome.* JCI Insight, 2021. **6**(5).
298. Jonasch, E., et al., *Belzutifan for Renal Cell Carcinoma in von Hippel–Lindau Disease.* New England Journal of Medicine, 2021. **385**(22): p. 2036-2046.
299. Kamihara, J., et al., *Belzutifan, a Potent HIF2α Inhibitor, in the Pacak-Zhuang Syndrome.* N Engl J Med, 2021. **385**(22): p. 2059-2065.
300. Jochmanova, I., et al., *Clinical characteristics and outcomes of SDHB-related pheochromocytoma and paraganglioma in children and adolescents.* J Cancer Res Clin Oncol, 2020. **146**(4): p. 1051-1063.
301. Ciftci, A.O., et al., *Pheochromocytoma in children.* J Pediatr Surg, 2001. **36**(3): p. 447-52.
302. Barontini, M., G. Levin, and G. Sanso, *Characteristics of pheochromocytoma in a 4- to 20-year-old population.* Ann N Y Acad Sci, 2006. **1073**: p. 30-7.
303. Bausch, B., et al., *Long-term prognosis of patients with pediatric pheochromocytoma.* Endocr Relat Cancer, 2014. **21**(1): p. 17-25.
304. Rednam, S.P., et al., *Von Hippel-Lindau and Hereditary Pheochromocytoma/Paraganglioma Syndromes: Clinical Features, Genetics, and Surveillance Recommendations in Childhood.* Clin Cancer Res, 2017. **23**(12): p. e68-e75.
305. Redlich, A., et al., *Pseudohypoxic pheochromocytomas and paragangliomas dominate in children.* Pediatr Blood Cancer, 2021. **68**(7): p. e28981.
306. Beilan, J.A., et al., *Pheochromocytoma of the urinary bladder: a systematic review of the contemporary literature.* BMC Urology, 2013. **13**(1): p. 22.
307. Cheng, L., et al., *Paraganglioma of the urinary bladder.* Cancer, 2000. **88**(4): p. 844-852.
308. de Tersant, M., et al., *Pheochromocytoma and Paraganglioma in Children and Adolescents: Experience of the French Society of Pediatric Oncology (SFCE).* J Endocr Soc, 2020. **4**(5): p. bvaa039.
309. King, K.S., et al., *Metastatic pheochromocytoma/paraganglioma related to primary tumor development in childhood or adolescence: significant link to SDHB mutations.* J Clin Oncol, 2011. **29**(31): p. 4137-42.
310. Buffet, A., et al., *Positive Impact of Genetic Test on the Management and Outcome of Patients With Paraganglioma and/or Pheochromocytoma.* J Clin Endocrinol Metab, 2019. **104**(4): p. 1109-1118.
311. Davidoff, D.F., et al., *Surveillance Improves Outcomes for Carriers of SDHB Pathogenic Variants: A Multicenter Study.* J Clin Endocrinol Metab, 2022. **107**(5): p. e1907-e1916.

312. Gill, A.J., et al., *Immunohistochemistry for SDHB triages genetic testing of SDHB, SDHC, and SDHD in paraganglioma-pheochromocytoma syndromes.* Hum Pathol, 2010. **41**(6): p. 805-14.
313. Papathomas, T.G., et al., *SDHB/SDHA immunohistochemistry in pheochromocytomas and paragangliomas: a multicenter interobserver variation analysis using virtual microscopy: a Multinational Study of the European Network for the Study of Adrenal Tumors (ENS@T).* Mod Pathol, 2015. **28**(6): p. 807-21.
314. De Sousa, S.M.C., et al., *Aberrant Splicing of SDHC in Families With Unexplained Succinate Dehydrogenase-Deficient Paragangliomas.* J Endocr Soc, 2020. **4**(12): p. bvaa071.
315. Nosé, V., et al., *Overview of the 2022 WHO Classification of Familial Endocrine Tumor Syndromes.* Endocr Pathol, 2022. **33**(1): p. 197-227.
316. Kühlbrandt, W., *Structure and function of mitochondrial membrane protein complexes.* BMC Biology, 2015. **13**(1): p. 89.
317. Gammage, P.A. and C. Frezza, *Mitochondrial DNA: the overlooked oncogenome?* BMC Biol, 2019. **17**(1): p. 53.
318. Scheffler, I.E., *A century of mitochondrial research: achievements and perspectives.* Mitochondrion, 2001. **1**(1): p. 3-31.
319. Gorman, G.S., et al., *Mitochondrial diseases.* Nat Rev Dis Primers, 2016. **2**: p. 16080.
320. Clay Montier, L.L., J.J. Deng, and Y. Bai, *Number matters: control of mammalian mitochondrial DNA copy number.* J Genet Genomics, 2009. **36**(3): p. 125-31.
321. Area-Gomez, E. and E.A. Schon, *Mitochondrial genetics and disease.* J Child Neurol, 2014. **29**(9): p. 1208-15.
322. Chinnery, P.F., et al., *MELAS and MERRF. The relationship between maternal mutation load and the frequency of clinically affected offspring.* Brain, 1998. **121 (Pt 10)**: p. 1889-94.
323. Gorman, G.S., et al., *Prevalence of nuclear and mitochondrial DNA mutations related to adult mitochondrial disease.* Annals of Neurology, 2015. **77**(5): p. 753-759.
324. Alston, C.L., et al., *The genetics and pathology of mitochondrial disease.* J Pathol, 2017. **241**(2): p. 236-250.
325. Hanahan, D., *Hallmarks of Cancer: New Dimensions.* Cancer Discovery, 2022. **12**(1): p. 31-46.
326. Ju, Y.S., et al., *Origins and functional consequences of somatic mitochondrial DNA mutations in human cancer.* Elife, 2014. **3**.
327. Kim, M., et al., *Mitochondrial DNA is a major source of driver mutations in cancer.* Trends in Cancer, 2022. **8**(12): p. 1046-1059.
328. Yuan, Y., et al., *Comprehensive molecular characterization of mitochondrial genomes in human cancers.* Nat Genet, 2020. **52**(3): p. 342-352.
329. Gorelick, A.N., et al., *Respiratory complex and tissue lineage drive recurrent mutations in tumour mtDNA.* Nat Metab, 2021. **3**(4): p. 558-570.
330. Lendvai, N., et al., *Succinate-to-fumarate ratio as a new metabolic marker to detect the presence of SDHB/D-related paraganglioma: initial experimental and ex vivo findings.* Endocrinology, 2014. **155**(1): p. 27-32.
331. Favier, J., et al., *Hereditary paraganglioma/pheochromocytoma and inherited succinate dehydrogenase deficiency.* Horm Res, 2005. **63**(4): p. 171-9.
332. Puttick, C., et al., *mity: A highly sensitive mitochondrial variant analysis pipeline for whole genome sequencing data.* bioRxiv, 2019: p. 852210.

333. Shen, L., et al., *MSeqDR mvTool: A mitochondrial DNA Web and API resource for comprehensive variant annotation, universal nomenclature collation, and reference genome conversion.* Hum Mutat, 2018. **39**(6): p. 806-810.
334. McLaren, W., et al., *The Ensembl Variant Effect Predictor.* Genome Biology, 2016. **17**(1): p. 122.
335. Castellana, S., et al., *High-confidence assessment of functional impact of human mitochondrial non-synonymous genome variations by APOGEE.* PLoS Comput Biol, 2017. **13**(6): p. e1005628.
336. *Pan-cancer analysis of whole genomes.* Nature, 2020. **578**(7793): p. 82-93.
337. Barthel, F.P., et al., *Systematic analysis of telomere length and somatic alterations in 31 cancer types.* Nat Genet, 2017. **49**(3): p. 349-357.
338. Kim, S., et al., *The telomere maintenance mechanism spectrum and its dynamics in gliomas.* Genome Medicine, 2022. **14**(1): p. 88.
339. Gordon, D.M. and J.H. Santos, *The emerging role of telomerase reverse transcriptase in mitochondrial DNA metabolism.* J Nucleic Acids, 2010. **2010**.
340. Heaphy, C.M., et al., *Altered Telomeres in Tumors with ATRX and DAXX Mutations.* Science, 2011. **333**(6041): p. 425-425.
341. Grandhi, S., et al., *Heteroplasmic shifts in tumor mitochondrial genomes reveal tissue-specific signals of relaxed and positive selection.* Hum Mol Genet, 2017. **26**(15): p. 2912-2922.
342. Lam, A.K., *Update on Adrenal Tumours in 2017 World Health Organization (WHO) of Endocrine Tumours.* Endocr Pathol, 2017. **28**(3): p. 213-227.
343. Hamidi, O., et al., *Malignant Pheochromocytoma and Paraganglioma: 272 Patients Over 55 Years.* J Clin Endocrinol Metab, 2017. **102**(9): p. 3296-3305.
344. Hescot, S., et al., *Prognosis of Malignant Pheochromocytoma and Paraganglioma (MAPP-Prono Study): A European Network for the Study of Adrenal Tumors Retrospective Study.* J Clin Endocrinol Metab, 2019. **104**(6): p. 2367-2374.
345. Fishbein, L., et al., *SDHB mutation carriers with malignant pheochromocytoma respond better to CVD.* Endocr Relat Cancer, 2017. **24**(8): p. L51-l55.
346. Dahia, P.L., *Pheochromocytomas and Paragangliomas, Genetically Diverse and Minimalist, All at Once!* Cancer Cell, 2017. **31**(2): p. 159-161.
347. Jimenez, C., *Treatment for Patients With Malignant Pheochromocytomas and Paragangliomas: A Perspective From the Hallmarks of Cancer.* Front Endocrinol (Lausanne), 2018. **9**: p. 277.
348. Niemeijer, N.D., et al., *Chemotherapy with cyclophosphamide, vincristine and dacarbazine for malignant paraganglioma and pheochromocytoma: systematic review and meta-analysis.* Clin Endocrinol (Oxf), 2014. **81**(5): p. 642-51.
349. O'Kane, G.M., et al., *A phase 2 trial of sunitinib in patients with progressive paraganglioma or pheochromocytoma: the SNIPP trial.* Br J Cancer, 2019. **120**(12): p. 1113-1119.
350. Kayano, D. and S. Kinuya, *Current Consensus on I-131 MIBG Therapy.* Nucl Med Mol Imaging, 2018. **52**(4): p. 254-265.
351. Zandee, W.T., et al., *Treatment of inoperable or metastatic paragangliomas and pheochromocytomas with peptide receptor radionuclide therapy using 177Lu-DOTATATE.* Eur J Endocrinol, 2019. **181**(1): p. 45-53.

352. Vallabhajosula, S. and A. Nikolopoulou, *Radioiodinated metaiodobenzylguanidine (MIBG): radiochemistry, biology, and pharmacology.* Semin Nucl Med, 2011. **41**(5): p. 324-33.
353. Dhingra, J. and R. Halkar, *I-131 MIBG therapy has been used as the first line therapy in pheochromocytoma.* Journal of Nuclear Medicine, 2020. **61**(supplement 1): p. 1452-1452.
354. Pryma, D.A., et al., *Efficacy and Safety of High-Specific-Activity (131)I-MIBG Therapy in Patients with Advanced Pheochromocytoma or Paraganglioma.* J Nucl Med, 2019. **60**(5): p. 623-630.
355. Strosberg, J., et al., *Phase 3 Trial of (177)Lu-Dotatate for Midgut Neuroendocrine Tumors.* N Engl J Med, 2017. **376**(2): p. 125-135.
356. Giammarile, F., et al., *EANM procedure guidelines for 131I-meta-iodobenzylguanidine (131I-mIBG) therapy.* Eur J Nucl Med Mol Imaging, 2008. **35**(5): p. 1039-47.
357. NSW, N.M.N.a.C.I. *NSW Lutate therapy referral and protocol for neuroendocrine cancer patients Sydney, Australia*. 2017; Available from: https://www.aci.health.nsw.gov.au/__data/assets/pdf_file/0004/255451/NSW-Lutate-therapy-referral-protocol–to2017.pdf.
358. Eisenhauer, E.A., et al., *New response evaluation criteria in solid tumours: revised RECIST guideline (version 1.1).* Eur J Cancer, 2009. **45**(2): p. 228-47.
359. Green, S. and G.R. Weiss, *Southwest Oncology Group standard response criteria, endpoint definitions and toxicity criteria.* Invest New Drugs, 1992. **10**(4): p. 239-53.
360. Thorpe, M.P., et al., *Long-Term Outcomes of 125 Patients With Metastatic Pheochromocytoma or Paraganglioma Treated With 131-I MIBG.* J Clin Endocrinol Metab, 2020. **105**(3): p. e494-501.
361. Safford, S.D., et al., *Iodine -131 metaiodobenzylguanidine is an effective treatment for malignant pheochromocytoma and paraganglioma.* Surgery, 2003. **134**(6): p. 956-62; discussion 962-3.
362. Satapathy, S., B.R. Mittal, and A. Bhansali, *'Peptide receptor radionuclide therapy in the management of advanced pheochromocytoma and paraganglioma: A systematic review and meta-analysis'.* Clin Endocrinol (Oxf), 2019. **91**(6): p. 718-727.
363. Yadav, M.P., S. Ballal, and C. Bal, *Concomitant (177)Lu-DOTATATE and capecitabine therapy in malignant paragangliomas.* EJNMMI Res, 2019. **9**(1): p. 13.
364. Prejbisz, A., et al., *Cardiovascular manifestations of phaeochromocytoma.* J Hypertens, 2011. **29**(11): p. 2049-60.
365. Manger, W.M., R.W. Gifford, Jr., and B.B. Hoffman, *Pheochromocytoma: a clinical and experimental overview.* Curr Probl Cancer, 1985. **9**(5): p. 1-89.
366. Brouwers, F.M., et al., *Emergencies caused by pheochromocytoma, neuroblastoma, or ganglioneuroma.* Endocrinol Metab Clin North Am, 2006. **35**(4): p. 699-724, viii.
367. Timmers, H.J., et al., *Metastases but not cardiovascular mortality reduces life expectancy following surgical resection of apparently benign pheochromocytoma.* Endocr Relat Cancer, 2008. **15**(4): p. 1127-33.
368. Kolasinska-Ćwikła, A., et al., *A Clinical Efficacy of PRRT in Patients with Advanced, Nonresectable, Paraganglioma-Pheochromocytoma, Related to SDHx Gene Mutation.* J Clin Med, 2019. **8**(7).
369. Gedik, G.K., et al., *131I-MIBG therapy in metastatic phaeochromocytoma and paraganglioma.* Eur J Nucl Med Mol Imaging, 2008. **35**(4): p. 725-33.

370. Shilkrut, M., et al., *Low-dose iodine-131 metaiodobenzylguanidine therapy for patients with malignant pheochromocytoma and paraganglioma: single center experience.* Am J Clin Oncol, 2010. **33**(1): p. 79-82.
371. Shapiro, B., et al., *Radiopharmaceutical therapy of malignant pheochromocytoma with [131I]metaiodobenzylguanidine: results from ten years of experience.* J Nucl Biol Med (1991), 1991. **35**(4): p. 269-76.
372. Krempf, M., et al., *Use of m-[131I]iodobenzylguanidine in the treatment of malignant pheochromocytoma.* J Clin Endocrinol Metab, 1991. **72**(2): p. 455-61.
373. Nastos, K., et al., *Peptide Receptor Radionuclide Treatment and (131)I-MIBG in the management of patients with metastatic/progressive phaeochromocytomas and paragangliomas.* J Surg Oncol, 2017. **115**(4): p. 425-434.
374. Gonias, S., et al., *Phase II study of high-dose [131I]metaiodobenzylguanidine therapy for patients with metastatic pheochromocytoma and paraganglioma.* J Clin Oncol, 2009. **27**(25): p. 4162-8.
375. Carrasquillo, J.A., N. Pandit-Taskar, and C.C. Chen, *I-131 Metaiodobenzylguanidine Therapy of Pheochromocytoma and Paraganglioma.* Semin Nucl Med, 2016. **46**(3): p. 203-14.
376. Sabet, A., et al., *Long-term hematotoxicity after peptide receptor radionuclide therapy with 177Lu-octreotate.* J Nucl Med, 2013. **54**(11): p. 1857-61.
377. Vyakaranam, A.R., et al., *Favorable Outcome in Patients with Pheochromocytoma and Paraganglioma Treated with (177)Lu-DOTATATE.* Cancers (Basel), 2019. **11**(7).

Appendices

Appendix 1. Electropherograms following RNA extraction from PC/PGL harbour *TMEM127* variants.

Ladder

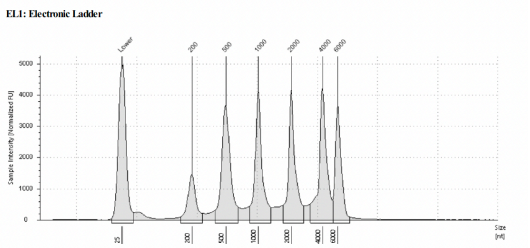

Sample Table

Well	RINe	28S/18S (Area)	Conc. [ng/µl]	Sample Description	Alert	Observations
EL1	-	-	84.9	Electronic Ladder		Ladder

Peak Table

Size [nt]	Calibrated Conc. [ng/µl]	Assigned Conc. [ng/µl]	Peak Molarity [nmol/l]	% Integrated Area	Peak Comment	Observations
25	40.0	40.0	4710	-		Lower Marker
200	5.94	-	87.4	7.80		
500	15.9	-	93.6	20.88		
1000	14.2	-	41.8	18.62		
2000	13.8	-	20.3	18.11		
4000	15.5	-	11.4	20.38		
6000	10.8	-	5.31	14.22		

VPH-80T

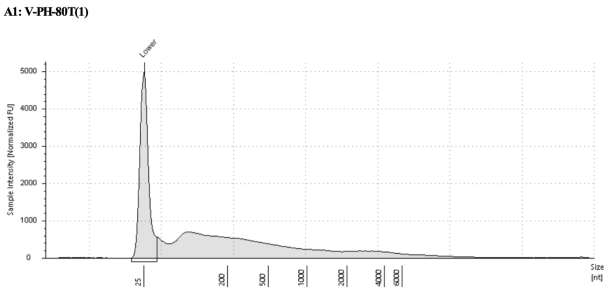

VPH-81T

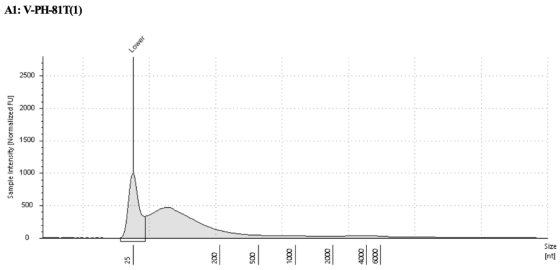

VP-82T

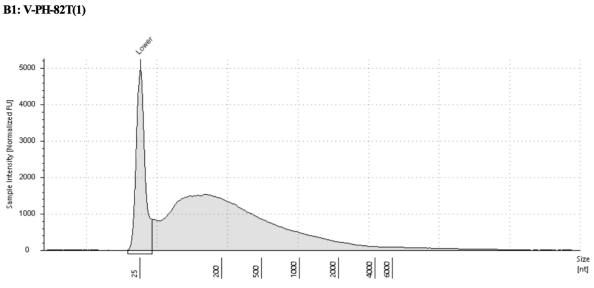

VPH 83-T

VPH-84T

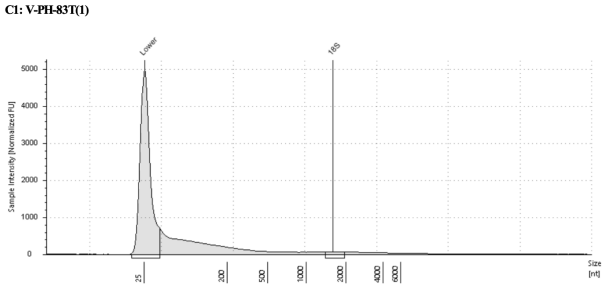

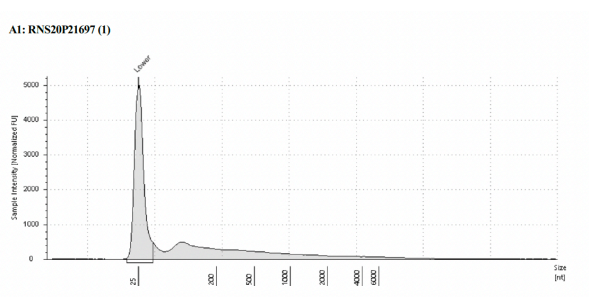

VPH-85T

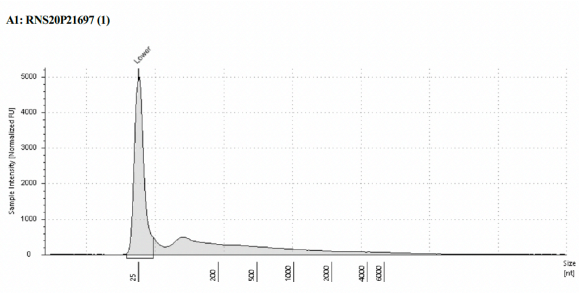

VPH-86T

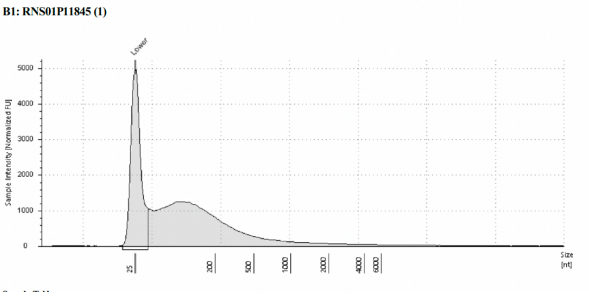

VPH-87T

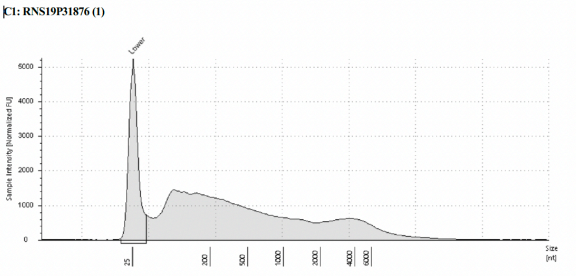

VPH-88T

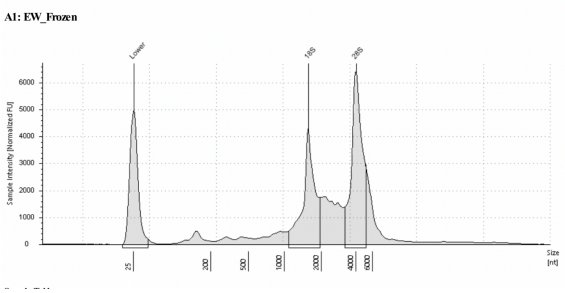

Appendix 2. *TMEM127* PC/PGL samples CNV analysis – chromosome view

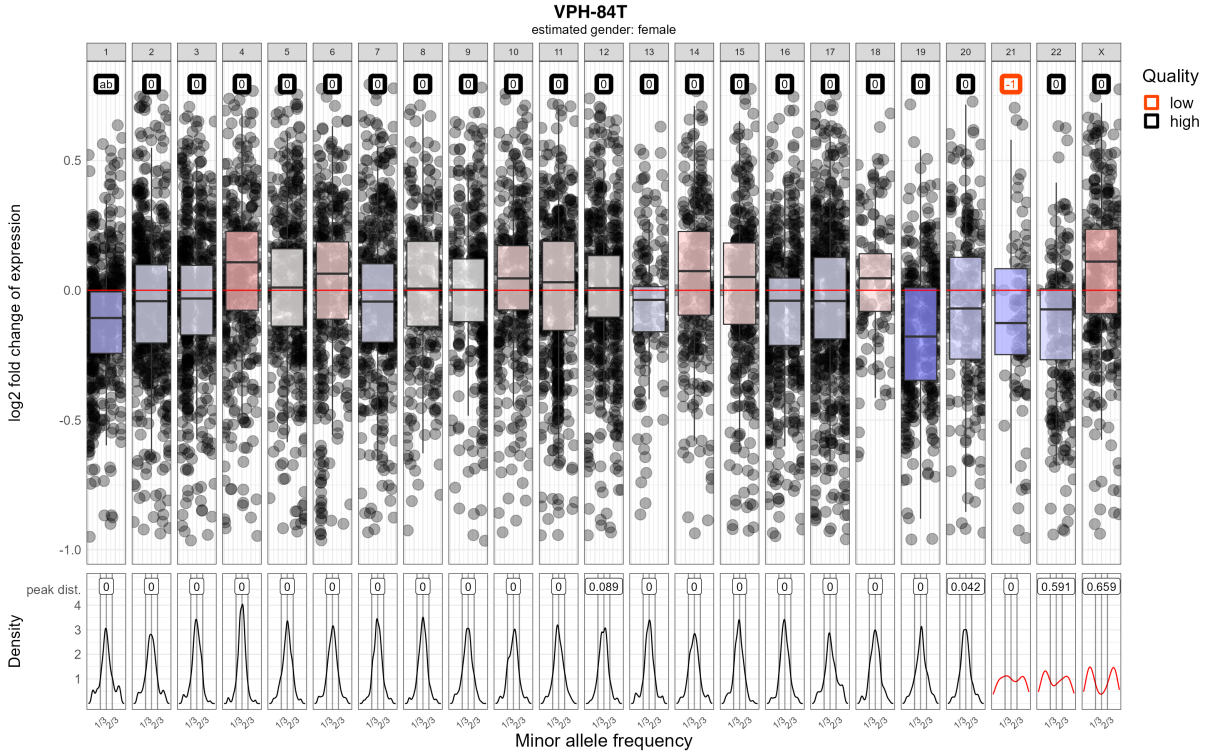

Appendix 2a. VPH-84T

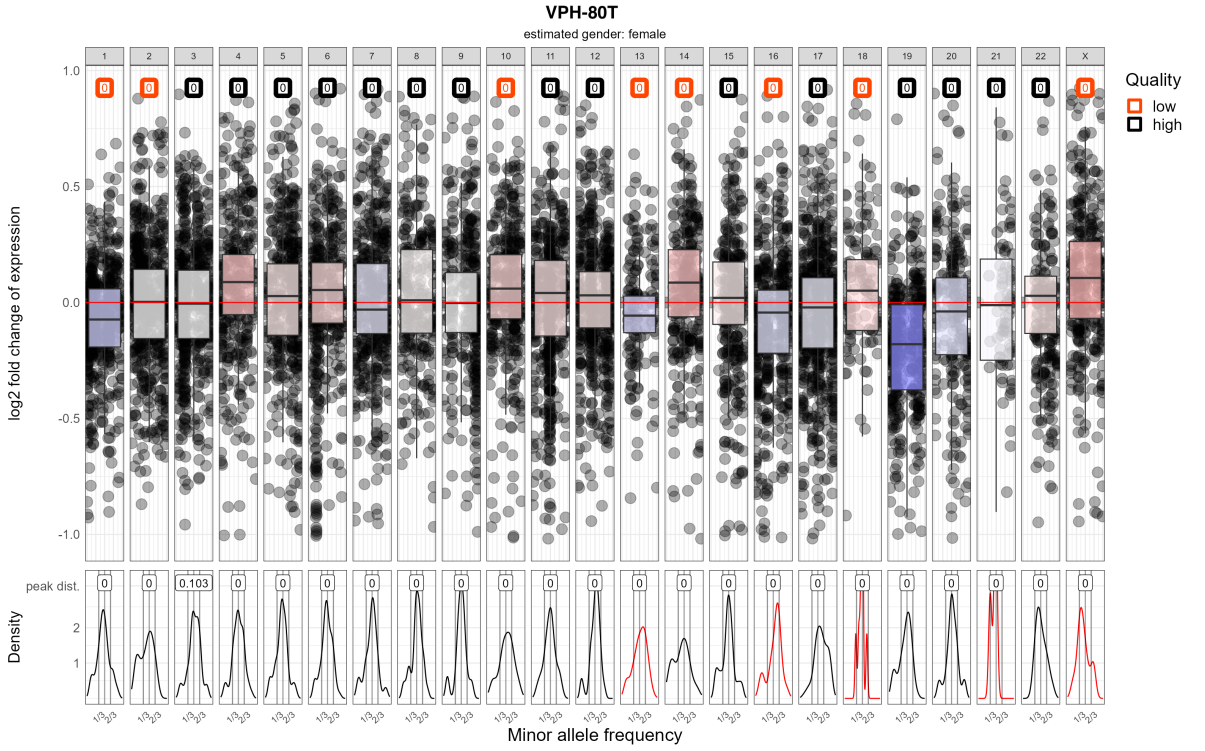

Appendix 2b. VPH-80T

Upper panel showing per chromosome gene expression level. Y axis displays log2 fold change of gene expression against reference samples; x axis shows 23 chromosomes from 1-22-X (Y chromosome excluded). x axis displays the position of genes on each chromosome. A weighed box plot represents the distribution of normalised gene expression with a Random Forest algorithm used to estimate CNV for each chromosome. CNV with low quality are highlighted in red. The lower panel displays the density graphs of MAF for each chromosome using the MAF of heterozygous SNVs (0.05-0.9) to determine CNVs. The peak distance measures the distance between the two highest peaks in the MAF density plot.

The median expression level for both VPH-80T and VPH84T were centred around zero with the highest peaks in the MAF density graph at 0.5. There was evidence of a partial loss in Fig. 4b. chromosome 1. Red represents elevated with low MAF > single copy gain. Normal distribution with low MAF > copy neutral LOH.

Appendix 3. *TMEM127* PC/PGL samples CNV analysis –- arm level figure

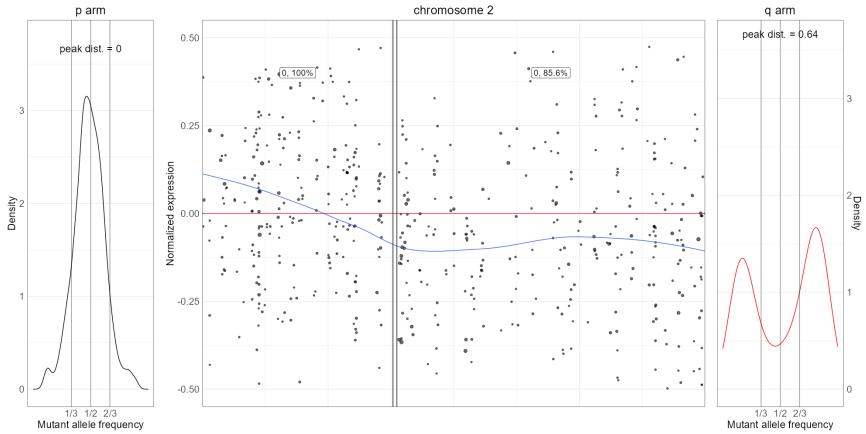

Appendix 3a. VPH-84T

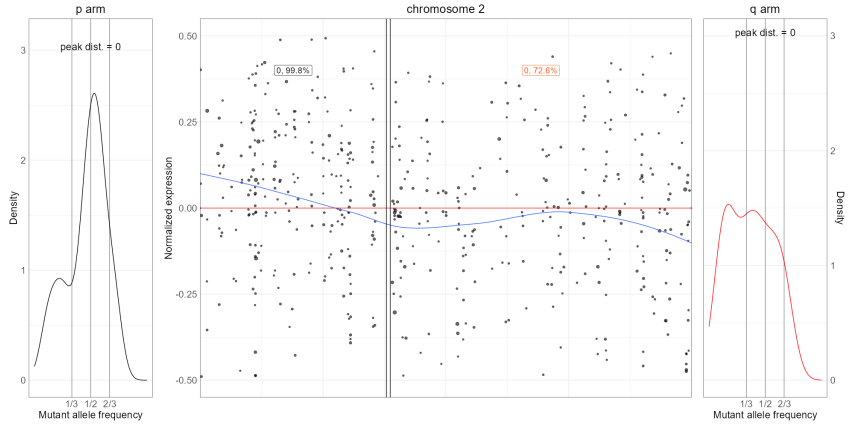

Appendix 3b. VPH-80T

The central panel represents chromosome 2 displaying the random forest estimated alteration with the percentage of trees in the model that agreed upon this alteration. The p- and q-chromosome arms MAF density graphs are shown on either side. The peak distribution is the distance between the peaks of the MAF density graph

Appendices 4-5. Contributions of the candidate and coauthors to the publications arising from this thesis.

Appendix 4. Multiple Endocrine Tumors Associated with Germline *MAX* Mutations: Multiple Endocrine Neoplasia Type 5? **Seabrook A**[+], Harris J[+], Velosa S, Kim E, McInerney-Leo A, Dwight T, Hockings J, Hockings N, Kirk J, Leo P, Love A, Luxford C, Marshall M, Mete O, Pennisi D, Brown M, Gill A, Hockings G*, Clifton-Bligh R*, Duncan E*, *The Journal of Clinical Endocrinology & Metabolism*, Volume 106, Issue 4, April 2021, Pages e1163–e1182

Appendix 5. Genotype–phenotype correlations in paediatric and adolescent phaeochromocytoma and paraganglioma: a cross-sectional study. **Seabrook A**, Vasudevan A, Neville K, Gerstl B, Benn D, Smith J, Kirk J, Gill A, Clifton-Bligh R, Tucker K. *Archives of Disease in Childhood* 2024;**109:**201-208.